The design and testing of a horizontal axis wind turbine with sailfoil blades

Thesis

THE DESIGN AND TESTING OF A HORIZONTAL AXIS WIND TURBINE WITH SAILFOIL BLADES

by

Derek Alan Taylor
AA Dip Arch, M Des RCA Industrial Design (Engineering)

October 1985

A thesis submitted for tne degree of
Doctor of Philosophy of the Open University

Alternative Technology Group/Design Discipline
Faculty of Technology
Open University
Milton Keynes

THE DESIGN AND TESTING OF A HORIZONTAL AXIS WIND TURBINE WITH SAILFOIL BLADES

Derek Taylor

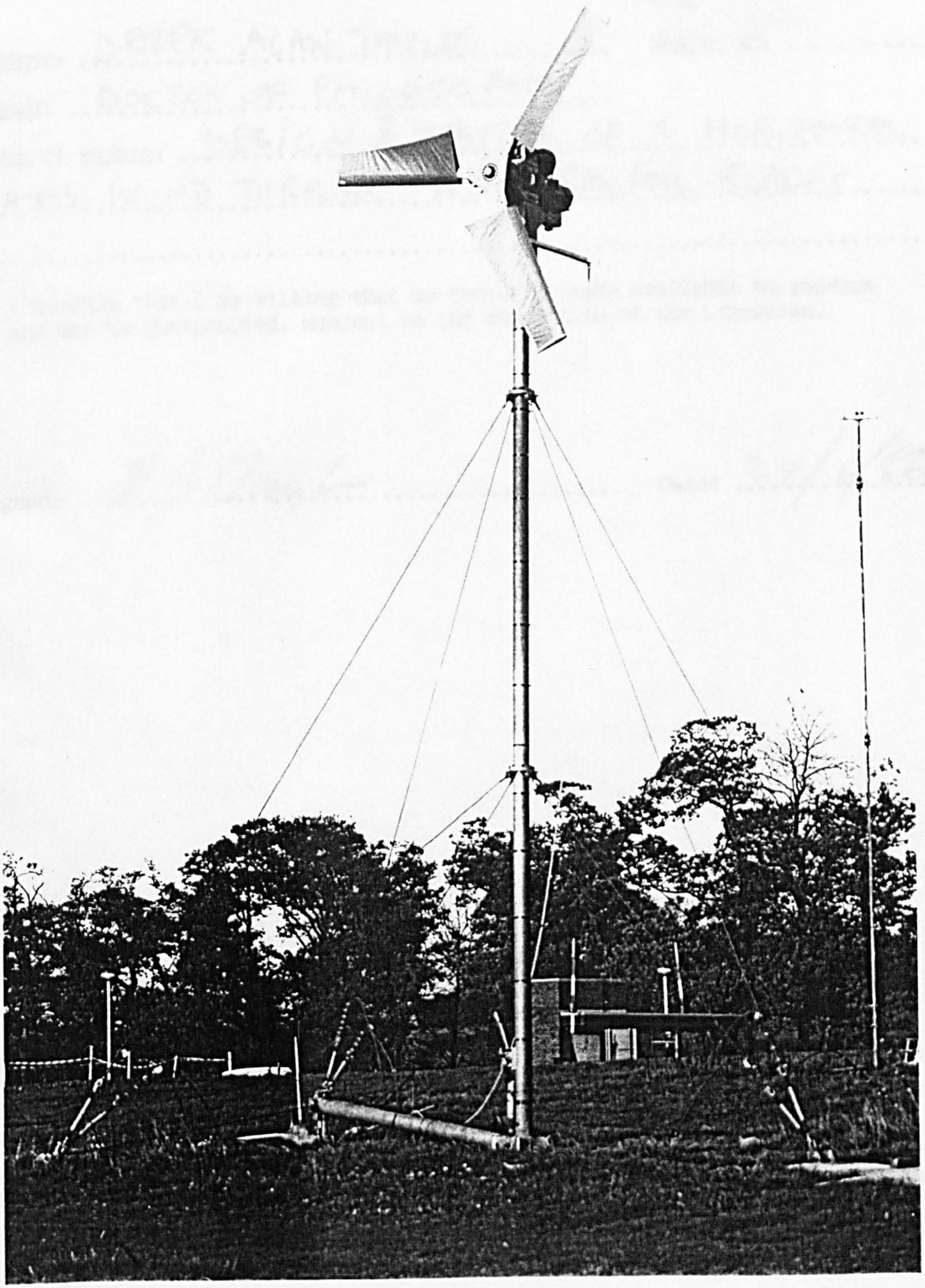

ABSTRACT

The work contained in this thesis covers the design, development and testing of a horizontal axis wind turbine (HAWT) with Sailfoil blades.

Included is a brief history of wind turbine technology, its revival, a review of current wind energy developments and a literature survey of previous work on wind turbines with sail type blades.

The Sailfoil blade consists of a framework of a leading edge D spar and a rigid trailing edge spar over which is stretched a fabric sock, forming a wing-like surface.

The aerodynamic performance theories of HAWTs are described, as is the aerodynamic, structural and mechanical design of a 4 metre diameter, 3 bladed HAWT with Sailfoil blades.

A wind turbine test facility was designed and developed for free air testing of wind turbines and is described.

Free air tests were carried out on the Sailfoil wind turbine on the test facility to obtain power coefficient versus tip speed ratio curves and power versus wind speed curves for the wind turbine. These are presented and compared to predicted values.

ACKNOWLEDGEMENTS

The author expresses his gratitude and thanks to the following people:

Mr Godfrey Boyle, whose interest in wind energy and electronics support has been invaluable, and for his encouragement throughout this work.

Mr Scott Forrest for the considerable manufacturing work carried out on the 4 metre Sailfoil wind turbine and the field test facility as well as his assistance during the testing of the wind turbine.

Mrs Biff Forrest for her expertise in making the sailsocks for the Sailfoil wind turbine blades.

Mr Tony Robotham for his support and assistance during some of the testing and his contributions to the instrumentataion and control system.

Mr Jim Frederickson for project support and contributions to the instrumentation.

Mr David Sharpe of Queen Mary College, who provided his acceleration test software.

Ms Judy Collins for her assistance throughout this project and for typing the manuscript.

The author also wishes to thank the following for their contributions:

The members of the Open University's Alternative Technology Group for their ongoing support and for obtaining the necessary equipment for the completion of this work.

The Open University Electronics Common Facility for designing and producing various parts of the instrumentation components. Also for installing and wiring up the instrumentation components and the instrumentation system for the wind turbine test facility.

The Open University Science and Technology Mechanical Workshop for producing some of the mechanical components.

The Open University Estates Department for carrying out the site works and installing mains services to the wind turbine test facility.

Northumbrian Energy Workshop, who designed and manufactured the wind turbine mast to the author's specifications, and who also supplied some of the instrumentation and the anemometer masts.

SKF Steel of Newport Pagnell, who donated the steel for

the wind turbine shafts.

Finally, the Open University Research Committee, Faculty of Technology, Design Discipline and the Science and Engineering Research Council who contributed financial support to the project.

LIST OF CONTENTS

LIST OF FIGURES FOR CHAPTER 3

LIST OF FIGURES IN CHAPTER 4

LIST OF FIGURES IN CHAPTER 5

LIST OF FIGURES FOR CHAPTER 6

LIST OF FIGURES FOR CHAPTER 7

LIST OF FIGURES IN CHAPTER 8

FIGURES FOR CHAPTER 9

LIST OF FIGURES FOR CHAPTER 10

LIST OF FIGURES IN CHAPTER 11

CHAPTER 1

SYNOPSIS

SYNOPSIS

This thesis covers the design, development and testing of a horizontal axis wind turbine with a novel form of blade construction known as the Sailfoil.

The work includes a brief history of wind turbine technology and its recent renaissance, together with its growing importance to a world becoming increasingly aware of the dangers of pollution and the limited nature of conventional forms of energy.

There is a chapter on the established aerodynamic theories relating to horizontal axis wind turbines. A computer program, CPHAWT, based on these theories was developed to predict the performance of a horizontal axis wind turbine with known aerofoil data.

Chapter 5 consists of a review of prior art relating to wind turbines employing soft-sailed blades, including the Princeton sailwing.

There is a description of the Sailfoil blade utilised in this project which is essentially an improved sailwing. It consists of a rigid framework of a load bearing leading edge D spar and a rigid training edge spar over which is stretched a fabric sock, forming a wing-like surface.

The Sailfoil form of blade was investigated as it simplifies the sailwing and offers a relatively uncomplicated means of blade construction for achieving the complex twisted and tapered blade surface preferred for horizontal axis wind turbines.

A 4 metre diameter, 3 bladed horizontal axis wind turbine which utilises Sailfoil blades was designed and constructed to evaluate the performance of such a turbine in free air conditions.

The aerodynamic design procedure used to design this wind turbine is described. A computer program, WINDROTOR, based on this procedure was developed to produce the initial design, assuming an idealised optimum performance Sailfoil rotor blade. As the leading and trailing edges of the Sailfoil are straight, the degree of blade taper in the idealised design was then modified to a linearised taper that was achievable within the construction constraints.

The performance of the Sailfoil wind turbine with linearised blades was predicted using the CPHAWT program.

The structural and mechanical design of the Sailfoil wind turbine is described.

In order to test the wind turbine under free air condition, an open air wind turbine field test facility was designed by the author and developed by the Alternative Technology Group on the Open University's Walton Hall campus. This test facility is described.

Two different types of testing methods were employed to evaluate the performance of this wind turbine.

A technique developed from wind tunnel testing of wind turbines, known as the 'acceleration technique', was adapted and modified for testing variable speed wind turbines in the free wind. This was used to measure the power coefficient versus tip speed ratio characteristics of the turbine.

The other type of testing procedure entailed measuring the shaft and electrical power together with wind speed. Employing an established binning technique, this data was smoothed and measured power versus wind speed curves were produced.

These two testing techniques are described and the experimental results are compared to the predicted values.

CHAPTER 2

INTRODUCTION

2.1 INTRODUCTION

From about the 12th Century until the industrial revolution, wind energy was an important component in the economy of Britain and at the climax of its popularity in the 18th and 19th centuries there were reckoned to be over 10,000 windmills in Great Britain (Wailes 1948). These windmills were used principally for milling grain and pumping water. They were located mainly in the eastern and south-eastern counties of England and over 2000 windmills were used for draining the Fens of East Anglia.

With the advent of the steam engine a source of energy then became available when required and not limited by geographical location. This began the decline of wind energy and by the mid 20th century these windmills had simply become merely examples of architectural conservation and tourist attractions.

The cheapness and convenience of fossil fuels meant that wind energy was not taken seriously as a viable source of energy, apart from the 'American' multiblade water pumping windmills and a number of periodic experiments into wind generated electricity in several countries.

However, a renaissance of interest in wind energy began

in the late 1960s and early 1970s as environmental awareness started to grow, especially with regard to air, water and thermal pollution, the abuse of natural resources, the increasing problems of waste disposal, and concern about the risks of nuclear power.

2.2 FOSSIL FUELS

The fossil fuels, ie, coal, oil and gas, which were originally derived from the sun, are effectively finite reserves: the greater the rate at which they are used the shorter their lifetime.

In addition to providing fuel, fossil fuels are an important source of feed-stock for the chemical industry, especially for plastics. Therefore it would seem sensible that, if possible, these fossil resources should preferably be used as a source of materials rather than being burned.

There are other problems associated with the burning of fossil fuels. The transportation of oil at sea can contribute to serious marine pollution if a tanker leaks its cargo. Whole eco-systems may be damaged, taking perhaps several years to recover, if at all.

The combustion of fossil fuels also causes major atmospheric pollution problems which gave rise to

concern in the past and continues to do so. These problems include acid rain, carbon dioxide build up and waste heat.

2.2.1 Acid Rain

There is growing concern that sulphur dioxide emissions from fossil fuel powered stations may have a damaging effect on wildlife, most noticeably in lakes and on forests.

Such emissions also cause structural damage to a substantial part of the building stock.

2.2.2 Carbon Dioxide and Waste Heat

The combustion of fossil fuel also generates carbon dioxide (CO2). In itself this might appear innocuous but carbon dioxide has increased as a proportion of the Earth's atmosphere as a result, and there is some concern that this could affect the Earth's surface temperature.

The theory is that carbon dioxide in the atmosphere creates a phenomenon known as the 'greenhouse effect'. In other words, like glass in a greenhouse, carbon dioxide is transparent to incoming short wave solar radiation but tends to absorb and re-radiate to earth the infra-red waves which would otherwise be emittted

from the surface of the earth. And as a result, the surface temperature of the earth should tend to rise as the proportion of CO2 in the atmosphere increases.

Although there is some dispute as to whether this effect will be counteracted by other effects (such as reduced incoming solar radiation caused by particulate matter in the atmosphere, also caused by burning fossil fuels) there is concern that if the temperature of the Earth's surface does rise, it could adversely affect ecological and agricultural systems.

More directly, waste heat is pumped into the atmosphere by both fossil and nuclear power stations. This also contributes to raising the temperature of the atmosphere and could eventually cause adverse climatic change. (Chapman, 1975).

2.3 NUCLEAR POWER

Whilst nuclear power does not produce acid rain or carbon dioxide, there is growing public and scientific concern about the safety of nuclear power stations in operation and about the various types of radioactive waste produced.

Nuclear power stations may appear, under laboratory conditions, to be an attractive means of energy

conversion; but in practice there are numerous disquieting aspects. These include the potential release of large quantities of highly poisonous radioactive materials into the atmosphere, into watercourses and the sea, and the whole problem of handling, transportation, storing and dumping of the highly toxic fuel and other wastes.

2.4 ALTERNATIVE ENERGY TECHNOLOGIES

Concern about the above problems during the 1960s and 1970s spawned both the environmental activists, who adopted a 'fire fighting' role, attempting to stop wastes, pollution and nuclear power, and the alternative technologists, who attempted to take a more positive approach by endeavouring to develop technologies that would have minimal impact on the environment and be of little hazard to human beings.

Alternative technologists have concerned themselves with a wide variety of human activity including material resources, food, shelter, transport, health, working and living conditions, but their main activity has been in energy conservation and what have become known as 'alternative energy technologies'. These include a variety of energy conversion technologies, most of which utilise a number of forms of energy derived from solar energy. They include:

a) Direct Solar Energy Technologies - that employ the radiation of the sun directly. These include solar thermal energy conversion systems for space, water or process heating; and solar photo-voltaic cells for electricity generation.

b) Indirect Solar Energy Technologies - that utilise energy derived from the indirect effects of solar radiation, such as wind, rainfall, waves and photosynthesis. This category also includes biological sources of energy collectively known as 'biomass'; the energy of falling water (eg, hydroelectricity); wave energy; and wind energy for mechanical applications, electricity generation, water pumping and heat generation.

The term 'alternative energy technology' also includes the following non-solar energy technologies:

c) Geothermal Energy, used for water, space or process heat and for electricity generation.

d) Tidal Energy, now used mainly for electricity generation and, in the past, for corn milling.

Apart from (c), these forms of energy are also known as 'renewable' or 'income' forms of energy (compared to fossil and nuclear fuels, which are 'capital' forms of energy). They are usually considered to be benign in

terms of their environmental effects, but whether or not this is so depends to a large extent on the physical scale of a particular installation, and the degree of care with which it is designed, constructed and operated. These factors are influenced by those who control the installation and by goverment policies.

2.5 WIND POWER

Under the right climatic conditions and with careful design, the use of direct solar energy is a very effective way of obtaining heat energy, but it is not yet a very economic means of obtaining mechanical or electrical energy except in very small quantities. This position may change when photovoltaic solar cells become significantly cheaper.

The wind, on the other hand, is ideally suited as a source of mechanical and hence, via an electrical generator, as a source of electrical energy. In addition, in terms of the area of capture surface required to generate a given amount of energy, wind has a higher annual energy flux density than solar energy in many locations.

To become economically successful, however, the devices for extracting wind energy, known as wind turbines, need to become cheaper, less complex and more reliable than currently available devices.

One method which could make a contribution in this area forms the basis of the work described in this Thesis: the design and testing of a novel wind turbine blade.

2.6 AIMS

The main aim of the work described here is the design, development and testing of a Horizontal Axis Wind Turbine (HAWT) which employs a novel blade design conceived by the author. This blade concept is known as the SAILFOIL, on which the Open University has taken out a patent (Taylor 1981).

At the present time most small to medium scale wind turbines (ie, those with rated powers of < 200 kW) are produced in low volume, frequently by small engineering companies.

It is generally within the capability of these companies to fabricate many of the elements utilised in wind turbines, by employing traditional metalwork and machining techniques and/or assembling the turbine from mass produced components such as bearings, gear boxes and generators etc.

However, these companies, especially in Third World Countries, are rarely able to cope with the more exotic, capital-intensive, highly skilled and quality sensitive

processes required for the manufacture of reliable blades for horizontal axis wind turbines. These are highly stressed components, subject to severe fatigue loading. The sophistication of the technology required to manufacture wind turbine blades is far greater than that required for making glass reinforced plastic (GRP) boats.

For maximum performance and reliable self-starting capability, the blades of HAWTs are required to have built in twist and taper, which further complicates the fabrication process.

Current blade designs for HAWTs utilise wood, glass fibre reinforced plastics (GRP), and fabricated steel (riveted or welded).

Solid wood blades require careful selection, detailed knowledge of the material, and skill with and access to complex machining equipment, the cost of which may not be justified for low volume production. They also require elaborate and careful treatment for weather proofing against rot, and can be subject to warping.

Epoxy laminated wood results in a more satisfactory blade but the process is highly skilled and is an expensive technique for small scale wind turbine blades, due to the amount of skilled labour involved and because of the small physical size it is difficult to lay up

with available veneers. This generally precludes its use on wind turbine blades under about 5 metres. This technique also requires careful selection of the material (in veneers) and good quality control.

Similar criteria apply to the manufacture of GRP blades. Manufacturing highly stressed GRP blades is not as straight forward as the manufacture of GRP boats and careful quality control is necessary.

Metal blades require somewhat more familiar skills, though achieving accurate twist and taper is by no means as easy as it may appear. Also corrosion protection is a difficult area as is the use of welds in joints which are subject to fatigue loads.

Taking all these factors into consideration, therefore, there would seem to be scope for a simpler blade design which could help overcome some of the limitations of the above techniques. In particular, it seemed to the author that if the stresses in the blade could be carried mainly by an element which is already mass produced to high quality control standards and which is of standard shape, and if the blade could be assembled around this element, then it could provide scope for a satisfactory blade manufacturing technique for low volume production by small companies. This would depend on devising a simple technique for obtaining the complex surface shape required, using readily available rather

than exotic skills.

Such a technique does exist and there are numerous craftsmen around the world who have the necessary skills and are operating in a similar industry: these are sailmakers. They not only produce sails for boats, but also for wind surfing sailboards, hang gliders and micro-light aircraft.

The use of sail type fabrics in harnessing wind for marine propulsion has been successful for thousands of years. Their use in low speed aviation has also more recently been successful following the introduction of new strong lightweight fabrics

The use of a hybrid concept combining a framework from mass produced elements with fabric surfaces therefore seemed worth exploring. Provided that reasonable performance could be achieved, then perhaps it could form the basis for the development of a novel technique for low volume production of high performance wind turbine blades.

That is the main aim of the work described in this thesis.

REFERENCES FOR CHAPTER 2

Chapman, P (1975): Fuel's Paradise, Penguin

Taylor, DA (1981): Rigid Trailing Edge Sailwing (Sailfoil), Patent Office, London

Wailes, R (1948): The English Windmill, Arcnitectural Press

CHAPTER 3

WIND ENERGY

3.1 HISTORY

Wind energy is believed to have been first exploited in ancient times through the use of sailing boats.

The first windmills, which were used for grinding grain or pumping water, evolved from sailing boats either in China or Persia sometime around 2000 BC (see Figure 3.1 and 5.2) and bore a strong resemblance to sailing boats, though rotating about a vertical axis.

These early windmills were 'drag' type wind machines. Wind pressure pushing against a high drag (or highly resistant to air flow) surface causes a difference in pressure either side of the surface and if the surface or sail is free to rotate, then the high wind pressure pushes the sail around. If a number of sails are set radially in a manner similar to a wide paddle wheel with its shaft vertical, then each sail will contribute work to spin the wheel.

However there is one fundamental difficulty with this simple arrangement. This is to do with the fact that as the paddle wheel is spinning on a vertical shaft and the wind is blowing from one side and if we view the paddle wheel from the upwind side, it will be observed that the paddle wheel on one side of the shaft is able to move with the wind, but on the other side of the shaft it

wants to move against the wind. So, as the wind presssure is the same on both sides of the shaft, the paddle wheel will not rotate unless something is done to reduce the wind pressure on the side that is tending to rotate against the wind.

A wide variety of vertical axis windmills therfore evolved which used a number of measures to overcome this limitation and are frequently 're-invented' today. They fall into the following categories.

(i) 'Screen' type vertical axis windmills: these include the Persian Sistan windmills and the 'merry-go-round' windmills developed in the 19th century in Nebraska, (Fig 3.1)

(ii) 'Clapper' or 'flapping type' vertical axis windmills: In these devices the sails are supported on pivots and 'clap' up against radial support arms on the driving half of their cycle. On the other part of their cycle, when they are moving towards the wind, they trail behind their pivot so that they present minimal sail area to the wind (Fig 3.3).

(iii) Vertical axis windmills with epicyclically pivoting blades: In these devices each sail is constantly changing its angle in relation to its radial support arm in such a way that it is able to extract torque for a large part of its cycle. This

is a complex concept (Fig 3.4), which requires sensing of wind direction.

(iv) Differential drag type vertical axis windmills: These windmills utilise concave sails or blades so that the drag presented to the wind on the driving part of the cycle is greater than on the non driving part of the cycle. The cup anemometer and the Savonius rotor are examples of this type of device (Fig 3.5 and 3.6).

However, the main impetus to the technological development of windmills came with the horizontal axis type of windmill known as traditional North European windmills.

These are what most people think of when windmills are mentioned. They took two basic forms, the post mill and the tower mill (see Figs 3.7 and 3.8).

The earliest recorded English windmill dates from 1191 (Golding, 1955) and was a post mill. Tower mills, introduced around the 14th Century, were generally more popular and successful than post mills as they provided enclosure for the machinery and raised the windmill rotor into a higher wind speed zone.

Traditional European windmills, together with watermills, provided the main motive power for industry

in the 17th century, before the age of steam. Windmills were used for sawing wood, paintmaking, papermaking and the preparation of spices as well as for grinding grain and raising water. These windmills flourished in 17th Century England, the Netherlands, Denmark and Germany where the numbers peaked at around 10000, 8000, 6000 and 18000 respectively.

The traditional horizontal axis windmills initially utilised canvas 'common' sails laid across a lattice framework. These evolved through various stages which included 'shutter sails', 'spring sails', 'patent sails', and 'Dekkerised sails'(Fig 3.9), until in the Netherlands in the early part of this century the sails took the form of an aeroplane wing with an airfoil cross section.

The first experiments using windmills for generating electricity took place in Denmark towards the end of the 19th century and were carried out by Professor Poul La Cour with a 22.8 m diameter rotor which generated electricity for a school in Askov (Fig 3.10).

The Lykkegard wind generator, which evolved out of La Cour's experimental windmill, was manufactured in large numbers in the early part of this century. These horizontal axis windmills used traditional shutter type sails supported on a lattice tower (Fig 3.11).

Wind generator developments have continued in Denmark during this century. These developments include machines manufactured by F L Schmidt during the second world war, which were followed by a 200 kW three bladed Horizontal Axis Wind Turbines (HAWT) designed by J Juul and erected at Gedser in 1957 (Fig 3.12). This machine was very successful and is still in existence (Lundsager,1978).

In addition to the developments in Denmark, wind generator projects took place in the USA, France, Germany and the UK. Most of these projects were medium or large scale turbines (see Figs 3.13 to 3.15) but they met with little success (Putnam, 1948 and Golding, 1955)

During this period there were also a number of manufacturers producing small battery charging wind generators (up to about 5 kW) in the 1940s and 1950s, mainly in the USA. One of the best of these was produced by the Jacobs company based in Minnesota.

This took the now classical wind-charger form of a 3 bladed, horizontal axis, propeller-type rotor with centrifugally controlled variable pitch wooden blades. This rotor was directly coupled to a dc generator. It was kept pointed into the wind by a rudder-like tail vane and was supported by a free standing steel lattice tower (Fig 3.16).

With the spread of electricity grids in the 50s, these wind chargers almost disappeared because they were unable to compete with the Utilities' low priced electricity based on cheap fossil fuels, or to supply enough electricity for the innumerable appliances being promoted by these utilities.

However, concern about the environmental effects of fossil fuel and nuclear based sources of energy in the late 1960s and early 70s led to a revival of interest in such 'alternative energy technologies'.

After 1973, as a result of the oil crisis, the development of alternative energy technologies was given a further boost in the oil dependent 'developed' Western nations, and principally in the USA where federal resources were invested by the Carter administration (1975-79). Initially, research and development was directed towards direct solar technologies, predominantly for water and space heating, but there was also a growing interest in wind energy, not only in the USA but also in Denmark, the Netherlands, Canada, Sweden and West Germany.

In these countries there were (and are) research and development programmes focussing on large scale wind generators in the megawatt range (Figs 3.17 - 3.19). This involvement in very large wind turbines has been relatively unsuccessful so far, and indeed may have

impeded the development of wind energy for a number of reasons:

(i) Large scale wind generators are much more expensive to design, analyse and build than small or medium-scale machines. Because of this they have tended to consume practically all the available funds (which are not large) for wind energy R & D. Consequently, small and medium-scale wind turbine developments have been starved of funds.

(ii) Because of the substantial time taken to design, construct and test a large wind turbine, it takes a long time, for technological improvements to be recognised and incorporated. Moreover, partly because of the variability of government decisions that affect the financing of wind energy, if a large machine is built and is not completely successful, funding has tended to be withdrawn.

By contrast, small and medium scale wind turbines have a relatively fast 'learning curve' and are cheaper to develop. But they have not received major government support, at least in the UK (although this may now be changing).

(iii)Even if large scale wind turbines eventually prove successful, they are too expensive to be purchased by private organisations and have to be

bought by government organisations or utilities such as the Central Electricity Generating Board (CEGB), or the North of Scotland Hydro-Electric Board (NSHEB). So far at least this has not happened, apart from orders for experimental one-off machines, largely because there appears to be a political preference for large, nuclear power stations or for coal and oil fired stations.

However, in spite of the limited direct Goverment support for small and medium scale wind turbines, private companies are beginning to make headway with the development of these systems in the USA and Denmark. Their success has been at least partially due to tax credits, which, in California for example, are available from both the State and Federal Governments. Nuclear power stations have, in California, proved to be a financial burden to the utilities, whereas wind conditions are excellent and so this has led to the establishment of quite large numbers (>8000) of small or medium scale wind turbines, mainly installed in clusters known as 'wind farms' or 'wind parks' in this region (Fig 3.20). These wind farms operate much like conventional power stations by selling the electricity produced to the utilities who then distribute it to their customers.

The Californian wind farms have shown that small to medium scale wind turbines can operate satisfactorily

and produce electricity to the standards required for mains distribution. Elsewhere (apart from Denmark where wind turbines are being used widely in agriculture) the use of wind energy is so far limited to a few off shore islands and remote locations such as the Orkney and Shetland islands in the UK.

3.2 GLOBAL POTENTIAL WIND RESOURCE

Due to the more direct angle at which the sun is able to strike the equatorial regions of the Earth, they are warmed to a higher temperature than the polar regions. The lighter, warm air from the equator rises and flows towards the poles while the cooler, heavier air moves from the poles to replace it, see Figure 3.21 (Eldridge, 1975). However, these winds do not blow in a northerly or southerly direction as the earth is rotating. The Earth's spin from west to east bends the northern hemisphere's winds to the right of the wind direction and southern hemisphere's winds are bent to the left of the wind direction, Figure 3.22. Surface winds in the equatorial and polar regions are mainly easterly and those of the middle latitudes are usually westerly.

A further effect on these planetary winds is the inclination of the earth's axis to the sun, so that for half the year the northern hemisphere is tilted towards sun and then the southern hemisphere has its turn. This causes seasonal changes in the direction and strength of

the winds due to the variation in heat received from the sun at different times of the year.

During daylight hours the air above large bodies of water, such as lakes, seas or oceans, remains relatively cool because the sun's energy is absorbed by the water due to its large thermal mass, or consumed in evaporation. The air over land, in contrast, is heated more during the day because the land absorbs less solar energy and less moisture is evaporated. The warmed air over land expands, becomes lighter and rises, whilst the cooler, heavier air over the body of water flows landward to replace it, thus creating local coastal breezes (Fig 3.23). During the night the water cools more slowly than the land. Because of this, the coastal breezes reverse direction (Fig 3.24).

Local breezes of a similar nature occur between mountains and valleys. During the day the heated air rises along the valley sides, warmed by the sun's rays and during the night the cool, heavy air on the valley sides moves down into the valleys (Figs 3.25 & 3.26).

The content of the energy of these winds over the earth is estimated on the basis of thermodynamic considerations to be sufficient to maintain a total power capacity of 10^{11} gigawatts (Eldridge, 1978).

Fig 3.27 shows the World Meteorological Organisation

wind energy map which shows the predicted annual energy available from the wind around the earth on a regional basis, (WMO 1981).

3.3 UK POTENTIAL WIND RESOURCE

The UK is one of the countries best suited to making use of wind energy because it has such a long coastline and is located so that it receives substantial unimpeded winds from the bodies of sea surrounding it. Figure 3.28 shows the geographical wind energy distribution over the UK (Caton, 1976).

The size of the UK wind energy resource which is technically exploitable for electricity generation by land based or off shore wind turbines is very substantial, amounting to perhaps hundreds of terawatt hours per year (one terawatt hour = 10^{12}Wh) (ETSU, 1982).

A number of estimates have been made of the UK potential wind energy resource based primarily on the output from large scale multi-megawatt wind turbine. One such estimate,(BWEA, 1982) shows that 10,000 land-based machines of 91 m diameter on low wind speed sites would each produce 10 GWh pa, and would therefore produce a total of 100TWh of electricity per year. This represents 40% of UK demand in 1982.

A study carried out by the CEGB, (Rockingham, 1981), identified eight major off shore areas around the coast of the UK that might be suitable for clusters of wind generators, and a further 29 smaller dispersed sites each of less than 150 square kilometres. These sites are shown in Fig 3.29 and their installed capacity was estimated to be 165 GW representing an annual energy of about 240 TWh.

However, widespread implementation of off shore wind energy is unlikely to take place until the large scale wind turbines have been operating successfully on land. There will also have to be the political will to proceed, since the financing of such major projects would almost certainly require government involvement, or at least government incentives.

As regards the contribution to the UK energy needs that could be made by small scale wind turbines (<100 kW), ETSU, (1982) estimated that the energy resource that could be converted by small scale wind turbines was 26 TWh/year: 10TWh in the domestic sector; 4 TWh/year in agriculture; 0.2 TWh/year in industry; and 12 TWh/year in commercial and institutional buildings. 26 TWh represents a 10th of current electricity demand. However, no account was taken, in these calculations of the possible energy contribution that could be made by wind farms consisting of clusters of small or medium

scale wind turbines. A Department of Energy study to investigate the potential of wind energy in agriculture is currently underway and should provide a more detailed picture.

There are a number of factors which will affect the implementation of small scale wind turbines in the UK.

(i) System Cost

Small/medium scale wind turbines have to be competitive with conventional electricity sources. This means that turbine designs have to be simple and not rely on expensive, elaborate designs which require aerospace companies to manufacture them, but instead can be manufactured by small engineering companies.

(ii) Positive Climate

Wind turbines are much more likely to be implemented if there is a positive political climate towards them which encourages rather than impedes their use.

(iii) Equitable Treatment

If all the different sources of energy are treated equally then there is a stronger likelyhood that wind turbines would be installed.

For instance, the valuation placed on private generators (such as wind turbines) in local rating

assessments is substantially higher than that levied on the generating boards. Thus the cost of electricity production for private consumption may be doubled by rates charges alone, (BWEA 1984).

Mains electricity charges currently levied by the electricity boards appear excessive, and the Energy Act may have increased these difficulties, despite the Government intention to use the act to facilitate small wind power development (BWEA 1984). Electricity Boards pay low rates (and have very complex tariffs) for buying power, and charge very high rates for selling standby power to independent producers.

(iv) Early Market Incentives

If the UK had financial incentive programmes, as in many overseas contries, by way of capital grants, tax allowances and government purchase of early machines, this would allow British technology the opportunity to offer established machines in the home and world market.

3.4 OVERSEAS POTENTIAL MARKET

A number of studies have been carried out which examined the overseas potential market for small to medium scale (< 100 kW) wind turbines.

3.4.1 Department of Industry Study

A study commissioned by the UK Department of Industry, (Calnan, 1980), which investigated the potential for wind turbines < 50 kW, found that there is a world demand for new wind driven water pumps which could amount to 400,000 machines worth \1200 million (1979 pounds), see table 3.1, and an on-going replacement market of 2300 machines per year worth \69 million per year.

The potential for wind turbines for electricity generation for agriculture and residential purposes is even greater. The study found that there is a World potential market for over 650000 machines, see table 3.2, in the 2.5 to 15 kW range worth \3100 million (in 1979) pounds.

This study did not take into account the additional potential demand for turbines for use in US wind farms.

3.4.2 Rocky Flats Study

The potential market for small to medium scale wind turbines in the USA was investigated in a study by JBF Scientific Corporation, (Healy, 1981), for the US Department of Energy's Small Wind Turbine Test Centre at Rocky Flats, Colorado.

This study found that there was a potential market in the USA for 17 400 000 machines. This study also did not take wind farms into account.

3.4.3 Overseas Development Administration Study

A study of the world market for medium sized wind turbines, (50-200 kW) was carried out for the Overseas Development Administration by the Crown Agents, (Leicester, 1981).

This study estimated that there are at least 85 countries which could possibly be markets for wind energy systems.

On the assumption that wind energy systems would compete with diesel generation on a fuel saving basis, the report indicates that wind energy systems will have a good chance of being economic at sites with annual mean wind speeds over 6 m/s or in very remote areas.

It estimated that the world market for medium scale wind turbines would be of the order of only 100 machines per year, but this study also failed to include the USA where the number of machines installed this year will be 8,000, mainly on wind farms.

3.5 Conclusion

The wind is attractive as a source of energy on environmental and fuel conservation grounds and is widely distributed around the planet.

However, most current designs of wind turbines use exotic materials or complex manufacturing techniques for their blades and are consequently expensive to manufacture.

Apart from the blades themselves, the techniques involved in assembling wind turbine systems are quite well suited to the manufacturing capabilities of small companies, since many mass-produced, off-the-shelf components can be utilised.

However when it comes to the manufacture of the blades, then few small companies have the necessary skills or manufacturing equipment to design and produce inexpensive, safe, and reliable blades.

This is even more the case when it comes to Third World countries where the large potential for harnessing wind energy can only be realised if it can be exploited reliably and at very low cost. If this could be achieved, then windpower could be an extremely valuable asset, generally improving the quality of life of considerable numbers of the world's population.

REFERENCES FOR CHAPTER 3

Calnan, PG & Moughton, EA (1980) : Export Market Prospects for Small and Medium Wind Turbine Generators, ERA Technology Report No ERA 80-15, February

BWEA (1982) : Wind Energy for the Eighties, Peter Peregrinus

BWEA (1984) : British Wind Energy a Development Strategy, BWEA

Eldridge, FR (1979) : Wind Machines, Energy Research and Development Administration

ETSU (1982) : Strategic Review of Renewable Energy Technologies, ETSU, Department of Energy, November, HMSO

Golding, EW (1955 & 1976) : The Generation of Electricity of Wind Power, Spon

Leicester, RJ (1981) : ODA Study of World Market for Medium Sized Wind Turbine Generators, Crown Agents, July

Lundsager,P (1978): Measurements of Performance and Structural Response of the Danish 200 kW Gedser Windmill, 2nd International Symposium on Wind Energy Systems, Amsterdam, Netherlands

Putnam, P (1948): Power of the Wind, Van Nostrand

Rockingham, AP; Taylor, RH; Walker, JF : (1981) Offshore Wind and Wave Power - A Preliminary Estimate of the Resource, Proceedings of 3rd BWEA Conference, Cranfield, April 1981

Healy, TJ (1981) : Rocky Flats Small Wind Systems Program : An Update, Proceedings of 5th US Biennial Wind Energy Conference & Workshop, DOE, Washington, USA

World Meteorological Organisation (1981) : World Map of Energy Potential, WMO

Table 3.1: Total market for wind pumping plant in selected countries and UK share (Calhan, 1980)

	Total potential (Table 4.3)	Currently in use *(Table X.3)	'Actual' market 1980	Share for UK %	Share for UK No.
Europe					
France	10485		5367	-	-
Greece	8993		4603	14.1	649
Italy	41027		21001	8.3	1743
Malta	643		329	55.1	181
Portugal	1535		786	21.3	167
Spain	9390		4807	13.3	639
	72073	35180	36893		3379
North America					
USA	62637	158000	-	-	-
South America					
Argentina	642	145000	-	-	-
Chile	50697	13000	37697	6.2	2337
	51339	158000	37697		2337
Australasia					
Australia	12336	11000	1336	-	-
Africa					
Libya	196619		191750	16.6	31831
Madagascar	3505		3418	3.1	106
Morocco	746		728	8.2	60
Somalia	13136		12811	27.4	3510
South Africa	26983		26315	-	-
Sudan	55025		53662	50.6	27153
Tunisia	22988		22418	5.6	1255
	319002	7900	311102		63915
Asia					
Jordan	128		128	25.2	32
Lebanon	657		657	18.9	124
Pakistan	1223		1223	21.6	265
Syria	289		289	13.3	38
Various, not known		35320			
	2297	35320	2297		459
TOTAL	519684	405400	389325		70090

*Omitted from this report

Table 3.2: Total market for WIGs for electrical generation in selected countries and UK share (Calhan, 1980)

	Total potential (Table 4.7)	Currently in use *(Table X.2)	Projected market 1980	Share for UK %	Share for UK No.
Scandinavia					
Finland	480		407	19.3	78
Norway	354		300	28.4	85
Sweden	80		68	27.2	18
(Iceland)	40		34	21.2	7
	954	145	809		188
Rest of Europe					
France	1000		987	14.5	143
Greece	779		768	17.1	131
Italy	46000		45380	11.1	5037
Portugal	72000		71029	23.5	16691
Spain	10000		9865	15.7	1548
	129779	1750	128029		23550
North America					
Canada	4000	15	3985	4.7	187
USA	1000	1130	-	-	-
	5000	1145	3985[a]		187
South America					
Argentina	3075	610	2465	-	-
Brazil	19000		19000	6.8	1292
Chile	1125	170	955	6.5	62
Peru	48000		48000	8.8	4224
Uruguay	4000		4000	11.9	476
	75200	780	74420[a]		6054
Australasia					
Australia	-	600	-	-	-
New Zealand	320		320	31.6	101
	320	600	320		101
Africa					
Algeria	236000		235253	9.6	22620
Madagascar	3620		3609	9.6	346
Morocco	24000		23924	19.7	4713
Nigeria	1000		997	46.3	461
South Africa	5000		4984	32.8	1635
Sudan	62000		61804	51.3	31705
Tanzania	1008		1005	66.1	664
Tunisia	100000		99682	13.3	13258
	432628	1370	431258		75402
Island countries[b]					
Canaries	2557		2393	15.7[c]	376
Faeroes	4		4	100.0	4
Falklands	140		140	100.0	140
Malta	589		551	60.9	336
St. Helena	300		300	100.0	300
Others					
Jordan	4200		3931	30.6	1203
Panama	22000		20589	4.5	927
Syria	275		257	15.7	40
Various, not known		1900			
	30065	1900	28165[a]		3326
TOTAL	673946	7690	667056		108808

Notes: a - total of countries treated individually where possible.

b - these countries are not included in their appropriate 'regions' because the information obtained relates specifically to the islands.

c - separate statistics not available, treated as Spain.

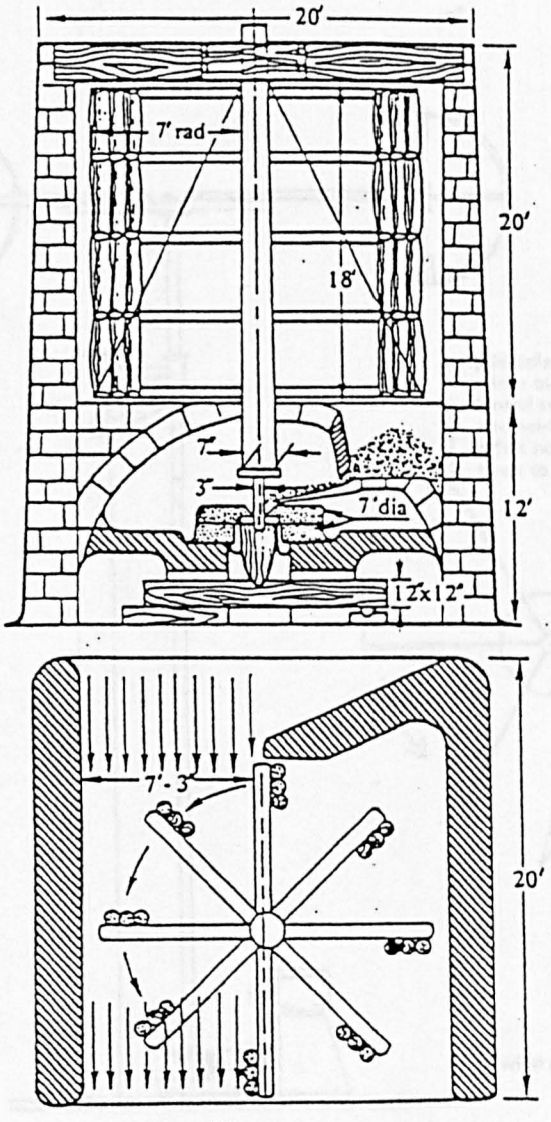

Figure 3.1: Persian sistan screen type vertical axis windmill, 600 a.d.

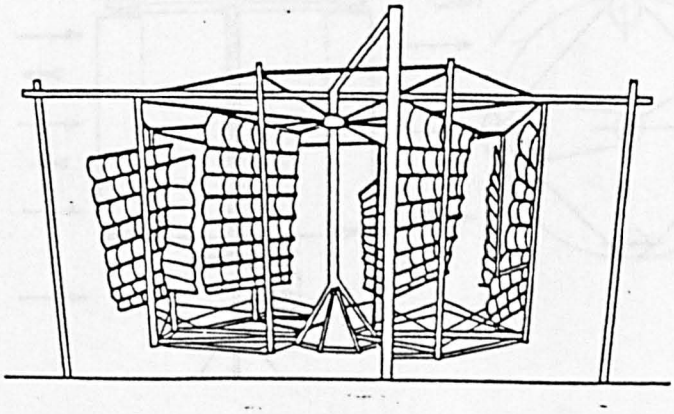

Figure 3.2: Chinese flapping sail type vertical axis windmill

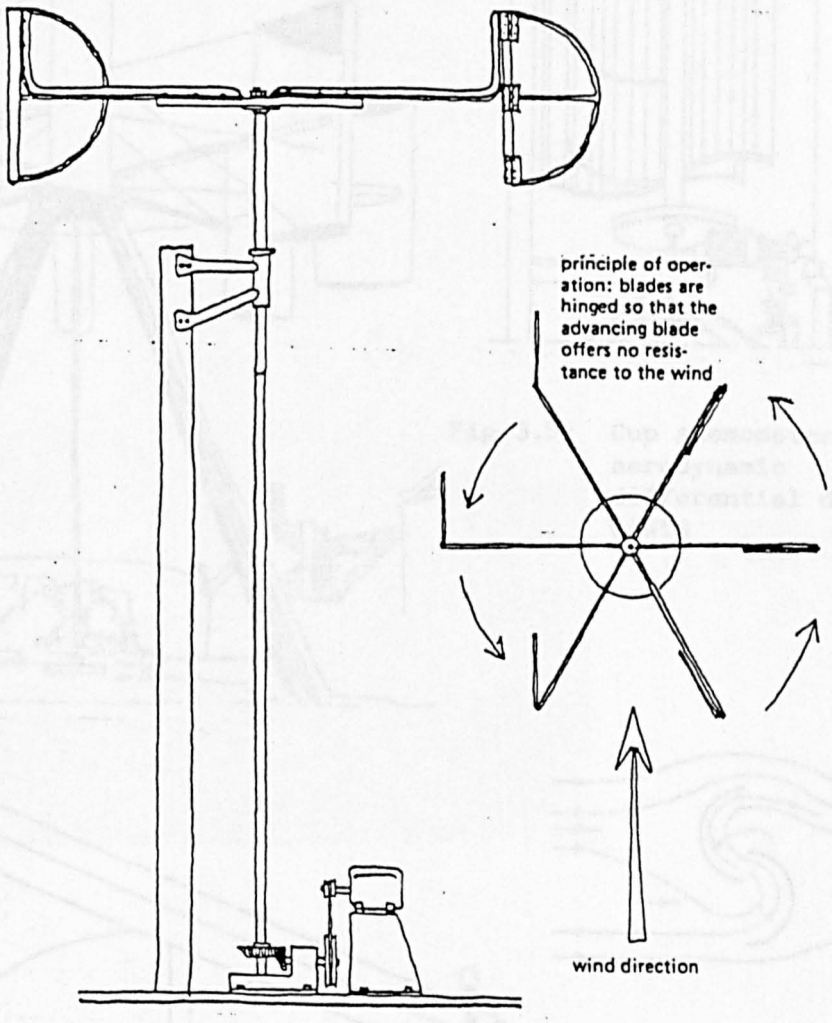

Figure 3.3: French clapper type windmill

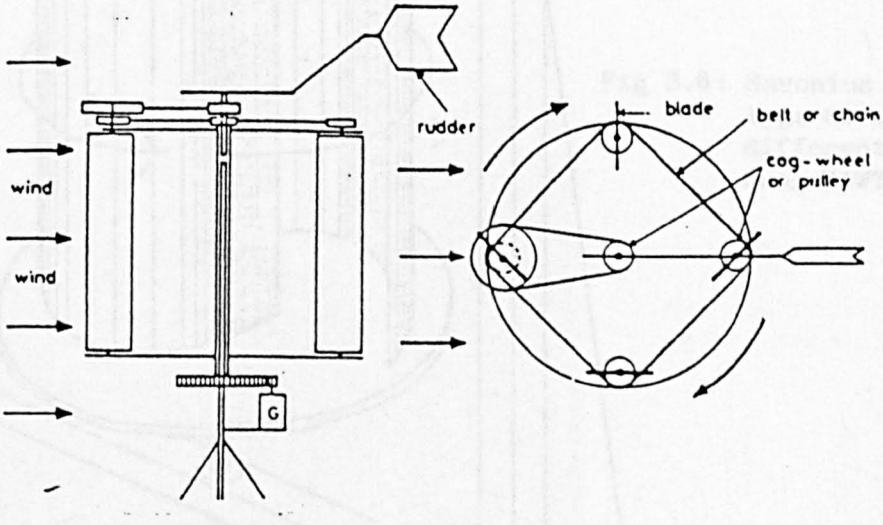

Figure 3.4: Vertical axis windmill with epicyclically pitching blades

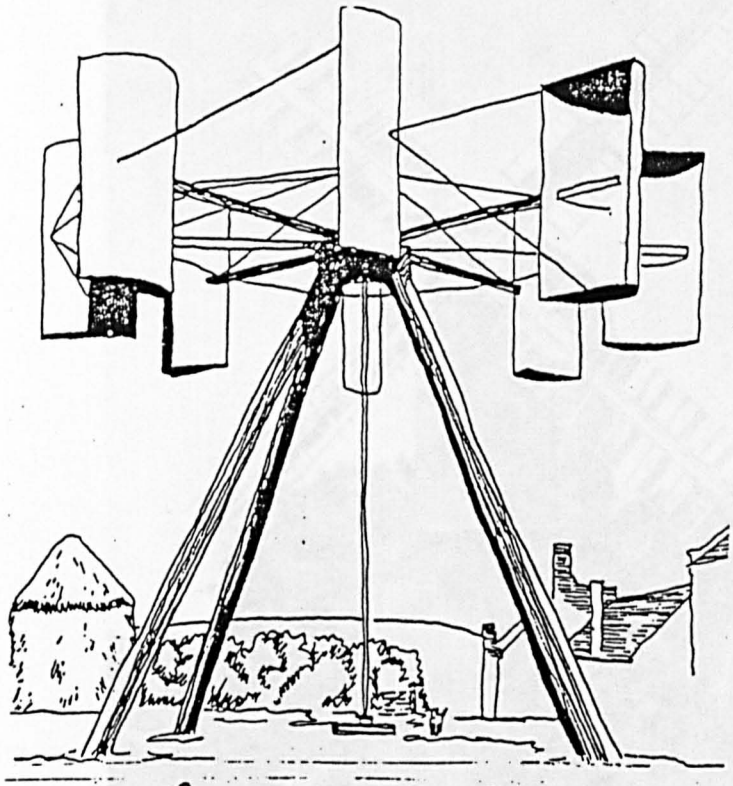

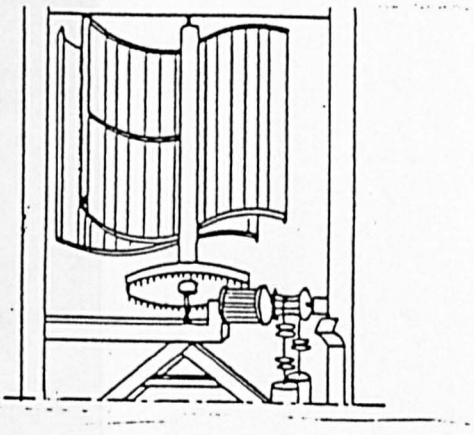

Fig 3.5: Cup anemometer type aerodynamic differential drag VAWTS

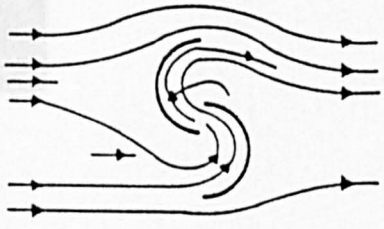

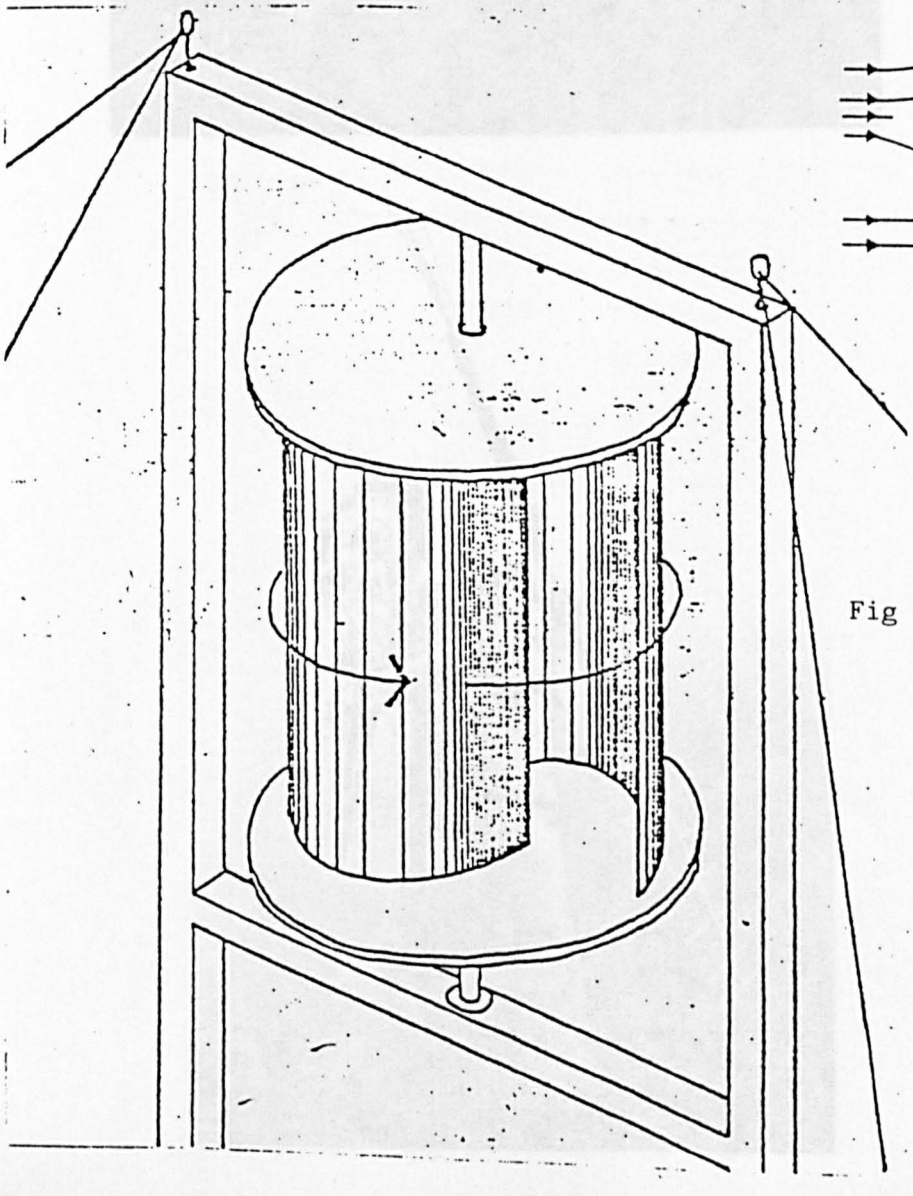

Fig 3.6: Savonius rotor type aerodynamic differential drag VAWT

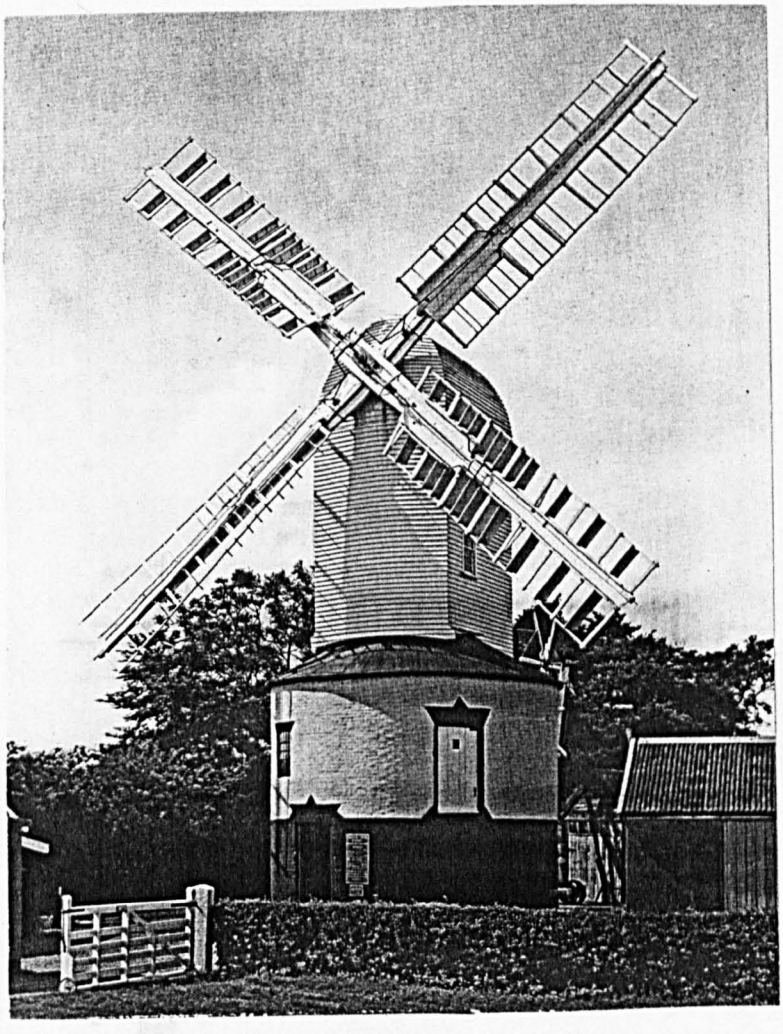

Fig 3.7:
North European
post windmill

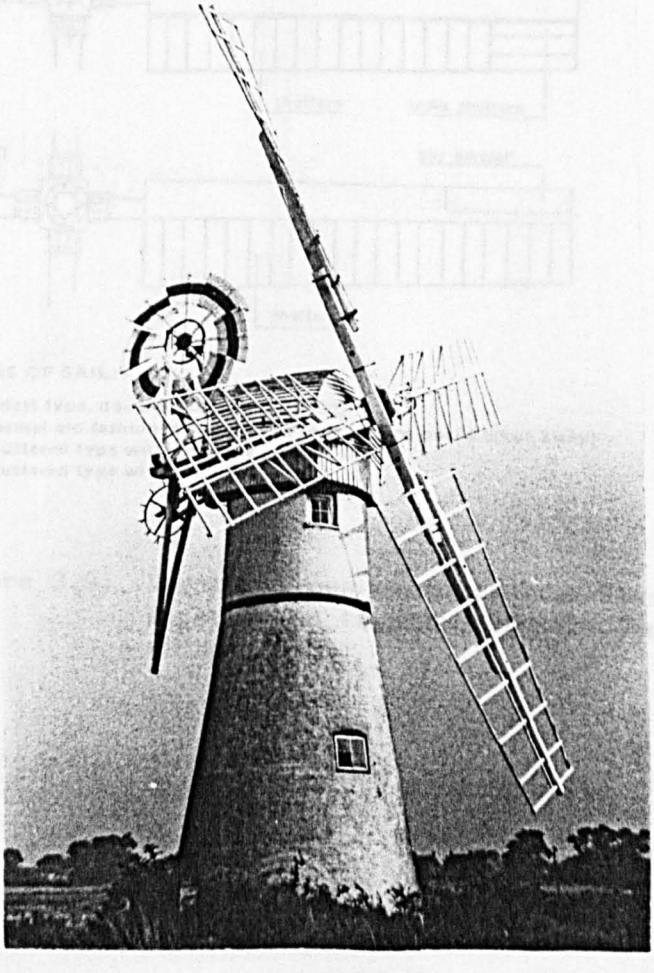

Fig 3.8:
North European
tower windmill

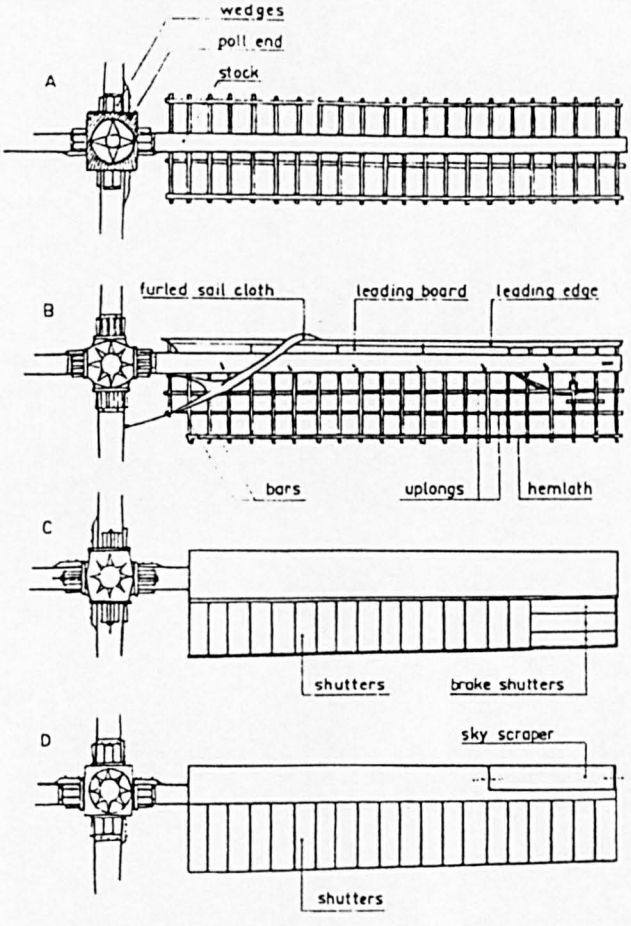

TYPES OF SAIL:

A. oldest type, double-sided (about 1600)
B. normal old-fashioned Dutch type (one leading board taken away)
C. shuttered type with air brake
D. shuttered type with sky scraper.

Figure 3.9: Various types of 'sails' or blades employed on traditional European windmills

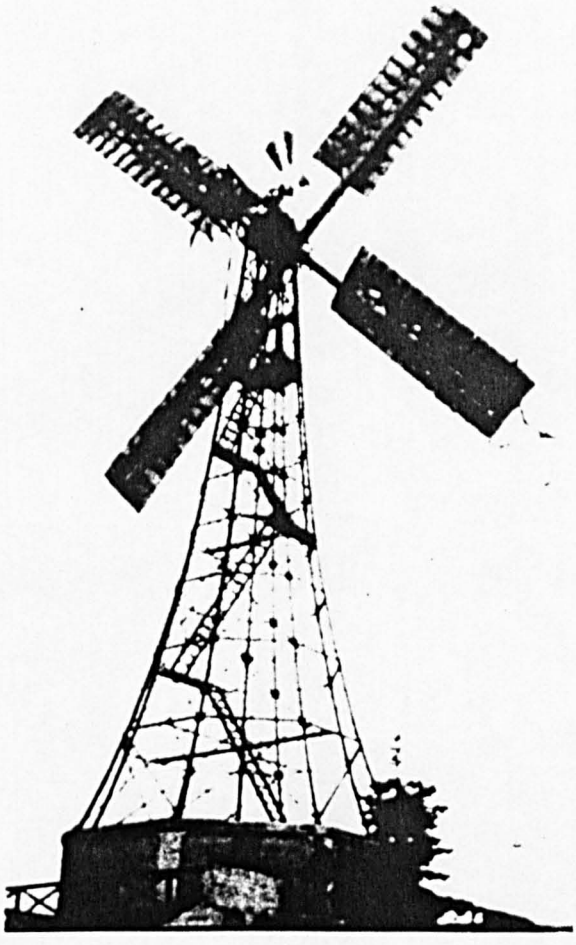

Fig 3.10:
Professor La Car's wind turbine used for electrical generation experiments, ca 1890's

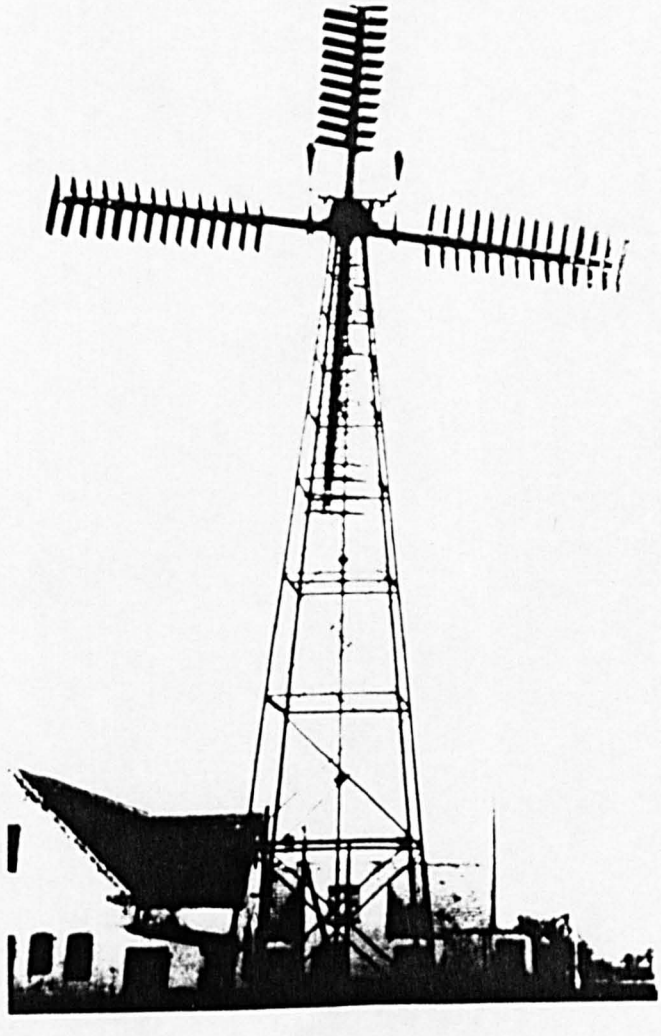

Fig 3.11:
Lykkegard wind generator

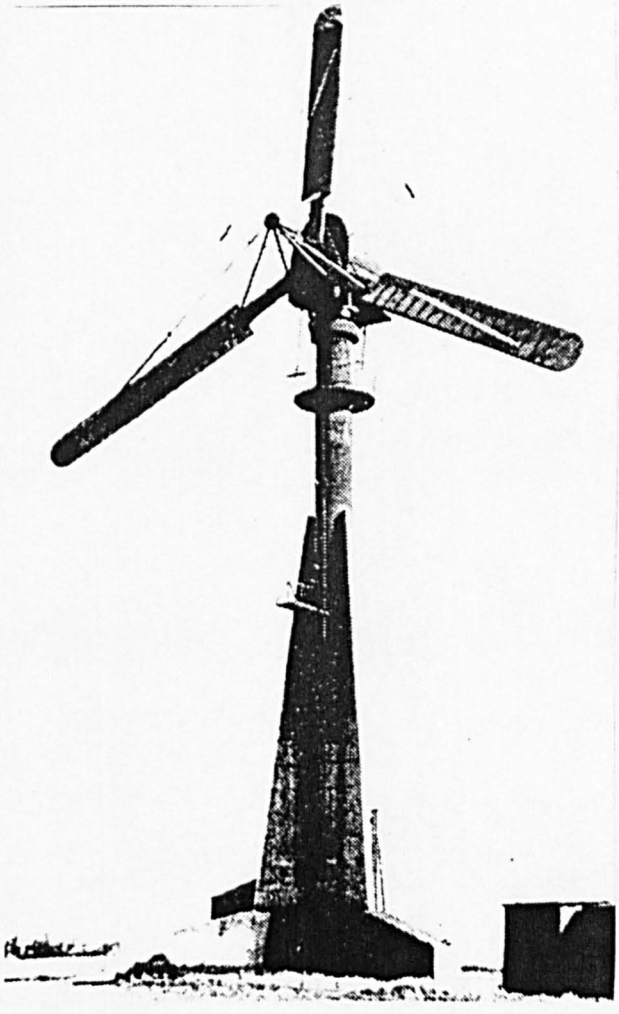

Fig 3.12:
200kW HAWT
generator at
Gedser, ca 1957

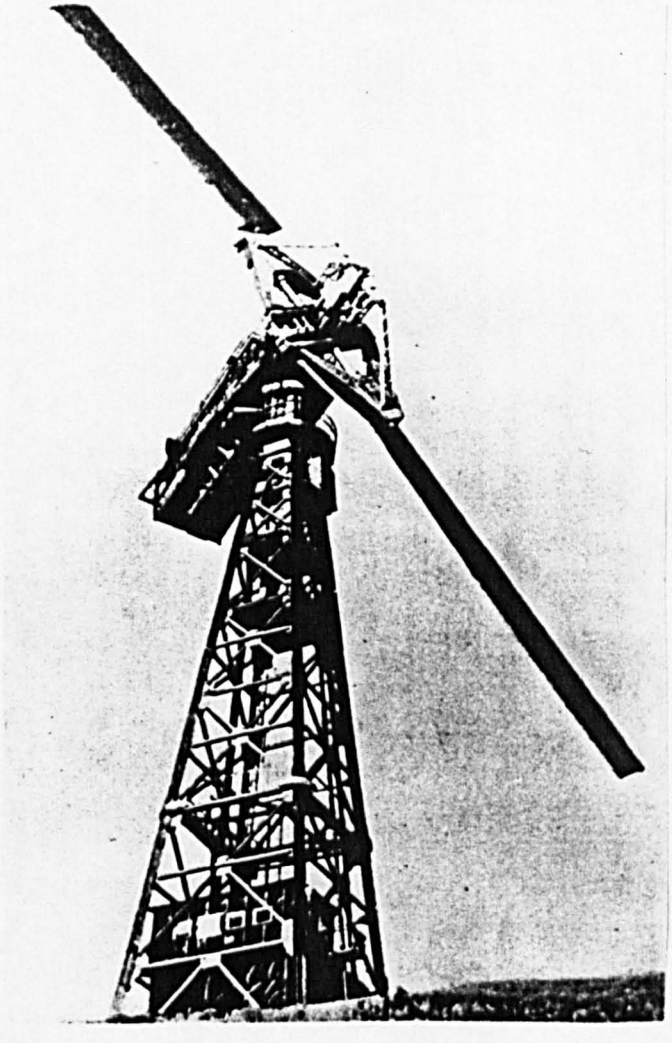

Fig 3.13:
Smith Putnam 1250kW
HAWT generator,
ca 1944

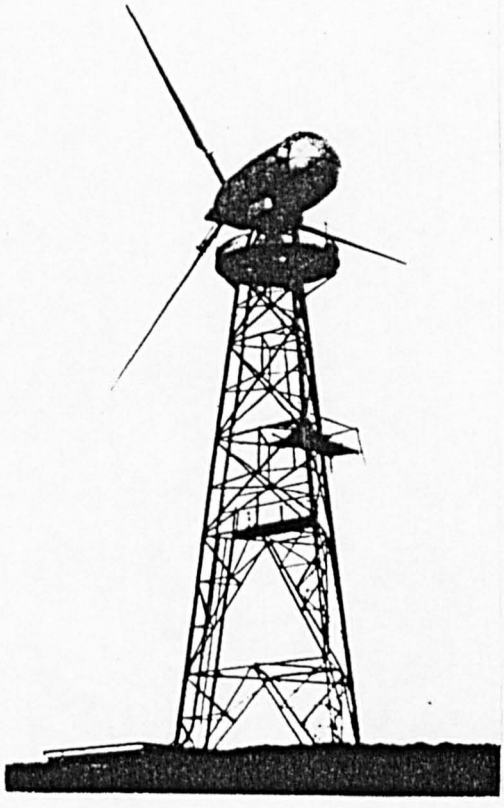

Figure 3.14:
100kW HAWT generator on
Costa Hill, Orkney

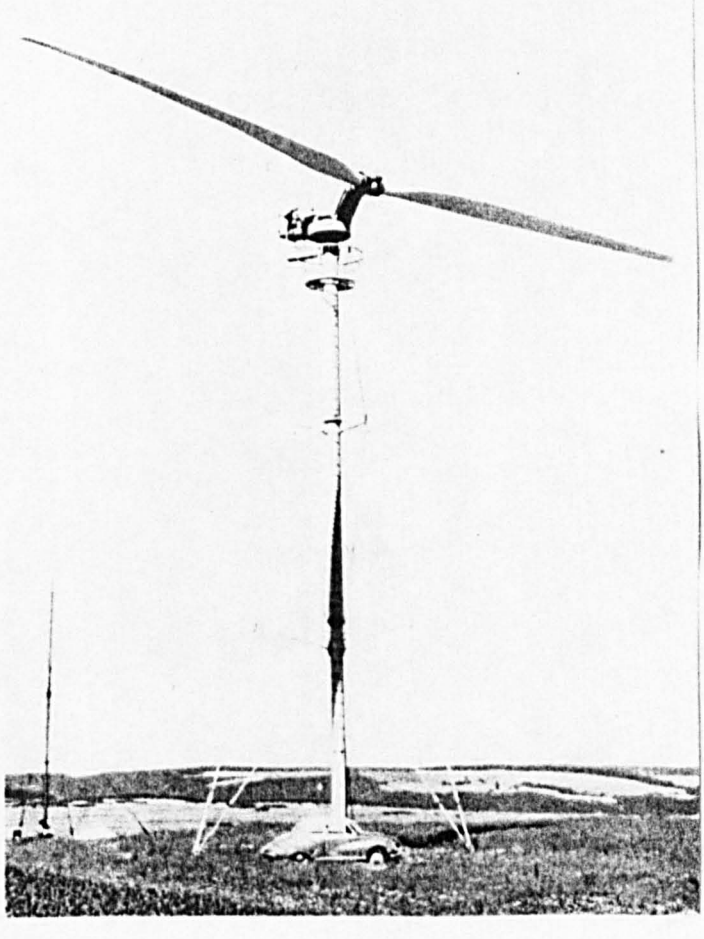

Figure 3.15:
HAWT generator at Stotten,
West Germany, ca 1957

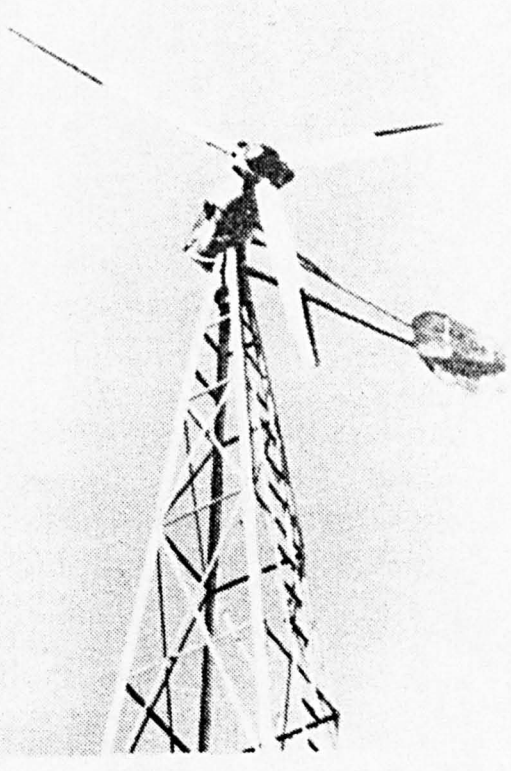

Figure 3.16: Jacobs 3 bladed horizontal axis wind charger, ca 1950s

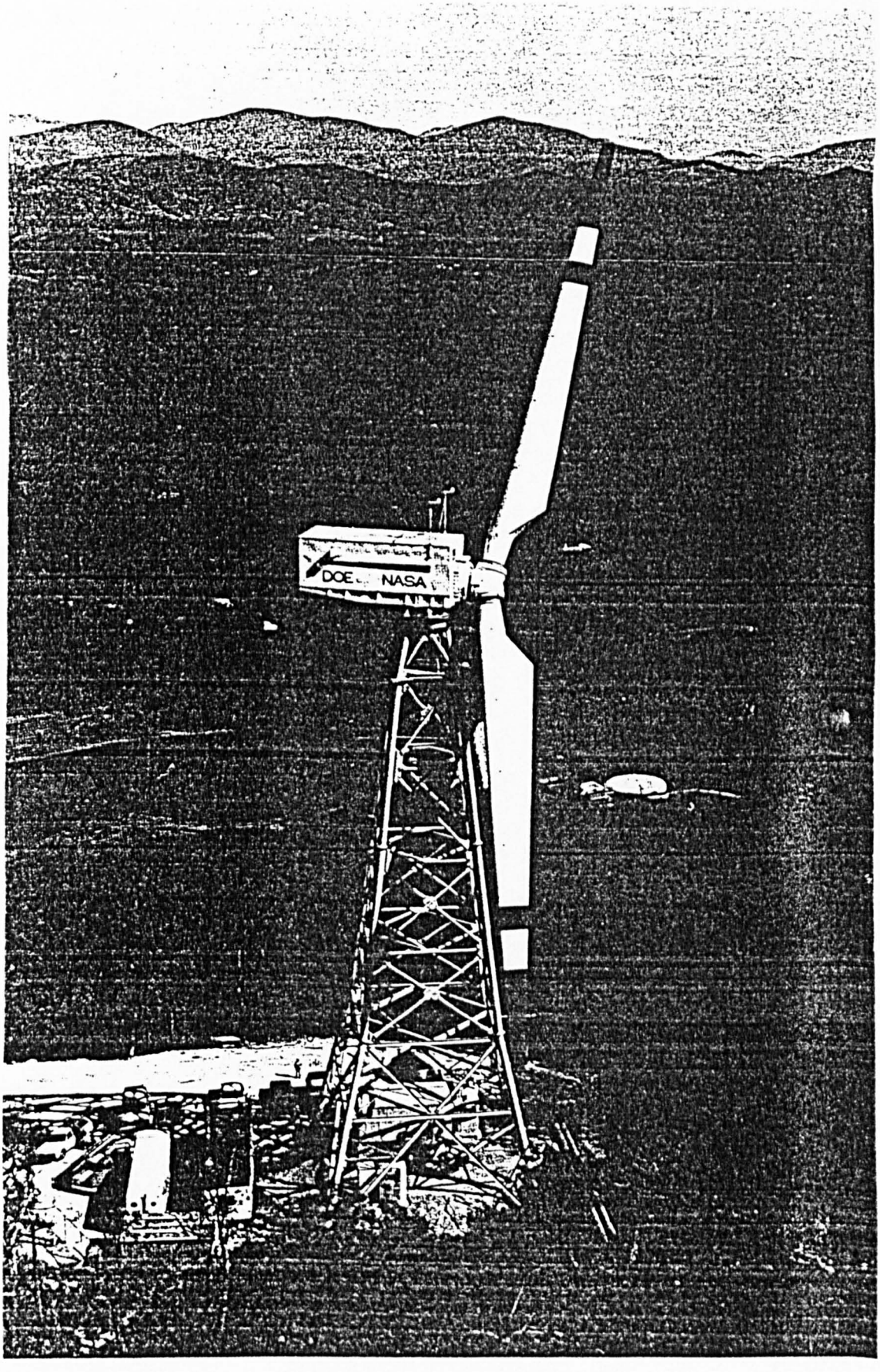

Figure 3.17: Mod 1 HAWT generator - US Dept of Energy

Figure 3.18: Mod 2 2.5kW HAWT generator - US Dept of Energy

Fig 3.19: Two 40 m diameter 630kW HAWT generators at Nibe, Denmark

Figure 3.20: Wind farm in California

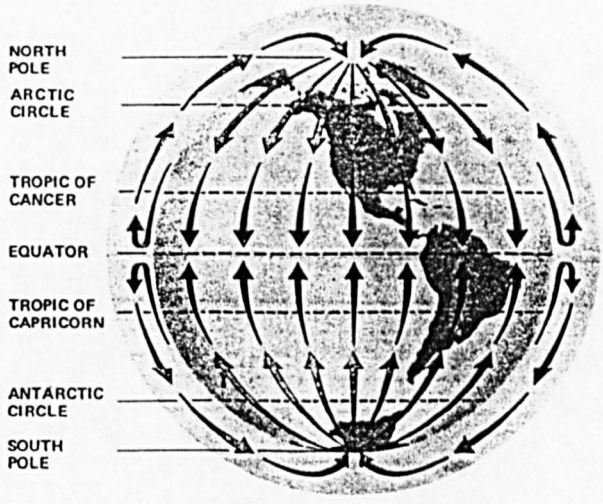

Figure 3.21: Global wind pattern excluding the effect of the Earth's rotation

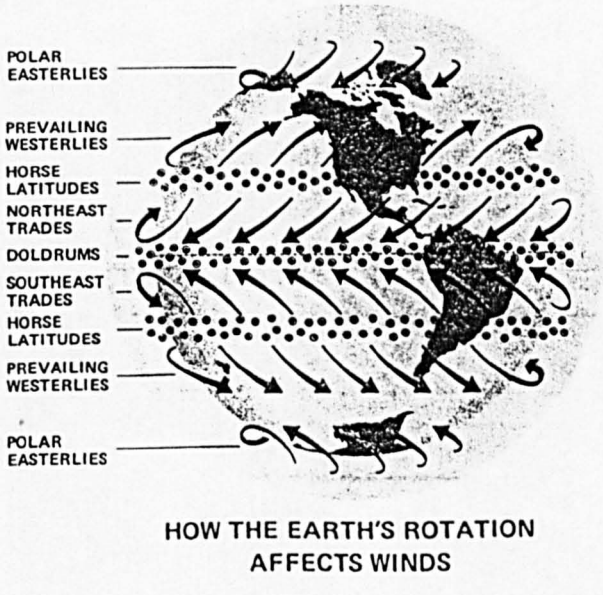

Figure 3.22: Global wind pattern including the effect of the Earth's rotation

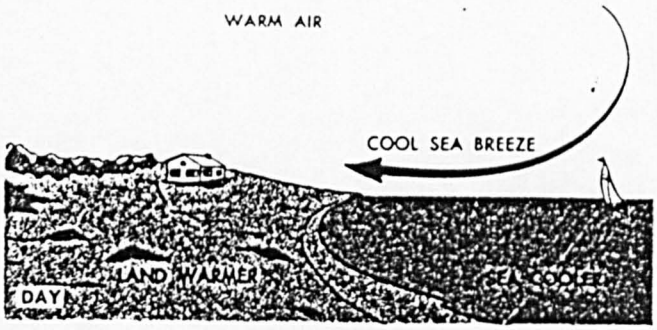

HOW LAND AND SEA BREEZES ARE CAUSED

Figure 3.23: Daytime coastal breezes blow towards the land

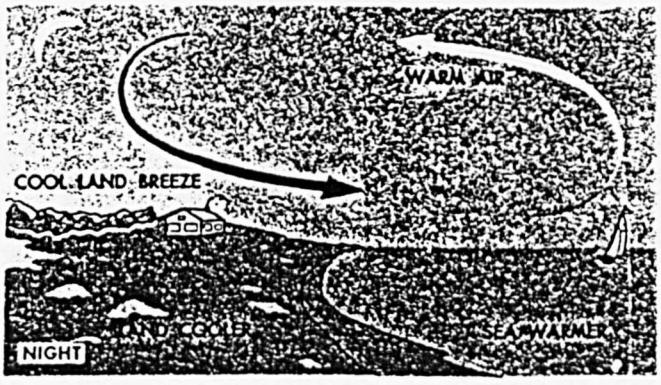

Figure 3.24: Night-time coastal breezes blow towards the sea

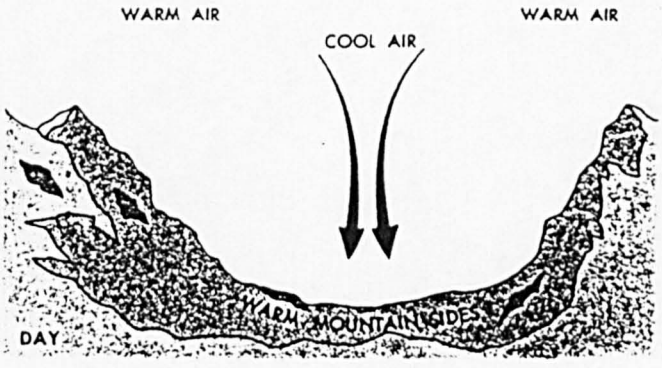

HOW MOUNTAIN AND VALLEY BREEZES OCCUR

Figure 3.25: Daytime mountain/valley winds

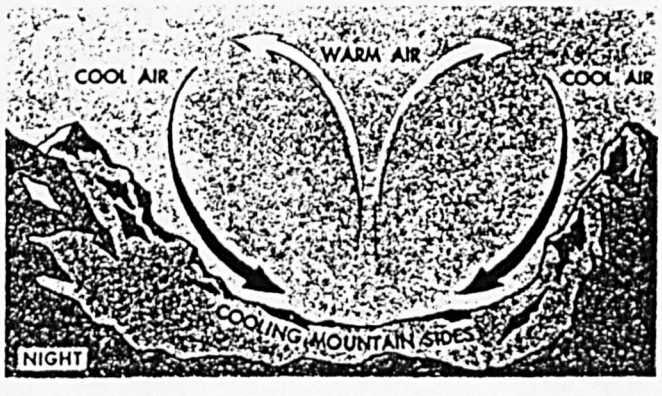

Figure 3.26: Night-time mountain/valley winds

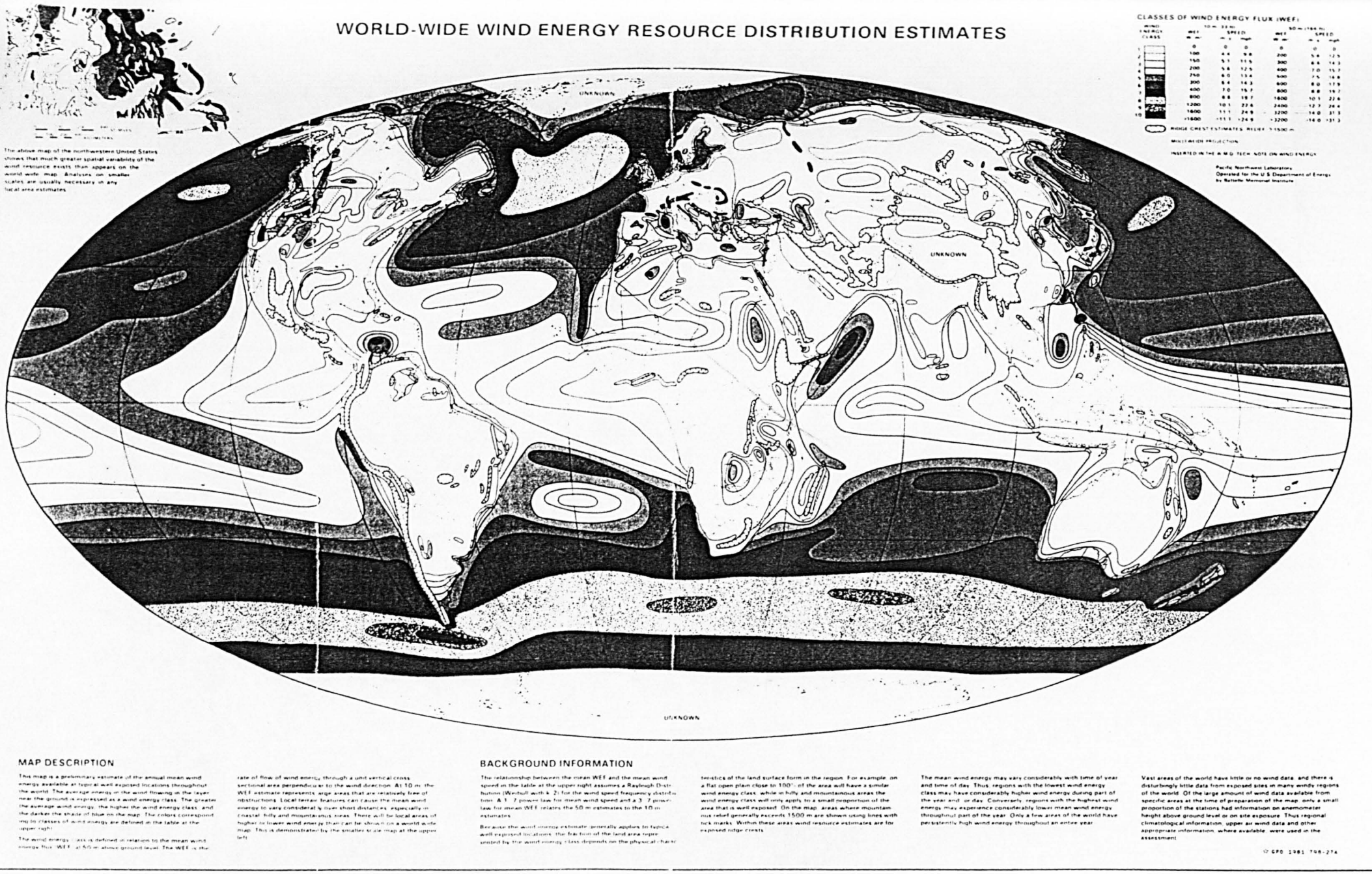

Figure 3.27: World Meteorological Organisation - World wind energy map

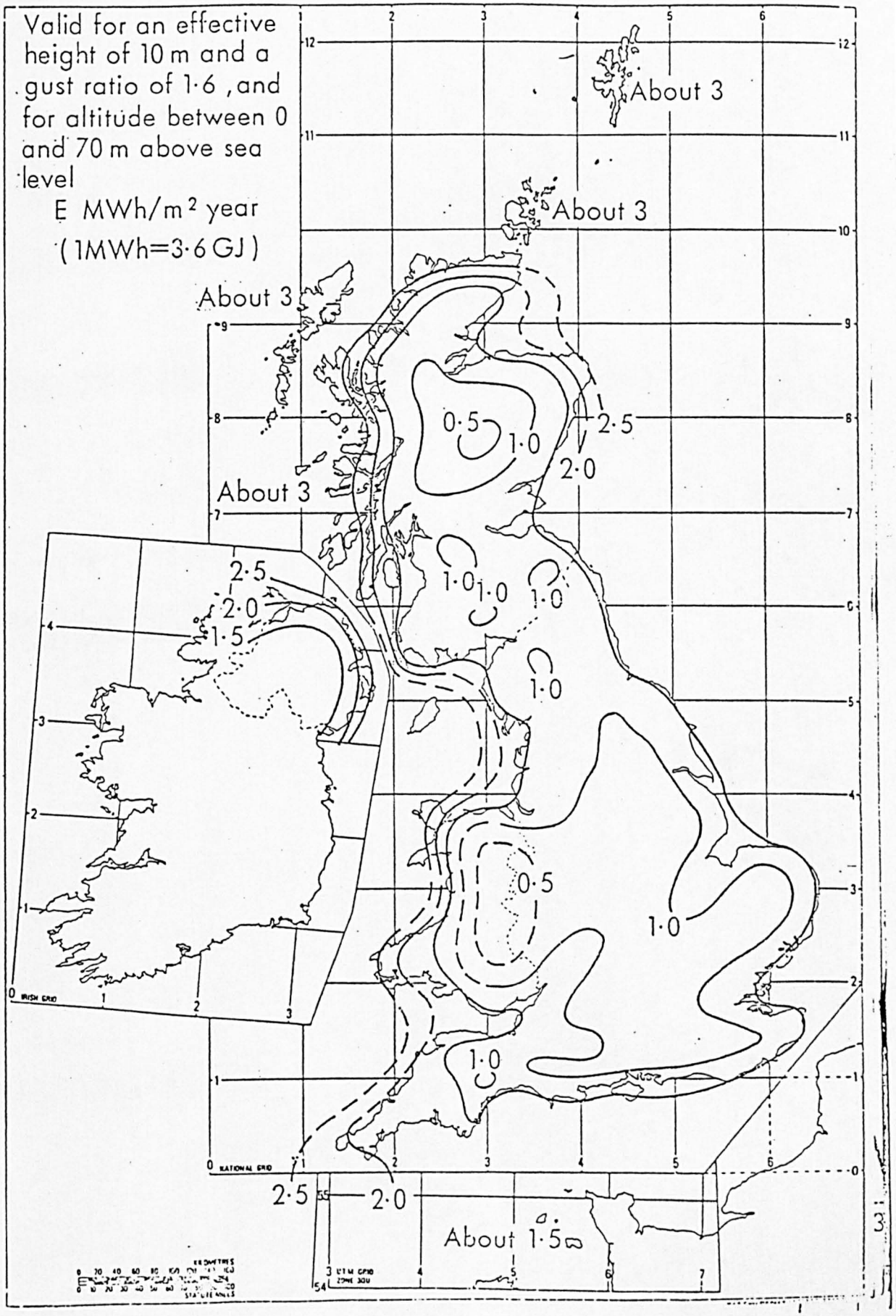

Figure 3.28: Wind energy distribution over the UK

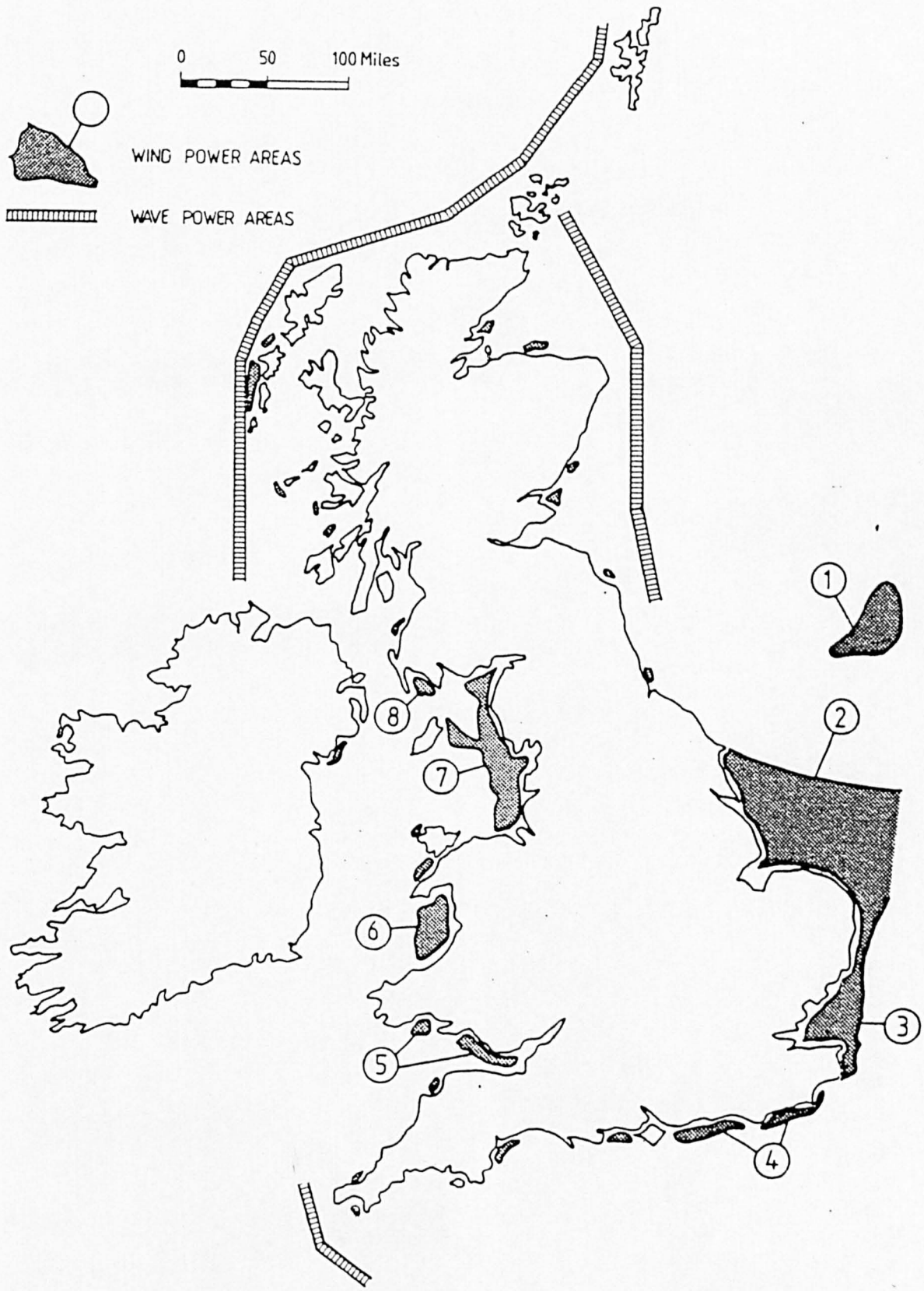

Figure 3.29: Sites located for UK offshore wind energy potential by CEGB (Rockingham, 1981)

CHAPTER 4

HORIZONTAL AXIS WIND TURBINES

LIST OF SYMBOLS IN CHAPTER 4

A = swept area of wind turbine rotor, eq (4-1)

Ao = cross sectional area of windstream upwind of rotor, eq (4-1)

Al = cross sectional area of windstream down wind of rotor, eq (4-1)

a = axial interference factor, eq (4-9c)

a' = angular interference factor, eq (4-18)

dAb = incremental planwise blade element area of one blade

B = number of blades, eq (4-53), (4-54)

C = blade chord width

CD = drag coefficient

CL = lift coefficient

CP = P / ((1/2) ρ A Vo^3) power coefficient, eq, (4-13)

CPmax = maximum power coefficient

CQ = torque coefficient

Cw = wind turbine rotor drag, eq (4-70) to (4-75)

Cx = axial force coefficient, eq (4-48)

Cy = tangential force coefficient, eq (4-49)

Ft = tangential force (eq (4-28)

Fx = thrust force

dFx = incremental thrust force at blade element, eq (4-44)

Fy = tangential force

dFy = incremental tangential force at blade element, eq (4-45)

F = Prandtl Tip Loss Factor, eq (4-78)

f = Prandtl factor, eq (4-79)

L = lift force

dL = lift force

'm = mass flow rate through the rotor, eq (4-2)

P = power extracted by rotor, eq (4-10), (4-11), (4-12)

Pw = power contained in the wind

po = atmospheric pressure, eq (4-3, (4-4)

pu = pressure in front of the rotor disc, eq (4-3)

pd = pressure behind rotor disc, eq (4-4)

dp = pressure drop through the rotor disc, eq (4-15), (4-16), (4-20), (4-30)

Q = torque generated by rotor, eq (4-33)

dQ = incremental torque at blade element at radius R, eq (4-29)

R = tip radius of wind turbine rotor

r = radius of blade element

dr = incremental radial length of the blade element at radius r

s = local solidity at the blade element at radius r eq (4-61)

Sl = distance between successive vortex sheets, eq (4-76)

T = thrust load acting on wind turbine rotor due to wind, eq (4-2), (4-6), (4-24)

dt = incremental thrust at annulus, eq (4-17), (4-25), (4-26)

U = tangential speed of blade tip

u = tangential speed of blade element at radius r

Uw = tangential speed of wake, eq (4-28)

V = wind velocity at the wind turbine rotor (m/s), eq (4-7), (4-8)

Vo = undisturbed wind velocity upwind of wind turbine rotor, eq (4-76), (4-8a), (4-9a)

Vl = wind velocity downwind of wind turbine rotor eq (4-7a), (4-9)

V_r = relative wind velocity, eq (4-56), (4-57)

w = angular velocity of wake, eq (4-19)

X = tip speed ratio of rotor

x = axis of rotation of rotor, eq (4-22)

x = local speed ratio of blade element at radius r, eq (4-22)

y = plane of rotation of rotor

α = alpha = angle of attack of blade element eq (4-42)

ϕ = Phi = relative wind vector angle, eq (4-42), (4-43)

$\phi(t)$ = Phi(t) = helix angle of the flow at boundary of slipstream, eq (4-76)

ρ = rho = density of the air, eq (4-2)

Ω = Omega = angular velocity of wind turbine rotor, eq (4-22)

w = omega = angular velocity imparted to the airflow eq (4-19)

θ = Theta = blade pitch angle of blade element, eq (4-42)

4.1 HORIZONTAL AXIS WIND TURBINE

Horizontal Axis Wind Turbines (HAWTs) are the most popular and, at the present time, the most successful of all devices used to extract energy from the wind.

They are axial-flow type rotating machines, ie, the axis of rotation or shaft is in line with the direction of the flow of the wind. In order to operate, therefore, HAWT rotors have to be pointed into the wind.

As they rotate, the blades of axial flow HAWTs sweep a disc shaped area. HAWTs which have blades that largely 'fill up' the disc area are defined as having high solidity, and turbines with few blades are defined as having low solidity and are sometimes described as 'propeller' type HAWTs (because of their resemblance to an aircraft propeller).

HAWTs include the following types of wind turbine:

- North European or Dutch type 'classical' windmills (Fig 4.1).

- Multiblade windpumps (Figure 4.2).

- The triangular, cloth-sailed Mediterranean or 'Cretan' windmills (Fig 4.3).

- Modern medium and high-speed 'propeller' type turbines (Fig 4.4).

The multiblade type and the mediterranean sail type devices are slow speed, high solidity wind turbines which have 6 or more blades. They are less efficient than the more modern high-speed, low solidity wind turbines but are still used for applications that require high starting torque, such as high lift water pumping from deep wells.

The North European windmills, which most frequently had 4 blades (though there are some 5, 6 and 8 bladed versions in existence) were medium speed, medium velocity wind turbines used for grinding grain, saw milling, paper making and low head water pumping, principally in the Netherlands and East Anglia.

Modern Propeller type HAWTs are a development of the traditional windmill, but with rotors that owe their design to aeroplane propeller and helicopter rotor technology.

Techniques for understanding the operation and design of HAWT rotors are derived from developments in aeroplane and ship propeller design.

4.2 'PROPELLER' TYPE HORIZONTAL AXIS WIND TURBINES

Whilst it is not strictly correct to describe the rotors of these wind turbines as 'propellers', the term does indicate the appearance of these machines. At first glance there does not seem to be any difference between an aircraft propeller and a propeller-type HAWT rotor, but there is a fundamental difference in the two types of 'airscrew'. This is due to their different functions: The aircraft propeller is used for the production of thrust and the wind turbine rotor is intended to produce torque.

The most noticeable difference is that on an aircraft propeller the cambered or convex curved surface and leading edge of the blades faces the 'airflow' (ie, the direction opposite to aircraft movement), whereas in the case of HAWTs, the blades' leading edges still face into the 'airflow' or wind, but the cambered surface of the blades faces away from the wind and the flat or concave surface is towards the wind.

It is therefore not possible to use an aircraft propeller as a propeller type HAWT successfully.

The first propeller type HAWTs were probably constructed in the early 1900s (Golding, 1955) but ideas on optimising the performance of propeller type HAWTs were developed by Betz (1927), Glauert (1935), and

Theodoresen (1944 & 48), amongst others.

4.2.1 CHARACTERISTICS OF PROPELLER TYPE HAWTs

1) These wind turbines have a small number of relatively narrow blades of airfoil cross section. Two and three blades are the most popular, though a number of Propeller type wind turbines with one or four blades have been built.

2) As propeller type HAWTs are axial flow machines they require a 'yawing' mechanism to slew the rotor around a vertical axis so that the shaft axis can be maintained in alignment with the wind direction whenever the wind direction changes. Such mechanisms include the tail vane or rudder, fantail, and yaw motors. It is also possible in certain circumstances to obtain passive or free yawing characteristics by positioning the rotor downwind of the support tower.

3) Propeller type HAWTs have medium to high rotation speeds, with rotor tip velocities ranging from 3 to 12 times the wind speed or greater.

4) Compared to multiblade HAWTs, which produce power at low rotation speeds but with high torque, propeller type HAWTs produce their power at their higher rotation speeds and have relatively lower characteristic torque output. Large propeller type

HAWTs, however, do generate substantial torque values, and therefore require gear boxes that can cope with high torque inputs.

5) Propeller type HAWTs tend to be the most efficient of wind turbines currently in use and are certainly the most popular.

6) Propeller type HAWTs require a support structure consisting of a freestanding steel lattice (tower), or free-standing steel or concrete cylindrical structures, or guyed tubular or pole structures.

7) Propeller type HAWTs perform best at relatively high working wind speeds and can seldom make use of very light winds.

8) Propeller type HAWTs are generally self-starting apart from certain designs such as very high tip speed ratio rotors and some rotors with untwisted blades.

4.2.2 PROPELLER TYPE HORIZONTAL WIND TURBINE VARIATIONS

4.2.2.1 Upwind Versus Downwind Rotors:

- Wind turbine rotors located downwind of the support tower can achieve passive or free yaw.

- For active yawing systems, the required yawing

effort is less for a downwind wind turbine compared to an upwind turbine, which strives to position itself downwind of the yawing axis and has, therefore, to be constantly restrained.

- Downwind operation results in a cyclic loading of the blades as they pass through the wake of the tower, an effect commonly known as 'tower shadow'. The tower shadow can also generate noise problems. Upwind operation reduces the tower shadow effect.

- Upwind turbines tend to be marginally more efficient due to the undisturbed airflow, ie, no tower wake.

4.2.2.2 Number of Blades:

- Single blade rotors achieve very high rotation speeds thus reducing gearbox size, but are less energy efficient than two or three bladed rotors, and are also subject to vibrations which have to be damped out.

- Single and two bladed rotors when spinning have a markedly fluctuating moment of inertia about the vertical axis. This causes the rotor to experience very high fluctuating loads during yaw. These blade loads can be reduced by allowing the rotor to 'teeter' or 'see-saw' about an axis at 90 degrees to the shaft and across the blade chord.

- Single and two bladed teetered rotors produce cyclic torque variations which require torsionally 'soft' or compliant transmissions to reduce the strains on gearboxes.

- Teetered rotors require the amplitude of the teeter motion to be limited to prevent the blades hitting the tower (usually around 6 degrees) and teeter stops are provided. The impact of the rotor on these stops can cause serious problems due to the very large forces transmitted to the whole structure.

  Apart from a few instances, teetered rotors have only been employed on medium and large scale HAWTs, mainly because three bladed rotors are the most popular configuration under 200kW in size.

- The choice of bearing for teeter hinges is very critical and has to be maintenance free. Also, there is the further complication of the need to provide a means of transmitting actuating forces for controlling blade pitch.

- Independently hinged or free coning of blades achieves a similar result to teetering, but have only rarely been employed, because teetering tends to be the cheaper mechanism as it requires only one flapping hinge per rotor instead of a hinge per blade.

- The dynamics of teetered and free coning blades are very complex and difficult to model: this can lead to increased costs.

- Three bladed rotors are not subject to the high fluctuating loads that affect single and two bladed rotors as the rotor moment of inertia does not vary significantly. They are also slightly more efficient and are able to produce a more even torque output.

- Three bladed rotors are often claimed to be more expensive than two bladed rotors because of the cost of the extra blade, but when the teeter hub and mechanism are taken into account, the differences are marginal. Currently, most commercial manufacturers of small to medium scale wind turbines are producing 3 bladed HAWTs but most large wind turbines (which are experimental) have 2 blades. However, the US Department of Energy, the main proponents hitherto of 2 bladed teetered rotors, have commenced work at NASA on medium scale 3 bladed HAWT rotors (Pintz, 1985).

4.2.2.3 Fixed or Variable Pitch Blades:

- Wind turbine rotor blades can be mounted with the ability to rotate in bearings at the hub about their span-wise axis. This rotation is known as pitch and blades mounted in this manner are known as variable pitch blades. Blades attached rigidly to the hub and

not able to pitch are known as fixed pitch blades.

- Variable pitch blades require a complex mechanism that has to operate under all conditions throughout the life of the turbine. As the root end of a variable pitch blade has to be designed to terminate into a bearing, this necessitates a substantial bearing as it has to cope with high bending and tensile loads on the blades. The roots of fixed pitch blades do not have this restriction, and this allows the loads to be catered for more simply.

- Variable pitch blades can be used to enhance starting, for maintaining constant rotation speed, overspeed control, and for bringing the rotor to a standstill.

- However similar results can be achieved with a fixed pitch rotor where only the outer portion of the blade has variable pitch. Most wind turbines produced in Denmark use this type of blade.

- If the wind turbine starts satisfactorily, then a fixed pitch rotor with drag spoilers such as flaps, ailerons or retractable plates for aerodynamic speed control is probably the least expensive solution.

- Fixed pitch, constant speed rotors can also be designed to operate with stall control by careful

selection of the aerofoil. Because the rotor speed is constant when the wind speed increases, the tip speed ratio reduces. This results in the blades' angle of attack increasing and approaching stall. When the blade is in stall it is no longer generating torque.

- Current wind turbine manufacturers are evenly divided in their use of fixed and variable pitch blades. Both variable pitch and fixed pitch blades are produced for small to large scale wind turbines.

4.2.2.4 Blade Shapes:

- Each portion of the blade of a Propeller type Horizontal Axis Wind Turbine rotor is moving at a different tangential speed, u. This speed linearly increases as the distance from the hub towards the tip. The Relative Wind vector angle o (Phi) is also progressively decreasing as the distance from the hub increases (Fig 4.4a).

- However, for maximum power extraction an aerofoil with a high Lift to Drag Ratio is normally chosen, but this ratio is only a maximum at a particular Angle of Attack, @ (alpha), of the aerofoil in relation to the airflow.

- As the Angle o (Phi) of the Relative Wind Direction is progressively decreasing from the hub to the tip, in order to operate at max L/D ratio, the blade will

therefore have to be twisted in such a way that the Angle of Attack in relation to the relative wind direction at each point along the blade remains constant.

- To maintain constant Lift (which is dependent on the Angle of Attack) along the length of the blade, the blade chord width, c, should ideally reduce progressively from the hub towards the tip, in order to take account of variations in tangential speed.

4.3 AERODYNAMIC THEORIES OF PROPELLER TYPE HORIZONTAL AXIS WIND TURBINES

Three different aerodynamic theories have been developed for describing the operation of Propeller type Horizontal Axis Wind Turbine (HAWTs). They are:

a) Momentum Theory or Actuatory Disc Theory
b) Blade Element Theory
c) Vortex Theory

4.3.1 MOMENTUM THEORY (MT)

The Momentum Theory is essentially concerned with the airflow through the disc shaped area swept by the HAWT rotor.

By applying basic physical laws of conservation (of mass, momentum and energy) to the wind energy conversion device (the rotor), it gives an indication of the changes in wind speed due to loss of kinetic energy caused by the interaction of the rotor with the air.

The theory also predicts the maximum energy conversion efficiency attainable but gives no indication of the ideal blade shape required to achieve it. The simplest form of this theory is the Axial Momentum Theory.

4.3.1.1 Axial Momentum (AM) Theory

The Axial Momentum Theory was first developed by WJM Rankine (1865) and subsequently refined by RE Froude (1889).

The AM Theory makes the following assumptions:

1 The wind is assumed to be one dimensional.
2 The wind is uniformly distributed across the rotor swept area.
3 The wind is assumed to be incompressible.
4 The wind is assumed to be non viscous.
5 The flow is entirely axial in direction with no rotation.
6 No friction occurs when the wind passes through the rotor.

In order to simplify the analysis the rotor is assumed

to be an 'Actuator Disc', ie, a simple device that absorbs kinetic energy from the wind.

Figure 4.5 shows a streamtube with an actuator disc representing a rotor with swept area A = pi R^2.

The wind velocity V at the disc and Vl downstream of the disc will be slower than the upstream wind velocity Vo, because of the fact that the disc is absorbing kinetic energy and in the process having a retarding effect on the wind speed. The streamtube that contains the disc has a cross sectional area upsteam, Ao, smaller than that of the disc, A, and an area Al, downsteam larger than that of the disc, A. This is because the mass flow rate, 'm, must be the same everywhere within the streamtube. This explains the shape of the flow in Fig 4.5 and leads to the continuity equation:

$$Vo\ Ao = V\ A = Vl\ Al \qquad (4\text{-}1)$$

In retarding the windstream the rotor or actuator disc is subjected to a Thrust load T which is equal to the rate of change of axial momentum:

$$T = 'm\ (Vo - Vl) = \rho\ A\ V\ (Vo - Vl) \qquad (4\text{-}2)$$

where 'm is the mass flow rate through the rotor and rho is the density of the air.

An increase in pressure builds up on the upstream side

of the rotor (with a consequent pressure drop on the downstream side) due to the thrust loading caused by the retardation of the wind stream.

To determine the difference in pressure on the upwind and downwind side of the rotor, Bernoulli's Theorem is applied, separately, to the upwind and downwind sections of the streamtube. Separate equations are necessary because the total energy is different upwind and downwind. Bernoulli's Theorem states that, under steady conditions, the total energy in tne flow, comprising kinetic energy, static pressure energy and gravitational potential energy, remains constant provided no work is done on or by the fluid. Thus applying Bernoulli's Theorem to the flow upwind of the rotor one obtains:

upwind of the rotor:

$$po + [(1/2)\ \rho\ Vo^2] = pu + [(1/2)\ \rho\ V^2] \qquad (4\text{-}3)$$

and downwind of the rotor:

$$po + [(1/2)\ \rho\ Vl^2] = pd + [(1/2)\ \rho\ V^2] \qquad (4\text{-}4)$$

where po is the atmospheric pressure

pu is the pressure in front of the rotor disc

pd is the pressure behind the rotor disc

ρ = rho = air density

Subtracting (4-4) from (4-3) gives:

$$pu - pd = do = (1/2)\ \rho\ (Vo^2 - Vl^2) \qquad (4\text{-}5)$$

The Thrust T can therefore also be described in terms of pressure drop through the disc:

$$T = A\ dp = A\ (1/2)\ \rho\ (Vo^2 - Vl^2) \qquad (4\text{-}6)$$

combining (4-2) and (4-6) yields:

$$V = (Vo + Vl) / 2 \qquad (4\text{-}7)$$

$$Vl = 2V - Vo \qquad (4\text{-}7a)$$

$$Vo = 2V - Vl \qquad (4\text{-}7b)$$

V is the wind velocity at the rotor and is the mean of the Upstream Vo and Downstream Vl wind velocities.

The actuator disc induces a velocity variation which must be superimposed on the free stream velocity. The streamwise component of this induced flow is given by a V, where a = 1-(V/Vo) and is called the 'axial interference factor'. In propeller theory it is also known as the inflow factor. It is a measure of the turbines' influence on the retardation of the velocity between the Undisturbed Upwind velocity, Vo, the wind velocity, V, at the rotor and the Downstream wind velocity Vl:

$$V = (1 - a)\ Vo \qquad (4\text{-}8)$$

$$Vo = V / (1 - a) \qquad (4\text{-}8a)$$

$$(1 - a) = V / Vo \qquad (4\text{-}8b)$$

Equation (4-7) becomes (4-9):

$$Vl = (1 - 2a)\ Vo \qquad (4\text{-}9)$$

and we also obtain the following relationships:

$$Vo = Vl / (1 - 2a) \qquad (4\text{-}9a)$$

$$2a = 1 - (V/Vo) \qquad (4\text{-}9b)$$

$$a = (1 - (Vl/Vo))/2 \qquad (4\text{-}9c)$$

$$Vo - Vl = 2a\ Vo \qquad (4\text{-}9d)$$

$$Vo - V = a\ Vo \qquad (4\text{-}9e)$$

The Power extracted by the rotor, P, is equal to the rate of change of the kinetic energy from upstream to downstream:

$$P = (1/2)\ 'm\ (Vo^2 - Vl^2)$$

$$= (1/2)\ \rho\ A\ V\ (Vo^2 - Vl^2) \qquad (4\text{-}10)$$

Substituting equations (4-8) and (4-9) into (4-10) we get:

$$P = (1/2)\ \rho\ A\ Vo^3\ 4a\ (1 - a)^2 \qquad (4\text{-}11)$$

The actual power contained in a free wind stream passing through an area A is given by:

$$Pw = (1/2)\ \rho\ A\ V0^3 \qquad (4\text{-}12)$$

The non-dimensional Power coefficient (a measure of the rotor's power conversion efficiency) can now be established:

$$CP = P\ /\ Pw = P\ /\ ((1/2)\ \rho\ A\ Vo^3)$$

$$= 4a\ (1 - a)^2 \qquad (4\text{-}13)$$

It can be quickly shown by differentiation of CP with respect to a (see Fig 4.6) that CP attains a maximum value when a = 1/3, which yields:

$$CPmax = 4\ (1/3)\ (1 - (1/3)^2 = 16/27 = 0.593 \qquad (4\text{-}14)$$

This value of 16/27 is known as the Betz Coefficient or the Betz Limit, after its originator Albert Betz (1927). It essentially implies that the maximum power extraction

attainable by the best wind turbine rotor is 59% of the power contained in the free windstream.

4.3.1.2 GENERAL MOMENTUM THEORY (GMT)

A fact which the Axial Momentum Theory does not take into account is that the wind actually imparts its energy to the wind turbine rotor by causing it to spin. The rotor thus has a Torque, Q, and an Angular Velocity, O (Omega), in the plane of rotation.

This turbine rotation is taken into account in the General Momentum Theory.

The Torque in the rotor produces an opposite reaction into the wind as it moves through the rotor, causing the wake to rotate. The higher the torque generated, the higher the downstream angular momentum in the wake. Angular velocity, w, is also imparted to the airflow in the opposite direction to the turbine's rotation (see Fig 4.7).

Joukowski (1912) considered the effect of wake rotation in an analysis of aircraft propellers, and Wilson & Lissaman (1974) applied this analysis to wind turbines. They have shown that for wind turbines with Tip Speed Ratios greater than 2, very little energy will be lost to the wake. Glauert (1935) came to a similar conclusion.

We can therefore assume that the wake rotation, w, is very small compared with the Angular Velocity of the rotor, and that the pressure drop due to wake rotation between a position far upstream of the rotor and a position far downstream is also very small, ie, po = p1 (See Fig 7.7).

If we imagine the airflow relative to the blades, then the relative angular velocity at the rotor increases from Omega on the windward side to $\Omega + w$ on the leeward side.

If we take an annulus of radius, r, (see Fig 4.8) and radial thickness dr and area dA, the pressure drop through the rotor can be redefined as:

$$dp = (1/2)\ \rho\ r^2\ ((\Omega + w)^2 - \Omega^2) \qquad (4\text{-}15)$$

$$= \rho\ r^2\ w\ (\Omega + (w/2)) \qquad (4\text{-}16)$$

where dp = pu - pd

Ω = Omega = rotor angular velocity

w = angular velocity of the wake

r = radius of annulus

This is the pressure drop across the annulus. The thrust is then given by:

$$dT = dp\ dA$$

where $dA = 2\ pi\ r\ dr$

$$dT = [\rho\ r^2\ w\ (\Omega + (w/2))] * [2\ pi\ r\ dr]$$

$$= 2\ \pi\ r^3 \rho\ w\ (\Omega + (w/2))\ dr \qquad (4\text{-}17)$$

Or by introducing the 'angular interference factor', a':

$$a' = \frac{\text{angular velocity of the wind at the rotor}}{2 * \text{angular velocity of the rotor}}$$

$$= w/(2\ \Omega) \qquad (4\text{-}18)$$

$$\&\ w = 2\ a'\ \Omega \qquad (4\text{-}19)$$

The expressions for pressure (4-15) becomes by substitution (4-19):

$$dp = \rho\ r^2\ 2\ a'\ \Omega\ (\Omega + (2\ a'\ \Omega\ /\ 2)$$

$$= \rho\ r^2\ 2\ a'\ \Omega^2\ (1 + a') \qquad (4\text{-}20)$$

and equation (4-17) becomes:

$$dT = 4\ pi\ r^3\ \rho\ \Omega^2\ a'\ (1 + a')\ dr \qquad (4\text{-}21)$$

The Local Speed Ratio ,x, is the ratio of the Tangential speed u at radius r, to the undisturbed upstream wind velocity Vo and is defined as:

$$x = u\ /\ Vo = (\Omega\ r)\ /\ Vo \qquad (4\text{-}22)$$

The Tip Speed Ratio X of the rotor as a whole is the ratio of the Tangential speed U at the Tip of Radius R

of the rotor to the undisturbed upstream wind velocity Vo and is defined as:

$$X = U / Vo = (\Omega R) / Vo \qquad (4\text{-}23)$$

Assuming that the axial wind velocity V at the rotor is the mean of the upsteam Vo and downstream V1 axial wind speeds (eq 4-7):

$$V = (Vo + V1) / 2 \qquad (4\text{-}7)$$

$$V1 = 2V - Vo \qquad (4\text{-}7a)$$

The Thrust from the Axial Momentum Theory derived from (4-2) is:

$$T = A \rho V (Vo - V1) \qquad (4\text{-}2)$$

Substituting equation (4-7a) into (4-2) we obtain:

$$T = A \rho [V (Vo - (2V - Vo))]$$
$$= A \rho [V (2Vo - 2V)]$$
$$= A \rho 2 V (Vo - V) \qquad (4\text{-}24)$$

The Thrust on the annulus from the Axial Momentum Theory is therefore:

$$dT = dA \rho 2 V (Vo - V)$$
$$= [2 \pi r dr] * [\rho 2 V (Vo - V)]$$
$$= 4 \pi \rho r dr V (Vo - V) \qquad (4\text{-}25)$$

If we now substitute the Axial Interference Factor ,a, into the equation (4-25) from (4-8) and 4-9d) we obtain:

$$dT = 4 \pi r\, dr\, \rho\, V\, a\, Vo$$
$$= 4 \pi r\, dr\, \rho\, Vo\, (1 - a)\, a\, Vo$$
$$= 4 \pi r\, dr\, \rho\, Vo^2\, a\, (1 - a) \qquad (4\text{-}26)$$

Equating the two formulae for the Thrust (4-21) and (4-26) leads to a relationship between the Interference Factors a and a':

$$4 \pi r^3 \rho\, a' \Omega^2 (1 + a')\, dr = 4 \pi r\, dr\, \rho\, Vo^2\, a\, (1 - a)$$

$$\frac{r^2 \Omega^2}{V^2} (1 + a')\, a' = (1 - a)\, a$$

$$x^2 (1 + a')\, a' = (1 - a)\, a \qquad (4\text{-}27)$$

where x = Local Speed Ratio at r.

The Torque generated in the annulus due to the rotating wake needs to be considered. The Tangential force dFt acting in the wake is the product of the mass flow rate through the annulus at radius r and the change in velocity in the tangential direction:

$$dFt = 'm\, dUw = \rho\, V\, dA\, w\, r$$
$$= 2 \pi r^2 \rho\, V\, w\, dr \qquad (4\text{-}28)$$

where 'm = mass flow rate

Uw = tangential speed of the wake

w = angular velocity of the wake

Ft = tangential force

The Torque due to this force acting on 'lever arm' of radius r is therefore:

$$dQ = dFt\ r = [2\pi\ r^2\ \rho\ V\ w\ dr] * r$$
$$= 2\pi\ r^3\ \rho\ V\ w\ dr \qquad (4\text{-}29)$$

and power extracted is equal to the Torque ,Q, times the Angular Velocity ,Ω (Omega), of the rotor, and is defined as:

$$dP = dQ\ \Omega$$
$$= [2\pi\ r^3\ \rho\ V\ w\ dr] * \Omega \qquad (4\text{-}30)$$

Integrating over the whole swept area gives the total Torque and Power extracted by the rotor:

$$Q = 2\pi\ \rho \int_0^R V\ w\ r^3\ dr \qquad (4\text{-}31)$$

$$P = 2\pi\ \rho\ \Omega \int_0^R V\ w\ r^3\ dr \qquad (4\text{-}32)$$

By substituting for V and w with equation (4-8) and (4-19) into (4-31) and (4-32):

$$V = (1 - a)\ Vo \qquad (4\text{-}8)$$

$$w = a'\ 2\Omega \qquad (4\text{-}19)$$

we obtain:

$$Q = 2\pi\ \rho \int_{o}^{R} Vo\ (1 - a)\ a'\ 2\Omega\ r^3\ dr \qquad (4\text{-}33)$$

$$P = 2\ \pi\ \rho\ \Omega \int_{o}^{R} Vo\ (1 - a)\ a'\ 2\Omega\ r^3\ dr \qquad (4\text{-}34)$$

Expressing equations (4-33) and (4-34) in terms of the dimensionless Torque Coefficient CQ and Power Coefficient CP we get:

$$CQ = \frac{Q}{(1/2)\ \rho\ \pi\ R^3\ Vo^2}$$

$$= \frac{8}{X^3} \int_{o}^{X} (1 - a)\ a'\ x^3\ dx \qquad (4\text{-}35)$$

and

$$CP = \frac{P}{(1/2\ \rho\ \pi\ R^2\ Vo^3}$$

$$= \frac{8}{X^2} \int_{o}^{X} (1 - a)\ a'\ x^3\ dx \qquad (4\text{-}36)$$

There is also a relationship between Torque Coefficient

CQ and the Power Coefficient CP given as follows:

$$CQ = CP / X \text{ and } CP = CQ\ X$$

4.3.2 MAXIMUM ATTAINABLE POWER COEFFICIENT

The expression for CP that takes account of the wake rotation can be used to evaluate the Maximum Power Coefficient.

For Maximum CP in equation (4-36), the expression (1 - a) a' must be a Maximum subject to the constraints of the equation (4-27):

$$x^2 (1 + a') a' = (1 - a) a \qquad (4\text{-}27)$$

If (1-a) a' is to be a maximum, then:

$$(d / da) [(1 - a) a'] = 0 \qquad (4\text{-}37)$$

or

$$[(1 - a) (da' / da)] - a' = 0 \qquad (4\text{-}38)$$

and from (4-27) by differentiating with respect to a:

$$(1 + 2a') x^2 (da' / da) = (1 - 2a) \qquad (4\text{-}39)$$

Substituting (4-38) into (4-39) and then recombining with (4-27) we obtain:

$$a' = (1 - 3a) / (4a - a) \qquad (4\text{-}40)$$

Tables 4.1 and 4.2 and Fig 4.9 give the relationship between a, $a'x^2$, x, X and CPmax.

Jansen (1976) derived an approximate relationship

between CPmax and Tip Speed Ratio shown in Fig 4,9 and expressed as following:

$$CP(approx) = (16/27)\ e^{-d} \qquad (4\text{-}41)$$

where $d = 0.3538\ X^{-1.2946}$

However to obtain these ideal values of CP, wind turbine rotors would need to be operating in a frictionless medium, have an infinite number of blades as well as an unlimited capability of blade pitch angles and chord widths.

As this is not possible and we also need to be able to determine the best blade chord width and blade pitch angle and the number of blades to obtain the best performance, we shall now refer to the Blade Element Theory.

4.3.3 BLADE ELEMENT THEORY

The Momentum Theory looks at the effect of the windflow on the rotor in terms of the wind velocities at different points. Relationships between the Thrust and Torque on the rotor and the rate of change of momentum of the wind have been determined.

An expression for the maximum possible Power Coefficient

attainable by an ideal rotor has also been established, but the theory cannot give information on the ideal shape of the blades of a rotor that will achieve a particular Power Coefficient, or indeed on the influence of the number of blades and of friction.

A technique which, when used in conjunction with the Momentum Theory, provides information on these aspects is the Blade Element Theory.

The Blade Element Theory was originated by W Froude (1878) and developed by S Drzeweicki (1892). The approach differs from that of the Momentum Theory in that it is entirely concerned with the forces produced on the blades as a result of the motion of the air.

The main assumption of this theory is that the windflow through the rotor is in a series of interacting circular stream tubes. Fig 4.10 shows one of these streamtubes.

According to Wilson & Lissaman (1974) this assumption is perfectly valid for 'lightly loaded' turbines, ie, those having medium to high tip speed ratio. Therefore, the flow at an element dr at the annulus at radius r may be regarded as two dimensional. In view of this it is possible to use known aerofoil sections with their measured two dimensional section characteristics to determine the aerodynamic forces generated at each element in the blade.

If we now can assume that the blade cross-section at the annulus to be an aerofoil section, then Fig 4.11 shows the blade in cross-section view, with the velocity and force diagram superimposed.

The axis, x, is the axis about which the HAWT rotor rotates (ie, the shaft) and, y, is the plane of rotation. When the rotor is spinning, the blade not only sees the axial wind velocity V, but also the Rotational Velocity $(1 + a')\,\Omega r$, in terms of the Relative Wind Velocity vector VR at an angle Phi (Relative Wind Angle) to the plane of rotation (y).

This Relative Wind Velocity Vr causes two aerodynamic forces to occur on the blade element at radius r. Both of these forces are towards the leeward side of the blade, one of which is acting in the same direction as Vr and is known as the Drag force dD, and the other, known as the Lift force dL, is acting in a direction perpendicular to Vr.

The Angle of Attack α (alpha) in the diagram is referred to as the angle between the chord line of the blade's aerofoil cross section and the Relative Wind Vr, and is defined as:

$$\alpha = \phi - \theta \qquad (4\text{-}42)$$

where

rotation y and Relative Wind Velocity vector Vr

θ = Blade Pitch Angle between the plane of rotation y and the chordline of the blade's cross section.

Using trigonometric expressions we can determine the following relationships:

$$\text{Tan } \phi = \frac{(1 - a)}{(1 + a')} * \frac{Vo}{\Omega r} \qquad (4\text{-}43)$$

$$dFx = [dL \cos\phi] + [dD \sin\phi] \qquad (4\text{-}44)$$

$$dFy = [dL \sin\phi] - [dD \cos\phi] \qquad (4\text{-}45)$$

Where dFx and dFy are the incremental forces in the axial (thrust) and tangential (torque) directions respectively.

Changing these forces into dimensionless coefficients we obtain the following expressions:

$$\text{Lift Coefficient: } CL = \frac{L}{(1/2)\ \rho\ Vr^2\ dAb} \qquad (4\text{-}46)$$

$$\text{Drag Coefficient: } CD = \frac{D}{(1/2)\ \rho\ Vr^2\ dAb} \qquad (4\text{-}47)$$

$$\text{Axial Force Coeff: } Cx = \frac{Fx}{(1/2)\ \rho\ Vr^2\ dAb} \qquad (4\text{-}48)$$

$$\text{Tangential Force Coeff: } Cy = \frac{Fy}{(1/2)\ \rho\ Vr^2\ dAb} \qquad (4\text{-}49)$$

Where dAb is the incremental planwise blade element area of one blade, defined as:

$$dAb = c\ dr \qquad (4\text{-}50)$$

where c = the blade chord width

dr = incremental radial length of the blade element at radius r.

Again using trigonometric relationships, the following expressions may also be obtained:

$$CX = [CL\ Cos\phi] + [CD\ Sin\phi] \qquad (4\text{-}51)$$

$$Cy = [CL\ Sin\phi] - [CD\ Cos\phi] \qquad (4\text{-}52)$$

Expressions for the incremental thrust and torque components of element dr at radius r now become:

$$dT = B\ c\ (1/2)\ \rho\ Vr^2\ Cx\ dr \qquad (4\text{-}53)$$

$$dQ = [B\ c\ (1/2)\ \rho\ V^2\ Cy\ dr] * r \qquad (4\text{-}54)$$

where B is the number of blades in the rotor.

4.3.4 COMBINED MOMENTUM AND BLADE ELEMENT THEORY

To combine the two theories we now need to equate the Thrust and Torque from the Blade Element Theory with the same components from the Momentum Theory. However, as the Momentum Theory assumes frictionless flow the drag components in (4-53) and (4-54) must be set to zero.

From the Momentum Theory we have:

$$dT = 4\ \pi\ r\ dr\ \rho\ Vo^2\ a\ (1 - a) \qquad (4\text{-}26)$$

$$dQ = 2\ \pi\ r^3\ \rho\ V\ w\ dr \qquad (4\text{-}29)$$

and from (4-8):

$$dQ = 2\ \pi\ r^3\ \rho\ Vo\ (1 - a)\ w\ dr \qquad (4\text{-}55)$$

From Fig 4.11 and using trigonometric relationships, we have:

$$Vr\ Sin\phi = Vo\ (1 - a) \qquad (4\text{-}56)$$

and

$$Vr\ Cos\phi = \Omega\ r\ (1 + a') \qquad (4\text{-}57)$$

Substituting Vr for eq (4-56) into (4-53) and equating Thrusts (assuming CD = 0) we obtain:

$$B\ c\ \frac{1}{2}\ \rho\ Vo^2\ \frac{(1 - a)^2}{Sin^2\phi}\ CL\ Cos\phi\ dr =$$

$$= 4\ \pi\ r\ \rho\ Vo^2\ (1 - a)\ a\ r\ dr \qquad (4\text{-}58)$$

and

$$\frac{a}{(1 - a)} = \frac{Bc}{2\ \pi\ r} = \frac{CL\ Cos\phi}{4\ Sin^2\phi} \qquad (4\text{-}59)$$

and

$$\frac{a}{(1 - a)} = \frac{s\ CL\ Cos\phi}{4\ Sin^2\phi} \qquad (4\text{-}60)$$

Where s is a term known as the Local Solidity at radius, r. It is a measure of the number of blades as well as the chord, c, of each blade and the effect of radial distance from the axis. It is defined as follows:

$$s = \frac{B\ c}{2\ \pi\ r} \qquad (4\text{-}61)$$

A similar relationship to that derived for the Thrust can also be derived for Torque:

$$B\ c\ \frac{1}{2}\ \frac{\rho\ (1 + a')^2\ \Omega^2\ r^2}{Cos^2\phi}\ CL\ Sin\phi\ r\ dr =$$

$$= 2\ \pi\ \rho\ Vo\ (1 - a)\ w\ r^3\ dr \qquad (4\text{-}62)$$

giving

$$\frac{a'}{(1 + a')} = \frac{s\ CL}{4\ Cos\phi} \qquad (4\text{-}63)$$

With the two expressions (equations (4-60) and (4-63)) that relate the axial and tangential wind flow to the shape of the rotor blades, it is possible to calculate the flow conditions at an element dr at radius r giving the performance characteristics for different Tip Speed Ratios X.

4.3.5 DRAG EFFECTS

In the previous section the drag component was reduced to zero in order to equate the Momentum Theory and the Blade Element Theory. However, a real wind turbine rotor blade is subject to drag forces which must be taken into account.

If we consider eq (4-54) which now contains a factor for the drag, it is possible to show how the maximum CP curves are affected by different Drag/Lift ratios, (Jansen, 1976) (see Fig 4.12) for wind turbines with the number of blades B equal to infinity. Wilson et al (1976) give a similar relationship between Lift/Drag ratio and the CP versus Tip Speed Ratio curves of single, two and three-bladed rotors (see Fig 4.13).

The Torque from the Blade Element theory is given by:

$$dQ = B\ c\ (1/2)\ \rho\ Vr^2\ Cy\ r\ dr \qquad (4\text{-}54)$$

and taking equation (4-52) into account we obtain:

$$dQ = B\ c\ (1/2)\ \rho\ Vr^2[(CL\ Sin\phi)-(CD\ Cos\phi)]\ r\ dr \qquad (4\text{-}64)$$

and

$$dP = \Omega\ dQ$$

$$= \Omega\ B\ c\ (1/2)\ \rho\ Vr^2\ *$$

$$[(CL\ Sin\phi)-(CD\ Cos\phi)]\ r\ dr \qquad (4\text{-}65)$$

and, taking into account the Drag/Lift ratios we obtain:

$$dP = \Omega\ B\ c\ (1/2)\ \rho\ Vr^2\ CL\ Sin\phi\ *$$

$$[1 -((CD/CL)\ Cot\phi]\ r\ dr \qquad (4\text{-}66)$$

The term outside the brackets of eq (4-66) is the idealised power and can be considered the same as that developed from a drag-less or friction-less rotor, see eqs (4-30) to (4-36). Converting eq (4-36) to dimensionless form, we obtain an expression for ideal CP which includes the effect of rotor drag:

$$CP = \frac{8}{X^2}\int_0^X (1-a)\ a'\ x^3\ [1 - (\frac{CD}{CL}\ Cot\phi)]dx \qquad (4\text{-}67)$$

$$= CPideal - Cw \qquad (4\text{-}68)$$

$$\text{where } Cw = \frac{8}{X^2} \int_0^X (1 - a)\, a'\, x^3\, \frac{CD}{CL} \cot\phi \; dx \qquad (4\text{-}69)$$

and substituting eq (4-43) into eq (4-69) we obtain:

$$Cw = \frac{8}{X^2} \int_0^X (1 - a) a'\, x^3\, \frac{CD}{CL} \frac{[(1 + a')\Omega r]}{(1 - a)\, Vo} \, dx \qquad (4\text{-}70)$$

$$Cw = \frac{8}{X^2} \int_0^X (1 - a) a'\, x^3\, \frac{CD\ (1 + a')}{CL\ (1 - a)}\, x \, dx \qquad (4\text{-}71)$$

Assuming that the angle of attack along the blade remains constant and that the aerofoil section does not change along the length of the blade, we can obtain:

$$Cw = \frac{8}{X^2} \frac{CD}{CL} \int_0^X a'(1 + a)\, x^4 \, dx \qquad (4\text{-}72)$$

and taking into account eq (4-27)

$$x^2\, (1 + a')\, a' = (1 - a)\, a \qquad (4\text{-}27)$$

we obtain:

$$Cw = \frac{8}{X^2} \frac{CD}{CL} \int_0^X (1 - a)\, a\, x^2\, dx \qquad (4\text{-}73)$$

Referring back to table (4-1) for values of x greater than 2; (1 -a)a and $a'.x^2$ are virtually constant and equal to 2/9 and $a'\Omega$.

Cw now becomes:

$$Cw = \frac{8}{X^2} \frac{CD}{CL} \int_0^X \frac{2}{9} x^2\, dx \qquad (4\text{-}74)$$

$$Cw = \frac{CD}{CL} \frac{16}{27} x \qquad (4\text{-}75)$$

The relationship for the maximum attainable Power Coefficient is therefore:

$$CP = CPideal - \left[\frac{CD}{CL} \frac{16}{27} x\right] \qquad (4\text{-}76)$$

As can be seen from Fig 4.12, wind turbine rotor blades that have aerofoil cross sections which generate Drag/Lift ratios of less than 0.05 (and Lift/Drag ratios greater than about 20) should prove to have satisfactory performance.

4.3.6 THE EFFECT OF A FINITE NUMBER OF BLADES

Up to now the theory described has been based on the assumption that the wake is rotationally symmetric. With a finite number of blades this assumption breaks down, and increasingly unsymmetric flow in the wake occurs with a decreasing number of blades.

Another assumption was that the flow at any element is two dimensional, but radial acceleration and wake induced flow at the tip may alter the assumed flow pattern.

According to Wilson et al (1974), it is safe to ignore this effect, as the wake angular velocity ,w, is small compared to the rotor angular velocity Ω (Omega).

A finite number of blades does involve performance losses, however, compared to an ideal rotor with an infinite number of blades, and these losses (which are concentrated around the tips) are known as tip losses.

Several approaches have been developed to cope with this phenomenon but the two principal methods are the Prandtl and Goldstein Tip Loss Models (Prandtl 1919 and Goldstein 1929).

Goldstein's Tip Loss Model is more complex and

sophisticated than the Prandtl model which is relatively simple to implement, and according to Wilson et al (1976), there is little difference in the results. That being the case, only the Prandtl Tip Loss Model will be described here.

Essentially, what occurs when there is an airflow around the upper and lower surfaces (or more accurately for HAWT rotors, the blade section's leeward and windward surfaces) of an aerofoil is that the pressure is reduced on the leeward surface and increased on the windward surface.

In the centre of the blade, the flow diverted from the windward to the leeward surface is negligible, but towards the tip and root there is a considerable increase in the mixing of the airflows which tends to reduce the torque acting on the blade because of the reduction in the pressure difference on either side of the rotor blade (see Fig 4.14). As the largest portion of the torque contribution occurs towards the blade tip, it is important that the tip losses are not neglected as they will have a marked affect on performance.

There is also a similar effect at the blade root, but this is less important as the torque contribution is low in this region of the blade. Wilson et al (1976) also give an approximation for root or hub losses.

4.3.7 PRANDTL TIP LOSS MODEL

Prandtl's Tip Loss Model uses a Tip Loss Factor F to approximate the radial flow near the blade tip.

Prandtl assumed that it was possible to replace the vortex sheets shed from the blade with a series of parallel planes (Fig 4.15). If the number of blades is B, then the normal distance between successive sheets is given by:

$$Sl = \frac{2\pi R}{B} \text{Sin } \phi(t) \qquad (4\text{-}76)$$

where $\phi(t)$ is the angle (helix) of the flow at the boundary of the slipstream.

At the boundary of the slipstream, the induced velocities will be zero and so:

$$\tan o(t) = \frac{Vo}{R\,\lambda L} = \frac{1}{X} \qquad (4\text{-}77)$$

It is, however, more convenient to replace the term (R Sin $\phi(t)$) with (r Sin ϕ). This does not invalidate the result, as local values of ϕ are used when calculating the flow at any radius.

The Prandtl Tip Loss Model is described fully by Glauert (1935), where the Tip Loss Factor is derived as:

$$F = \frac{2}{\pi} \text{Arc Cos } e^{(-f)} \qquad (4\text{-}78)$$

and

$$f = \frac{B\,(R - r)}{2\,r\,\text{Sin}\phi} \qquad (4\text{-}79)$$

The interpretation of this result is that the maximum change of axial velocity (2 a V) only occurs on the vortex sheets and the average change is only a fraction of this, giving (2 a F V). Similarly, the angular velocity, instead of being (2 a' Ω) should become (2 a' F Ω).

This assumption of the Tip Loss Factor F affecting only the wake velocities is the one most commonly used.

Wilson (1974), however, suggested that F also reduces the axial velocity at the rotor by a.F instead of just a. This introduces a second order term into the flow around the blades and has meant that there is uncertainty as to which method to adopt, though Wilson (1976) claims that the calculation iterations required to compute are fewer with the Wilson modification.

The effect of the Tip Loss Factor on the flow equations (4-59) and (4-63) can be calculated by substituting:

for $V1 = Vo\ (1 - 2a)$; the expression $V1 = (1 - 2aF)\ Vo$

(4-80)

and for $w = 2\,a'\,\Omega$; $w = 2\,a'\,F\,\Omega$ (4-81)

and also for the Wilson method:

$V = (1 - a)\,Vo$ by $V = (1 - aF)\,Vo$ (4-82)

Equations (4-59) and (4-63) become:

$$\frac{aF}{(1 - a)} = \frac{s\,CL\,Cos\,\phi}{4\,Sin^2\,\phi} \qquad (4\text{-}83)$$

and

$$\frac{a'F}{(1 + a')} = \frac{s\,CL}{4\,Cos\,\phi} \qquad (4\text{-}84)$$

or by Wilson:

$$\frac{aF\,(1 - aF)}{(1 - a)^2} = \frac{s\,CL\,Cos\,\phi}{4\,Sin^2\,\phi} \qquad (4\text{-}85)$$

and

$$\frac{a'F\,(1 - aF)}{(1 - a)(1 + a')} = \frac{s\,CL}{4\,Cos\,\phi} \qquad (4\text{-}86)$$

With the incorporation of tip losses into the above relationships, the overall theory is now complete.

Further work was carried out by Anderson (1981) on cyclic effects but concluded that any improvement to the

Theory attributable to cyclic effects were questionable.

4.3.8 VORTEX WAKE THEORY (VWT)

A very much more elaborate technique is the Vortex Wake Theory.

In the Vortex Wake Theory, an analysis technique is used to model the vortex generated in the wake of a wind turbine rotor having a finite number of blades.

When induced velocities are small with respect to the wind velocity, the helical vortex sheets move downstream with a velocity almost equal to the wind velocity. The vortex sheets are assumed to move downstream like a rigid body.

Anderson (1980 & 1981) has developed a Vortex Wake Analysis for HAWT rotors derived from techniques employed in the design of helicopter rotors.

Anderson also compared the results obtained from the Vortex Wake Analysis to those obtained using the Blade Element Theory and found very close correlation with the BET provided a tip loss model was employed. The best correlation occurred with the Goldstein Tip Loss Model.

He concluded that unless information is required about the wake itself, it is satisfactory to use the BET with

a tip loss model.

In view of these conclusions and the considerable amount of computing time required in order to predict performance using this theory, the Vortex Wake Theory has not been employed on this project.

4.4 CPHAWT PROGRAM

A computer program, shown in the appendix, has been developed by the author for use with a microcomputer and is based on the Combined Momentum and Blade Element Theory. This program enables a predicted CP - X curve to be plotted for a wind turbine rotor having known blade shapes and aerofoil section. (See Chapter 6).

REFERENCES FOR CHAPTER 4

Anderson, MB (1980): A Vortex Wake Analysis of a HAWT & A Comparison with a Modified Blade Element Theory, presented at the 3rd International Symposium on Wind Energy System, Copenhagen.

Anderson, MB (1981): An Experimental & Theoretical Study of HAWTs, University of Cambridge.

Betz, A (1927): Windmills in the Light of Modern Research, NACA Tech. Memorandum No 474.

Froude, RE (1889): Transactions of Naval Architects, p390.

Glauert, H (1935): Airplane Propellers, in Durand, WF (ed) 'Aerodynamic Theory'.

Goldstein, S (1929): On the Vortex Theory of the Airscrew, Proc. Royal Society A123, 440.

Jansen, WAM (1976): Horizontal Axis Fast Running Wind Turbines for Developing Countries, SWD.

Joukowski, NE (1912) Soc Math Moscow, reprinted in: Theorie Tourbillionnaire de l'Helice Propulsive, Paris 1929.

Pintz, A et al (1985): Analysis of 1.9 meter Tip Controlled, Three Bladed Rotor for Mod 0 Test Bed, Windpower 85, San Francisco

Prandtl, L (1919): Appendix to Schrauben Propeller Mit Geringstem EnGergieuerlust, by Betz, a Gottinger Nachr.

Rankine, WJM (1865): Transactions, Institute of Naval Architects, Vol 6, p13, 1865).

Theodorsen, Theodore (1944): The Theory of Propellers, NACA Reports, 775, 776, 777, 778.

Theodorsen, Theodore (1948): Theory of Propellers, McGraw Hill.

Wilson, RE & Lissaman, PBS (1974): Applied Aerodynamic Performance of Wind Machines, Oregon State University

Wilson, RE; Lissaman, PBS & Walker, SN (1976): Aerodynamic Performance of Wind Turbines, Oregon State University

a	a'	a' x^2	x
0.25		0	0
0.26	5.5	0.030	0.073
0.27	2.375	0.058	0.157
0.28	1.333	0.086	0.255
0.29	0.812	0.114	0.374
0.30	0.500	0.140	0.529
0.31	0.292	0.166	0.753
0.32	0.143	0.190	1.154
0.33	0.031	0.214	2.619
1/3	0	2/9	

Table 4.1:

Relationships between interference factors and speed ratio.

X	$C_{P_{max}}$	$C_{P^*_{(approx)}}$
0	0	0
0.5	0.288	0.249
1.0	0.417	0.416
1.5	1.5	0.481
2.0	0.513	0.513
2.5	0.533	0.532
5.0	0.571	0.567
7.5	0.583	0.577
10.0	0.585	0.582
	0.593	0.592

Table 4.2:

Relationship between Cp and tip speed ratio.

* refers to equation (4-41)

Fig 4.1: North European 'Classical' traditional windmill

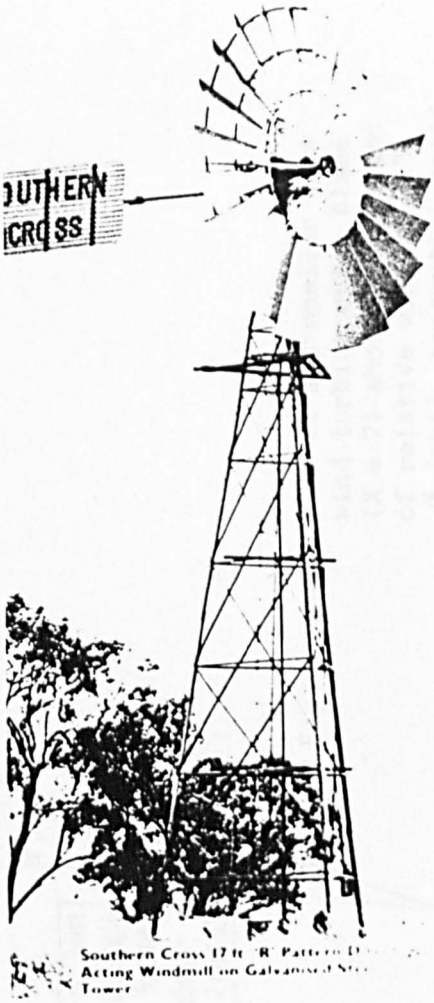

Fig 4.2: Multiblade water pumping windmill

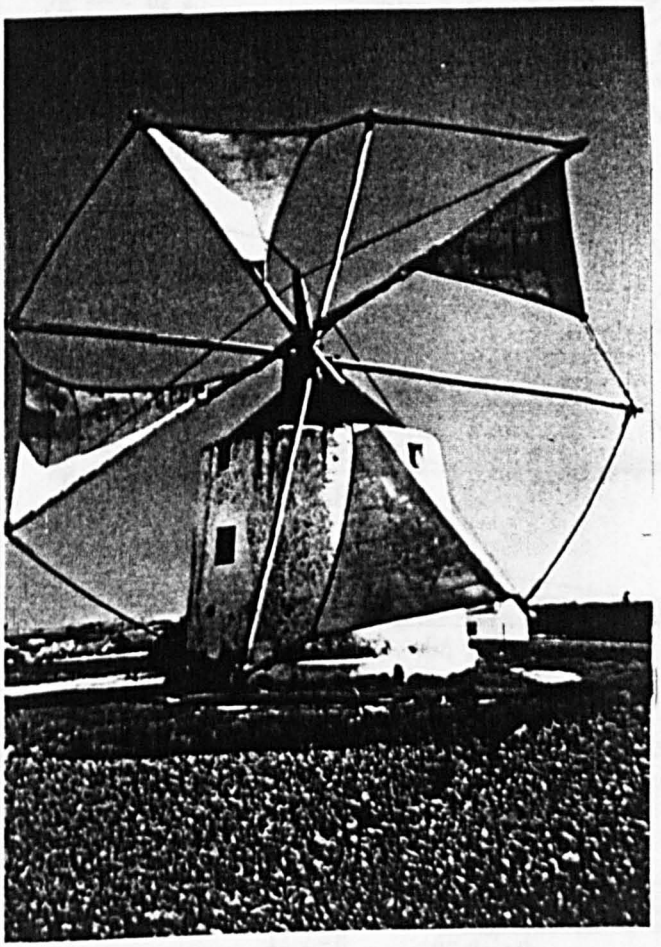

Fig 4.3: Mediterranean type sail windmill

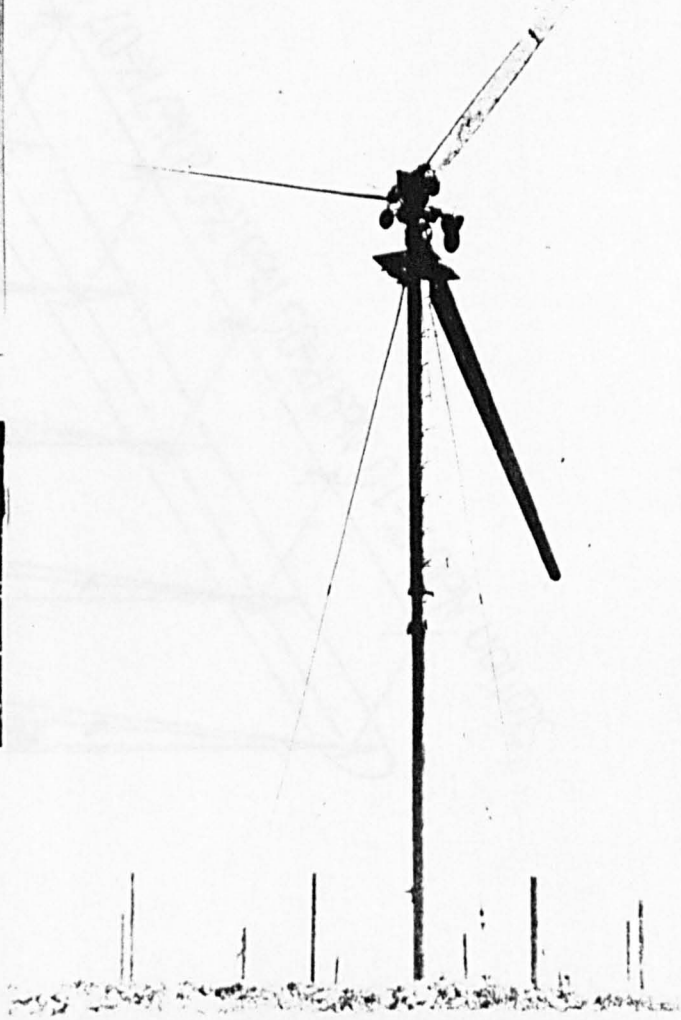

Fig 4.4: Propeller type horizontal axis wind turbine - electricity generating

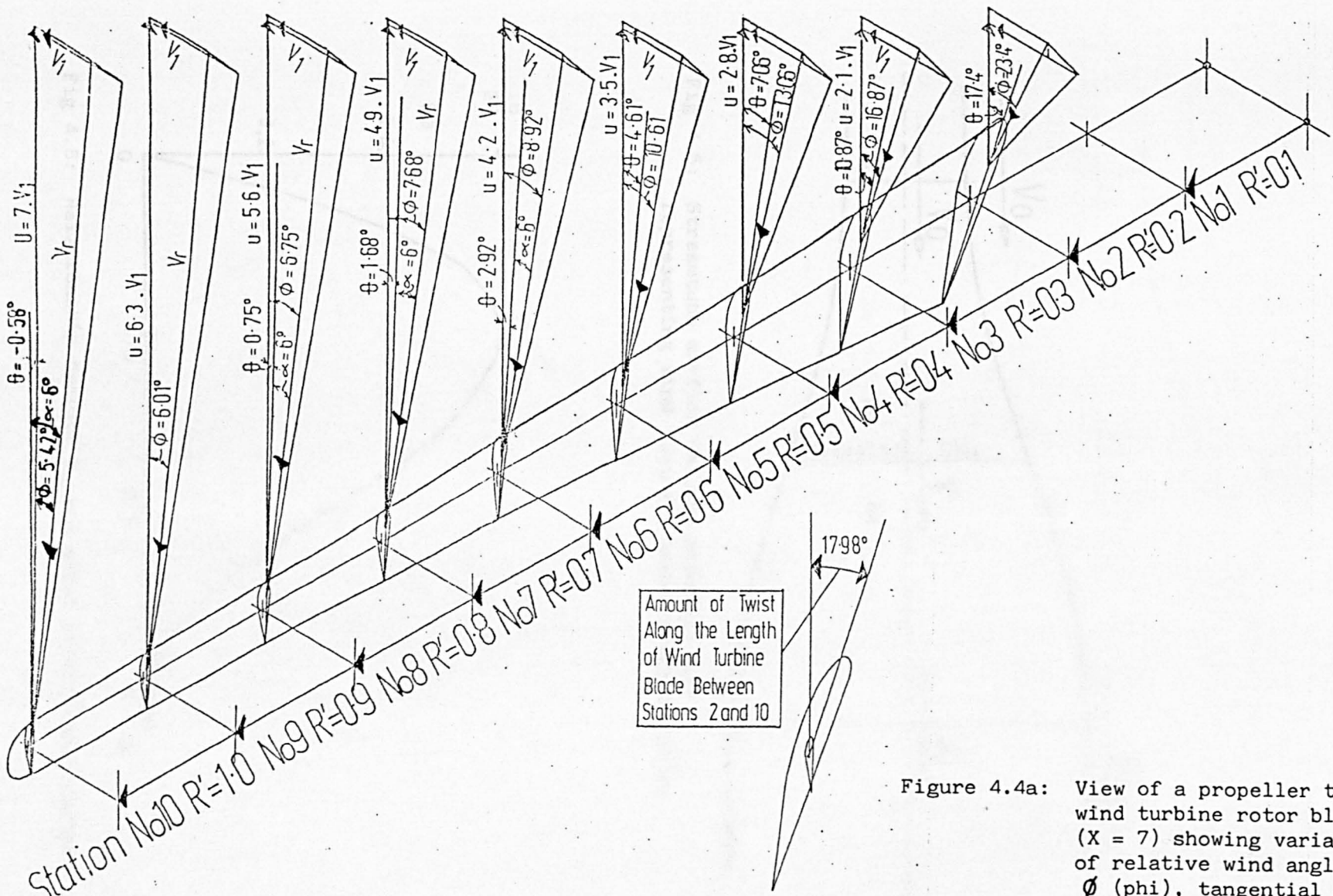

Figure 4.4a: View of a propeller type wind turbine rotor blade (X = 7) showing variation of relative wind angle Ø (phi), tangential speed, U, and blade chord, c, along blade span.

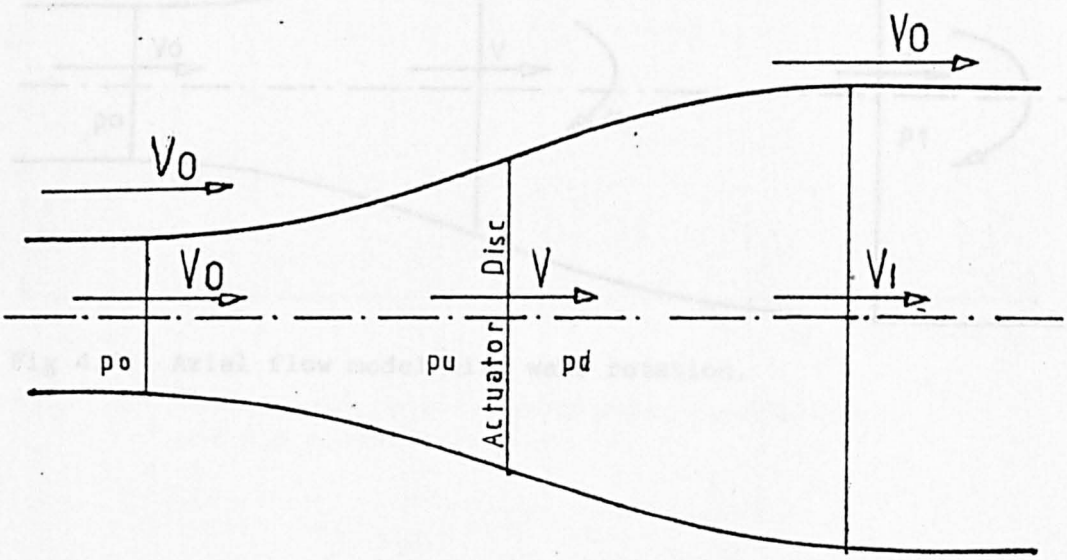

Fig 4.5: Streamtube airflow through actuator disc representing wind tubine - axial momentum theory.

Fig 4.6: Relationship between C_p and axial interference factor.

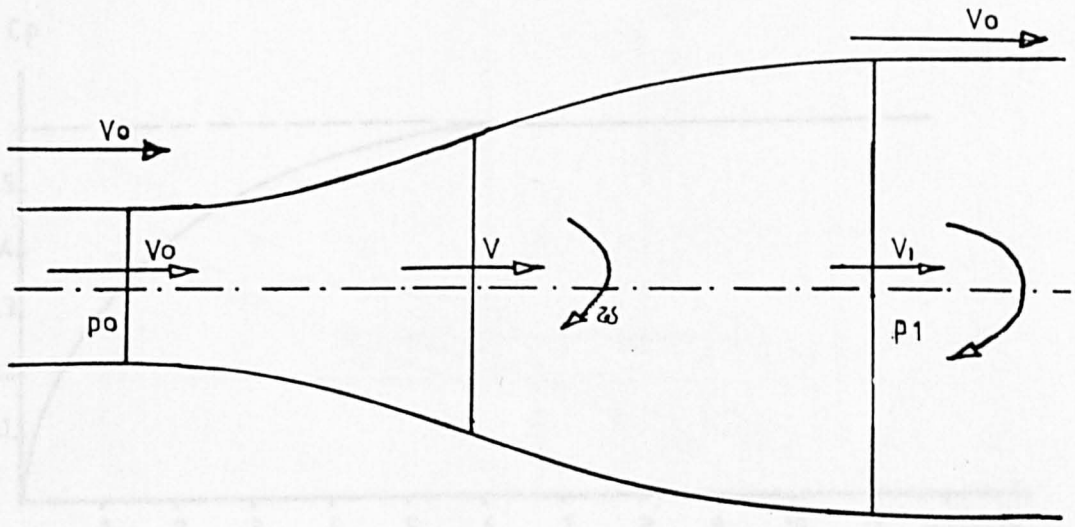

Fig 4.7: Axial flow model with wake rotation.

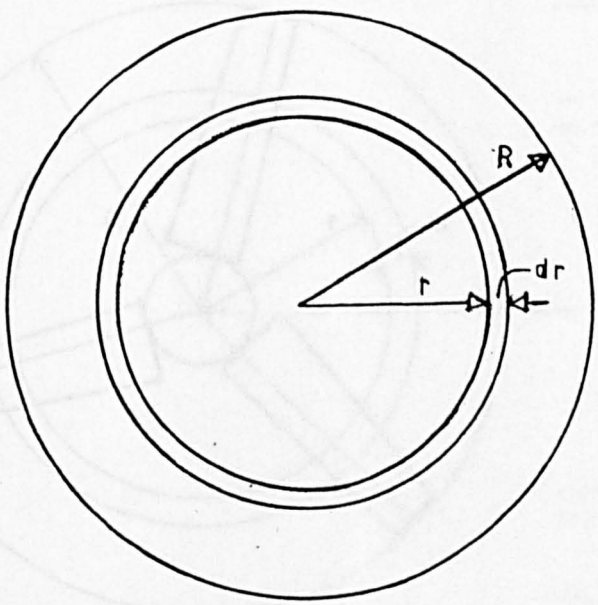

Fig 4.8: Annulus at radius r

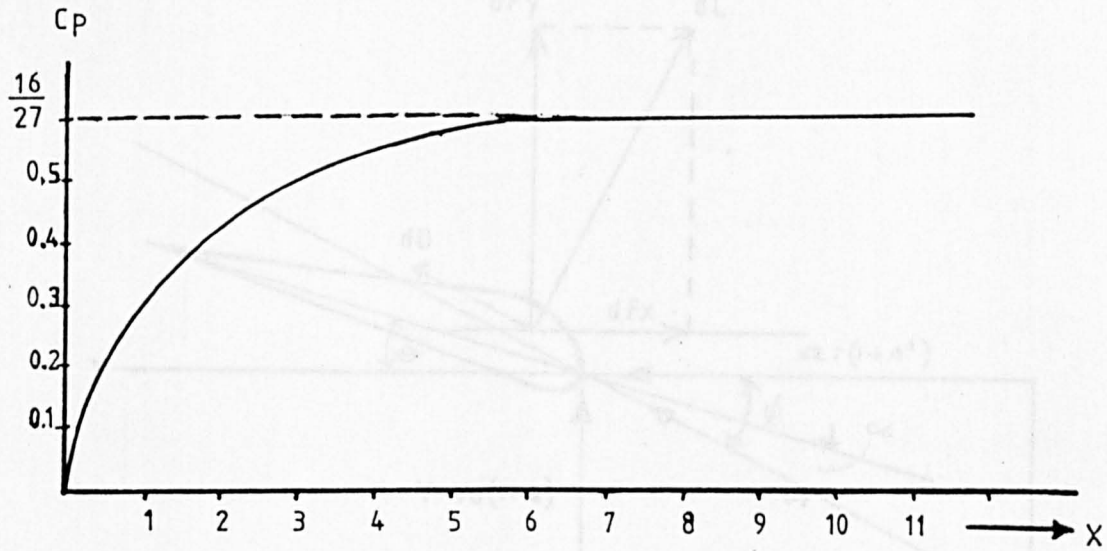

Fig 4.9: Relationship between peak power coefficient and tip speed ratio.

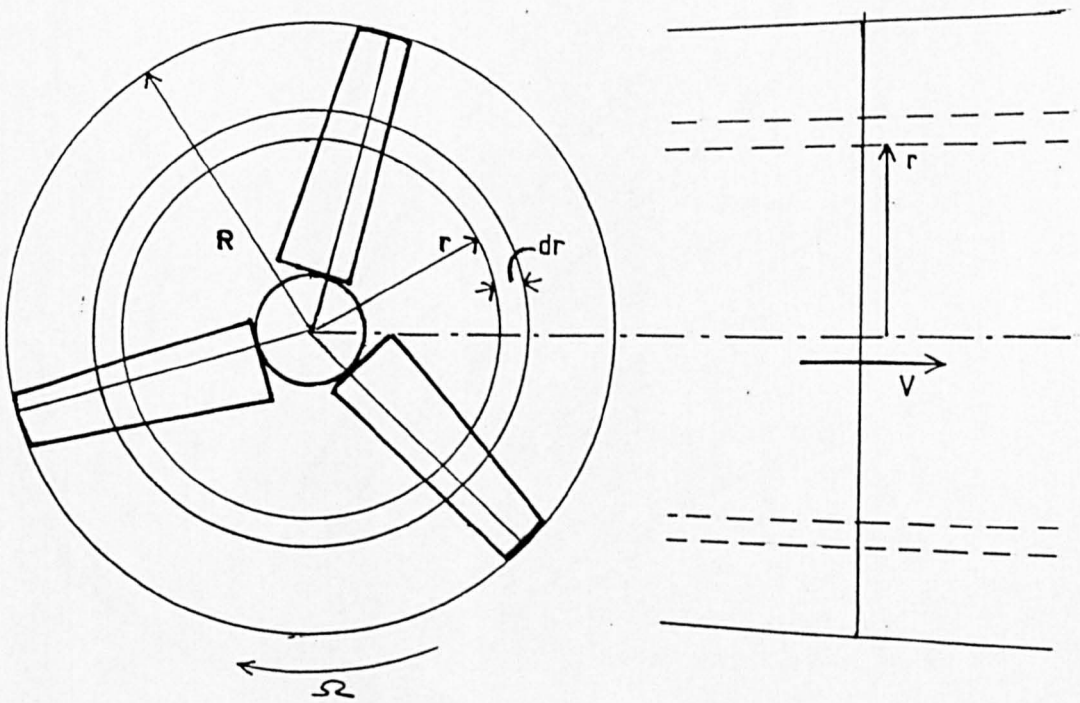

Fig 4.10: Streamtube flow and blade elements.

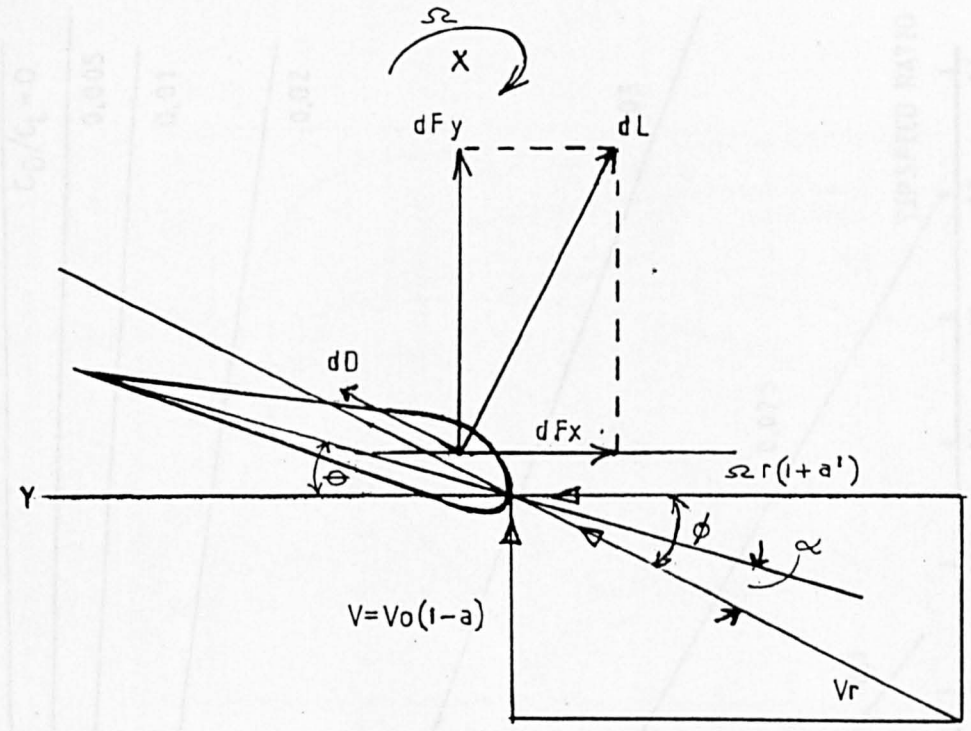

Fig 4.11: Velocity and forces on a blade element at local radius r.

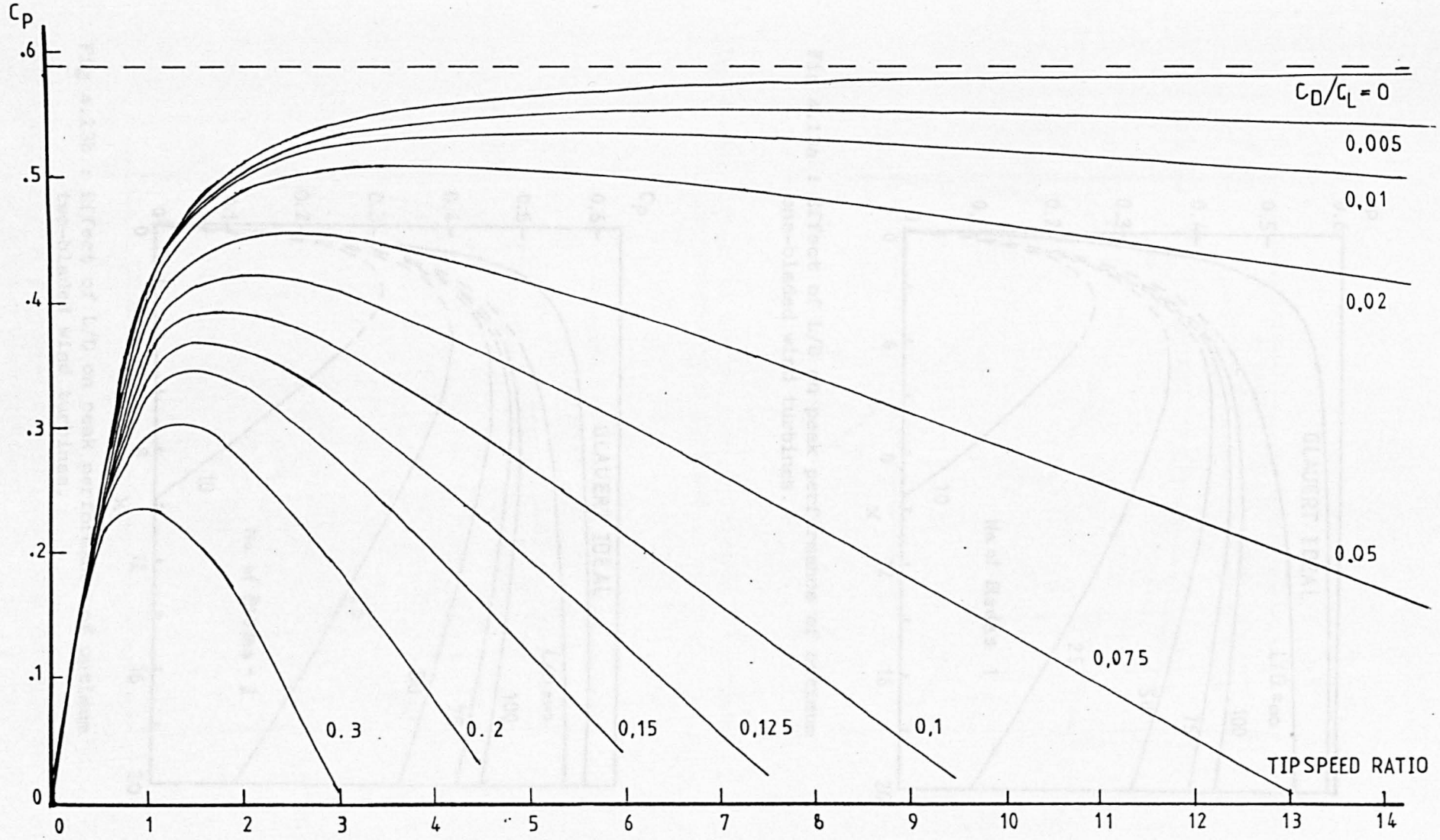

Fig 4.12: C_p-X characteristic of ideal windmills with B=∞

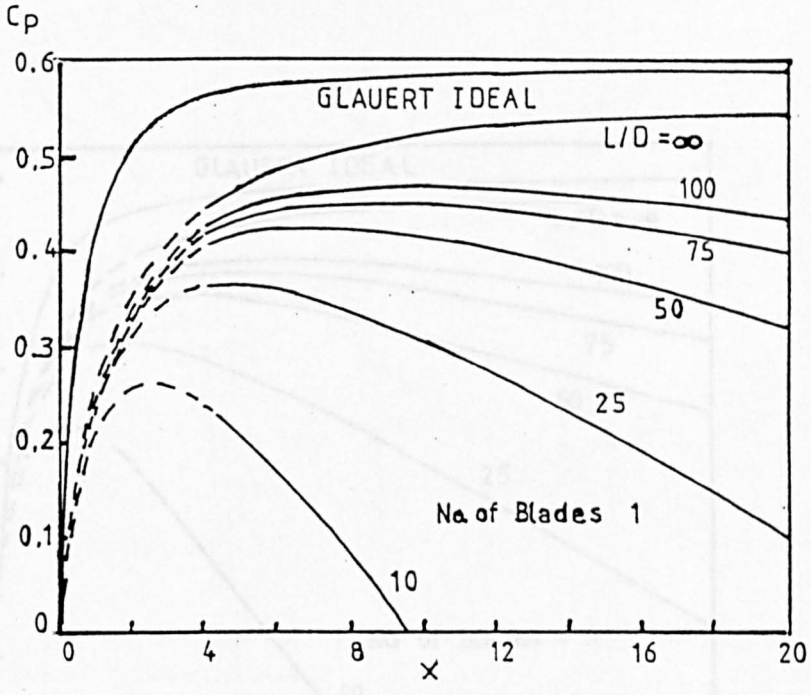

Fig 4.13a : Effect of L/D on peak performance of optimum one-bladed wind turbines.

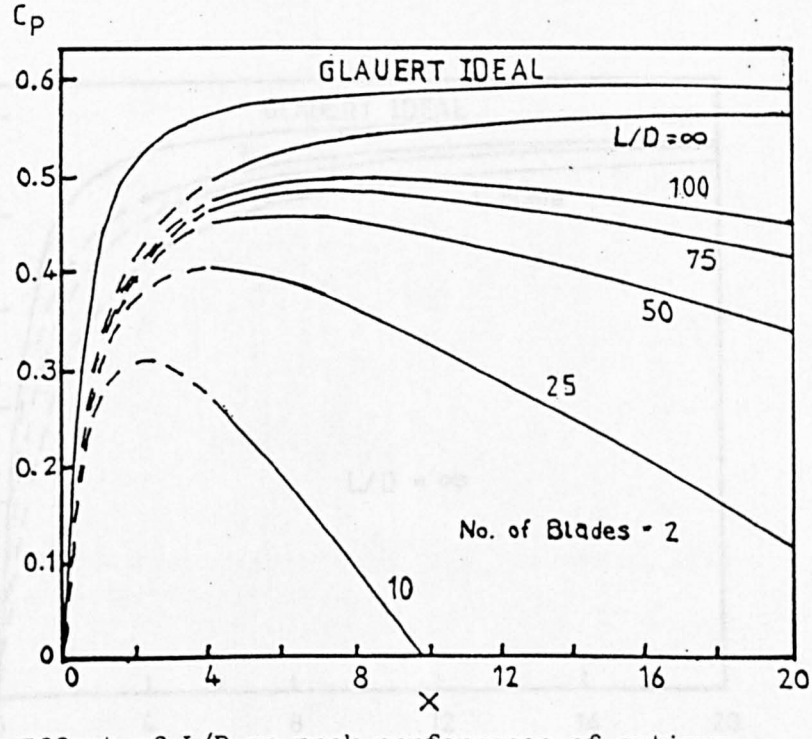

Fig 4.13b : Effect of L/D on peak performance of optimum two-bladed wind turbines.

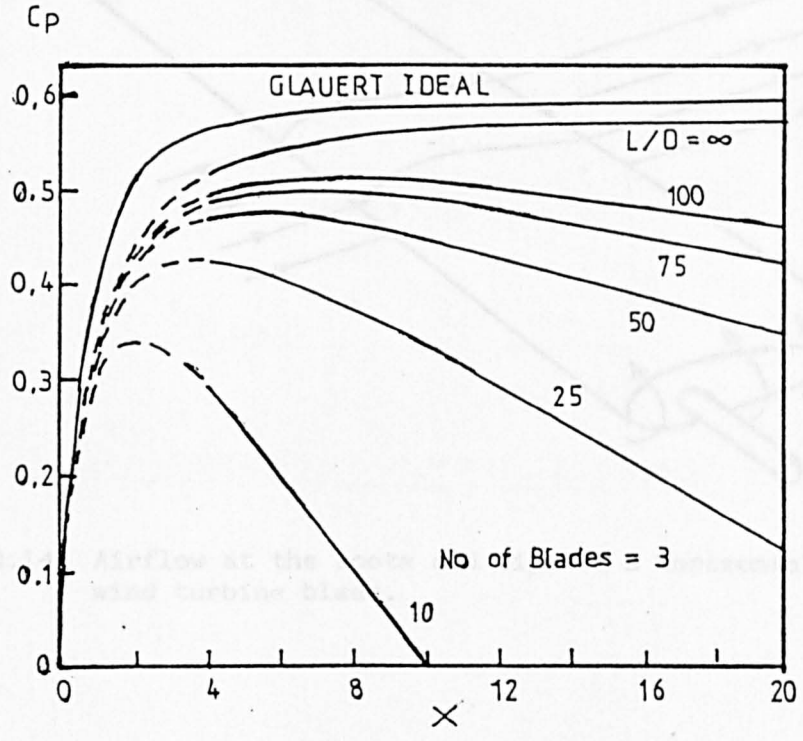

Fig 4.13c : Effect of L/D on peak performance of optimum three-bladed wind turbines.

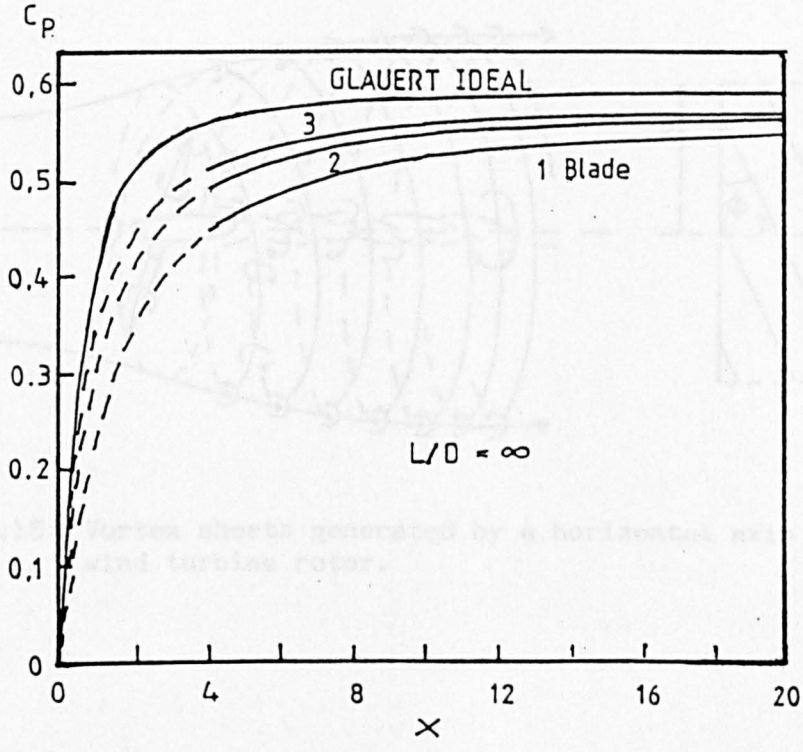

Fig 4.13d : Effect of number of blades on peak performance of optimum wind turbines.

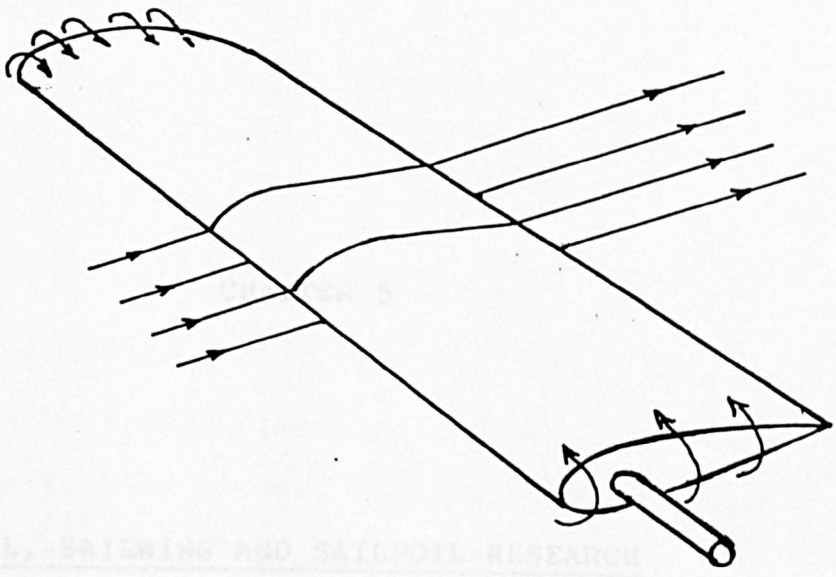

Fig 4.14: Airflow at the roots and tips of a horizontal axis wind turbine blade.

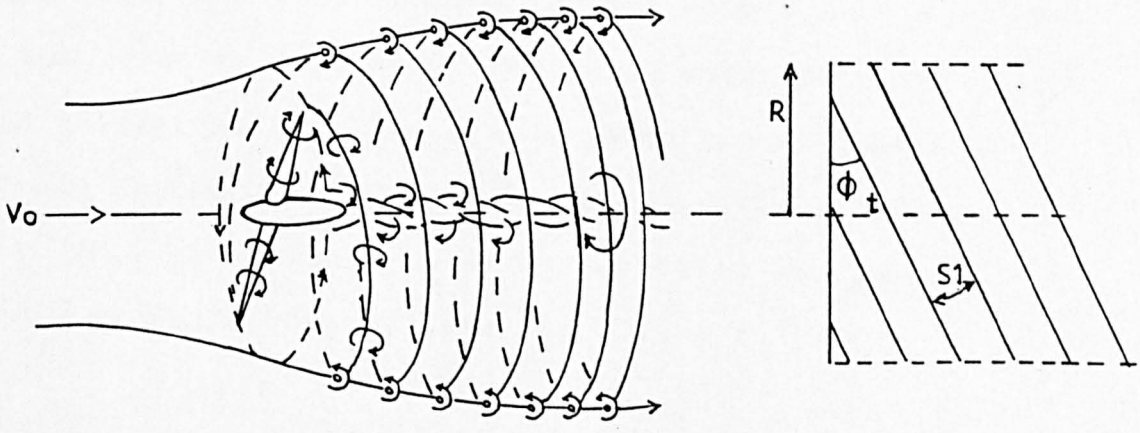

Fig 4.15: Vortex sheets generated by a horizontal axis wind turbine rotor.

CHAPTER 5

SAIL, SAILWING AND SAILFOIL RESEARCH

5.1 SAILS

For the purpose of this work the term 'sail' will be used to describe a wind propelled surface, as used on boats or wind turbine blades, consisting of a single flexible membrane, usually made of fabric.

The use of fabric sails on windmills almost certainly grew out of their use on sailing boats and ships (see Fig 5.1).

As the first sailing boats were 'drag' or 'impulse' devices (eg, they were 'pushed' by the wind); so too were the first sail powered windmills, which rotated around a vertical axis and are believed to have been developed around 2000 BC in China and Persia, (Golding 1955). They consisted of a series of sails attached to a number of radial spokes (see Figs 5.2 & 5.3).

However, probably the most familiar windmills to make use of sails or single membrane blades are the traditional, horizontal axis Mediterranean or Cretan windmills, found in Crete, other areas of Greece, Spain and Portugal, which use triangular shaped cloth sails (Figs 5.4 & 5.5). Also well known are the 'common sails' of the traditional North European or Dutch type

windmills (Figs 5.6 & 5.7), which consist of tanned canvas sheets stretched over a lattice framework (Fig 5.8).

In high winds the sail area exposed to the wind can be reduced, on both the Cretan and Dutch type windmills, by manually furling the sails, either by removing them completely or by rolling them up in a manner not unlike that used on sailing boats.

The Common Sail has been largely replaced by the Patent Sail, Roller Reefing or Shutter Sail and the more efficient Dekkerised Sail, but it is still used on a few Dutch windmills, preserved by the Association for the Preservation of Windmills in Netherlands.

There has been a revival in recent times in the use of the Cretan windmill type of sail rotor, mainly for low speed water pumping and mechanical applications. Various designs have been published, for example: Byrd (1976), Calvert (1975), Fleming & Probert (1982 & 1983), Fraenkel (1975), Mann (1979), National Centre for Alternative Technology (1975), Van de Ven (1977), WESCO (1979), and Windworks (1976). The Steering Group for Wind Energy in Developing Countries (SWD), in the Netherlands, has developed a sail wind turbine with sails similar to the Cretan, except that they are of rectangular planform instead of the triangular sails used previously, (Dekker, 1977).

However, single membrane sails have very poor aerodynamic characteristics, with Lift/Drag Ratios of around 8 (Sweeney, 1975) and most of the Cretan type rotors so far designed are difficult to regulate except by manually furling the sails.

5.2 IMPROVED SAIL TYPE BLADES

Improvements have been proposed in sail wind turbine blades which include:

a) The 'Sailvane', developed at Princeton (Maughmer, 1976): see Fig 5.9.

b) The 'Sailtrouser', developed by SWD (Dekker, 1977): see Fig 5.10.

c) The 'Semi-Sailwing', developed at Princeton (Maughmer 1976): see Fig 5.11

d) The 'Sailwing', developed at Princeton (Sweeney, 1973): see Fig 5.12..

Apart from the Sailvane, all of these design concepts involve the use of a double membrane (or partial double membrane.)

5.3 SAILVANE

The Sailvane is essentially a single membrane type of sail, attached to a streamlined spar of 'teardrop' shape with a tensioned wire Trailing Edge (TE). Various variants of the sailvane have been developed. These include Sailvanes 1 and 2 which have the sail membrane attached to the upper surface of the spar, and feature respectively a more rounded and less rounded Leading Edge (LE); and Sailvane 3 which has the membrane attached to the aft of the streamlined spar (see Fig 5.9).

In wind tunnel tests at Princeton University, Sailvanes 1 & 2 achieved lift to drag ratios of 16 and 18 respectively.

5.4 SAILTROUSER

The Sailtrouser concept, conceived by Jansen (1976) and Dekker (1977) and developed in the Netherlands by SWD, can best be described as a framework consisting of a tubular spar located at a point approximately one third of the chord aft of the Leading Edge, together with tensioned cables located at both the leading edge and trailing edge, over which is stretched a fabric sock (see Fig 5.10).

A horizontal axis Sailtrouser rotor was tested in an open jet wind tunnel of TNO-IWECO in Waddinxveen, in the Netherlands, where the maximum power coefficient CP was found to be 0.27 at a tip speed ratio of about 2.2, and a lift to drag ratio of 10 (Dekker, 1977).

5.5 SEMI-SAILWING

The Semi-Sailwing (see Fig 5.11) is a blade concept that lies half way between a sail and a sailwing (se below). It is a partial double membrane blade, with a rigid leading edge spar and a tensioned wire trailing edge.

Three types of Semi-Sailwing profile were proposed and tested at Princeton University (Maughmer, 1976).

Semi-Sailwing 1 was based on a streamlined tubular spar of teardrop cross section, with the more rounded edge of the tube as the leading edge. Semi-Sailwing 2 was similar to Semi-Sailwing 1, but with the sharper edge of the tube as the leading edge.

Semi-Sailwing 3 was similar to the other two, except that the tubular spar was of circular cross section.

Semi-Sailwings 1,2 & 3 achieved maximum lift to drag ratios of 21, 18, and 13.5 respectively.

So far as the author is aware, no complete wind turbine rotors utilising these blade concepts have been tested.

5.6 SAILWING

The Sailwing type of blade design was developed by Professor Thomas E Sweeney at Princeton University in 1948, (Sweeney, 1973), originally for sailing boats and lightweight aircraft. It has two forms:

1) the 'O Spar' Sailwing
2) the 'D Spar' Sailwing

In basic concept, the Sailwing consists of a rigid leading edge spar, rigid root and tip members, and a wire trailing edge, over all of which is stretched a fabric sock or 'sailsock', see Fig 5.12.

Of these two forms, the 'D Spar' type of Sailwing was found to have by far the best aerodynamic characteristics, having a lift to drag ratio of 29, (Maughmer, 1976) compared to 11 for the 'O Spar' Sailwing, (Sweeney, 1961).

5.6.1 'O SPAR' SAILWING

Despite its relatively poor characteristics, there has been considerable interest in the 'O Spar' Sailwing,

and several other groups apart from Princeton have carried out research on it. Wind tunnel tests on 'O Spar' Sailwing aerofoil profiles have been carried out at NASA Langley (Fink, 1967); McGill University (Robert, 1977); Warwick University (Revell, 1981); and Imperial College (Buehring 1977).

Robert found the best L/D ratio for an 'O Spar' Sailwing to be around 21 for a thickness to chord ratio of 10%.

Various Vertical Axis Wind Turbines (VAWTs) have been built with 'O Spar' Sailwing blades. (Current designs of 'D Spar' Sailwings are not suitable for VAWT application, due to their inability to reverse camber, a feature essential for VAWT operation). These include the New Age Access 'Minimill' (Watson et al, 1978): Low Energy Systems' VAWT (Hurley, 1979) Fig 5.13): and the VAWTs constructed at McGill University (Robert, 1977) and Warwick University (Revell & Everitt, 1980). However, none of these VAWT designs was very efficient.

There have also been a number of Horizontal Axis Wind Turbines utilising 'O Spar' Sailwing blades. These include machines built at Princeton University (Sweeney et al, 1975), the New Alchemy Institute (Sherman, 1973), SWD (Dekker, 1977), and the 'Trimblemill' (1979), see Fig 5.14.

Princeton University tested, on a mobile test facility, a three bladed 3 metre diameter design. This achieved a maximum power coefficient (CP) of 0.17 at a tip speed ratio of about 2.5 (Sweeney et al (1975). The SWD design achieved a maximum CP of 0.24 at a tip speed ratio of about 2.

5.6.2 D SPAR SAILWING

Most of the development work on the 'D Spar' Sailwing has been carried out at Princeton University (Sweeney et all, 1973, 1975) and (Maughmer, 1976).

A series of wind tunnel tests were carried out on 'D Spar' Sailwing profiles (Maughmer, 1976), a maximum L/D ratio of 29 being achieved. See Fig 5.15.

A variety of experimental wind turbines up to 7.6 metres in diameter were built and tested. A series of moving tests were carried out, using a mobile test facility based around a jeep.

Of these tests, a two bladed, 3.65 metre diameter 'D Spar' Sailwing rotor achieved a peak power coefficient CP of 0.4 at a tip speed ratio of around 4.3 (Maughmer, 1976); and a three bladed 3.0 metre diameter 'D Spar' Sailwing rotor achieved a CP of 0.44 at a tip speed ratio of 3.2 (Sweeney, 1975a). See fig

5.16).

The best results were obtained with a very taut trailing edge.

As far as the author is aware, no field testing of a complete 'D Spar' Sailwing wind turbine has taken place at Princeton University. However, a 3.65 metre diameter Princeton-designed 'D Spar' Sailwing HAWT with three blades was tested at Imperial College, (Buehring, 1980), with encouraging, though not conclusive, results due to considerable scatter on the test results which were not binned.

The US Solar Energy Research Institute (SERI) commissioned a study of the Sailwing Wind Turbine concept (Hohenemser et al, 1979). This study concentrated almost entirely on 'D Spar' Sailwing HAWTs.

It concluded that the 'D Spar' Sailwing wind turbine had promise and recommended further experimental work. So far as the author is aware, these recommendations were not acted upon.

The author understands that a company, WECSTECH, has been manufacturing 'D Spar' Sailwing HAWTs in the USA, but at the time of writing only scant information has been obtained.

5.7 SAILFOIL BLADE CONCEPT

Whilst the 'D Spar' Sailwing has been shown to operate successfully in aerodynamic terms, it seems to the author that it had two important disadvantages.

1) The first was associated with the wire trailing edge. In order to maintain the membrane in a smooth condition, the tensioned trailing edge has to take the form of a concave catenary curve. This necessitates very careful control over the tension in the trailing edge wire, both during manufacture and operation, and there is a need for complex tailoring of the trailing edge of the sailsock. This problem is exacerbated in long blades, because the wire needs to be supported by intermediate ribs between root and tip to avoid excessive sagging. Between each of these ribs the trailing edge forms intermediate catenary curves and therefore departs from the ideal shape.

2) The second disadvantage is associated with the ageing characteristics of Dacron, the sailsock material used by Princeton. Dacron has a life of only three to five years in the open air, due to the degrading effects of ultra violet light.

In order to reduce the complexity of the trailing edge

(thus minimising the first of these disadvantages) the author has developed the 'Sailfoil' blade concept, for which the Open University has obtained a Patent (See Fig 5.17).

This is essentially a 'D Spar' Sailwing but with a rigid trailing edge (it will be recalled that 'D Spar' Sailwings were found to perform best with the trailing edge kept very taut). This greatly simplifies the fabrication of the blade framework and the tailoring of the fabric sock. It allows for the possibility of producing quite long blades using this technique and it improves the structural integrity of the blade. In addition, the compressive stresses in the leading edge spar, due to the tension in the trailing edge wire, are eliminated when a rigid trailing edge is used.

The second problem mentioned above, caused by the short life of Dacron, is not so significant. Many wind turbines are designed with tiltable towers, allowing easy access to the rotor and thus facilitating replacement of the blade material. Furthermore, materials can be used which have longer life than plain Dacron, such as semi-synthetic fabrics like Rotex which can last five to seven years in tropical conditions (Dekker, 1977). Polyester fabrics protected against ultra violet light are now available and can have a life of five to ten years. Coating with neoprene or silicone should also extend the life of such materials. However,

cotton or canvas, if proofed against moisture and rot, may achieve satisfactory life spans in Third World countries where more exotic materials may be difficult or expensive to obtain.

It was also felt that the Sailfoil blades would be suitable for production by small wind turbine companies, given that the sailmaking skills are widely available and that mass-produced components, such as tubes, can be used for critical load-bearing elements like spars.

To evaluate the concept, it was therefore decided to design, build and field test a four metre diameter Horizontal Axis Wind Turbine using three sailfoil blades.

REFERENCES FOR CHAPTER 5

Bird, AB (1976): Reinforced Brickwork Windmill Tower, Structural Clay Products, SCP 12

Buehring, I (1977): Performance Characteristics of Simple Aerofoils for Windmill Applications, Imperial College

Buehring, I (1980): The Development, Control & Testing of an Aerogenerator, Imperial College

Calvert, NG (1975): The Mono-Kairos Windmills of Lasithi

Dekker, TAH (1977): Performance Characteristics of Some Sail & Steel Bladed Wind Rotors, SWD Publication 77-5

Fink, M (1969): Full Scale Investigation of the Aerodynamic Characteristics of a Sailwing of Aspect Ratio 5.9, NASA Langley Research Center

Fleming, PD & Probert, SD (1982): Design & Performance of a Small Shrouded Cretan Wind Wheel, Applied Energy, Vol 10, pp 121-139

Fleming, PD & Probert, SD (1983): 'Optimising the Designs of Flexible-Sail Wind Turbines', Proceedings, BWEA Conference

Fraenkel, P (1975): Food from Windmills, ITDG Publications

Golding, EW (1975): The Generation of Electricity by Wind Power, Spon

Hohenemser, KH et al (1979): A Definitive Generic Study for Sailwing Wind Energy Systems, SERI/TR-98003-05

Hurley, B (1979): A Novel Vertical Axis Sail Rotor, Proc, 1st BWEA Wind Energy Workshop

Jansen, WAM (1976): Horizontal Axis Fast Running Wind Turbines, SWD publication, SWD 76-3

Mann, RD (1979): How to Build a 'Cretan Sail' Wind Pump, ITDG Publications

Maughmer, MD (1976): Optimisation and Characteristics of a Sailwing Windmill Rotor, AMS Report No 1297, Princeton University

National Centre for Alternative Technology (1975): Construction Plans for a Cretan Type Sail Windmill

Revell, PS & Everitt, KW (1981): 'Wind tunnel Tests of

Sailwings for Darrieus Rotors', Wind Engineering, Vol 5 No 2, pp 73-90

Revell, PS & Everitt, KW (1980): 'Sailwing Darrieus Rotors', Wind Engineering, Vol 4 No 1, PP 11-31

Sherman, MM (1973), The Sailwing Windmill and its Adaptation for Use in Rural India, Proc, Wind Energy Conversion Systems Workshop, Washington

Sweeney, TE (1961): Exploratory Sailwing Research at Princeton, Dept of Aero Engineering, Princeton University, report 578

Sweeney, TE (1973): Princeton Windmill Program, AMS Report No 1093, Princeton University

Sweeney, TE & Nixon, WB (1973): An Introduction to the Princeton Sailwing Windmill, AMS Report No 1106, Princeton University

Sweeney, TE et al (1975a): Sailwing Windmill Characteristics & Related Topics, AMS Report No 1240, Princeton University

Sweeney, TE et al (1975b): The Performance of a 2 Bladed Sailwing Windmill Rotor & Related Topics, AMS Report No 1254, Princeton University

Trimble Windmills: Manufacturer's brochure about the Trimble-mill

Van de Ven, N (1977): Construction Manual for a Cretan Windmill, SWD Publication SWD 77-4

WESCO Windmills (1979): Manufacturer's brochure about Cretan windmill kit, WESCO Windmills, Peacehaven

Windworks, (1976): Construction Plans for 25 Feet Diameter Cretan Type Sail Rotor, Windworks, USA

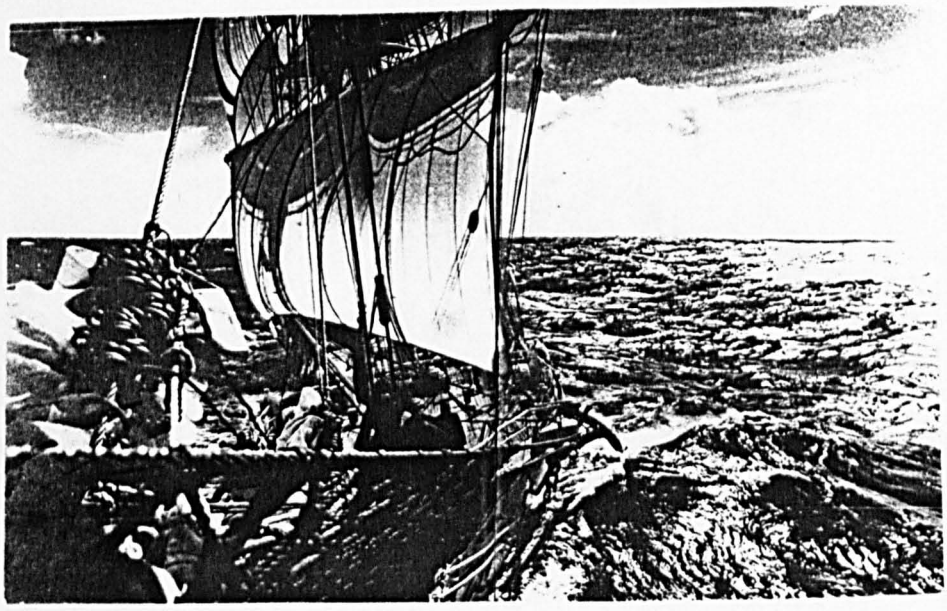

Fig 5.1: Sailing ships are thought to be the first application

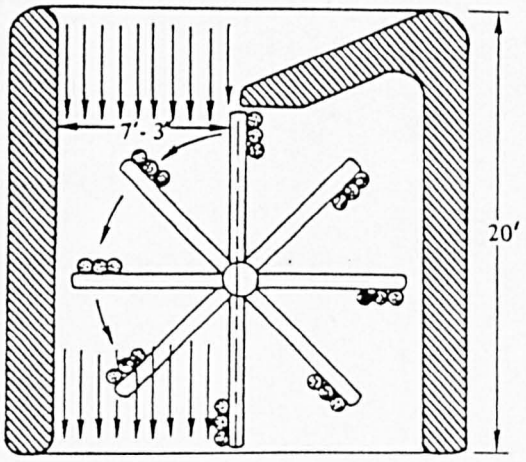

Fig 5.2: Persian Vertical Axis sail windmill (cross section)

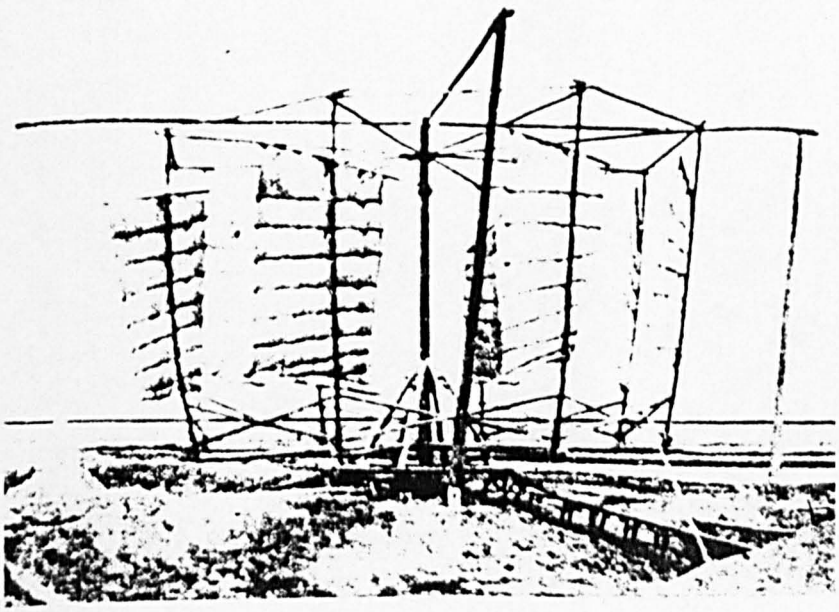

Fig 5.3: Chinese Vertical Axis sail windmill

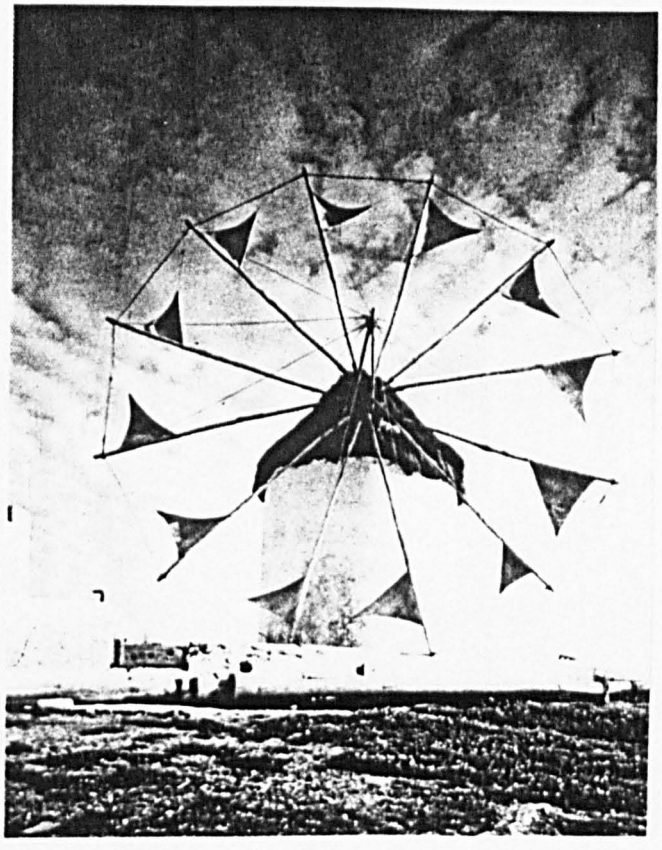

Fig 5.4: Mediterranean sail type windmill.
(Windmills of this basic shape are found all over the Mediterranean and in Portugal)

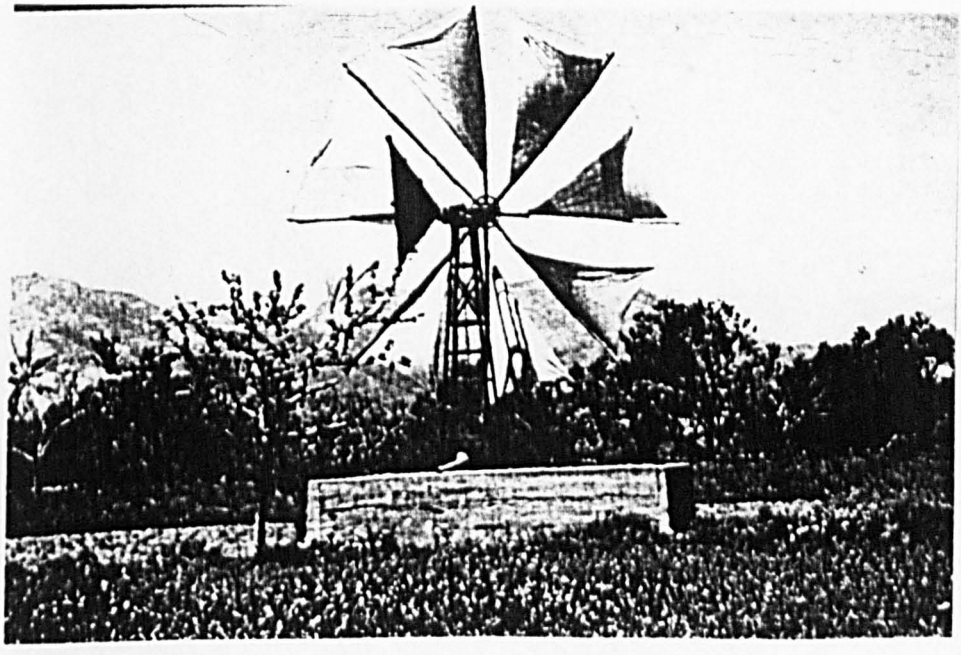

Fig 5.5: Cretan water pumping sail windmill used for irrigating vegetable plots

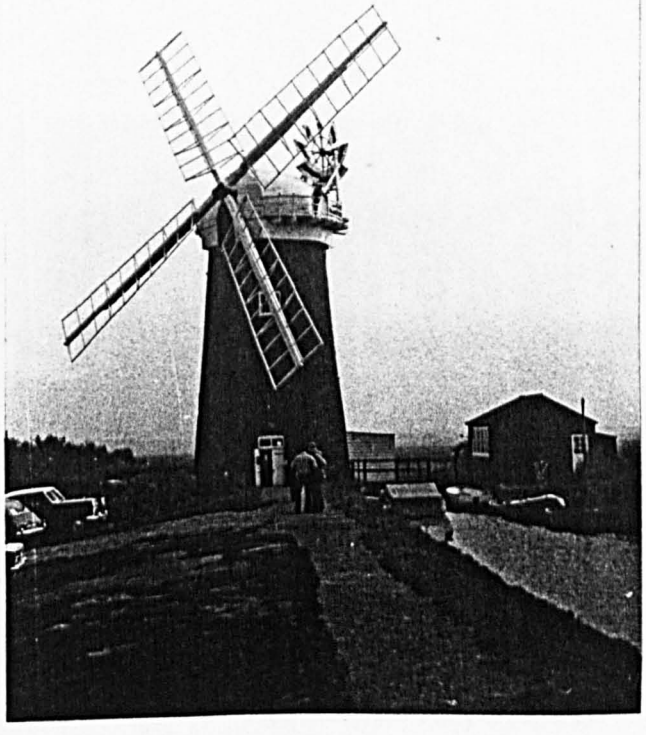

Fig 5.6: North European traditional windmill (English type) showing lattice framework over which 'Common sails' are stretched when working.

Fig 5.7:

Traditional windmill (Dutch type) showing slightly different lattice framework for sails.

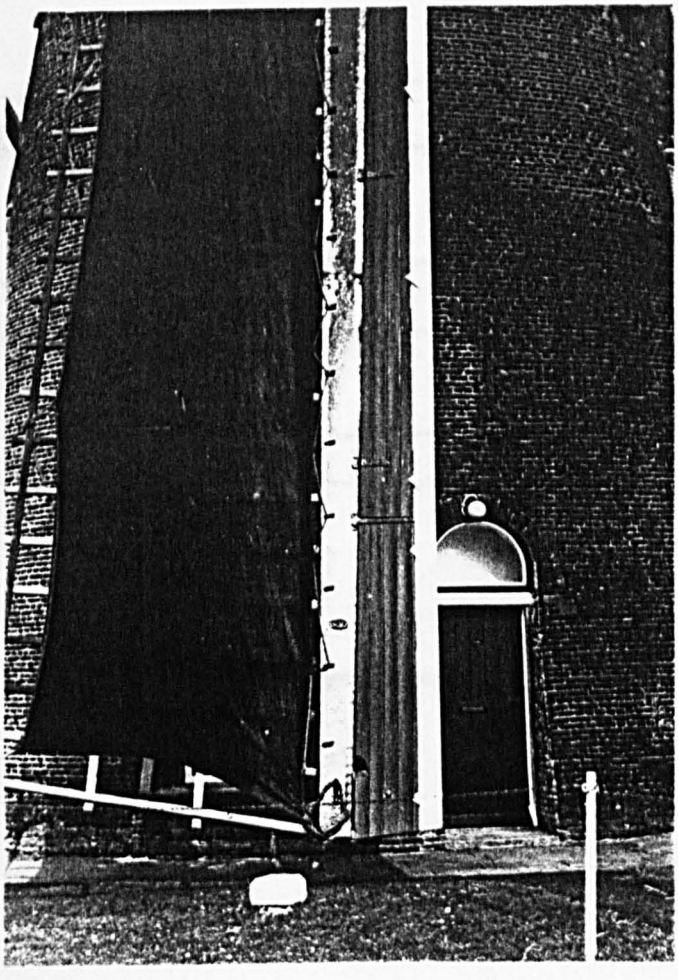

Fig 5.8 : Close up of common sail framework

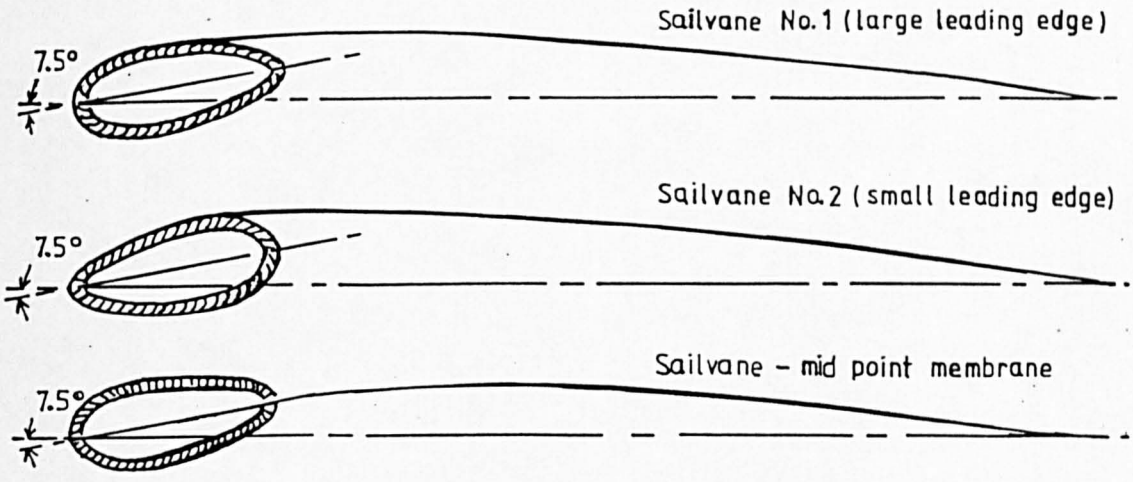

Fig 5.9: "Sailvane" profiles.

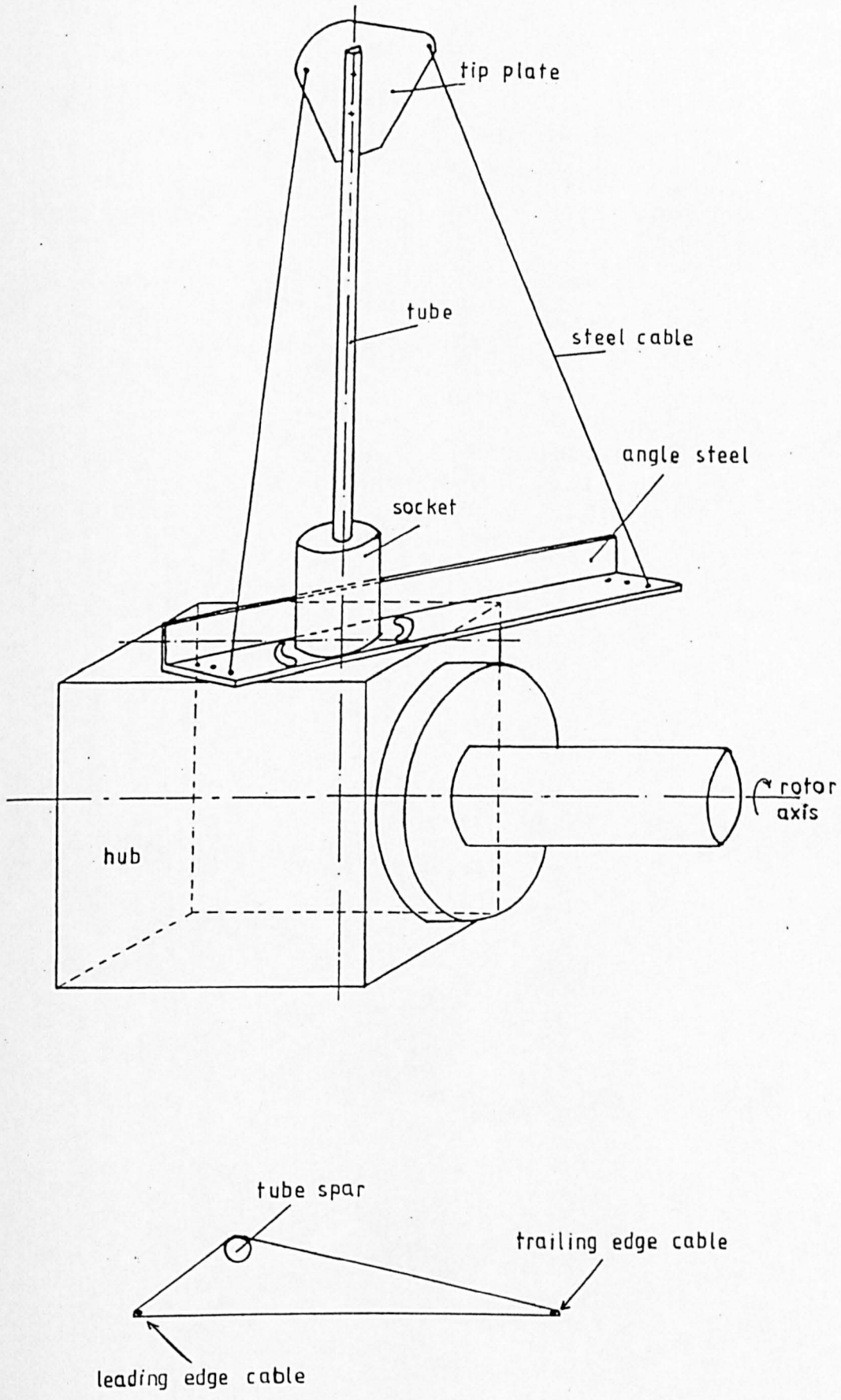

Fig 5.10: Sketch of the construction of a sailtrouser rotor blade mounted on a hub on the rotor axis.

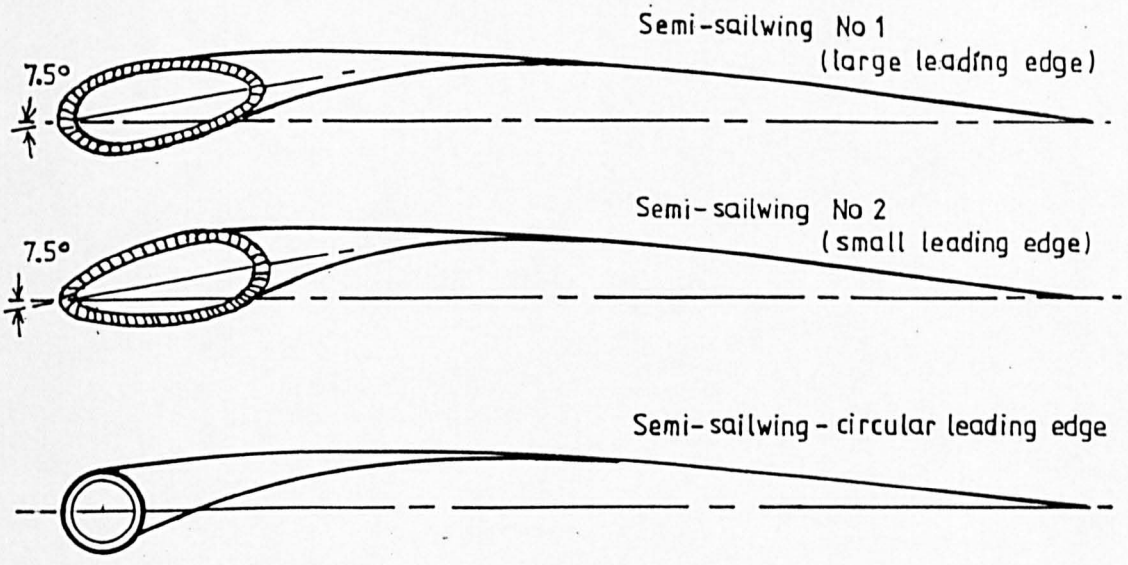

Fig 5.11: Semi-Sailwing profiles.

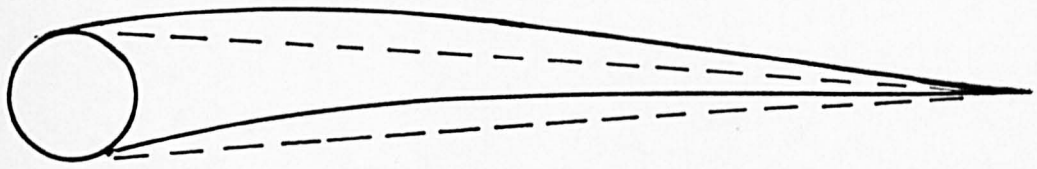

Round spar configuration.

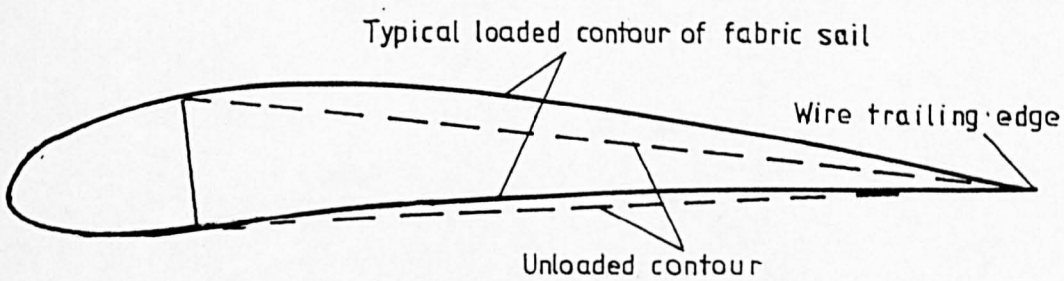

D spar configuration.

Fig 5.12: Typical cross-sectional views of the D spar and Round spar configurations.

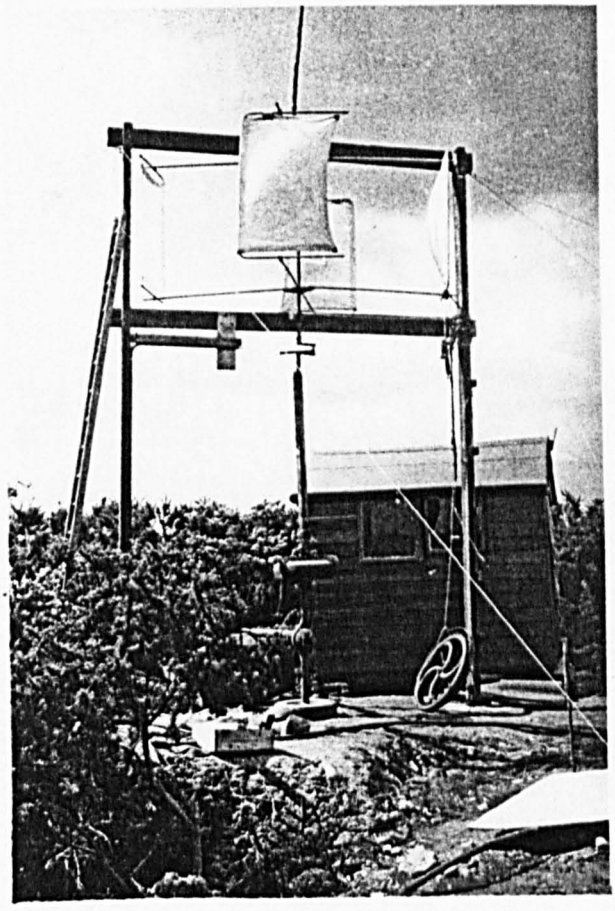

Fig 5.13:

Low Energy Systems vertical axis wind turbine utilising '0 Spar' sailwing blades.

(Hurley, 1979)

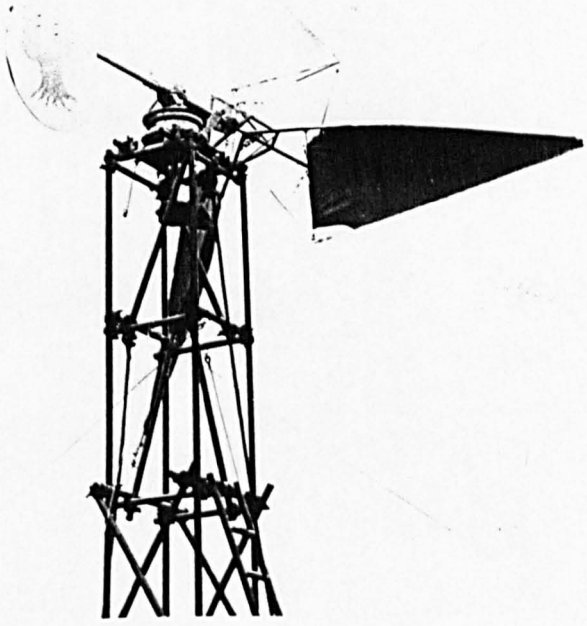

Fig 5.14:

Street Farmers horizontal axis wind turbine utilising '0 Spar' sailwing blades.

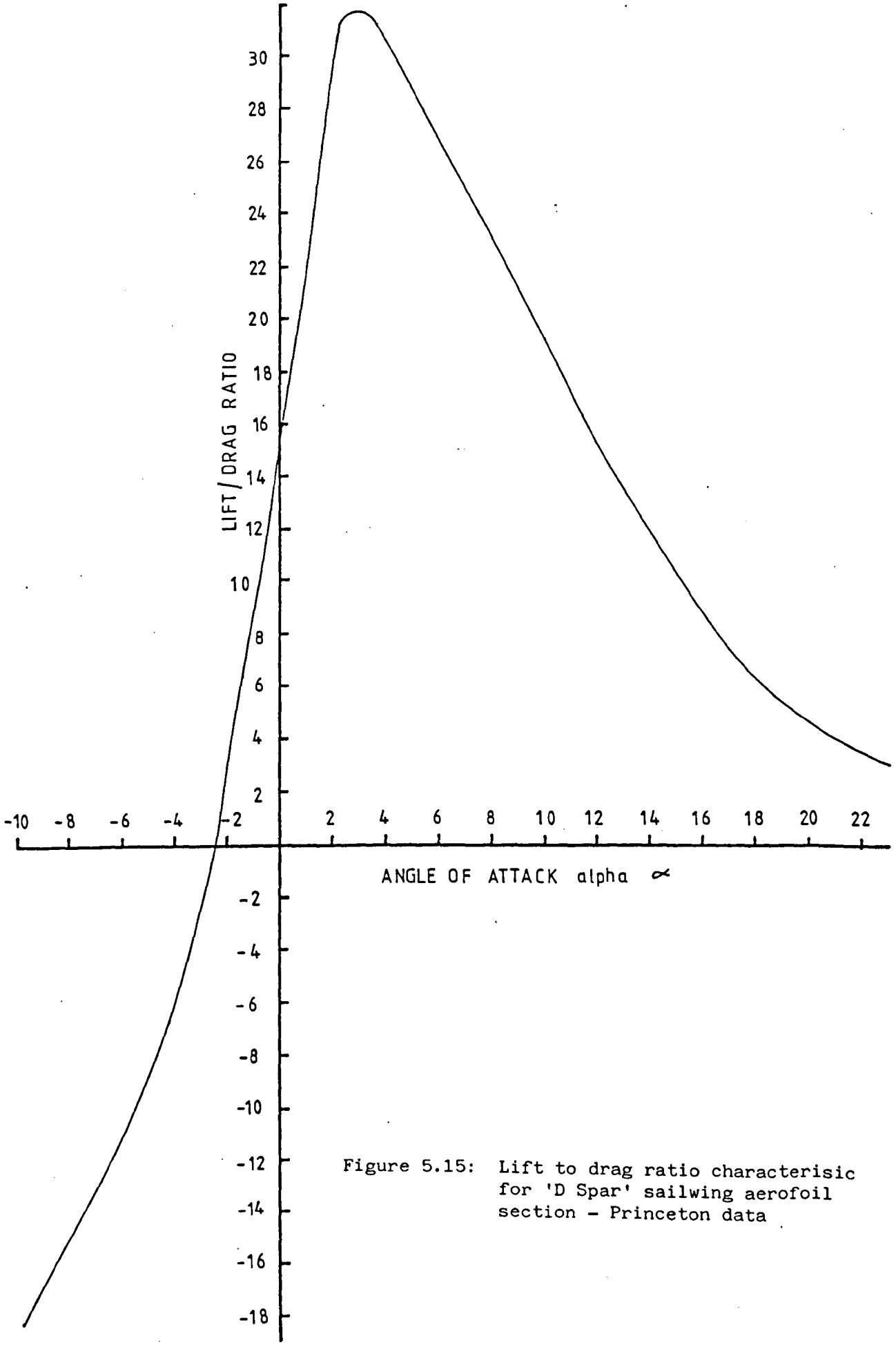

Figure 5.15: Lift to drag ratio characterisic for 'D Spar' sailwing aerofoil section - Princeton data

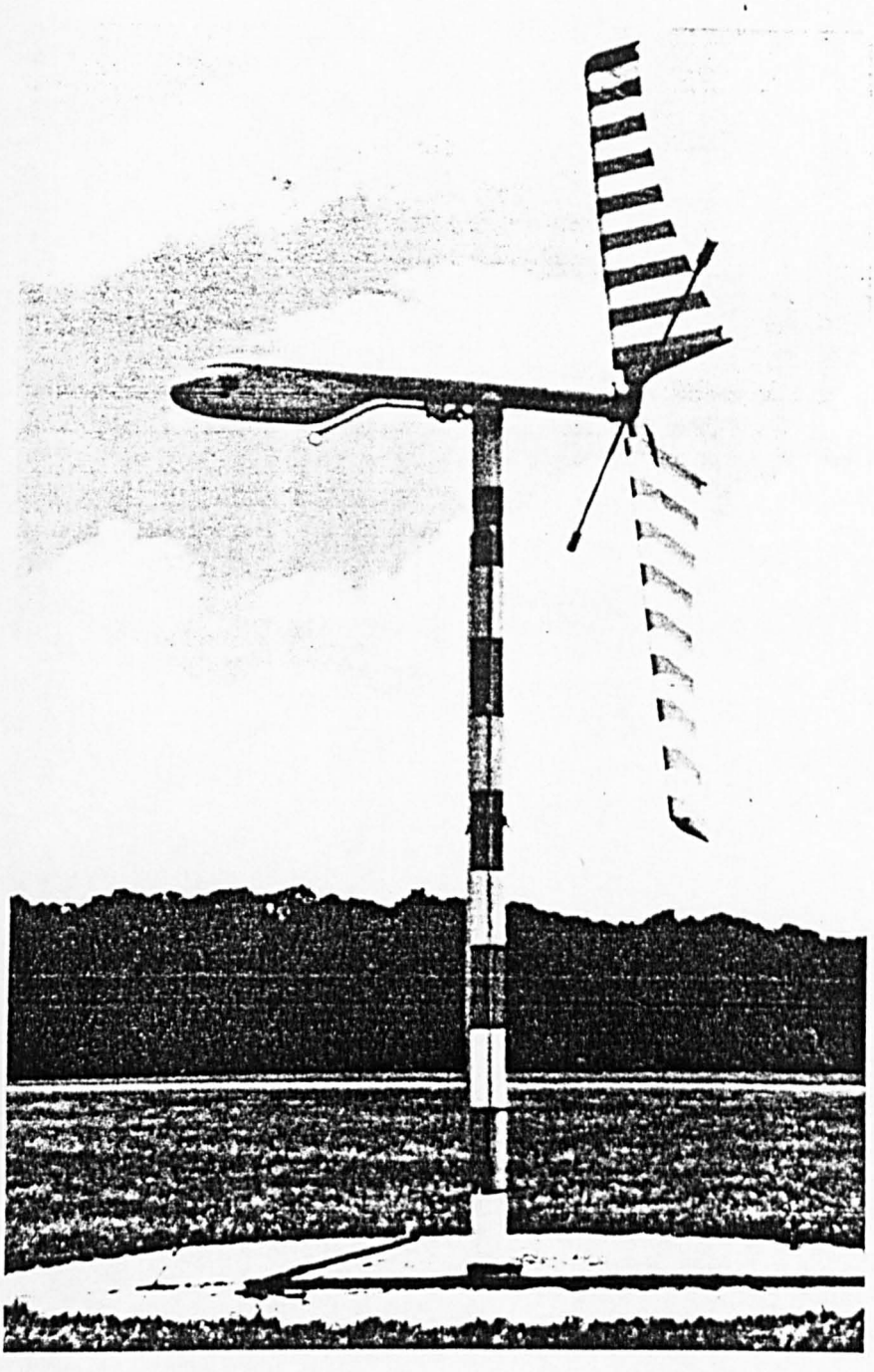

Figure 5.16a: Princeton University 25 ft diameter 'D Spar' Sailwing wind turbine

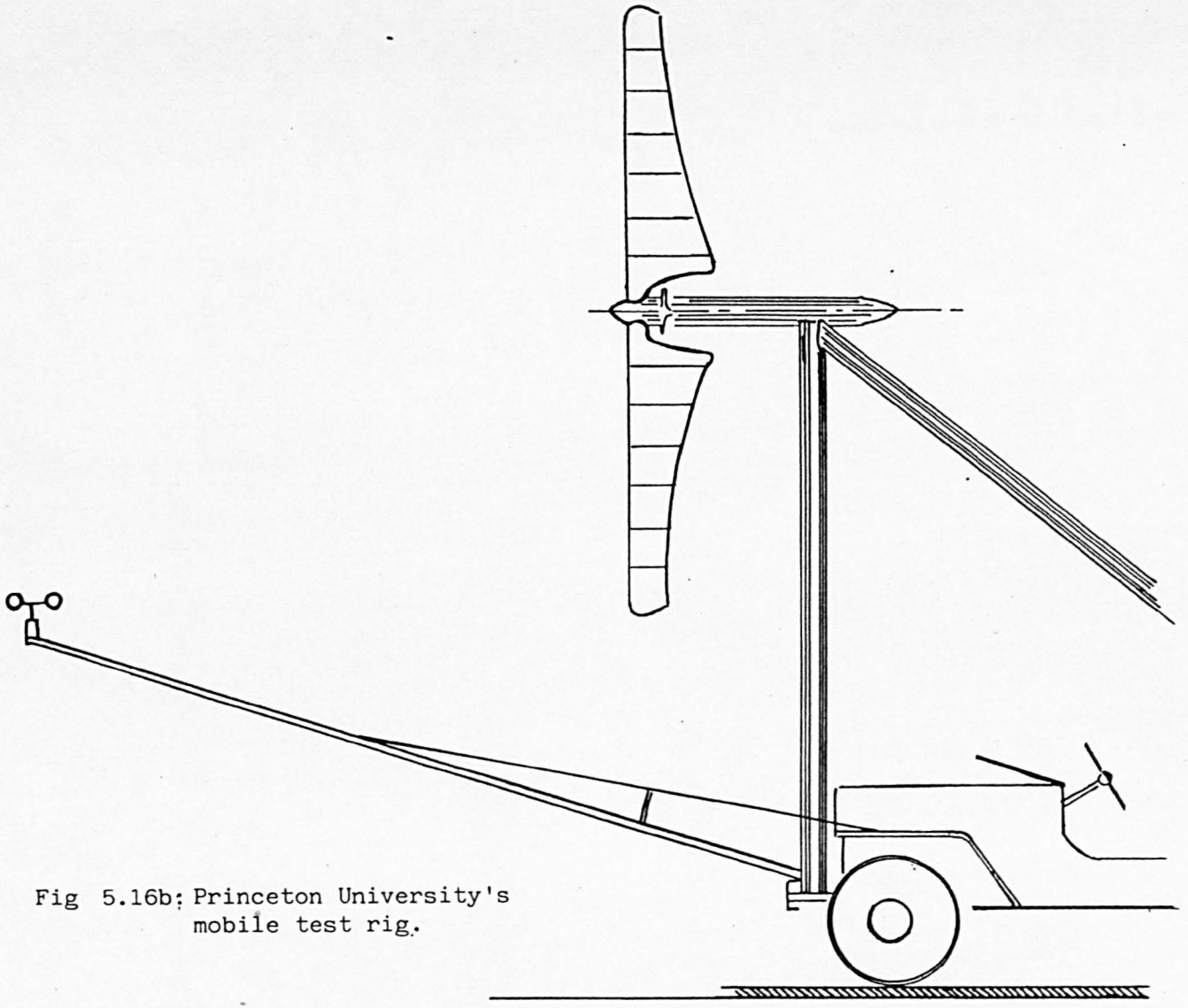

Fig 5.16b: Princeton University's mobile test rig.

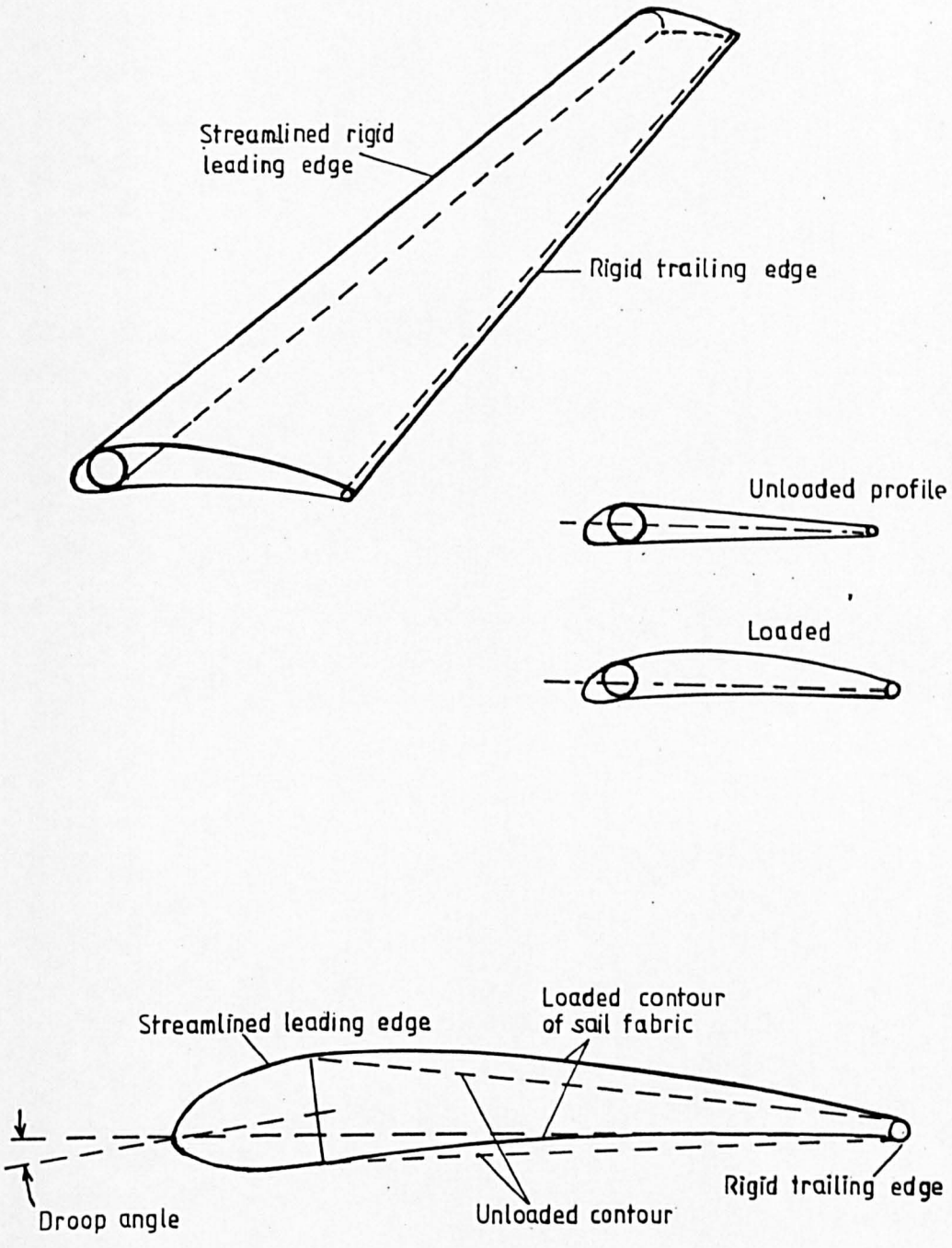

Fig 5.17a: "Sailfoil" wind turbine blade.

Fig 5.17b: Detailed view of sailfoil blade framework

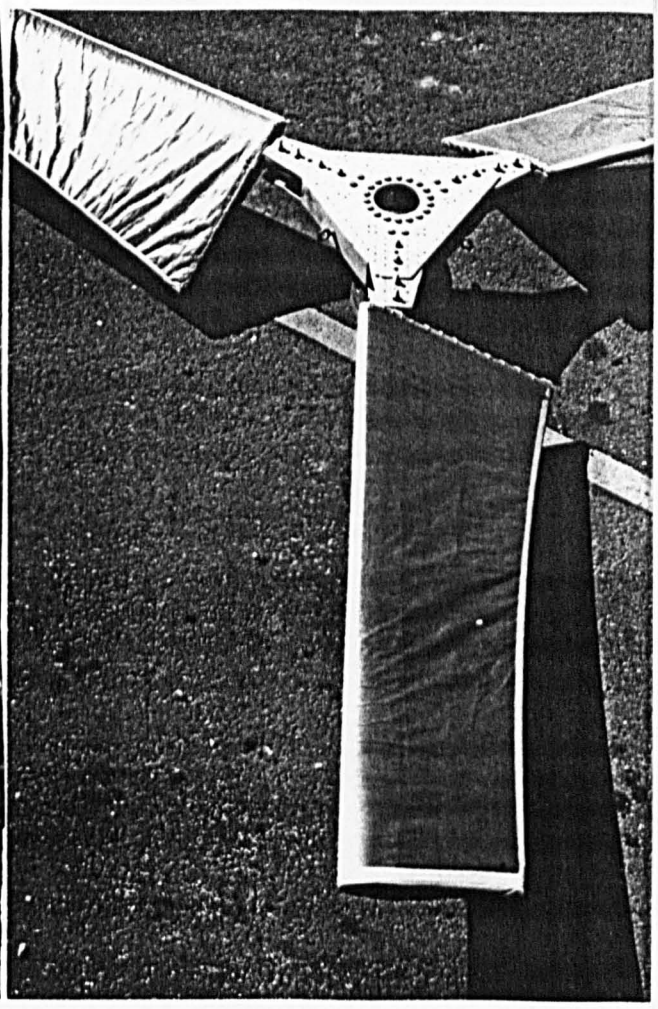

Fig 5.17c: Detailed view of sailfoil blade covered with polyester sock

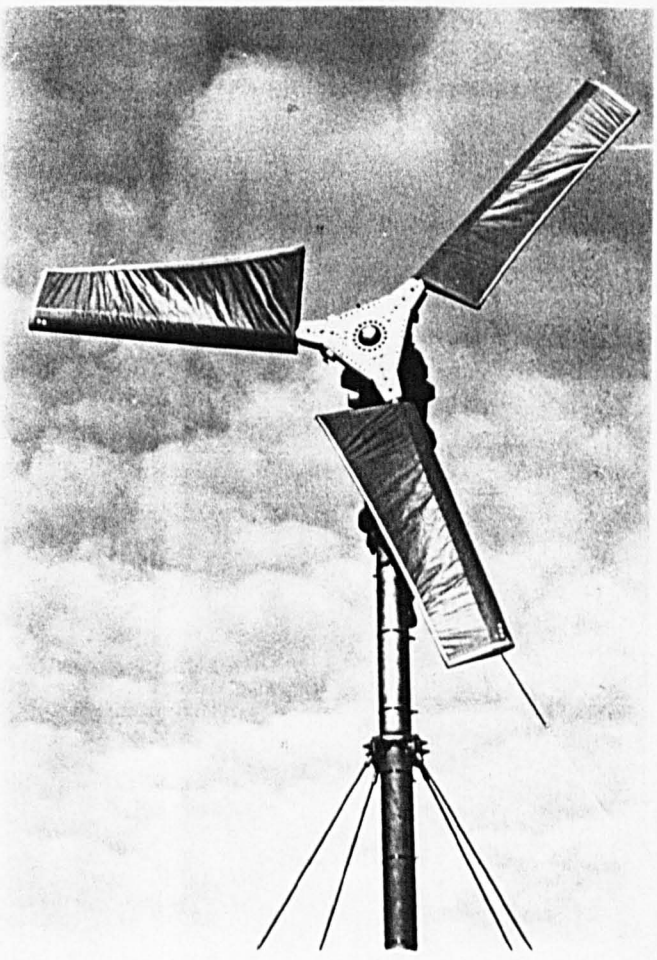

Fig 5.18:

4 m diameter horizontal axis wind turbine rotor utilising 3 sailfoil blades

CHAPTER 6

AERODYNAMIC DESIGN OF A SAILFOIL HORIZONTAL AXIS WIND TURBINE

LIST OF SYMBOLS FOR CHAPTER 6

al = Ω r Cos ϕ (see fig 6.4)

B = number of blades in rotor

bl = (Vo - dl) Sin ϕ (see fig 6.4)

c = chord width of blade element at radius eq (6-8), (6-9)

cl = dl Sin ϕ (see fig 6.4)

c(r) = chord of the blade at the root, eq (6-10)

c(t) = chord of the blade at the tip, eq (6-10)

CL = lift coefficient of aerofoil section, eq (6-8)

dl see fig 6.4

L/D = lift to drag ratio of aerofoil section

r = local radius of blade element or station (m) eq (6-1)

r(r) = radius of root of blade (m), eq (6-1)

R = tip radius of rotor (m), eq (6-1)

R' = station radius ratio = r/R, eq (6-1)

TC = the taper constant of linearised tapered blade, eq (6-10)

u = local tangential speed of blade element

Vo = undisturbed wind speed upstream of wind turbine rotor m/s, eq (6-2)

Vr = relative wind velocity m/s, eq (6-2)

W = induced velocity resultant at radius r m/s eq (6-2)

X = tip speed ratio of wind turbine rotor

x = local speed ratio of blade element at radius r (m), eq (6-2)

α = alpha = angle of attack of blade element at radius r, eq (6-7)

γ = gamma = arctan D/L ratio, eq (6-8)

ϕ = phi = relative wind angle at blade element at radius r, eq (6-7)

θ = theta = blade pitch angle

6 AERODYNAMIC DESIGN

Using procedures developed by the author (Taylor, 1978), and Jansen & Smulders (1977), a computer program 'Windrotor' was produced in order to assist in the aerodynamic design of a four metre diameter propeller-type HAWT with sailfoil blades.

6.1 DESIGN PROCEDURE

In the Windrotor program, the design procedure for the aerodynamic design of a HAWT rotor is carried out in the following sequence:

1) Selection of tip speed ratio and the number of blades

2) Selection of aerofoil aerodynamic data

3) Division of blade span into a number of equidistant stations

4) Calculation of local speed ratio (x) at local radius r

5) Calculation of relative wind angle (phi) at r

6) Calculation of blade pitch angle (theta) at r

7) Calculation of blade chord (c) at r

Steps 4 to 7 are repeated for each station.

The flow diagram for the Windrotor computer program is shown in the appendix.

6.2 SELECTION OF TIP SPEED RATIO X AND NUMBER OF BLADES B

Low speed wind turbines have tip speed ratios less than 2, medium speed wind turbines have tip speed ratios between 2 and 5, high speed turbines have tip speed ratios between 5 and 10, and very high speed wind turbines have tip speed ratios between 10 and 15.

The decision to design the sailfoil wind turbine as a medium speed rotor with a design tip speed ratio, X, of 4 was arrived at for the following reasons.

1) The sailfoil rotor was to be coupled to an alternator rather than a water pump (though there could be a water pumping variant) so there is no necessity for high starting torque, or for very low running speed.

2) On the other hand, high tip speed ratio, small scale wind turbines spin at fast rotation speeds. They are therefore more sensitive to imbalance in the rotor

and could be hazardous if not manufactured carefully.

3) A high tip speed ratio machine also accumulates more cycles of operation during a given time period and this has an adverse effect on the lifetime of the blades.

4) There was some uncertainty as to how the fabric blades could stand up to fast rotation speeds.

5) The Princeton experimental work on 'D Spar' sailwing HAWT rotors was carried out at tip speed ratios of around 4.

6) A high tip speed ratio was not required, since the alternator chosen could easily be geared to suit a moderate tip speed ratio rotor, and this did not have to be directly driven.

For all these reasons, therefore, it seemed sensible to opt for a medium speed machine with a design tip speed ratio of around 4.

As the main objective was to evaluate the performance of a sailfoil rotor, it was decided to keep the complexity of the rotor to a minimum so as not to interfere with the main purpose of the study.

As mentioned in Section 4.2.2.2, single and double

bladed rotors add greater complexity to the design because of the varying inertia loads experienced during yawing operations, and tend to require the blades to be hinged or teetered to alleviate the resulting stresses.

Four or more blades are not normally justified because of the additional expense, unless a higher starting torque is required.

For these reasons it was decided to opt for a three bladed rotor with fixed pitch blades.

6.3 AERODYNAMIC COEFFICIENTS

The lift and drag coefficients, CL and CD, are functions of the profile shape of the aerofoil section used in the blade, and of the angle of attack, α (alpha), presented by the aerofoil to the airflow (Vr for wind turbine blades).

The only lift and drag data appropriate to 'D Spar' sailwing aerofoils is that produced from the wind tunnel experiments at Princeton University (Maughmer, 1976). Figures 6.1 and 6.2 and Table 6.1 show lift and drag coefficients, together with lift/drag ratio characteristics for the 'D Spar' sailwing, used in the Princeton tests.

These figures constitute the basic aerodynamic data used

in the design of the sailfoil HAWT rotor described in this project.

6.4 LOCAL SPEED RATIO x

For each station the local speed ratio, x, is determined using the following relationship:

$$x = \frac{r\ X}{R} = R'\ X \qquad (6\text{-}1)$$

where x = local speed ratio = u/Vo

r = station local radius (m)

u = local tangential speed = Ω . r (m/s)

X = tip speed ratio = U/Vo

U = tip tangential speed = Ω . r (m/s)

R = tip radius (m)

R' = station radius ratio = r/R

Vo = undisturbed wind speed upstream of rotor (m/s)

Ω = Omega = angular velocity of wind turbine (shaft rad/sec)

Figure 6.3 shows the relationship between local speed ratio, x, and radius ratio R'.

6.5 RELATIVE WIND VELOCITY

The relative wind velocity, Vr, at a particular station or element along the blade span, is the resultant of the following velocities:

Undisturbed Wind Velocity	: Local Speed (Tangential) of the blade	: Induced Velocity Resultant at the station
Vo	: u	: W

The relationship between these velocities can be expressed trigonometrically as follows:

$$Vr = Vo \sin \phi + \Omega r \cos \phi$$

where Vo = Undisturbed free stream wind velocity upwind of the rotor

Ω = Omega = Angular velocity of the wind turbine shaft

= (X R) / Vo = (x r) / Vo

X = tip speed ratio of the rotor

x = local speed ratio at the station with radius r

= (Ω r) / Vo

ϕ = phi = Relative wind angle

Equation (6-2) was derived as follows (refer to Fig 6.4):

$$Vr = a1 + b1 + c1 \qquad (6\text{-}3)$$

where $a1 = \Omega r \cos \phi$

$b1 = (Vo - d1) \sin \phi$

$c1 = d1 \sin \phi$

Therefore

$$Vr = [\Omega r \cos \phi] + [(Vo - d1) \sin \phi]$$

$$b1 + c1 = [(Vr - d1) \sin \phi] + [d1 \sin \phi] =$$

$$= Vo \sin \phi \qquad (6\text{-}4)$$

$$Vr = (\Omega r \cos \phi) + (Vo \sin \phi)$$

as $x = (\Omega r) / Vo$; equation (6-2) becomes

$$Vr = Vo [\sin \phi) + (x \cos \phi)] \qquad (6\text{-}5)$$

6.6 RELATIVE WIND ANGLE ϕ (PHI)

The Relative wind angle, ϕ, is the angle which the relative wind vector, Vr, makes with the blade element at local radius r. The angle is dependent on the local speed ratio, x, at local radius r, and also therefore the tip speed ratio X of the rotor.

The relative wind angle is determined by means of an equation developed by Glauert (1935):

$$x = \frac{\sin \phi \ (2 \cos \phi) - 1}{1 + (2 \cos \phi)(1 - \cos \phi)} \qquad (6\text{-}6)$$

Figure 6.5 shows the graphical relationship between o and x.

6.7 BLADE PITCH ANGLE, θ, (THETA)

The blade pitch angle, θ, at each station is determined by subtracting the angle of attack, alpha, (for max L/D ratio) from the relative wind angle, ϕ, (phi) ie:

$$\theta = \phi - \alpha \qquad (6\text{-}7)$$

6.8 BLADE CHORD c

Once the relative wind angle, phi, is known, the blade chord c, at each station at radius r, can be determined by one of the following equations, (6-8) (Glauert, 1935) or (6-9) (Wilson, 1976).

$$c = \frac{4 \pi r}{CL\ B} * \frac{\sin^2 \phi}{\cos (\phi - \gamma)} \qquad (6\text{-}8)$$

$$c = \frac{8 \pi r}{CL\ B} * [1 - \cos \phi] \qquad (6\text{-}9)$$

where CL = lift coefficient at max L/D ratio

B = Number of blades

ϕ = phi = Relative wind angle

γ = Arctan D/L ratio

The results of applying this design procedure are given in Figure 6.7, which shows the shape of an optimum performance propeller type HAWT rotor with sailfoil blades. Table 6.2 gives the calculated parameters.

6.9 LINEARISED TAPER

However, given the characteristics of the Sailfoil blade concept, specifically its straight and rigid leading and trailing edges, it is clearly impossible to manufacture an optimally shaped sailfoil blade.

It is therefore necessary to approximate the optimum shape by linearising the taper and twist of the blade in such a way that the leading and trailing edges can be kept straight. The twist angle, beta, between the root and tip of the blade can be retained, however.

The leading edge of the blade is kept parallel to the blade span and the trailing edge is tapered between a root chord c(r) of 590 mm and a tip chord c(t) of 360 mm. The 'taper coefficient' TC (see Fig 6.6) is given by the following equation:

$$TC = (c(t) - c(r)) / (R - r(r)) \qquad (6\text{-}10)$$

$$= (0.36 - 0.59) / (2 - 0.4) = - 0.14$$

where r(r) = root radius

At a particular station with local radius r, the chord c is derived from the following expression:

$$c = TC\ (r - r(r)) + c(r) \qquad (6\text{-}11)$$
$$= (-\ 0.14)\ (r - 0.4) + 0.59$$

Table 6.3 and Figure 6.7 give the linearised shape of the sailfoil blade used and its twist. Figure 6.8 shows a sailfoil blade based on this design.

6.10 THEORETICAL PERFORMANCE OF A SAILFOIL HAWT ROTOR WITH LINEARISED BLADES

As the blade shape had departed from the optimum, the theoretical performance would be less than optimum. It was therefore considered important to ascertain the theoretical performance characteristics of the rotor with linearised blade shape in order to see if any adjustment in blade shape was warranted, and to obtain information about the difference in efficiency between the theoretically optimum and the practical linearised design.

Accordingly, a computer program CPHAWT was written, based on the Combined Blade Element and Momentum Theory described in Chapter 4, and incorporating the Prandtl

Tip Loss Model.

The flow diagram of the computer program CPHAWT used to compare the linearised blade and theoretically optimum rotors is shown in the Appendix.

Figures 6.9, 6.10, 6.11 and 6.12 are derived from the output of the CPHAWT program and show the predicted performance characteristics of the theoretically optimum and the practical linearised Sailfoil HAWT rotors. As can be seen, the theoretical power lost from linearising the rotor blades is small.

Figure 6.13 shows the Sailfoil HAWT rotor with linearised blades.

REFERENCES FOR CHAPTER 6

Glauert, H (1935): Aeroplane Propellers, Durand, WE (ed) 'Aerodynamic Theory'.

Jansen, WAM & Smulders, PT (1977): Rotor Design for Horizontal Axis Windmills, SWD 77-1, Netherlands.

Maughmer, MD (1976): Optimisation and Characteristics of a Sailwing Windmill rotor, AMS Report No 1297, Princeton University.

Taylor, DA (1978): Wind Power Primer, Design Manual School of Industrial Design (Engineering), Royal College of Art.

Wilson, RE et al (1976): Aerodynamic Performance of Wind Turbines, Oregon State University.

TABLE 6.2: PARAMETERS FOR BLADE SHAPE FOR OPTIMUM PERFORMANCE SAILFOIL ROTOR FROM 'WINDROTOR' PROGRAM

TIP RADIUS OF ROTOR R = 2m
DESIGN TIP SPEED RATIO = 4
NUMBER (B) OF BLADES = 3
AEROFOIL SECTION = Princeton 'D Spar' Sailwing
AEROFOIL MAXIMUM L/D RATIO = 29
AEROFOIL AT MAXIMUM L/D = 0.7
DESIGN ANGLE OF ATTACK = 3 degrees

LOCAL RADIUS r R1 (m)	LOCAL SPEED RATIO x XL	REL. WIND ANGLE phi FI (deg)	BLADE PITCH ANGLE theta T3 (deg)	CHORD WIDTH c C (m)
0.4	0.8	34	31	0.832
0.5	1	29.8	26.8	0.832
0.6	1.2	26.4	23.4	0.76
0.7	1.4	23.6	20.6	0.706
0.8	1.6	21.2	18.2	0.66
0.9	1.8	19.3	16.3	0.611
1	2	17.6	14.6	0.572
1.1	2.2	16.2	13.2	0.529
1.2	2.4	15	12	0.495
1.3	2.6	13.9	10.9	0.468
1.4	2.8	13	10	0.442
1.5	3	12.2	9.2	0.412
1.6	3.2	11.5	8.5	0.391
1.7	3.4	10.9	7.9	0.373
1.8	3.6	10.3	7.3	0.353
1.9	3.6	9.6	6.6	0.338
2	4	9.3	6.3	0.321

TABLE 6.3: PARAMETERS FOR LINEARISED BLADE SHAPE FOR SAILFOIL BLADE USED ON WIND TURBINE

TIP RADIUS OF ROTOR R = 2m
DESIGN TIP SPEED RATIO = 4
NUMBER (B) OF BLADES = 3
AEROFOIL SECTION = Princeton 'D Spar' Sailwing
AEROFOIL MAXIMUM L/D RATIO = 29
AEROFOIL AT MAXIMUM L/D = 0.7
DESIGN ANGLE OF ATTACK = 3 degrees

LOCAL RADIUS r R1 (m)	LOCAL SPEED RATIO x XL	REL. WIND ANGLE phi FI (deg)	BLADE PITCH ANGLE theta T3 (deg)	CHORD WIDTH c C (m)
0.4	0.8	34	31	0.589
0.5	1	29.8	26.8	0.575
0.6	1.2	26.4	23.4	0.561
0.7	1.4	23.6	20.6	0.546
0.8	1.6	21.2	18.2	0.532
0.9	1.8	19.3	16.3	0.518
1	2	17.6	14.6	0.503
1.1	2.2	16.2	13.2	0.489
1.2	2.4	15	12	0.474
1.3	2.6	13.9	10.9	0.46
1.4	2.8	13	10	0.446
1.5	3	12.2	9.2	0.431
1.6	3.2	11.5	8.5	0.417
1.7	3.4	10.9	7.9	0.403
1.8	3.6	10.3	7.3	0.388
1.9	3.8	9.6	6.6	0.374
2	4	9.3	6.3	0.359

ANGLE OF ATTACK	LIFT COEFFICIENT	DRAG COEFFICIENT	LIFT TO DRAG RATIO
(degrees)			
-10	-1.1	0.06	-18.33
-9	-0.9	0.055	-16.36
-8	-0.8	0.05	-16.00
-7	-0.6	0.045	-13.33
-6	-0.4	0.04	-10.00
-5	-0.3	0.035	- 8.57
-4	-0.23	0.033	- 6.97
-3	-0.1	0.03	- 3.33
-2	0.1	0.029	3.45
-1	0.27	0.027	10.00
0	0.35	0.026	13.46
1	0.47	0.024	19.6
2	0.6	0.023	26.08
3	0.7	0.022	31.818
4	0.88	0.03	29.33
5	0.92	0.032	28.75
6	1.0	0.038	26.316
7	1.1	0.044	25.00
8	1.2	0.052	23.07
9	1.3	0.06	21.66
10	1.33	0.068	19.55
11	1.37	0.076	18.00
12	1.45	0.093	15.6
13	1.48	0.1	14.8
14	1.505	0.13	11.57
15	1.5	0.16	9.3
16	1.49	0.17	8.76
17	1.45	0.2	7.25
18	1.42	0.23	6.17
19	1.35	0.27	5.00
20	1.3	0.3	4.33
21	1.25	0.31	4.03
22	1.2	0.34	3.53
23	1.1	0.35	3.143

Table 6.1: Lift and drag coefficients, lift to drag ratio characteristics for the 'D Spar' sailwing aerofoil section - Princeton data, (Maughmer, 1976)

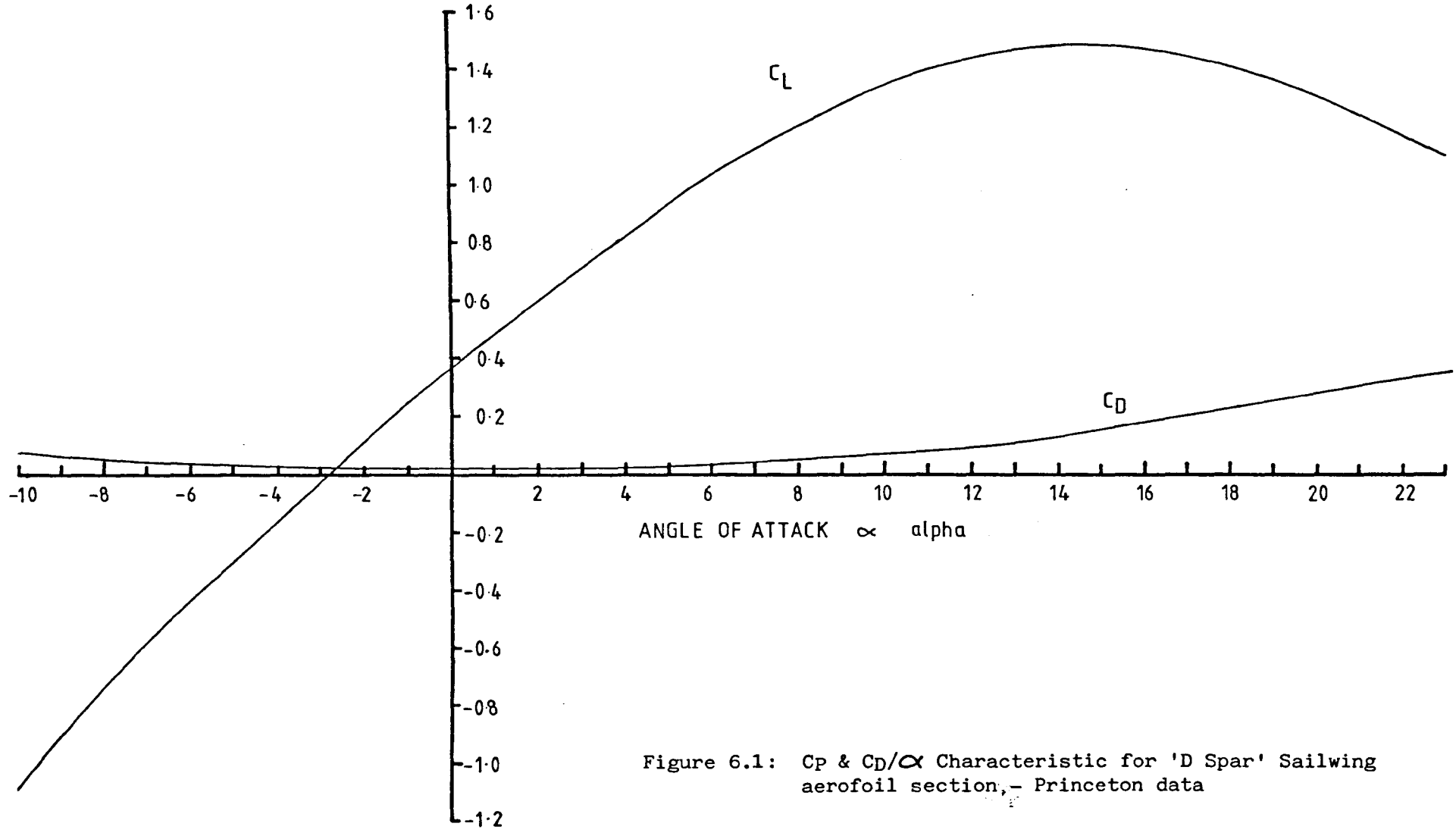

Figure 6.1: Cp & C_D/α Characteristic for 'D Spar' Sailwing aerofoil section,- Princeton data

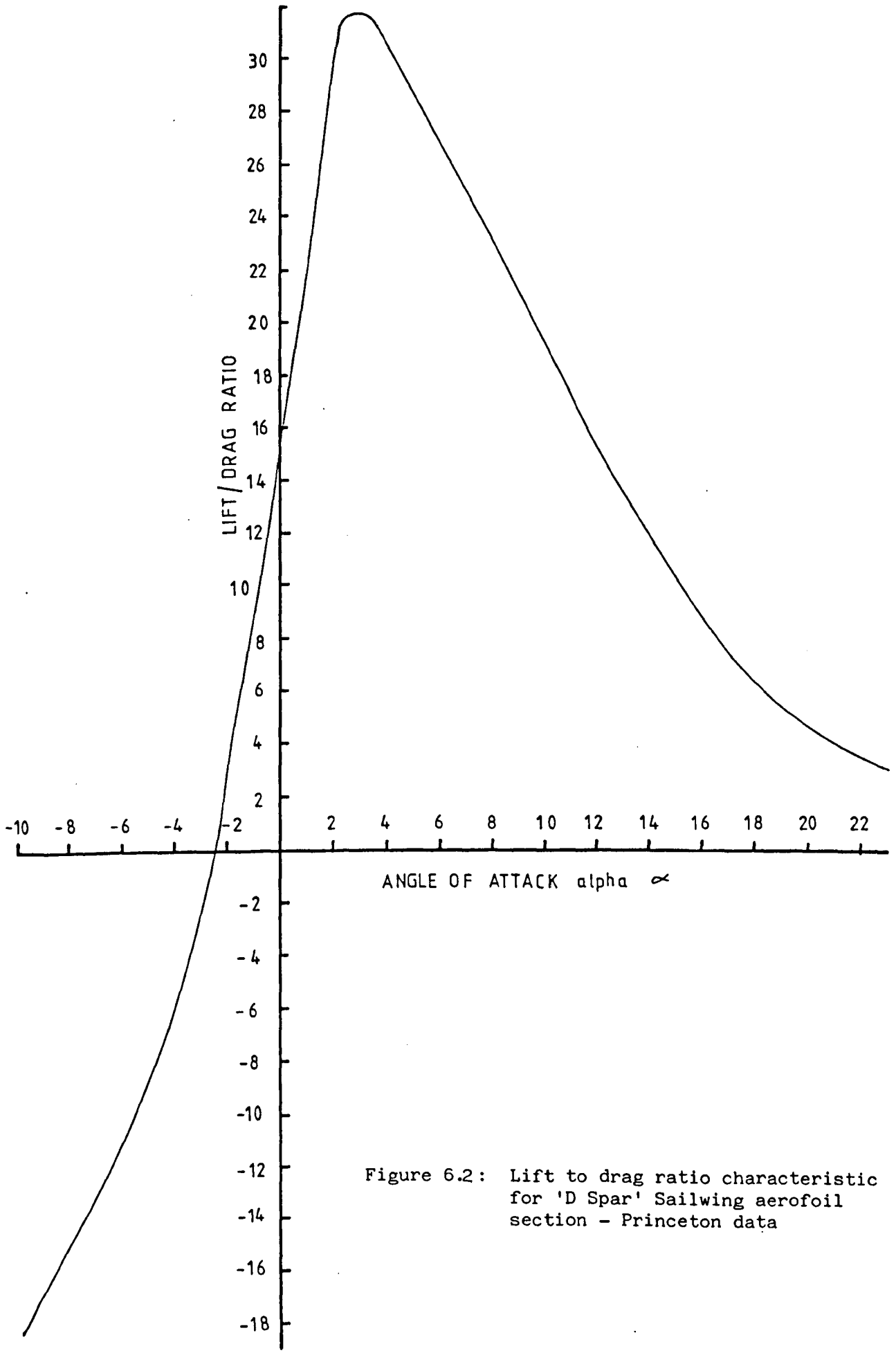

Figure 6.2: Lift to drag ratio characteristic for 'D Spar' Sailwing aerofoil section - Princeton data

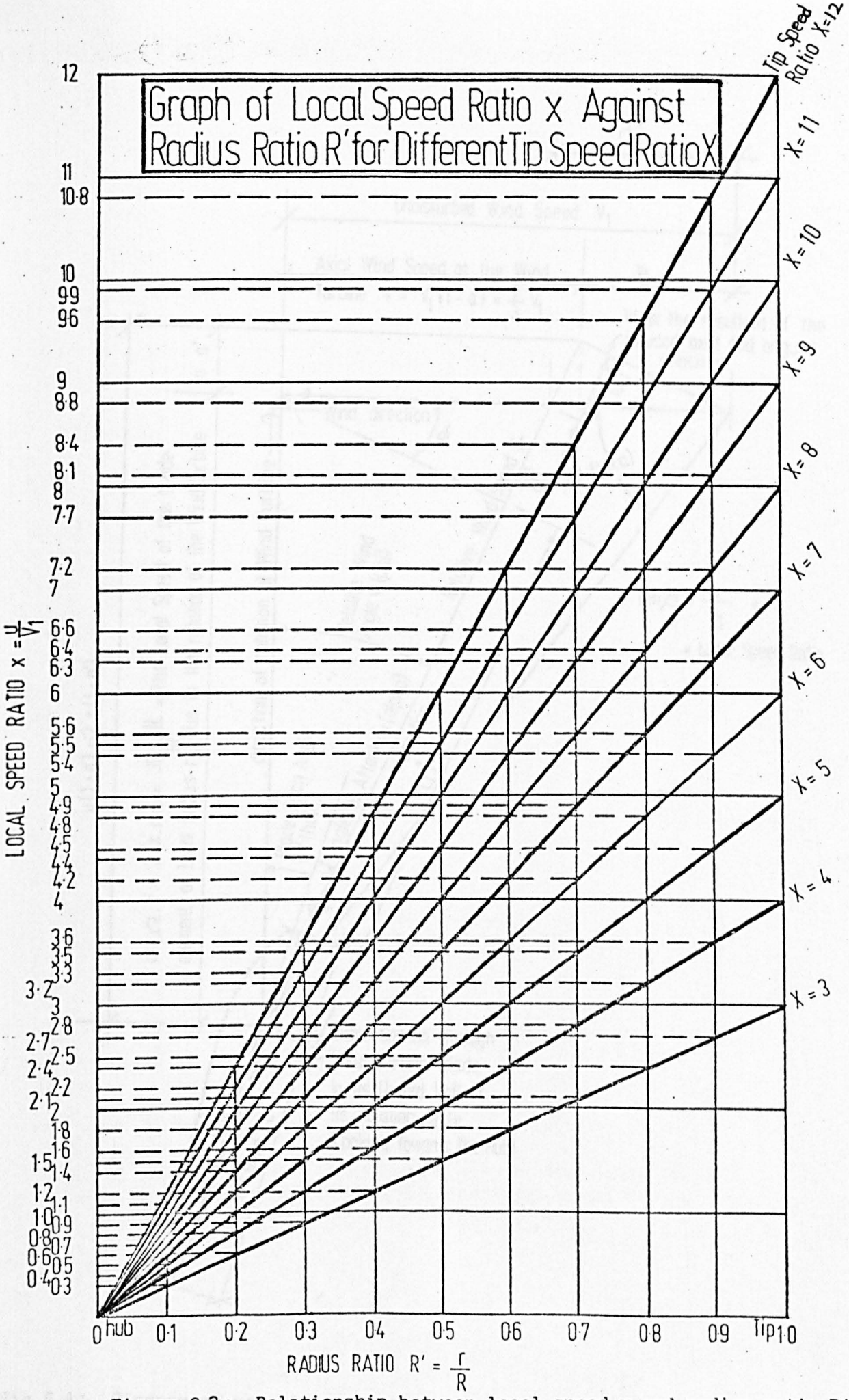

Figure 6.3: Relationship between local speed x and radius ratio R'

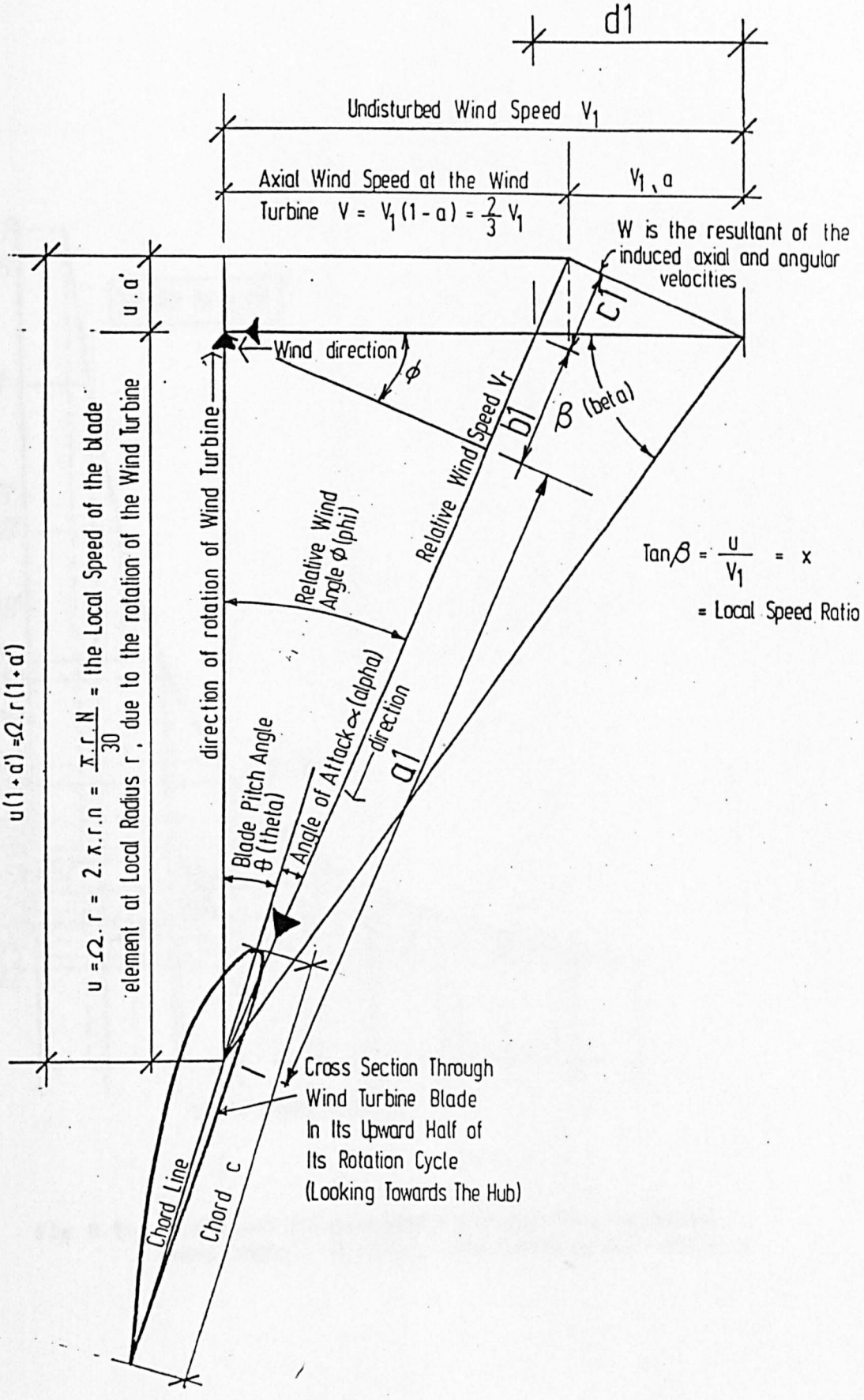

Fig 6.4: Diagram of velocities acting on a blade element at radius r

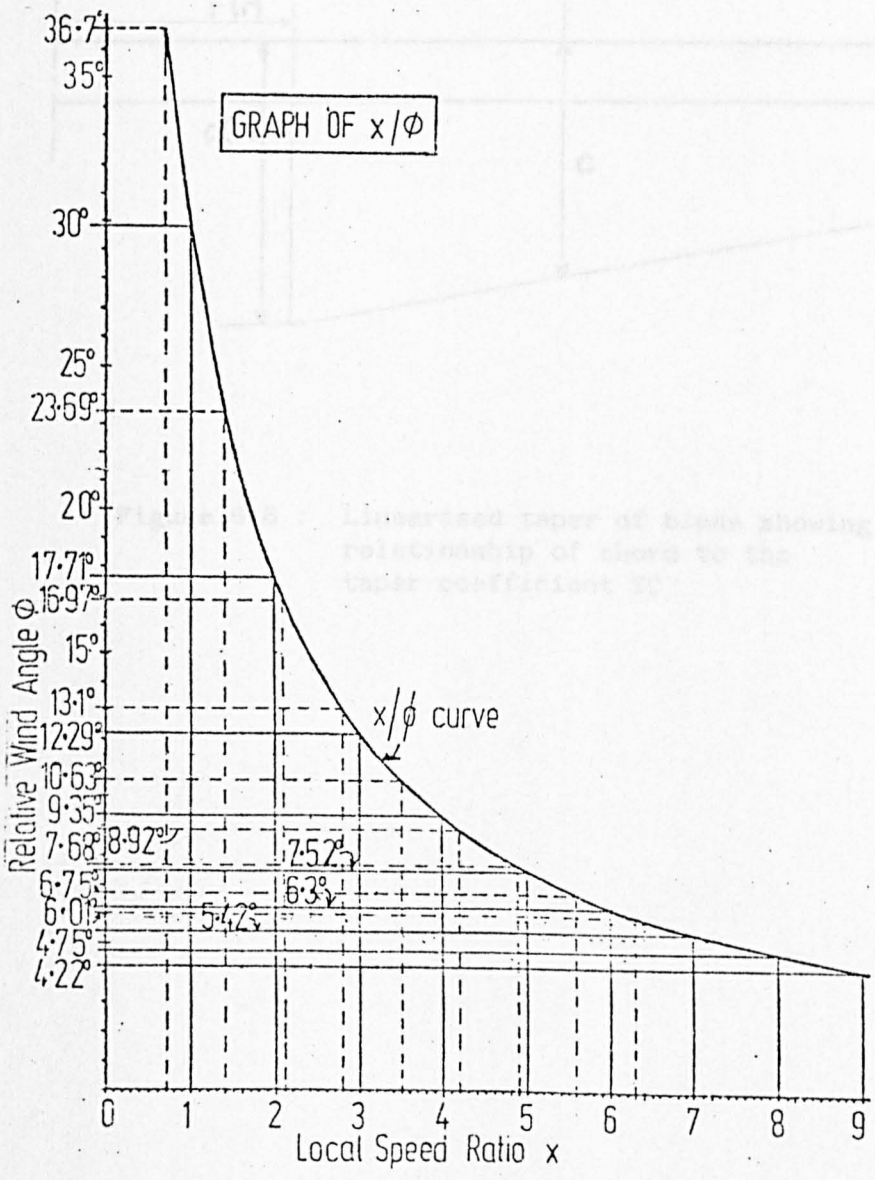

Fig 6.5: Graphical relationship between the relative wind angle, Ø (phi), and local speed ratio, x

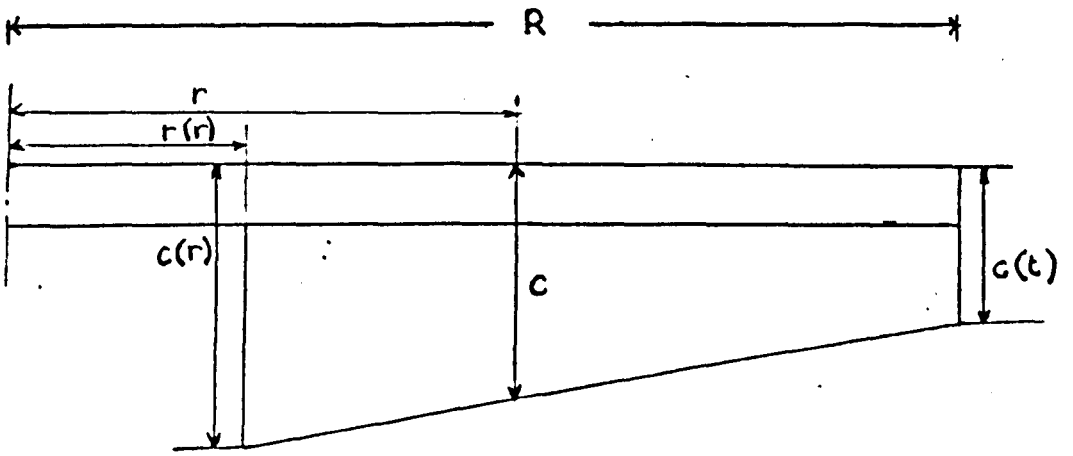

Figure 6.6 : Linearised taper of blade showing relationship of chord to the taper coefficient TC

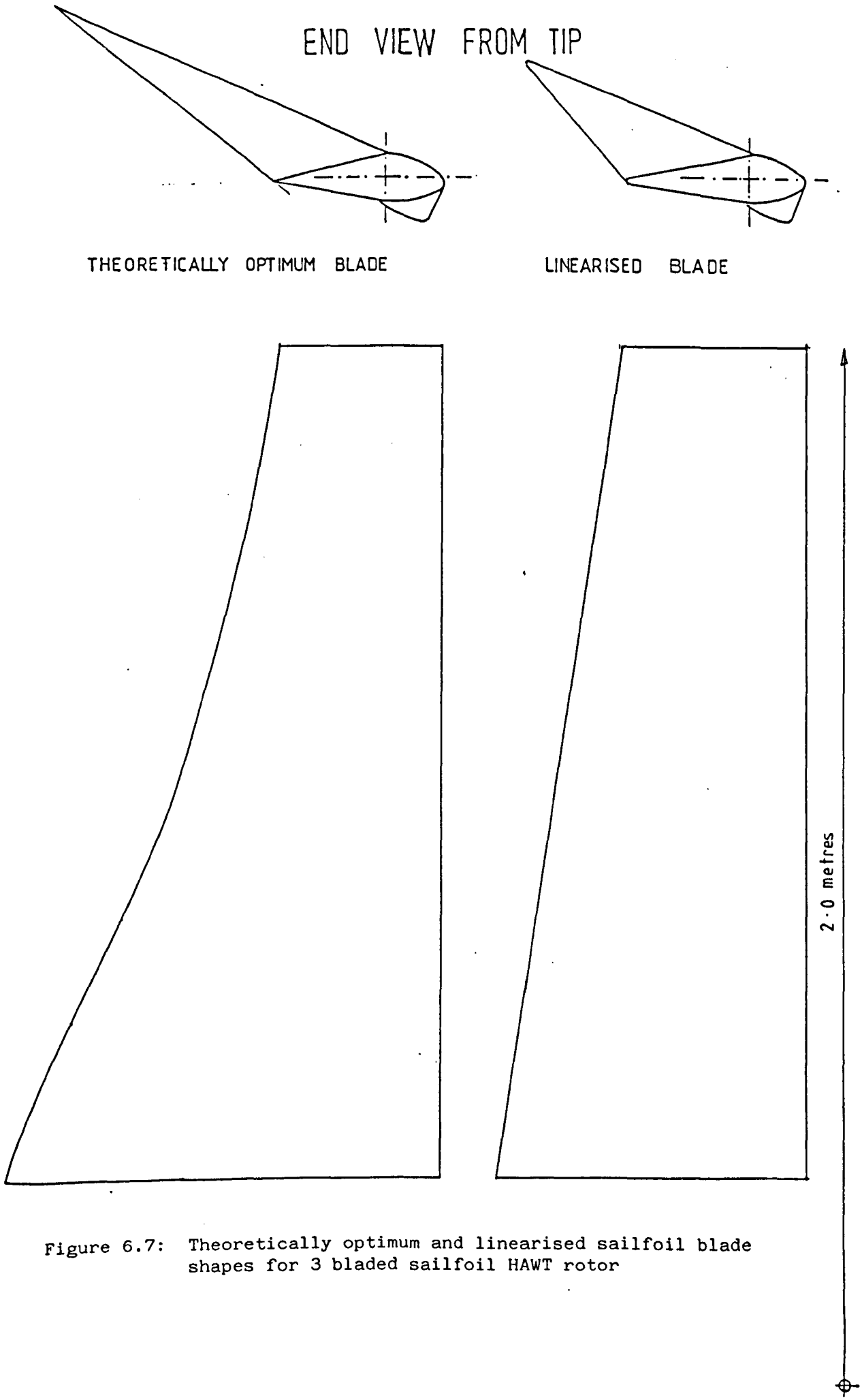

Figure 6.7: Theoretically optimum and linearised sailfoil blade shapes for 3 bladed sailfoil HAWT rotor

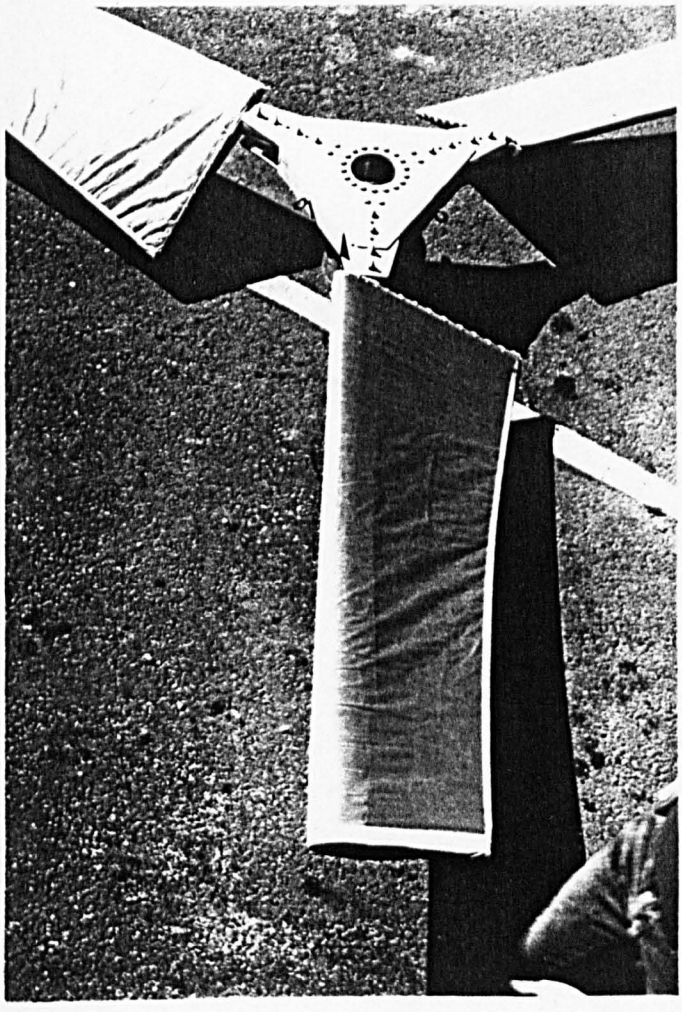

Fig. 6.8 Sailfoil blade used on wind turbine rotor.

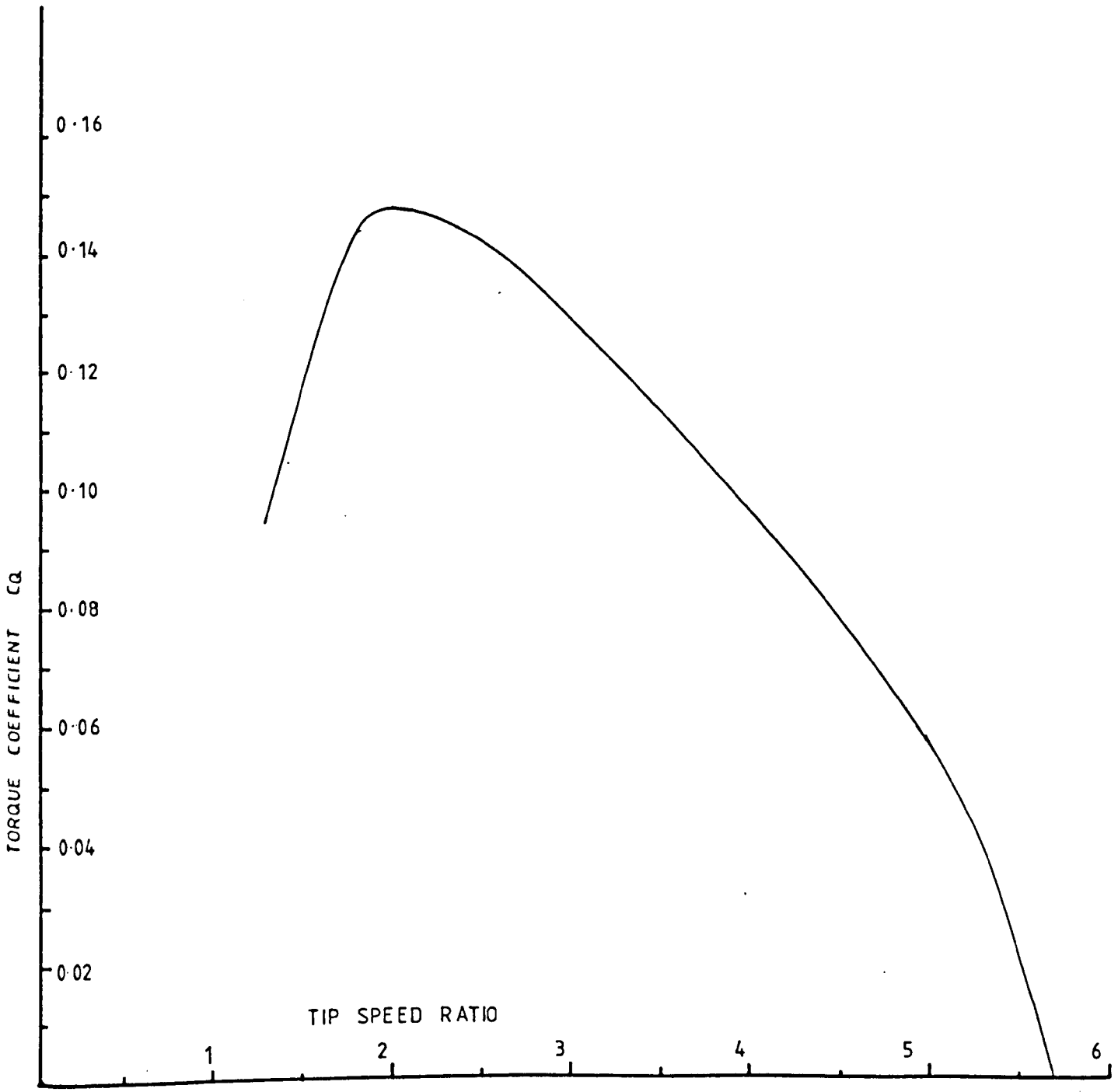

Figure 6.9 : C_Q/X Characteristics for 3 bladed sailfoil HAWT rotor with theoretically optimum blades

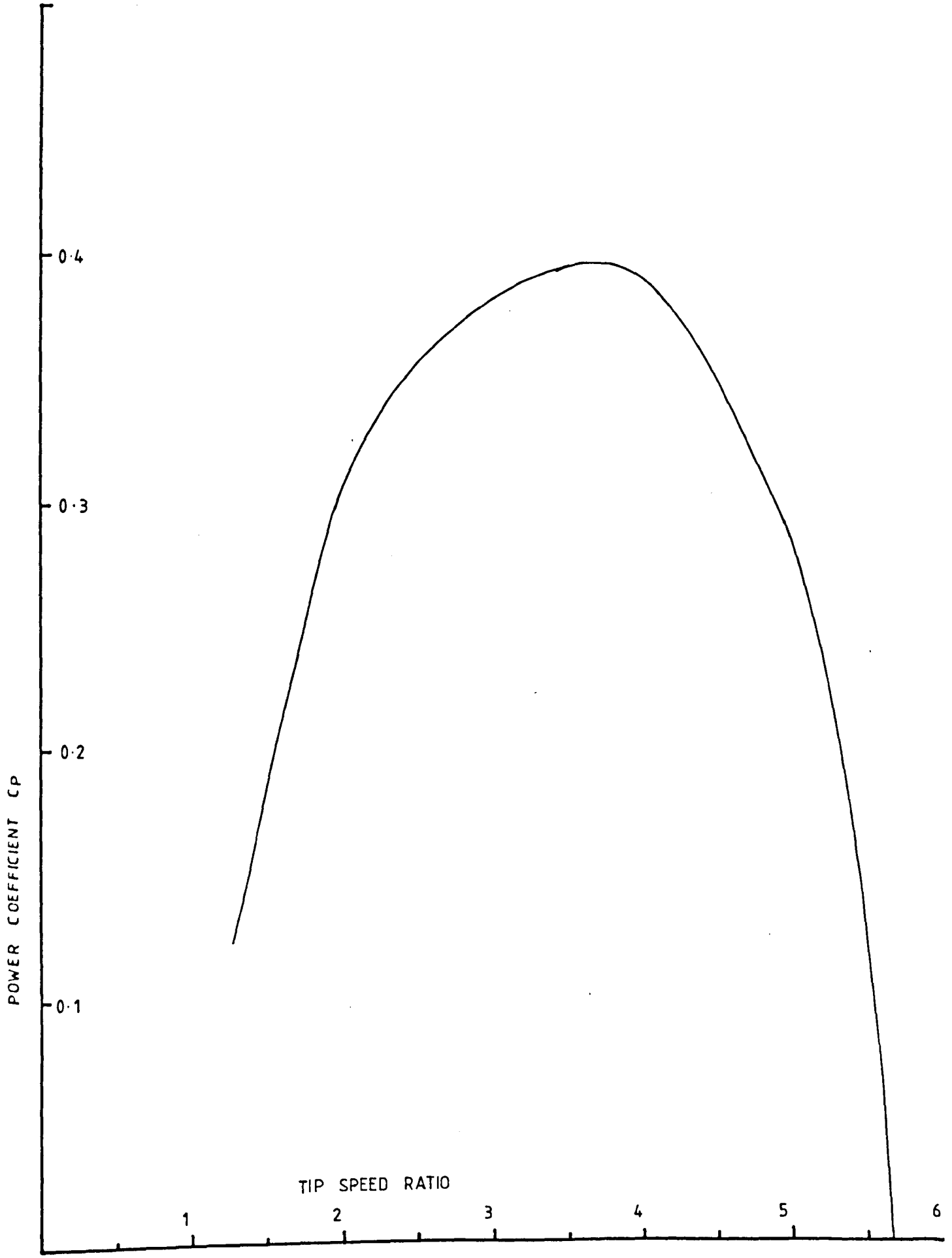

Figure 6.10 : Predicted Cp/X Characteristics for 3 bladed sailfoil HAWT rotor with theoretically optimum blades

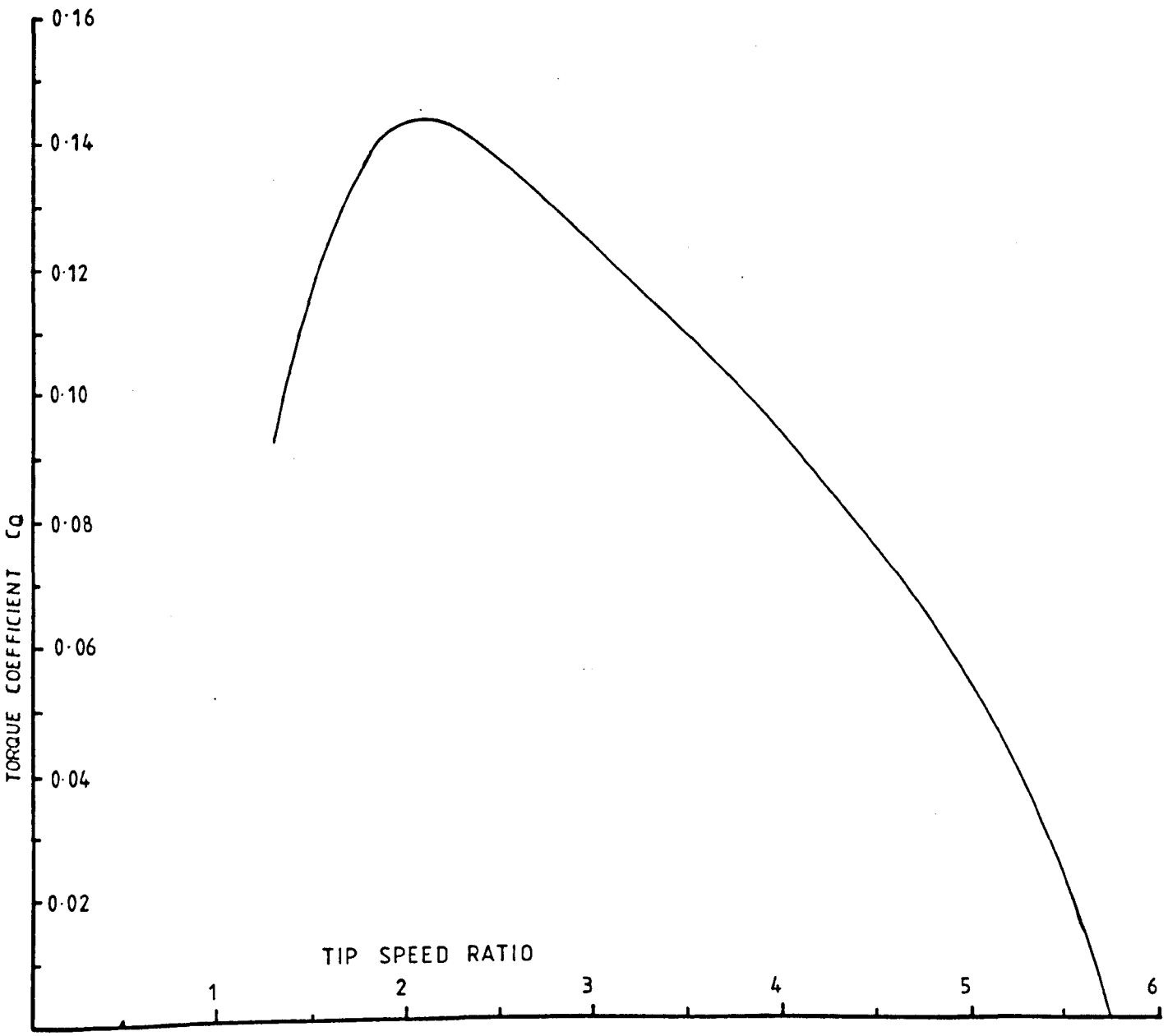

Figure 6.11: Predicted CQ/X Characteristics for 3 bladed sailfoil HAWT rotor with linearised blades

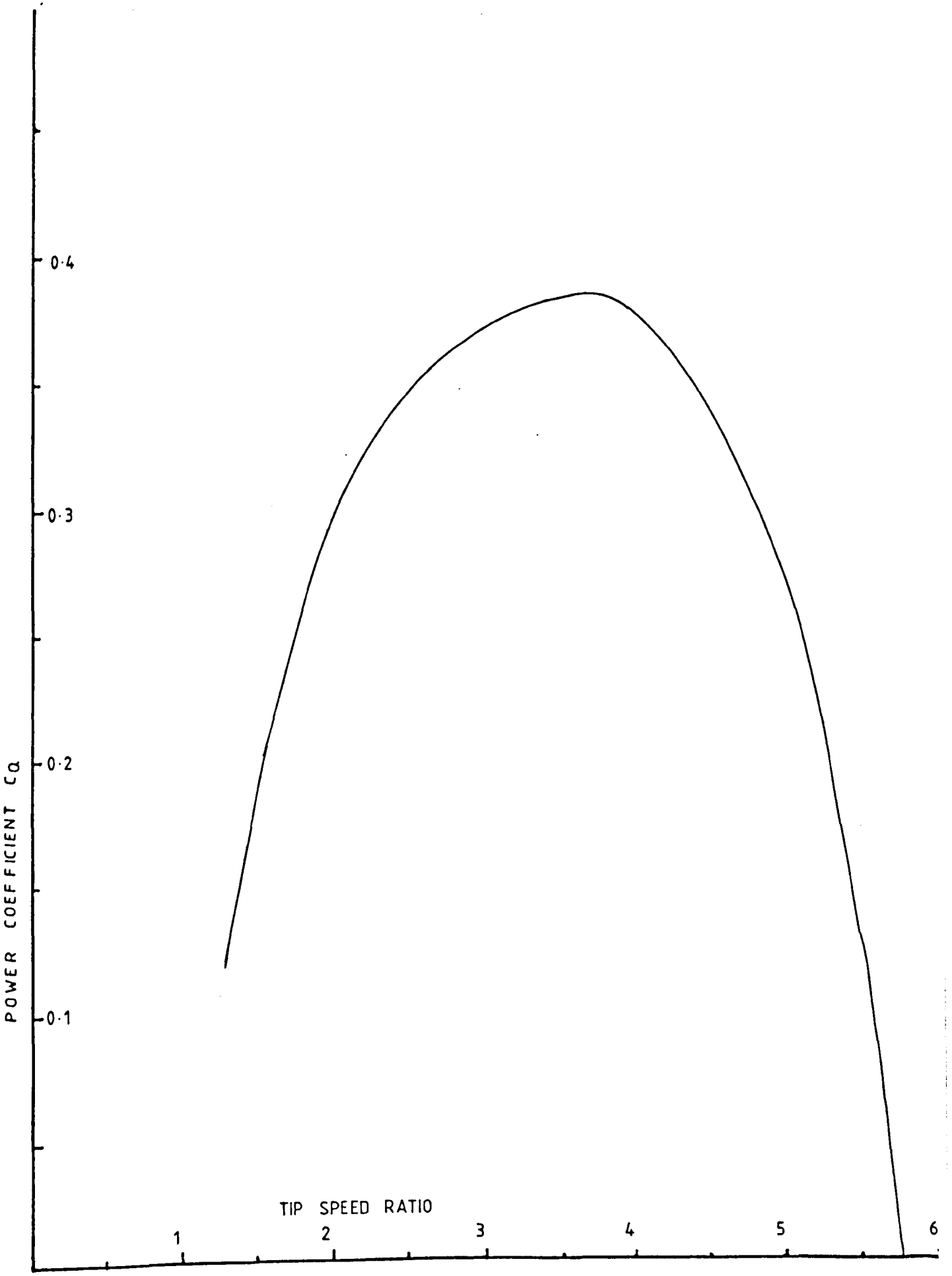

Figure 6.12: Predicted Cp/X Characteristics for sailfoil HAWT rotor with 3 linearised blades

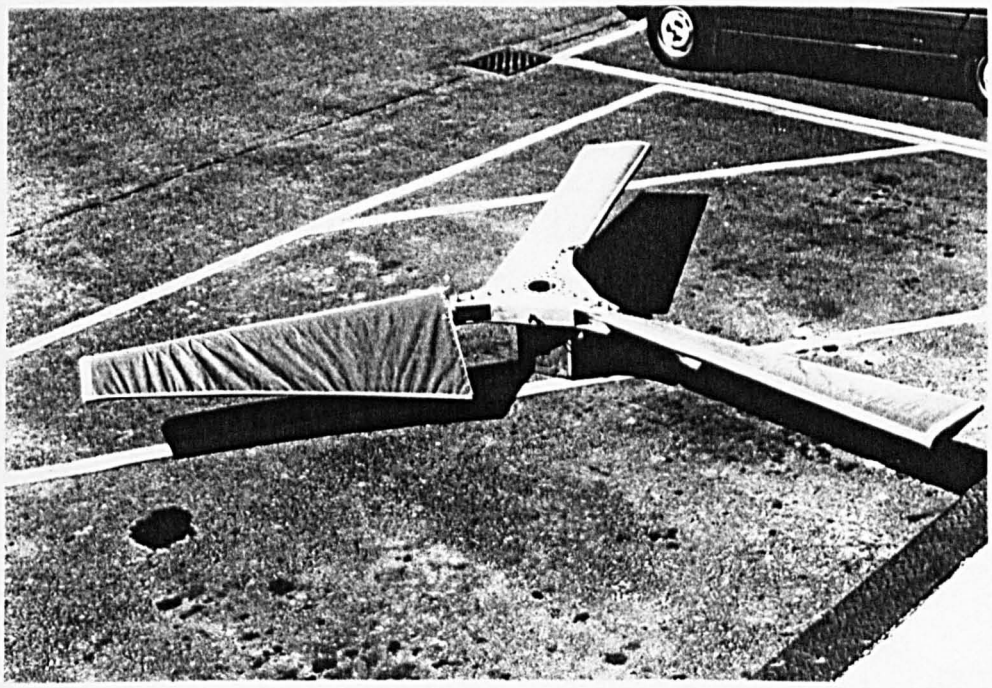

Fig. 6.14 Sailfoil HAWT rotor with linearised sailfoil blades.

CHAPTER 7

THE STRUCTURAL DESIGN OF A SAILFOIL HAWT ROTOR

LIST OF SYMBOLS FOR CHAPTER 7

A = A1 = Area of Rotor Swept Disc (m^2)

A2 = Area of Swept Disc Inboard of Blade Root

A3 = Area of Swept Disc Outboard of Blade Root

Ab = Frontal area of 1 blade presented to the wind (m^2)

As = Cross sectional area of blade spar

Bs = Bending Stress at blade spar rootN/mm^2

CF(r) = Centrifugal force acting on a blade element at local radius r (N)

Cs = Combined Bending and Centrifugal stress N/mm^2

Di = Inside Diameter of tubular blade spar

Do = Outside Diameter of tubular blade spar

Kt = Thrust constant for 4 m dia HAWT rotor

Lc = Lever arm of resultant of Thrust acting on blade measured from blade spar root (r = 0.420 m)

Mb = Mass of one blade (kg)

Mb(o) = Mass of blade outboard of local radius (kg)

N = Revolutions per minute of Wind turbine shaft

P = Power output

Pi = 3.14159

P(max) = Maximum power output

R = Tip Radius of wind turbine

r = Local radius of a blade element

r(c) = Radius of CG of blade portion outboard from blade element at local radius r

r(r) = Radius of blade spar root

T = Wind Thrust force acting on spinning wind turbine rotor (N)

Tb = Wind Thrust acting on 1 blade (spinning rotor) (N)

Tbp = Wind thrust acting on 1 blade (parked rotor) (N)

Tcs = Tensile stress due to Centrifugal Force N/mm^2

TM = Bending Moment acting on blade root spar due to the Wind Thrust load (N.m)

T(max)=Max thrust loading on spinning rotor

Vf = Furling wind speed

Vi = Incremental wind speed

Vm = Annual mean wind speed (m/s)

Vo = Undisturbed wind speed

VR = Rated wind speed

X = Rotor Tip Speed Ratio

Xmax = Runaway Rotor Tip Speed Ratio

Z = Section modulus of Tubular Spar

ρ = rho = air density

7.1 INTRODUCTION

Horizontal Axis Wind Turbine rotors are subjected to a number of forces which produce momentary stresses in the blades.

These forces and moments are due to:

(1) The effect of the wind thrust force acting on the rotor blade.

(2) The effect of centrifugal force due to the spinning mass of the blade.

(3) Tne effect of gravity on the mass of the blade and gyroscopic forces which occur if the rotor attempts to 'yaw' or 'slew' rapidly in response to changes in wind direction.

The gyroscopic force effects are considerably more severe with two-bladed HAWT rotors than with three-bladed rotors, due to the sharply varying moment of inertia about the vertical yaw axis when the rotor is spinning. With 3 bladed rotors this is not a major problem (because the variation in moment of inertia about the vertical axis is much smaller) provided the yawing speed does not exceed 0.5 rad/sec (Kinderen, 1976).

When the rotor is parked or stationary it is not subjected to centrifugal or gyroscopic forces but it has to be capable of withstanding the thrust forces caused by the maximum wind speed likely to occur on the wind turbine site.

7.2 WIND LOADS ON SPINNING HAWT ROTORS

In the action of rotating the turbine, the windflow subjects the rotor blade to aerodynamic forces (see Chapter 4) and moments.

The most significant of these for rotor structural design are the Thrust force (T), and the bending moments acting on the blade due to the Thrust force.

To determine the wind Thrust load, we need to refer back to the Momentum Theory (Chapter 4). Equation (4-6) gives the axial thrust on the rotor disc (Fig 7.1) as follows:

$$T = \rho \, (Vo^2 - Vl^2) \, A/2 \qquad (4\text{-}6)$$

Maximum power output is given by the Betz equation (Betz 1927);

$$P(max) = \frac{16}{27} \frac{1}{2} \rho \, A \, Vo^3 \qquad (7\text{-}1)$$

and the maximum Thrust on the rotor under these conditions is:

$$T(max) = \frac{P(max)}{V} = \frac{P(max)}{Vo\ (2/3)} \qquad (7\text{-}2)$$

this gives

$$T(max) = \frac{8}{9}\frac{1}{2}\rho\ A\ Vo^2 \qquad (7\text{-}3)$$

For maximum power extraction, therefore, the thrust force is only slightly less (1/9th) than that experienced by a solid disc with an area equal to the rotor swept area.

7.3 MECHANICAL LOADING ON A SPINNING HAWT ROTOR

When a wind turbine blade is spinning, it is subjected to centrifugal force acting on the mass of the blade.

For a given rotational speed, the centrifugal force acting on the blade is a non cyclic steady force which remains constant whatever the angular position of the blade.

The centrifugal force acting on a blade element at local radius, r, is derived from the equation:

$$CF(r) = \Omega^2\ r(c)\ Mb(o) \qquad (7\text{-}4)$$

Where CF(r) = Centrifugal Force

r(c) = Radius of centre of gravity of blade portion outboard from blade element at radius r

Mb(o) = Mass of blade portion outboard from blade element at local radius r

Ω = Omega = angular velocity of rotor

See Figure 7.2.

7.4.1 SAILFOIL HAWT ROTOR BLADE STRUCTURAL DESIGN

The load bearing member of the Sailfoil blade used in this project is a mass produced, aluminium alloy, drawn untapered tube with a circular cross section. Aluminium alloy was used in this case because of its preferable strength-to-weight ratio, though steel or wood would be possible. As this was to be an experimental project with a limited life, the poorer fatigue qualities of aluminium alloy was not a problem. For a production machine, steel or wooden spars would probably be more appropriate.

Whilst the circular cross section is not the ideal shape in terms of the mass-to-strength ratio, it does enable a readily available, standardised, high quality material to be used for this critical load bearing member. This in turn could allow the sailfoil type of blade to be

constructed by a small business without specialist equipment.

The use of a non-tapered tubular spar also simplifies the calculation of section constants and other parameters used in the structural design of a rotor blade.

The blade, being a cantilevered beam, experiences its highest stress levels due to bending and tension at the blade root.

This being the case, and because the structural spar is of constant cross-section, the structural design of the Sailfoil blades for the 4m dia HAWT was based on the calculation of the loads and stresses experienced at the spar root.

After investigating a number of possible spar materials and sizes, a non tapered tubular spar of 75mm outer diameter and 63mm inner diameter aluminium alloy HT30 was chosen as the main structural member.

Three conditions were assessed to ascertain the highest stress levels. These were firstly with the wind turbine operating at its normal tip speed ratio X and rotating at the furling wind speed Vf. Secondly with the wind turbine under runaway conditions at the furling wind speed Vf. Thirdly with the wind turbine parked and

facing into the wind in the maximum design wind speed, Vmax, likely to occur at the site.

The furling wind speed Vf is the maximum wind speed at which the wind turbine continues to operate. Above this wind speed the wind turbine is stopped to prevent damage. The choice of the furling wind speed depends on the strength of the rotor and the tower and the annual energy required from the site. Because of the low frequency of winds above the furling speed, the annual energy contained in these winds is low.

An estimate of the number of hours or minutes that the wind blows at a particular wind speed per year can be made by means of the Rayleigh distribution (Park, 1981) provided that the annual mean wind speed is known. From data obtained from Cardington, the annual mean wind speed (Taylor, 1980) is estimated to be 4 m/s. The number of hours that a wind speed Vi blows per year from the Rayleigh distribution is as follows.

$$Hi = 8760 \frac{\pi}{2} \frac{Vi}{Vm^2} e^{-k}$$

where Vi = wind speed

Vm = annual mean wind speed

e = 2.718

$$k = \frac{\pi}{4} \left(\frac{Vi}{Vm}\right)^2$$

In this wind turbine the furling wind speed Vf = 15 m/s, so the number of hours that this wind speed is estimated to occur is as follows.

$$k = \frac{\pi}{4}\left(\frac{Vf}{Vm}\right)^2$$

$$= \frac{\pi}{4}\left(\frac{15}{4}\right)^2 = 11.044$$

and

$$Hf = 8760 \cdot \frac{\pi}{2} \cdot \frac{Vf}{Vm^2} \cdot e^{-k}$$

$$= 8760 \cdot \frac{\pi}{2} \cdot \frac{15}{4^2} \cdot 2.718^{-11.044}$$

$$= 0.02 \text{ hours} = 13 \text{ minutes/year}$$

This means that the annual energy contribution from wind speed of 15 m/s or more is low, so it would not be justified to design the wind turbine to operate in wind speeds in excess of this value.

The normal operating tip speed ratio, X, on a variable speed wind turbine is the tip speed ratio that corresponds with the maximum power coefficient. From Figure 6.12 the predicted maximum coefficient for the Sailfoil wind turbine with three linearised blades occurs at a tip speed ratio of 4.

The runaway tip speed ratio is the tip speed ratio that the wind turbine rotor accelerates to in the event of

the rotor becoming decoupled from the load due to failure of the generator or V belt transmission.

From Figure 6.12 the predicted runaway tip speed ratio for the Sailfoil wind turbine with three linearised blades is 6.

7.4.2 WIND LOADS

Thrust acting on a 4 m diameter HAWT can be derived by applying equation (7-3) Thus:

$$T(max) = \frac{8}{9}\frac{1}{2}\rho A Vo^2 \qquad (7\text{-}3)$$

and Thrust constant, Kt, for the rotor is given:

$$Kt = \frac{8}{9}\frac{1}{2}\rho A \qquad (7\text{-}5)$$

$$= \frac{8}{9}\frac{1}{2}\rho \pi R^2$$

$$= \frac{8}{9} * \frac{1}{2} * 1.29 * \pi * 2^2$$

$$= 7.2047$$

$$T(max) = Vo^2 Kt \qquad (7\text{-}6)$$

$$= Vo^2 * 7.2047$$

Assuming Vo = 15 m/s,

Then $T(max) = 15^2 * 7.2047 = 1621$ N

As the swept area of a HAWT rotor is in in the form of a disc the Thrust distribution acting on the blades increases linearly outwards towards the tip. Figure 7.3 illustrates this relationship.

7.4.3 BENDING MOMENT ON BLADE SPAR AT ROOT (r=420mm) DUE TO THRUST (ROTOR SPINNING)

If we assume that the wind speed = Furling Wind Speed, ie, that VF = 15m/s, and that the rotor is spinning at a Tip Speed Ratio X = 4, then the thrust acting on the Rotor 'Disc', T = 1621 N, and the thrust acting on one blade, Tb = 1621/3 = 540 N

For cantilevered blades the lever arm of the resultant of the Thrust acting on the blade = Lc. To determine Lc we need to refer to Fig. 7.3.

The area of triangle ABC is equal to the entire swept area disc of the HAWT rotor. Triangle AED gives the area of the swept disc inboard from the blade root. Subtracting the area AED from the area ABC gives the area of EBCD, which corresponds to the area outboard from the blade root:

$$\text{Area ABC} = A1 = \pi R^2 \qquad (7\text{-}7)$$

$$= \pi * 2^2 = 12.5 \text{ m}^2$$

$$\text{Area AED} = A2 = \pi\, r(r)^2 \qquad (7\text{-}8)$$

$$= \pi * 0.42^2 = 0.554\ m^2$$

$$\text{Area EBCD} = A3 = A1 - A2 \qquad (7\text{-}9)$$

$$= 12.5 - 0.554 = 11.94\ m^2$$

Taking moments about A:

$$(x3 * A3) + (x2 * A2) = (x1 * A1) \qquad (7\text{-}10)$$

$$(x3 * A3) = (x1 * A1) - (x2 * A2)$$

$$x3 = [(x1 * A1) - (x2 - A2)] / A3$$

$$= [(1.33 * 12.5) - (0.28 * 0.554)] / 11.94$$

$$= 1.38\ m$$

$$Lc = x3 - r(r) \qquad (7\text{-}11)$$

$$= 1.38 - 0.42 = 0.96 \text{ metres}$$

The Bending Moment, TM, at the blade spar root due to the Thrust load is then given by the following equation (7-12):

$$TM = Lc * Tb \qquad (g\text{-}12)$$

$$= 0.96 * 540 = 557\ N.m$$

The bending stress in an element depends on the Bending Moment and Section Modulus Z of the element. For a circular hollow cross section the Section Modulus Z is given by the following relationship (Freer, 1977)(7-13):

$$Z = [(Do^4 - Di^4)/Do] * (\pi/32) \qquad (7\text{-}13)$$

$= [(75^4 - 63^4)/75] * (\pi/32)$

$= 20797\ mm^3$

Where Do = Outside diameter of the spar

Di = Inside diameter of the spar

The Bending Stress, Bs, at the blade spar root is given by the following equation (7-14):

$$Bs = TM/z \qquad (7\text{-}14)$$

$= 557 * 1000/20797$

$= 27\ N/mm^2$

The fatigue strength of HT30 aluminium alloy tube is 124 N/mm^2 at $5 * 10^6$ cycles (Aluminium Federation, 1980). Given that this experimental project is to have a limited life which is less than these cycles and the lack of design codes for wind turbine blades, the bending stress in the spar root is within acceptable levels.

7.4.4 CENTRIFUGAL LOADS ON SPINNING SAILFOIL HAWT ROTOR

The rotor is designed to operate up to a maximum rotational speed of 190 rpm (20 rad/sec). This corresponds to a tip speed ratio of 4 at a rated wind speed, VR, of 10 m/s, and also relates to the maximum rotational speed of the generator (1500 rpm) used. The rotor speed is kept fixed at this value for wind speeds at and above the rated value VR.

If the mass of one blade is known, together with the position of the blade's centre of gravity, then for a given angular velocity, O (Omega), the centrifugal force acting on the blade root (radius r(r)) (see Figure 7.2) is given bu the following equation (Greer, 1977):

$$CF(r) = \Omega^2 \, r(c) \, Mb \qquad (7\text{-}4)$$

Where CF(r) = the centrifugal force acting on the spar root

r(c) = the radius of the blade's centre of gravity

Mb = mass of the blade

The mass, Mb, of one blade is 12kg and the radius of the centre of gravity of the blade (CG) is 1.2 metres. Therefore, with an angular velocity of 20 rad/sec, the centrifugal force acting on the blade spar root is:

$$CF(r) = 20^2 * 1.2 * 12$$
$$= 5760 \text{ N}$$

The tensile stress Tcs at the blade root due to CF(r) depends on the cross sectional area, As, of the root spar. The cross sectional area As of the root spar is given by the following equation:

$$As = (Do^2 - Di^2) * \pi / 4 \qquad (7\text{-}15)$$
$$= (75^2 - 63^2) * \pi / 4$$
$$= 1300 \text{ mm}^2$$

Tensile stress Tcs is equal to the force per unit cross sectional area and is therefore determined by the following equation:

$$Tcs = CF(r) / As \qquad (7\text{-}16)$$
$$= 5760 / 1300$$
$$= 4.4 \text{ N/mm}^2$$

This value has to be added to the Thrust bending stress to give a Combined Stress Cs:

$$Cs = Bs + Tcs \qquad (7\text{-}17)$$

So for Vo = Vf = 15m/s and N = 190 rpm the combined stress due to Thrust Bending Moment and centrifugal force is:

$Cs = 27 + 4.4 = 31.4\ N/mm^2$

As fatique strength of HT30 aluminium alloy tube is $124N/mm^2$ at $5 * 10^6$ cycles, the spar is acceptable.

7.4.4.1 CENTRIFUGAL LOADS ON SPINNING SAILFOIL HAWT AT RUNAWAY TIP SPEED RATIO

Assume Vo = Vf = 15m/sec.

Each wind turbine rotor has a runaway tip speed ratio which it will accelerate up to if it becomes decoupled from its load. This depends on the number and shape of the blades, the aerofoil used and the design tip speed ratio. Referring to Figure 6.13 shows that the predicted runaway tip speed ratio is 6. Therefore the angular velocity of the rotor at runaway tip speed ratio, X(max), is derived from the following equation:

$$\Omega(R) = \frac{X(max)\ Vo}{R} \qquad (7\text{-}18)$$

Where $\Omega(R)$ = Omega(R) = angular velocity at runaway tip speed ratio at max operating wind speed.

X(max) = Runaway tip speed ratio.

As Vo = Vf = 15m/sec, $\Omega(R)$ is therefore:

$\Omega(R) = 6 * 15/2$

$= 45$ rad/sec

Centrifugal Force under these conditions is therefore:

$$CF(r) = 45^2 * 1.2 * 12$$
$$= 29160 \text{ N}$$

and Tensile stress Tcs becomes:

$$Tcs = 29160 / 1300$$
$$= 23 \text{ N/mm}^2$$

Combined Thrust bending stress and centrifugal stress becomes:

$$Cs = 27 + 23 = 50 \text{ N/mm}^2$$

Fatigue strength of HT30 aluminium alloy tube spar is 124N/mm^2 at $5 * 10^6$ cycles so this value is acceptable.

7.4.5 WIND LOAD ACTING ON A PARKED SAILFOIL HAWT FACING INTO WIND AT V = 50m/s

The wind Thrust load, Tbp, acting on each wind turbine rotor blade in parked position is determined by the following equation (7-19) (See Figure 7.4):

$$Tbp = (1/2)\ \rho\ Vo^2\ Ab \qquad (7\text{-}19)$$

Where Ab = blade frontal surface area presented to the wind

In this case Ab = 0.76 m^2

$$Tbp = (1/2) * 1.29 * 50^2 * .76$$
$$\doteq 1225 \text{ N}$$

Bending moment due to this load is:

$$TM = Lc\ Tbp$$
$$= 0.96 * 1225$$
$$= 1176 \text{ N.m}$$

Bending stress in the root of the blade spar becomes:

$$Bsp = TM / Z$$
$$= 1176 * 1000 / 20797$$
$$= 57 \text{ N/mm}^2$$

This value is therefore acceptable by the criteria for fatigue strength of aluminium already cited (124 N/mm^2 at $5 * 10^6$ cycles).

REFERENCES FOR CHAPTER 7

Aluminium Federation (1980): personal communication

Betz, A (1927): Windmills in the Light of Modern Research NACA Technical memorandum No 474

Greer, A (1977 : Tables, Data and Formulae for Engineers Thornes

der Kinderen, W & van Meel, J (1976): Field Performance of Wind Power Machines: System Analysis and Measuring Methods, Application to a Small Windgenerator, Eindhoven University of Technology, Dept of Physics, Netherlands

Park, J (1981): The Wind Power Book, Cheshire Books

Taylor, DA (1980): Wind and Solar Flux Densities for Milton Keynes, Alternative Technology Group, Open University, Milton Keynes

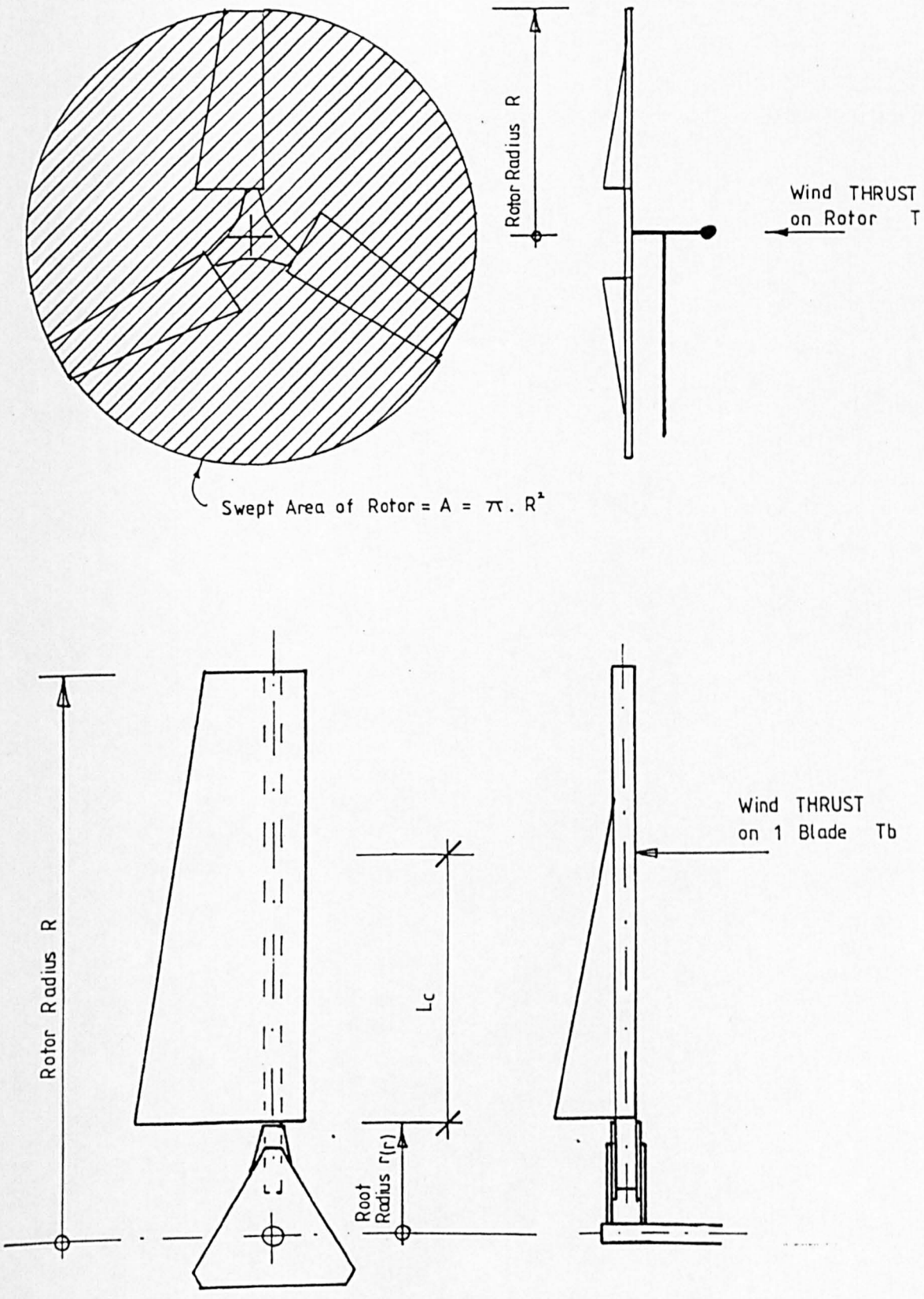

Fig 7.1: Wind Load on Sailfoil HAWT rotor

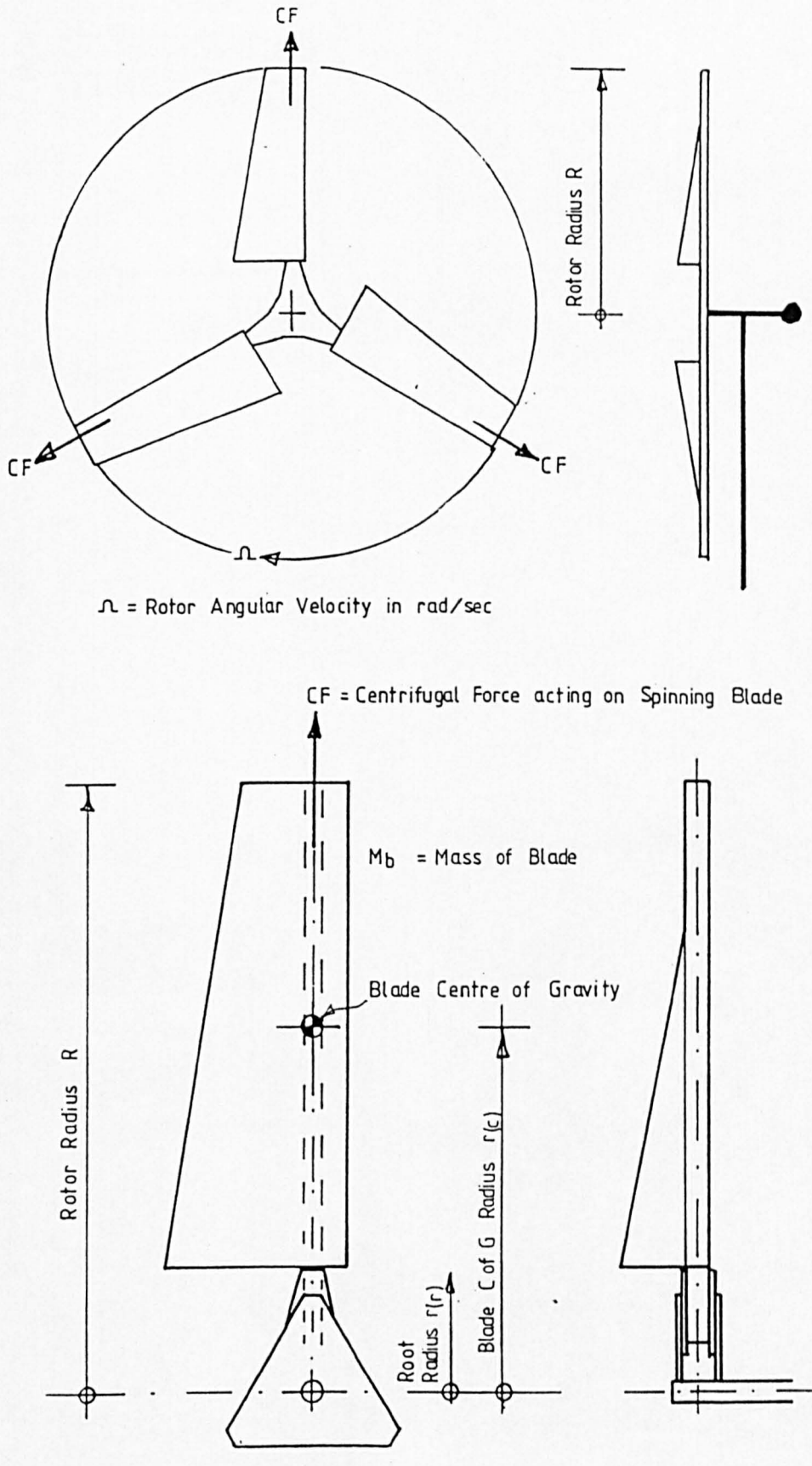

Fig 7.2: Centrifugal force on Sailfoil HAWT rotor

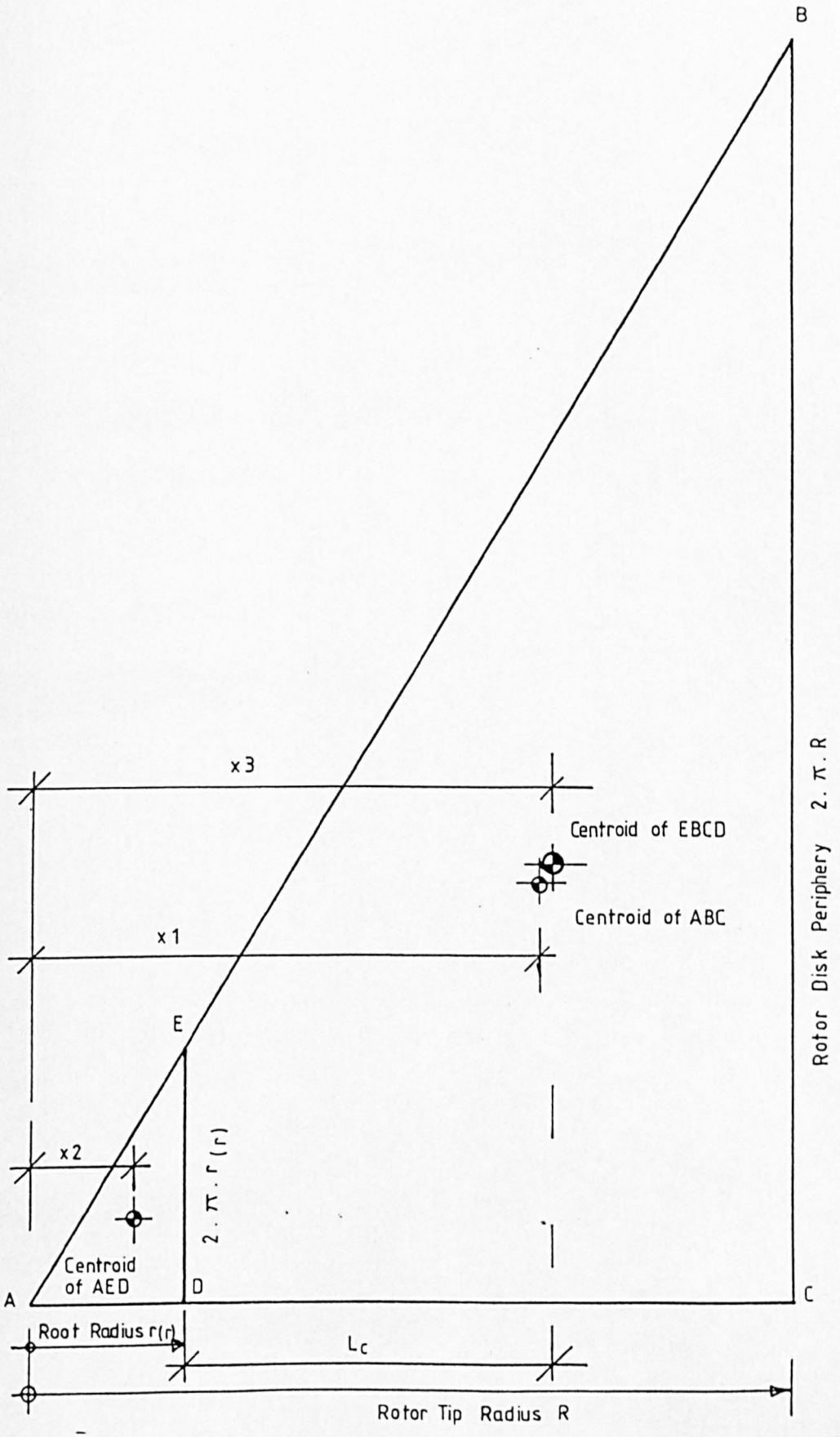

Fig 7.3: Relationship between rotor swept area and blade local radius r

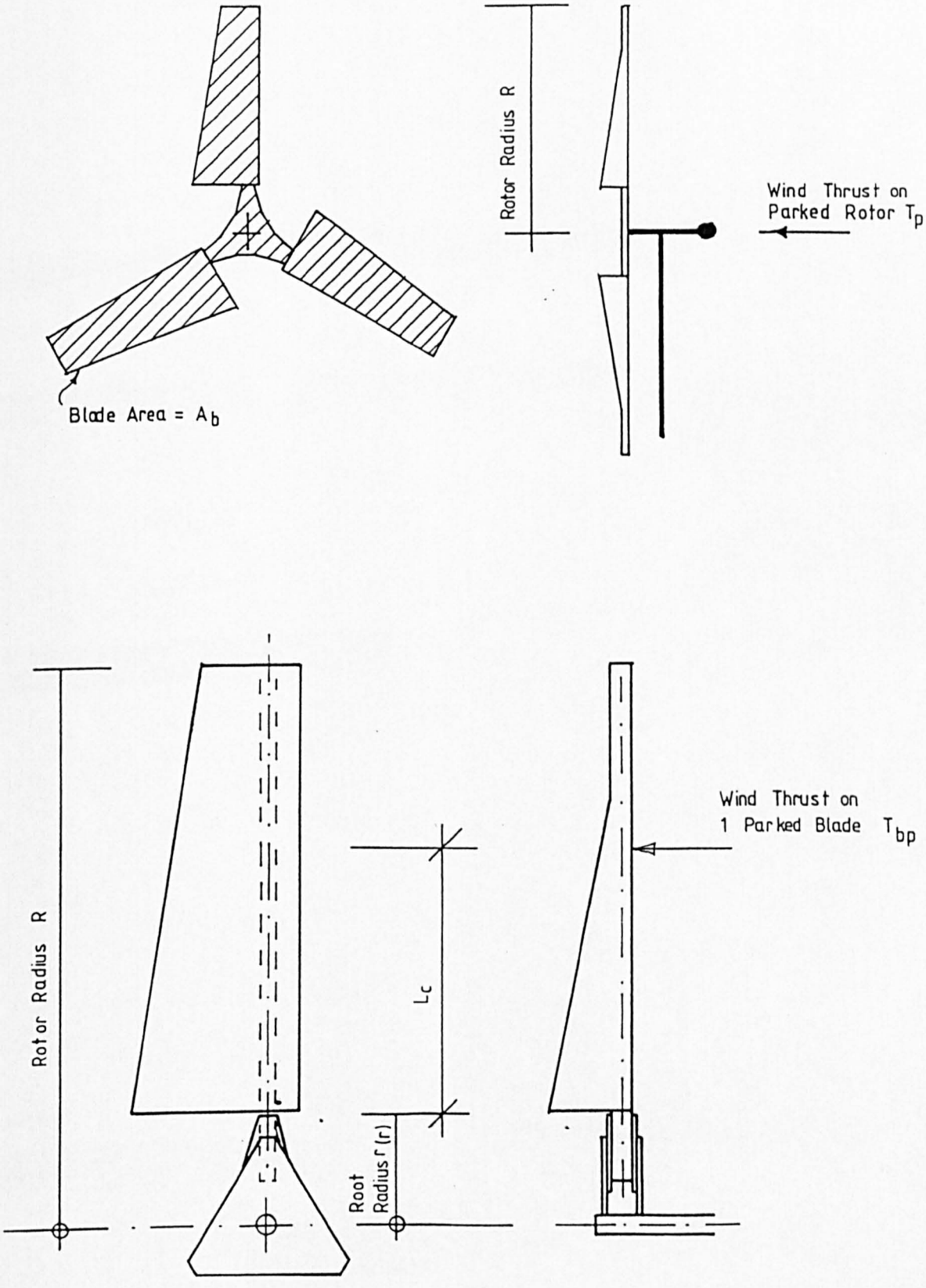

Fig 7.4: Wind load on parked Sailfoil rotor

CHAPTER 8

MECHANICAL DESIGN OF SAILFOIL HAWT & TEST RIG

LIST OF SYMBOLS IN CHAPTER 8

a = Lever arm of wind turbine from bearing 1.

ac = Arc of contact of belt to pulley on smaller pulley eq (8-2)

B1 = Reaction at bearing 1 eq (8-13)

B2 = Reaction at bearing 2 eq (8-12)

B3 = Reaction at bearing 3

B4 = Reaction at bearing 4

Bs = Belt speed eq (8-5)

BT1 = Belt tension in belt no. 1 (6 No) eq (8-7)

BT2 = Belt tension in belt no. 2 (3 No) see eq 8-8

b = Centre distance between bearing 1 & bearing 2 (see Fig 8.9)

Cor = Basic static load rating of bearing

CQ = Torque coefficient of wind turbine eq (4-35)

Cr = Basic dynamic load rating of bearing

Cs = Size factor for shaft from Fig 8-9

D = Pitch diameter of larger pulley at one stage

d = Pitch diameter of smaller pulley at one stage

d = Centre distance between bearing 3 & bearing 4 (see Fig 8.13)

Di = Inner diameter of hollow shaft

Do = Outer diameter of hollow shaft eq (8-6)

o = Outer diameter of solid secondary shaft eq (8-9)

e = Centre distance of pulley 2 from bearing 4 (see Fig 8.13)

f = Centre distance between pulley 2 & pulley 3 (see Fig 8.13)

Fr = Radial load at bearing

Fp = Peak axial force in N.
= wind thrust on rotor

= T. see eq (7-6) in chapter 7

h = Ratio of outer diameter to inner diameter
= Do/Di see eq (8-8)

J1 = 12/se eq (8-7)

J2 = Variable used in design of shafts eq (8-8)

J3 = Variable used in design of shafts eq (8-9)

J4 = Variable used in design of shafts eq (8-10)

J5 = Variable used in design of shafts eq (8-11)

K = Factor for bearing thrust loading

Ks = Stress coefficient appropriate to stress raising condition of shaft from Figs 8.10 & 8.11

Kt = Factor for thrust loading
= 7.2047

Life= Life of bearing eq (8-14)

Mp = Peak bending moment in shaft

Mp2 = Maximum bending moment acting on the secondary shaft

N = rpm of pulley/shaft eq (8-5)

nb = Number of belts at one stage eq (8-2)

P = P Peak power to be transmitted by belts

P1 = Weight of pulley No 1 eq (8-12)

P2 = Weight of pulley No 2 eq (8-7)

P3 = Weight of pulley No 3 eq (8-8)

Pb = Power transmitted by one belt

pd = Relationship between pulley diameters and centre distance eq (8-3)

Pf = Force required to deflect a belt 16mm per m span eq (8-2)

Q = Torque of wind turbine rotor eq (4-35)

Qb = Brake torque

Qp = Peak shaft torque eq (8-9)

R = Tip radius of wind turbine rotor eq (4-35)

Sl = Service factor for belts

Se = Endurance limit in rotating bending of shaft material

SF = Shock factor

T = Vo^2*Kt eq (7-6)

Tbc = Centrifugal belt tension, dependent on belt speed Bs

Tbs = Static belt tension eq (8-1)

Vo = Undisturbed wind velocity eq (4-35)

W2 = Weight of pulley 2 + weight of belt No 1 (6 No) see eq (8-7)

W3 = Weight of pulley 3 + weight of belt No 2 (3 No) see eq (8-9)

Wbl = Weight of belt No 1 (6 No) eq (8-7)

Wb2 = Weight of belt No 2 (3 No) eq (8-8)

Wbr = End load imposed on the shaft when running by belt tension eq (8-4)

Wbs = Total static end load Wbs eq (8-2)

WT = Weight of rotor, hub + brakedrum (N)

Ω = Omega = Angular velocity of shaft r/sec
ρ = Rho = Air density eq (4-35)

8.1 INTRODUCTION

The Sailfoil wind turbine rotor is designed to drive an electric generator. The turbine has been designed so that the generator and all the transmission equipment are located on a chassis that rotates about a vertical axis at the top of a 10 metre tall guyed mast (see Fig 8.1).

For small scale Horizontal Axis Wind Turbines this is generally the most popular arrangement. It avoids the need for a right-angle bevel gear if the generator is located at the top of the mast or tower, and it avoids the need for a long vertical shaft if the generator is to be located at or near ground level. However it necessitates the use of slip rings or flexible cables to transmit the power from the rotating chassis to the ground.

As a tilting mast was an integral part of the test rig, it was not necessary for the generator to be located near the ground as it could be accessed by tilting the mast to ground.

In order to make the turbine test rig as adaptable as possible (to allow other turbine rotors to be tested), a parallel shaft lay out was chosen for the gearing and power transmission. The power transmission was based on

readily available standard V belts and pulleys in a 2 stage step up arrangement. By changing the pulley sizes, different gear ratios can be readily obtained.

V belts were chosen because of their adaptability and also because of their ability to withstand extreme loads by slipping rather than breaking, as would be the case with toothed belts for example.

The two transmission shafts are supported on the chassis by standard off-the-shelf flange bearing units, two of the tapered roller and two of the ball bearing type. Taper bearings are used where the thrust and radial loads are higher than is acceptable for ball bearings of a given bore diameter.

A number of arrangements were examined to fit the confined space available (see Fig 8.2 for the final choice) which permits easy access for changing V belts, bearings and generator.

The wind turbine hub, which also supports a brake drum (needed for safety purposes), is attached to the cantilevered end of the wind turbine shaft via a taper lock hub adaptor. At the other end of the wind turbine shaft, pulley no. 1 is coupled via V belts to pulley no. 2 on the secondary shaft which is located above and parallel to the main wind turbine shaft (see Fig 8.2). The power is transmitted from the secondary shaft via

pulley no. 3 to pulley no. 4 on the alternator.

The wind turbine chassis is based around a Square Hollow Section (SHS) steel tube which slips over the top of the mast and is able to turn about the yaw axis by means of machined nylon bearings mounted between the mast top and the chassis pivot tube (Fig 8.3).

The advantage of using a square section tube as the main part of the chassis, is that the flat sides facilitate the attachment of the flanged bearing housings which are simply bolted to two sides of the SHS pivot tube. The brackets necessary for supporting the alternator and the lorry drum brake are also bolted (and blind permanent connections pop-riveted) to the pivot tube, thus avoiding the use of welding, providing for later modification, and resulting in a relatively simple and straightforward manufacturing process, without the need for elaborate manufacturing equipment (see Fig 8.4).

8.2 WIND TURBINE ROTOR HUB

The rotor blades are attached to the rotor shaft by means of a specially designed hub assembly (see Fig 8.5-8.6).

This hub assembly has been designed in such a way that the blades can be removed, allowing other types of

blades to be tested subsequently.

The hub is based around a steel ring into which a taper-lock hub adaptor is inserted. Two steel triangular plates are bolted to this ring and the blade spar ends are bolted to these plates. As there is the possibility of corrosion occuring due to different metals (steel and aluminium) being in contact with each other, stainless steel bolts and rivets were used between the spar and the hub plates and thin sacrificial sheets of aluminium have been inserted so that in the event of corrosion occuring, these sheets would be affected before the spar and they could then be replaced.

The hub has to be capable of absorbing the structural loads acting on the rotor as well as transmitting the power and torque to the rotor shaft.

The hub is also bolted to a lorry brake drum, see Fig 8.7, which is designed to absorb rotor torque in high wind speeds up to 50m/sec.

8.3 DESIGN OF WEDGE BELT POWER TRANSMISSION SYSTEM

Figure 8.8 shows a two stage wedge belt (a compact form of "V" belt) transmission which was designed to translate the wind turbine's relatively slow angular

velocity (peak 190 rpm) into the high rotation speed required by the alternator (peak of 1500 rpm). This requires an overall speed ratio of 1500/190 = 7.9. A combination of ratios 1 to 2.67 and 1 to 2.97 giving an overall speed ratio of 1 to 7.93 was chosen and the transmission system was designed with the aid of the manufacturers V-Belt Drive Design Handbook, (Fenner, 1980) as follows.

8.3.1 DESIGN OF 1ST STAGE WEDGE BELT TRANSMISSION

Peak Power P to be transmitted by belts = 5kW

Peak RPM of wind turbine shaft = 190rpm

Service factor, S1, was determined from the Fenner Handbook as 1.77 which takes into account the type of loading for class 3 (see appendix).

Design Power to be transmitted = P*S1 = 5*1.77 = 8.8kW

Belt type SPA was selected from the handbook, as being in the required power range.

Speed Ratio = 1 to 2.67

Pitch Dia of pulley No 1 = 315mm

Pitch Dia of pulley No 2 = 118mm

Pulley centre distance = 304mm

Belt length = 1320mm

The power, Pb, capable of being transmitted by one SPA belt in this arrangement was determined from the catalogue as = 1.49kW.

The number of belts required to carry the Design Power = 8.8/1.49 = 6 belts

Therefore each pulley has to have 6 grooves, ie, pulley No 1 is SPA/031A0336 which has a mass of 21.56kg and pulley No 2 is SPA/031A176 which has a mass of 2.96kg.

8.3.2 DESIGN OF 2ND STAGE WEDGE BELT TRANSMISSION

Peak Power P to be transmitted by belts = 5kW

Peak rpm of secondary shaft = 190 * 2.67 = 507 rpm.

Service factor, S1, is the same as for the first stage transmission, ie, 1.77 for class 3.

Design Power = P * S1 = 5 * 1.77 = 8.8kW

Belt type, SPA, was selected from the Fenner handbook.

Speed ratio = 1 to 2.97

Pitch Dia of pulley No 3 = 315mm

Pitch Dia of pulley No 4 = 106mm

Peak rpm of pulley no 4 (alternator) = 507 * 2.97

= 1500 rpm.

The power, Pb, capable of being transmitted by one SPA wedge belt in this arrangement was determined from the handbook as 3.39kW.

The number of belts required to carry the Design Power = 8.8/3.39 = 3 belts

So each pulley has to have 3 grooves, ie, pulley No 3 is SPA/031A0333 which has a mass of 13.61kg and pulley No 4 is SPA/031A0153 which has a mass of 1.53kg.

8.3.3 LOADS IMPOSED BY WEDGE BELT DRIVES

8.3.3.1 STATIC LOADS

8.3.3.1.a FIRST STAGE TRANSMISSION

Static Belt Tension, Tbs, is given by the following equation (Fenner, 1980):

$$Tbs = 16 * Pf \qquad (8\text{-}1)$$

Where Pf = the force required to deflect a belt 16mm per m span. Assume 80% of upper figure

from catalogue recommendations.

= 0.8 * 27 (from handbook)

= 21.6 N

Tbs = 16 * 21.6 = 345.6 N

The total static end load Wbs is the vector sum of the tensions in both sides, ie:

$$Wbs = 2 * Tbs * Sin\ (ac/2) * nb \qquad (8\text{-}2)$$

Where ac = arc of contact on the smaller pulley

nb = number of belts.

The arc of contact, ac, depends on the following relationship and is found from the Fenner handbook:

$$Pd = (D - d)/cd \qquad (8\text{-}3)$$

Where D = Dia of larger pulley

d = Dia of smaller pulley

cd = centre distance between pulleys

Pd = (315 - 118)/304 = 0.648

Arc of contact, ac, (corresponding to Pd = 0.648) is 140 deg from handbook. Inserting these values into equation (8-2) we obtain the static end load:

Wbs = 2 * 345.6 * Sin(140/2) * 6

= 4147 * Sin 70 = 3900 N

8.3.3.1.b SECOND STAGE TRANSMISSION

Pf = 0.8 * 27 = 21.6 N

Tbs = 16 * 21.6 = 345.6 N

Angle of contact, ac, of smallest pulley

Pd = (D - d)/cd

= (315 - 106)/312

So ac = 141 degrees from handbook

Wbs = 2 * Tbs * Sin(ac/2) * nb

= 2 * 345.6 * Sin 70.5 * 3

= 1955 N

8.3.3.2 RUNNING LOADS DUE TO WEDGE BELTS

8.3.3.2.a FIRST STAGE TRANSMISSION

To determine the approximate end load Wbr imposed by a drive when running, the centrifugal tension, Tbc,in each side of the pulley must be subtracted from the static

tension, Tbs, before the vectorial summation:

$$Wbr = 2((16\ Pf) - Tbc)\ Sin(ac/2)\ nb \qquad (8\text{-}4)$$

The centrifugal tension Tbc developed in a belt is a function of its weight and the square of the belt speed Bs. The belt speed Bs is given by the following equation (8-5) (Fenner, 1980):

$$Bs = (d\ N)/19100 \qquad (8\text{-}5)$$

Where d = dia of small pulley
N = rpm of the same pulley

$$Bs = 118 * 507/19100 = 3.13\ m/sec$$

Given the belt speed, the tension can be derived from table F.15 in the Fenner handbook (see appendix). Therefore belt tension, Tbc, for SPA wedge belt at a belt speed of Bs = 3.13 m/s, is 2.0 from Fenner handbook. Inserting this into equation (8-4), Wbr is determined as follows:

$$Wbr = 2((16 * 21.6) - 2.0) * Sin(140/2) * 6$$
$$= \underline{3875\ N}$$

8.3.3.2.b SECOND STAGE TRANSMISSION

Belt speed Bs = (d N)/19100

= (106 * 1500)/19100

= 8.32 m/s

So Tbc = 9.5 N for SPA belt per belt corresponding to Bs = 8.3 m/s

Wbr = 2((16 Pf) - Tbc) Sin(ac/2) nb

= 2((16 * 21.6) - 9.5) * Sin(141/2) * 3

= 1900 N

8.4 DESIGN OF POWER TRANSMISSION SHAFTS

The power transmission shafts were designed according to the Australian ASA-B249 shaft design method described by Stephenson & Callander (1974) and takes account of fatigue loadings. In the case of the wind turbine shaft, axial loads are also allowed for.

8.4.1 DESIGN OF WIND TURBINE SHAFT

Stephenson & Callander (1974) give the following formula, (equation 8-6) for designing shafts based on ASA-B249:

$$Do = (J1\ (J2 + J3)^{1/2})^{1/3} \qquad (8\text{-}6)$$

Where $J1 = 12/Se$ (8-7)

$$J2 = [Cs\ Ks\ SF\ (Mp+((Fp\ Do\ (1-h)^2)/8))]^2 \qquad (8\text{-}8)$$

$$J3 = (3/16)\ SF\ [(1+(Cs\ Ks))\ Qp]^2 \qquad (8\text{-}6)$$

Do = outer diameter of hollow shaft (mm)

Di = inner diameter of hollow shaft (mm)

h = Di/Do

Se = endurance limit in rotating bending of steel shaft material (0.45 * UTS) (N/mm^2)

Qp = Peak Shaft Torque (N.mm)

Mp = Peak Bending Moment (N.mm)

Fp = Peak Axial Force (N)
= Wind Thrust on Rotor = T in (N)

$T = Vo^2 * Kt$ (8-6)

Kt = 7.2047

Cs = size factor from Fig 8.10

Ks = stress coefficient appropriate to stress raising condition of shaft from Figs 8.11 & 8.12

SF = Shock Factor = 2 for heavy shocks

WT = Weight of Rotor, hub and brake drum

Assume Vo = 15 m/s

So Peak Torque Qp(at Omega = 20 r/sec)

= P/Omega = 5000/20

= 250 N.m = 250000 N.mm

Peak Bending Moment, Mp, due to weight of rotor, hub and break drum = WT * a

= 1100 * 370

= 407000 N.mm

Peak Axial Force Fp = Wind Thrust T acting on rotor.

Refering to equation (8-6)

$$T = Vo^2 * Kt \qquad (8\text{-}6)$$

$$T = 1542 * 7.2047 = 1621 \text{ N}$$

Assume shaft material is SKF214/ISOM19 (En14A) to BS970
Ultimate tensile strength ranges between 490 to
610 N/mm^2

So endurance limit for fatigue Se = 0.45 * 490
= 220 N/mm^2

Assume outer Dia, Do, = 76.2 mm (3 inches)
& inner Dia, Di, = 50.8 mm (2 inches)

$h = 2/3 = 0.666$

Assume Cs = 1.6 from Fig 8.10
Assume Ks = 2 from Fig 8.11

Inserting these values into equations 8-3, 8-4,8-5 & 8-6
we obtain:

$$J1 = 12/Se \qquad (8\text{-}4)$$

$$= 12/220 = \underline{0.0545}$$

$$J2 = [Cs\ Ks\ SF\ (Mp+((Fp\ Do\ (1 - h)^2))/8)]^2 \qquad (8\text{-}5)$$

$$= [1.6*2*2*((407000+((1621*76.2*(1-0.66)^2)/8]^2 \qquad (8\text{-}5)$$

$= [3.2 * 2\ (407000 + 1715.59]^2$

$= [3.2 * 2 * 408715.5]^2$

$= [2 * 1307889.7]^2$

$= [2615779.4]^2 = \underline{6.842E12}$

$J3 = (3/16) * SF\hat{}2 * [(1 + (Cs * Ks)) * Qp]^2$ (8-6)

$= (3/16) * 2^2 * [(1 + (1.6 * 2)) * 250000]^2$

$= 0.75 * [4.2 * 250000]^2$

$= 0.75 * [1050000]^2$

$= 0.75 * 1.1025E12 = \underline{8.268E11}$

Inserting these values into equation 8-3 we obtain

$Do = [J1 * (J2 + J3)^{(1/2)}]^{(1/3)}$ (8-3)

$= [0.0545 * (6.842E12 + 8.268E11)^{(1/2)}]^{(1/3)}$

$= [0.0545 * (7.668E12)^{(1/2)}]^{(1/3)}$

$= [0.0545 * 2769273.4]^{(1/3)}$

$= [150925.4]^{(1/3)} = \underline{53\ mm}$

Shaft with Do = 76.2 mm and Di = 50.8 mm is therefore satisfactory.

8.4.2 DESIGN OF SECONDARY SHAFT

8.4.2.1 LOADS ON SECONDARY SHAFT

Design conditions : Vo = 15 m/sec.

Refer to Figure 8.12

$$W2 = P2 + BT1 + Wb1 \qquad (8\text{-}7)$$

Where P2 = weight of pulley No.2 = 29 N
BT1 = static end load due to belt tension in belt No.1 (6 belts)
= Wbs = 3900N
Wb1 = weight of belt No.1 (6 belts) =11.5 N

$$W2 = 29 + 3900 + 11.5 = \underline{3941}\ N$$

and

$$W3 = P3 + BT2 + Wb2 \qquad (8\text{-}8)$$

Where P3 = weight of pulley No.3 = 133 N
BT2 = end load due to belt tension in belt No.2 (3 belts)
= Wbs2 = 1955N
Wb2 = weight of belt No.2 (3 belts) = 5.7 N

$$W3 = 133 + 1955 + 5.7 = \underline{2094}\ N$$

The maximum bending moment, Mp2, acting on the secondary shaft occurs at Bearing 4:

$$Mp2 = [W2\ e] + [W3\ (e + f)]$$
$$= [3941 * 120] + [2094 * 230]$$
$$= 472920 + 481620$$
$$= 954540\ N.mm$$

The secondary shaft was designed using the same procedure as for the wind turbine shaft except that a solid shaft was used and there is no axial force. The shaft design formula (8-3) becomes:

$$do = [J1\ (J4 + J5)^{(1/2)}]^{(1/3)} \qquad (8\text{-}9)$$

where $J4 = [Cs\ Ks\ Mp2]^2$ (8-10)

$J5 = (3/16)*[(1+(Cs*Ks))*Qp]^2$ (8-11)

Qp = peak torque = 97540 N.mm

do = outer dia. of solid shaft = 50.8mm (2 inches)

Se = endurance limit for fatigue for shaft material (SKF CEAX centreless ground shaft steel) (060 A47 to BS 970 UTS=590 N/mm^2)

$= 0.45 * 590 = 265\ N/mm^2$

Cs = 1.4 from Fig. 8.10

Ks = 1.8 from Fig. 8.11

Inserting these values into equations h-4, 8-6, 8-9, & 8-10 we obtain :

$$J1 = 12 / Se \qquad (8\text{-}4)$$

$$= 12 / 265 = 0.04528$$

$$J4 = [Cs\ Ks\ Mp2]^2 \qquad (8\text{-}10)$$

$$= [1.4 * 1.8 * 954540]^2$$

$$= 5.786E12$$

$$J5 = (3/16)\ [(1 + (Cs\ Ks))\ Qp2]^2 \qquad (8\text{-}11)$$

$$= (3/16) * [(1 + (1.4*1.8)) * 97540]^2$$

$$= 2.2103E10$$

Inserting into 8-9 we obtain the minimum permissible size of shaft:

$$do = [J1\ (J4 + J5)^{(1/2)}]^{(1/3)} \qquad (8\text{-}9)$$

$$= [0.04528 * (5.786E12 + 2.2103E10)^{(1/2)}]^{(1/3)}$$

$$= \underline{47.8\ mm}$$

Therefore a solid steel shaft of 50.8 mm Dia is satisfactory for the secondary shaft.

8.5.1 BEARING DESIGN

8.5.1.1 BEARINGS SUPPORTING THE WIND TURBINE SHAFT

Design conditions Vo =15 m/sec

Refer to Fig. 8.9

Taking moments about Bearing 1 (B1)

8.5.1.1.1 Reaction at Bearing 2:

$$(B2) = [((P1 + Wb1 - Bt1)\ (b + c)) - (WT\ a)]/\ b \qquad (8\text{-}12)$$

$$= [((272+11.5-3900)*(345+90))-(1100*370)]/345$$

$$= -\ 5740\ N$$

Taking moments about Bearing 2 (B2)

8.5.1.1.2 Reaction at Bearing 1:

$$(B1) = [((P1 + Wb1 - BT1)\ c) + (WT\ (a + b))]/\ b \qquad (8\text{-}13)$$

$$= [3616.5*90)+(1100*715)]/345$$

$$= 3224\ N$$

8.5.1.2 DESIGN OF BEARING NO.1

Radial load on Bearing No.1 = reaction at Bearing No.1:

B1 = 3224 N

Axial load due to Wind Thrust on Rotor at Vo = 15 m/sec) from equation (8-6):

$Fp = T = Vo^2 Kt = 15^2 * 7.2047$

= 1612N

Rpm, N, of Wind Turbine Shaft = 190 rpm

Try Wraxall Browning Tapered Roller Bearing Flange Block Bearing FB 901, 3 inch (76.2mm) bore.

From Browing catalogue K factor for Thrust loading = 0.4

Permissible load for a 30 000 hours minimum life from catalogue:

= 0.4 * 7712 = 3085 lbf = 13722 N

Bearing is therefore satisfactory.

8.5.1.3 DESIGN OF BEARING NO.2

Radial load on Bearing No.2 = reaction at Bearing No.2:

B2 = 5740 N

Rpm of shaft = 190 rpm

As the radial load is lower and thrust load is absorbed by bearing No1, a cheaper ball bearing type can be used.

Try RHP Self-lube flange bearing unit MSF 3, 3inch (76.2 mm) bore.

The design procedure adopted by RHP differs from the Wraxal/Browning and is based on calculating the minimum life of the bearing for a given load and speed.

Basic Dynamic load rating Cr = 55500 N from catalogue (RHP, 1980)
Basic Static load rating Cor = 44500 N from catalogue (RHP, 1980)

The minimum life of the bearing is given by the following equation (RHP, 1980):

$$\text{Life in Revs.} = [(Cr/Pr)^3] * 10^6 \qquad (8\text{-}14)$$

$$= [(55500/5740)^3] * 10^6$$

$$= 1.122E9 \text{ cycles}$$

$$= \underline{98480} \text{ continuous hours (11 years)}$$

Bearing is therefore suitable given the limited life of the project.

8.5.2 BEARINGS SUPPORTING SECONDARY SHAFT

Refering to Figure 8.13

Taking moments about B3

Reaction at Bearing No 4:

$$B4 = [(W2\ (e+d)) + (W3\ (e + f + d))]/d$$

$$= [(3941 * (120+330)) + (2094*(120+110+330))]/330$$

$$= \underline{7495}\ N$$

Taking moments about B4

Reaction at Bearing No.3:

$$B3 = [(W2 * e) + (W3 * (e + f))] / d$$

$$= [(3941 * 120) + (2094 * (120 + 110))]/330$$

$$= \underline{2892.5}\ N$$

8.5.2.1 DESIGN OF BEARING NO.3

Radial load, Fr = reaction @ Bearing 3 = B3 = 2893 N

Rpm of secondary shaft = 507 rpm

Try RHP Self-lube flange ball bearing unit MSF2, 2 inch (50.8 mm) bore.

Basic Dynamic Load Cr = 33400 N from catalogue

$$\text{Life in revs} = [(Cr/Fr)^3] * 10^6 \quad (8\text{-}14)$$

$$= [(33400/2893)^3] * 10^6$$

$$= 1.54E9 \text{ cycles}$$

= 50625continuous hours (5.8 years)

Bearing is therefore suitable for this project given its limited lifetime of 5 years.

8.5.2.2 DESIGN OF BEARING NO.4

Radial load = reaction at Bearing No.4 = B4 = 6300 N

RPM of secondary shaft = 507 RPM

Try Wraxall Browning tapered roller flange block bearing FB901, 2 inch (50.8 mm) bore.

Permissible radial load @ 500 rpm for 30 000 hours minimum life = 11566 N.

Bearing is therefore satisfactory.

8.6 BRAKE DESIGN FOR SAILFOIL HAWT

To be able to park the rotor for maintenance or to stop the wind turbine under emergency conditions and to prevent it from overspeeding and inducing very high centrifugal loads in the blades, it is necessary to have a mechanical brake in the system. (See Figure 8.14).

For safety and reliability in the event of failure of the transmission system, it is advisable to have the

brake on the low speed wind turbine shaft, even though this means that it has to cope with much higher torque values than a brake on the higher speed shaft. See Figure 8.13.

The worst case that the brake has to be designed for is that of the wind turbine facing directly into a 50m/sec wind.

The maximum theoretical torque coefficient for the Sailfoil HAWT rotor with linearised blades is assumed for design purposes to be 0.14 which occurs at a tip speed rato, X, of 2. See Figure 8.15.

Equation (4-35) gives the relationship of torque to wind speed:

$$CQ = Q / [0.5 \rho \pi R^3 Vo^2] \qquad (4\text{-}35)$$

which gives the following:

$$Q = 0.5 \rho \pi R^3 Vo^2 CQ \qquad (8\text{-}15)$$

Inserting the above values, the brake torque, Qb, required for a wind speed of 50 m/sec is given by the following:

$$Qb = 0.5 * 1.29 * \pi * 2^3 * 50^2 * 0.14$$

$$= \underline{5674} \text{ N.m}$$

We therefore need to have a brake which is capable of absorbing this torque input.

A number of types of brakes, were examined including disc brakes, but these were rejected as the size of disc was such that it would have been difficult to incorporate into the chassis and would have been difficult to protect from the weather.

For compactness it was therefore decided to use a drum type brake and the one chosen was a Lucas/Girling 12(3/8)" x 5" 2LS type Lorry brake.

This brake has a maximum design rated torque of 5800 N.m and is sufficient to cope with the maximum wind torque.

The brake is mechanically activated and is operated manually, from ground level. This is achieved by a lever mechanism located over the centre axis of the mast, Fig. 8.16. When this lever is pulled via a steel cable from ground level, the brake piston is pulled and the brake shoes come into contact with the spinning drum to slow or stop the rotor.

To allow for the turbine turning about the yaw axis, a cable swivel is employed between the yawing turntable and the base of the mast.

8.7 YAW OR TURNTABLE BEARING

Horizontal axis wind turbines have to be able to be turned about a vertical axis, so that the rotor can be moved to point into the wind when there is a change of wind direction.

This vertical axis which runs through the centre of the mast, is known as the "yaw axis" and the operation of turning the turbine to adjust for wind direction is known as "yaw".

In the wind turbine test rig, the yawing or turntable bearing consists of a thrust or pad bearing and two radial bearings. The turbine on the test rig is pointed into the wind or out of the wind manually.

As the yawing speed for a wind turbine is slow (< 5 rad/sec), ball or roller bearings are not required. Therefore nylon bearings were used which fit between the top of the mast and the pivot tube and the bearings have also been designed to be easily dismantled. To obtain ball or roller bearings of the necessary diameter would have been expensive.

The thrust bearing consists of a NYLATRON pad which sits on the top of the flat top of the mast cap. This is the surface upon which it turns. It is bolted to the

underside of a pad bolted to the inside of the square hollow section pivot tube.

The top and bottom radial bearings are identical and each is made up of machined NYLATRON which is bored to fit around the outer diameter of the mast about which it rotates and bolted to the inside of the pivot tube. The top radial bearing is located just below the thrust bearing and the bottom bearing is located at the bottom of the pivot tube.

Figure 8.18 shows the yaw bearing arrangement.

8.8 REFERENCES IN CHAPTER 8

ASA - B259 (1969) : Design of Shafts for Cranes and Hoists, Australian Standards Association

Fenner, JH (1980) :V-Belt Drive Design Handbook]

Lucas/Girling(1978): Leaflet on Drum brakes

Stephenson, J & Callander, (1974): Engineering Design, Wiley

RHP (1980) - Selflube Bearing Catalogue/Handbook

Wraxall (1979) - Browning Tapered Roller Bearing Catalogue

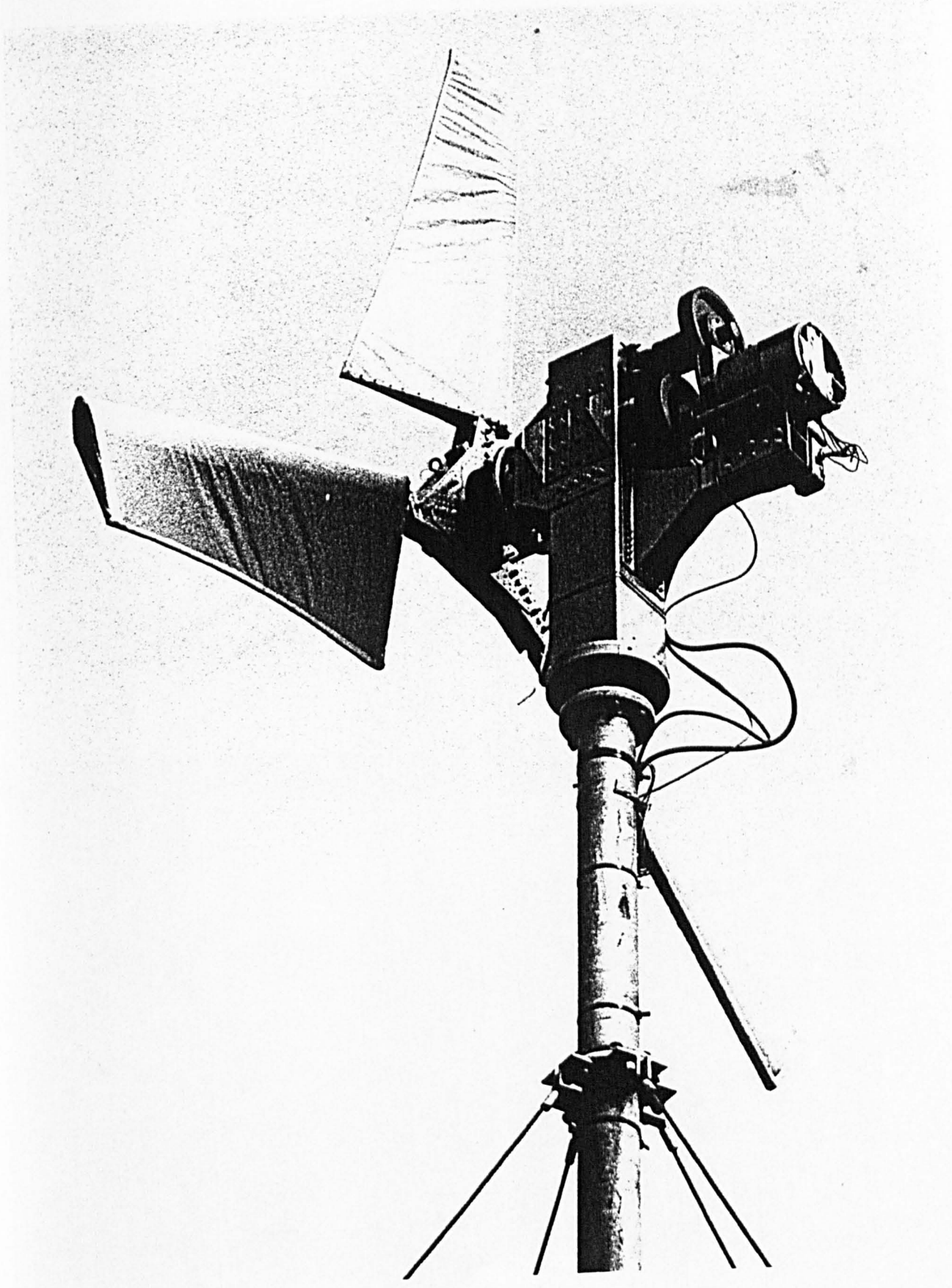

Figure 8.1: View of wind turbine at head of mast showing transmission arrangement with generator on chassis able to rotate about vertical axis (yaw)

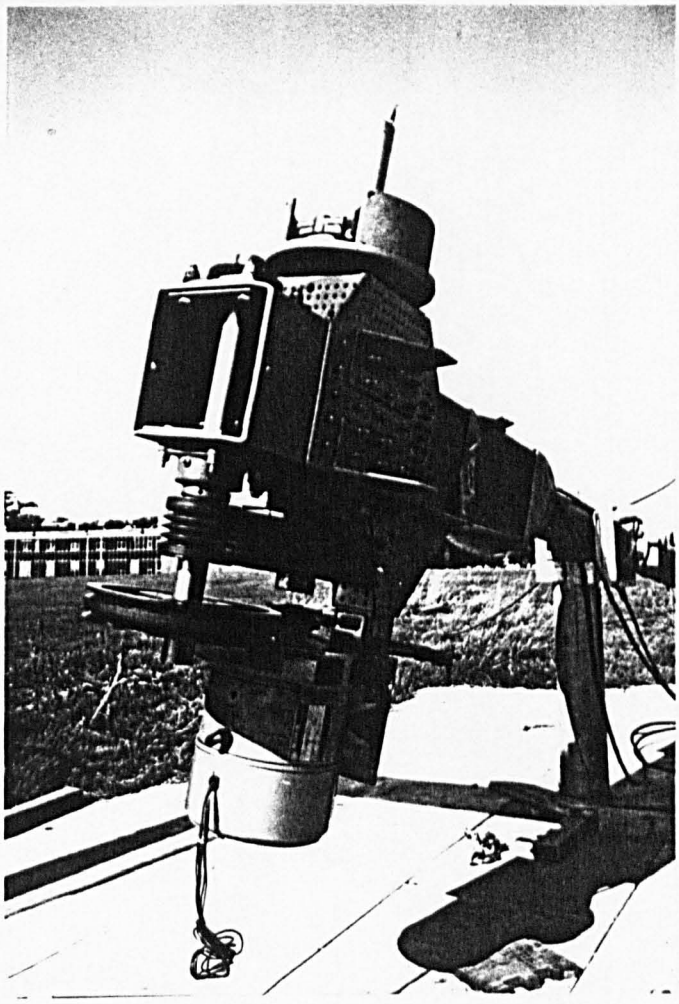

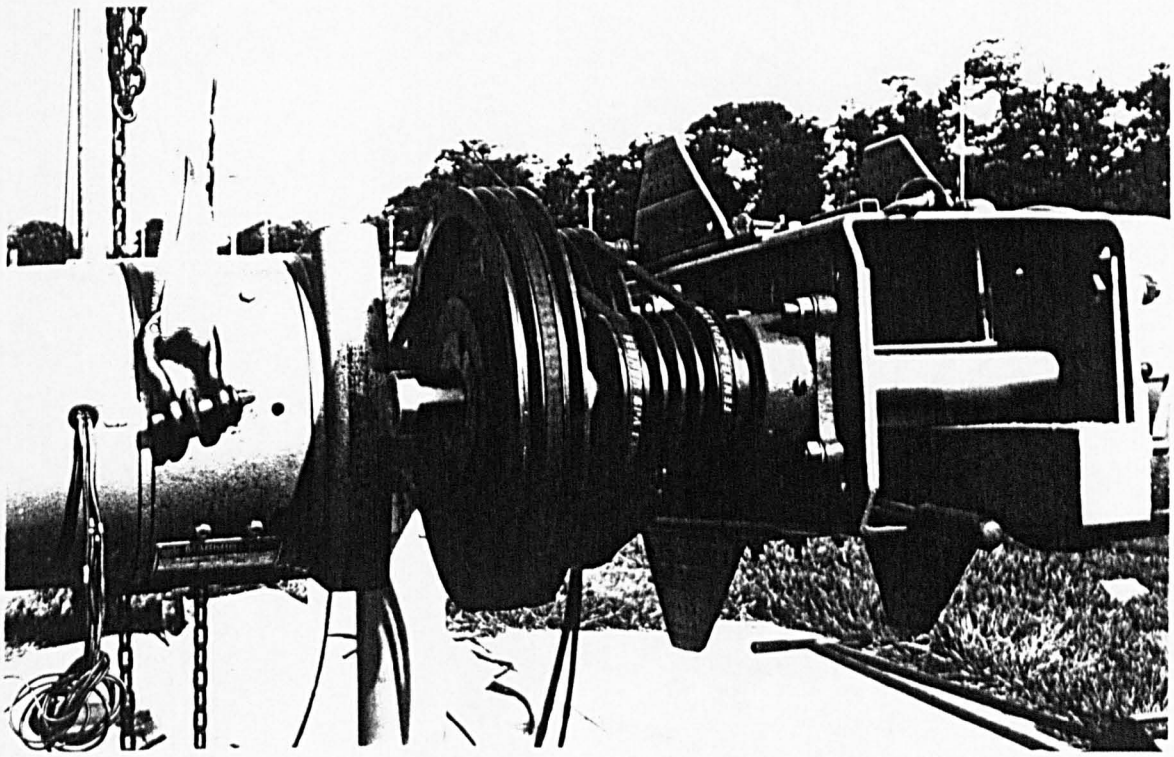

Figure 8.2: Arrangement of 2 stage V belt gearing transmission showing twin shafts

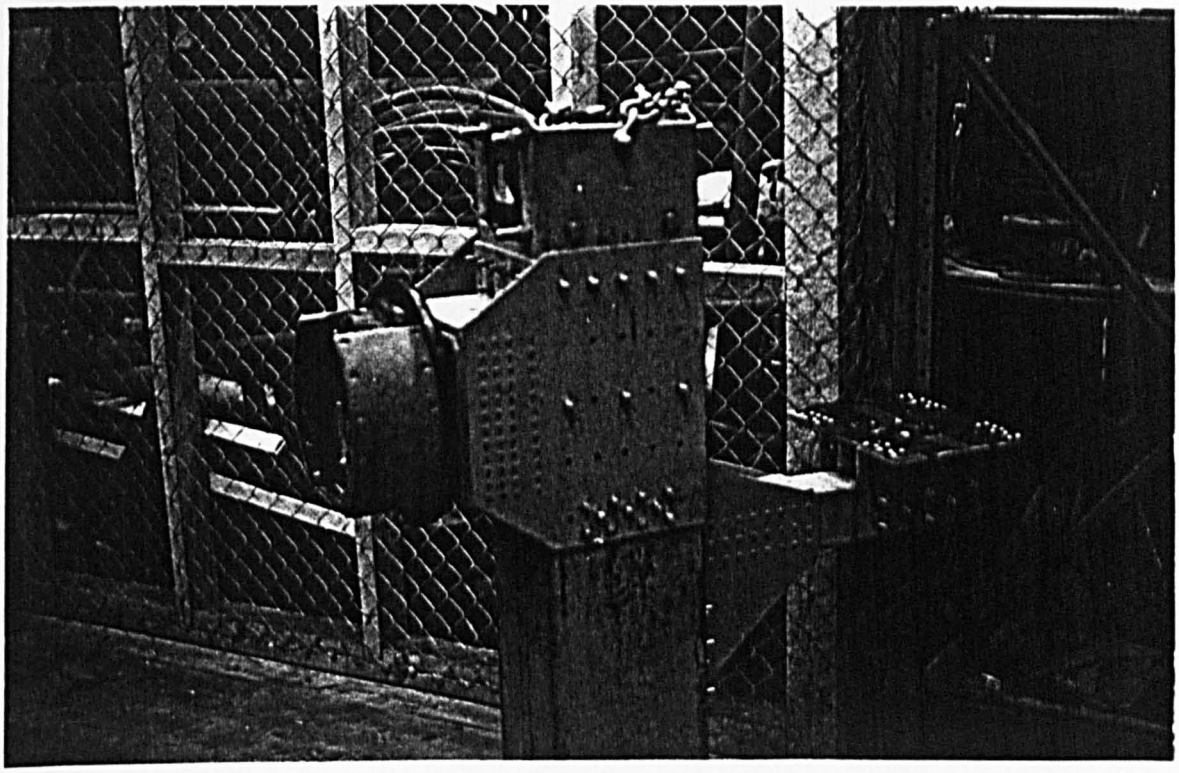

Fig 8.3a: (above)
Square hollow section (SHS) steel pivot tube forms the basis of the turbine chassis, and is mounted over the top section of the mast by machined nylon bearings

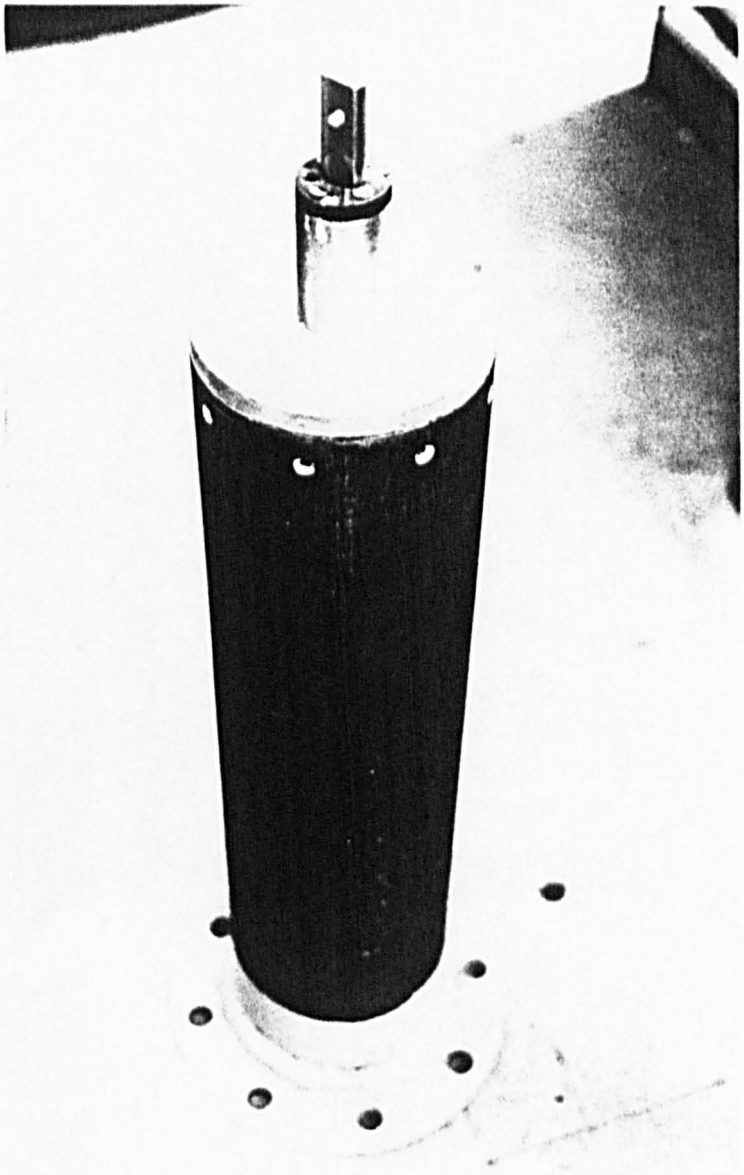

Fig 8.3b:
Mast top section showing machined cap (forming thrust bearing surface) and vertical spindle and vertical brake actuator

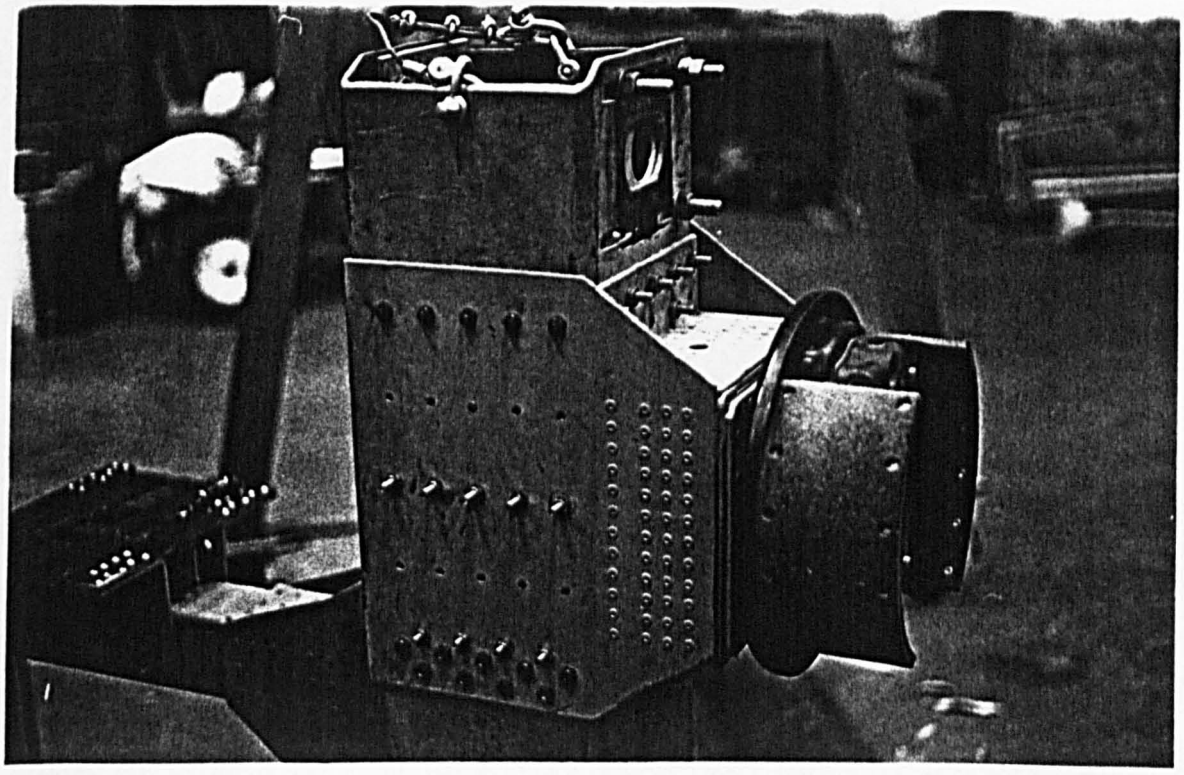

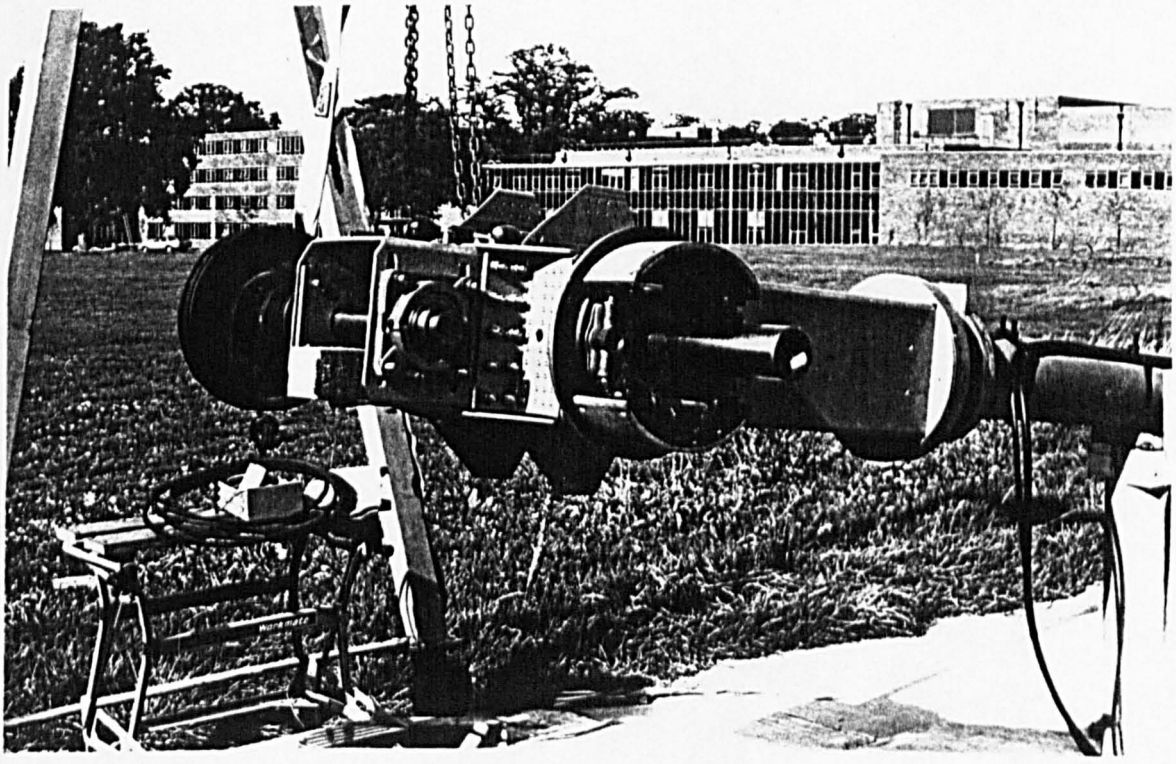

Figure 8.4: Views of chassis showing bolted and riveted construction and brake

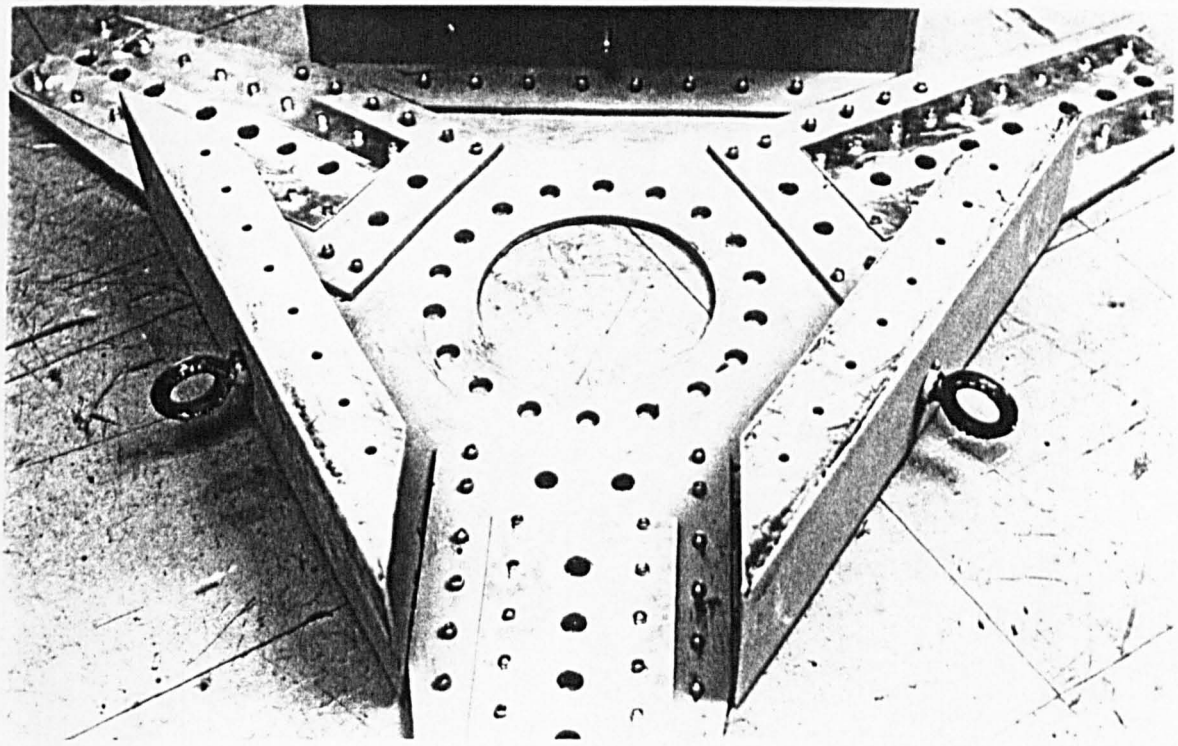

Figure 8.5: Wind turbine hub prior to assembly

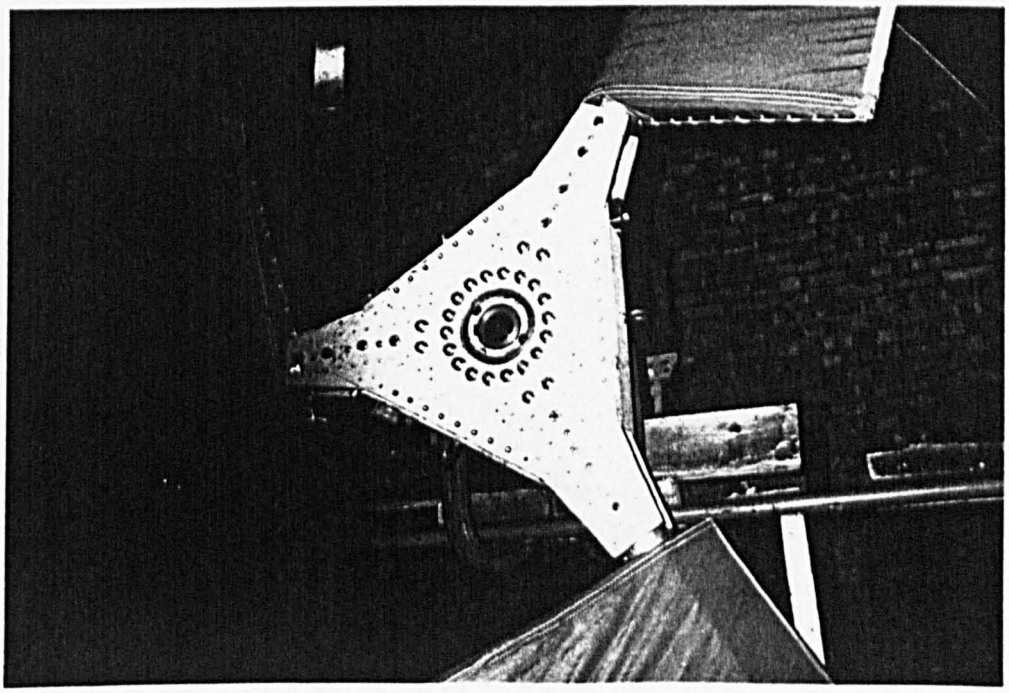

Figure 8.6: Wind turbine hub assembled and bladed attached

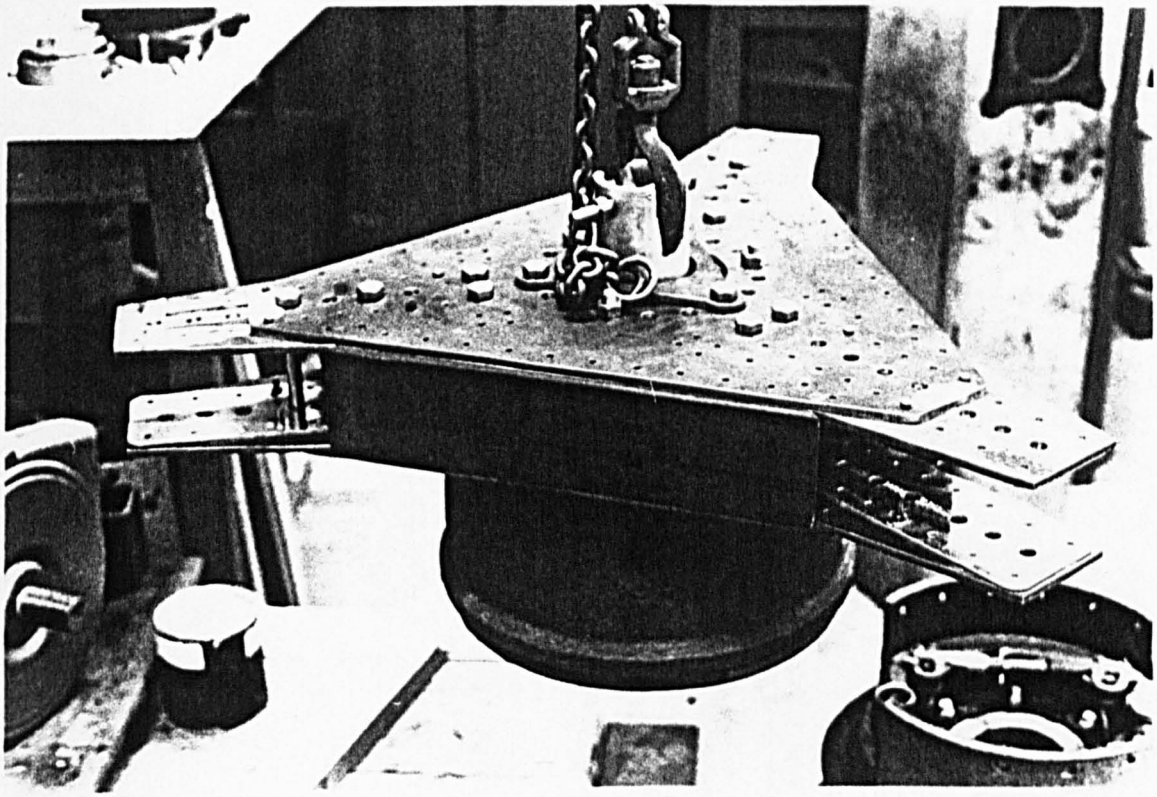

Figure 8.7: Wind turbine hub is attached to lorry brake drum

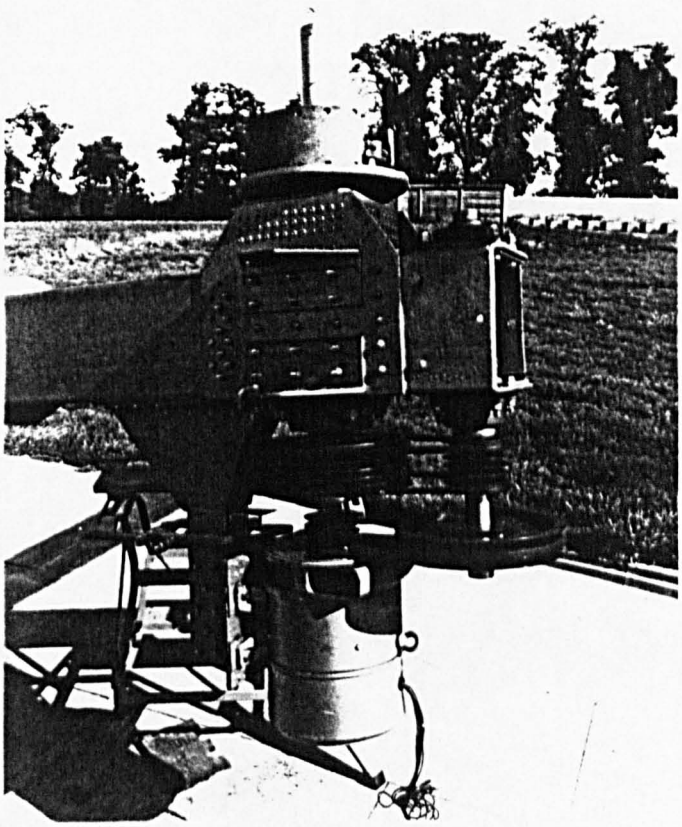

Figure 8.8: Two stage V belt transmission

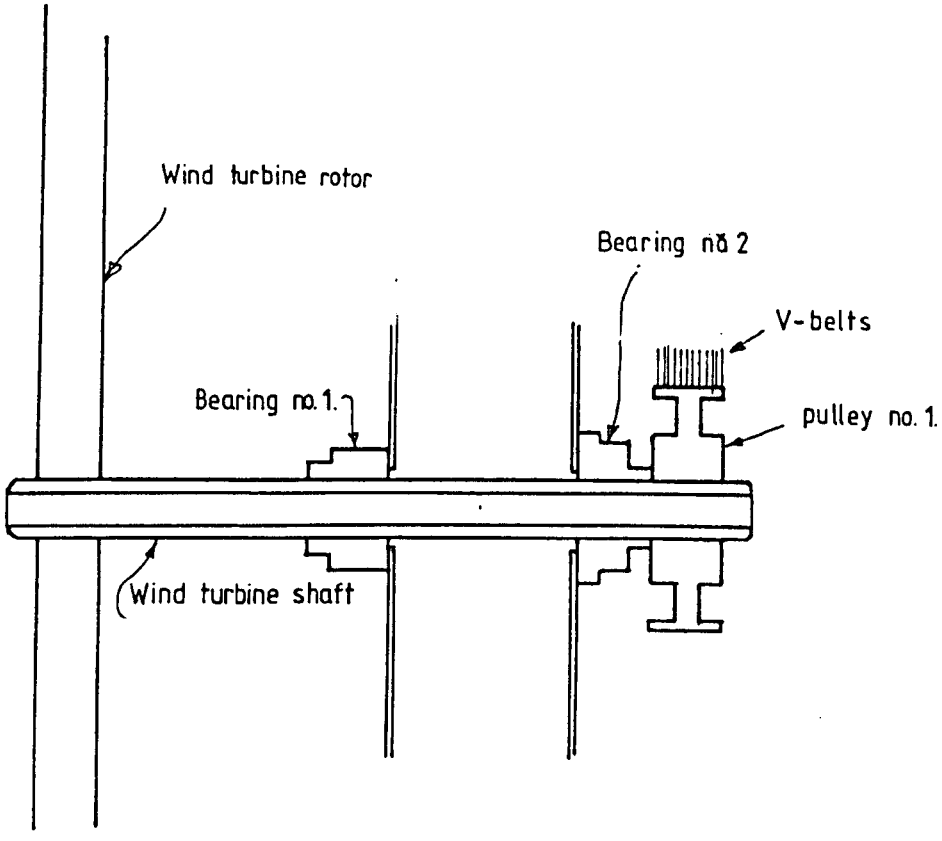

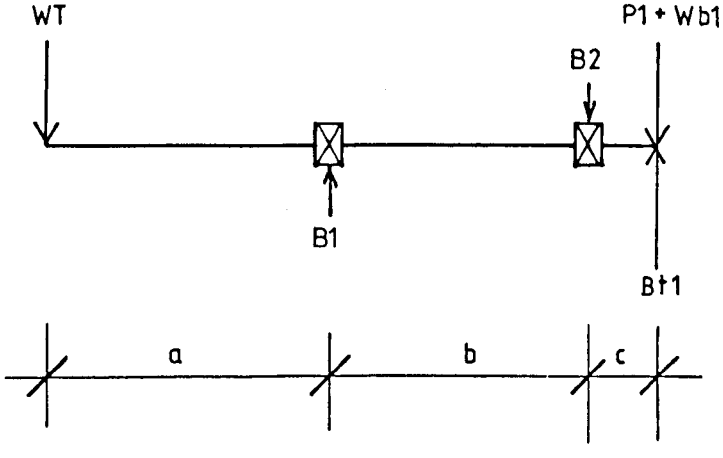

Figure 8.9 : Wind turbine shaft

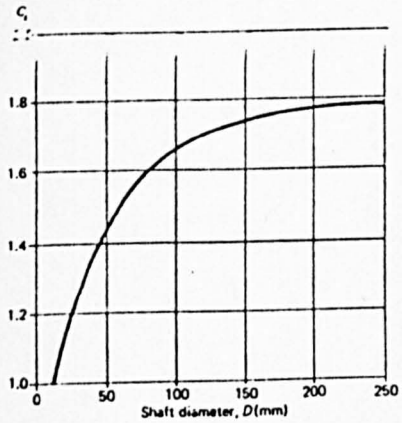

Fig 8.10: Cs Size factor for shaft (AS B1249, 1969)

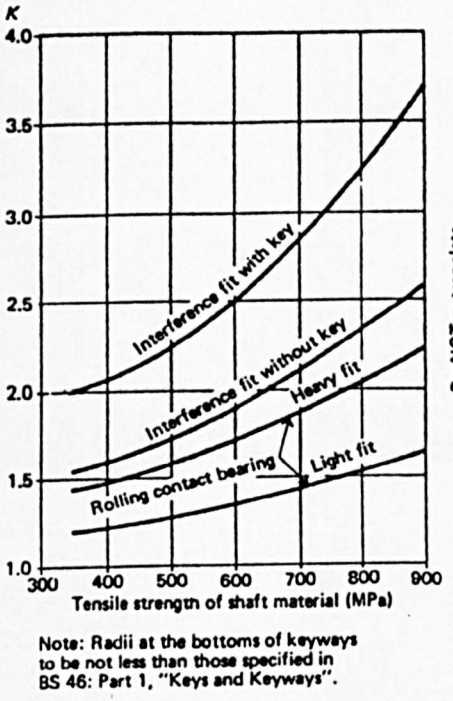

Fig 8.11: K_S stress coefficient for shafts with fitted components

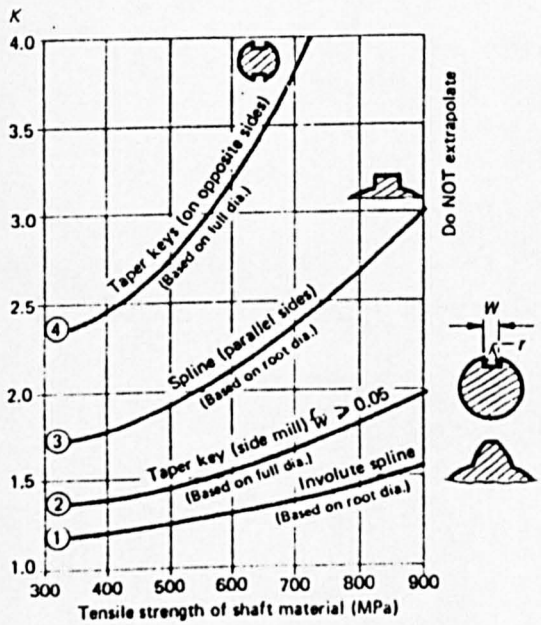

Fig 8.12: K, stress raising factor for shafts with splines or keyways

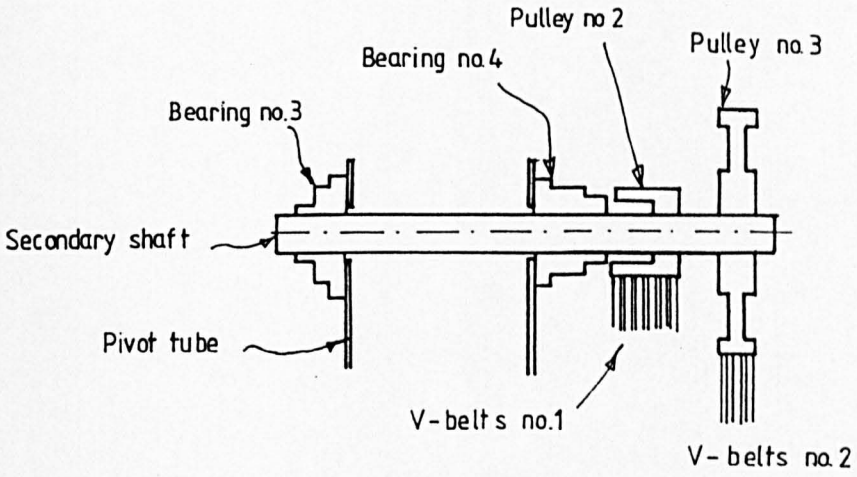

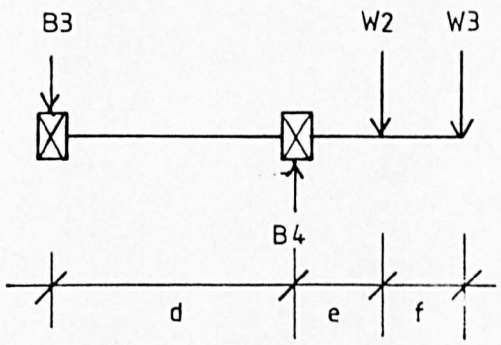

Figure 8.13: Secondary shaft

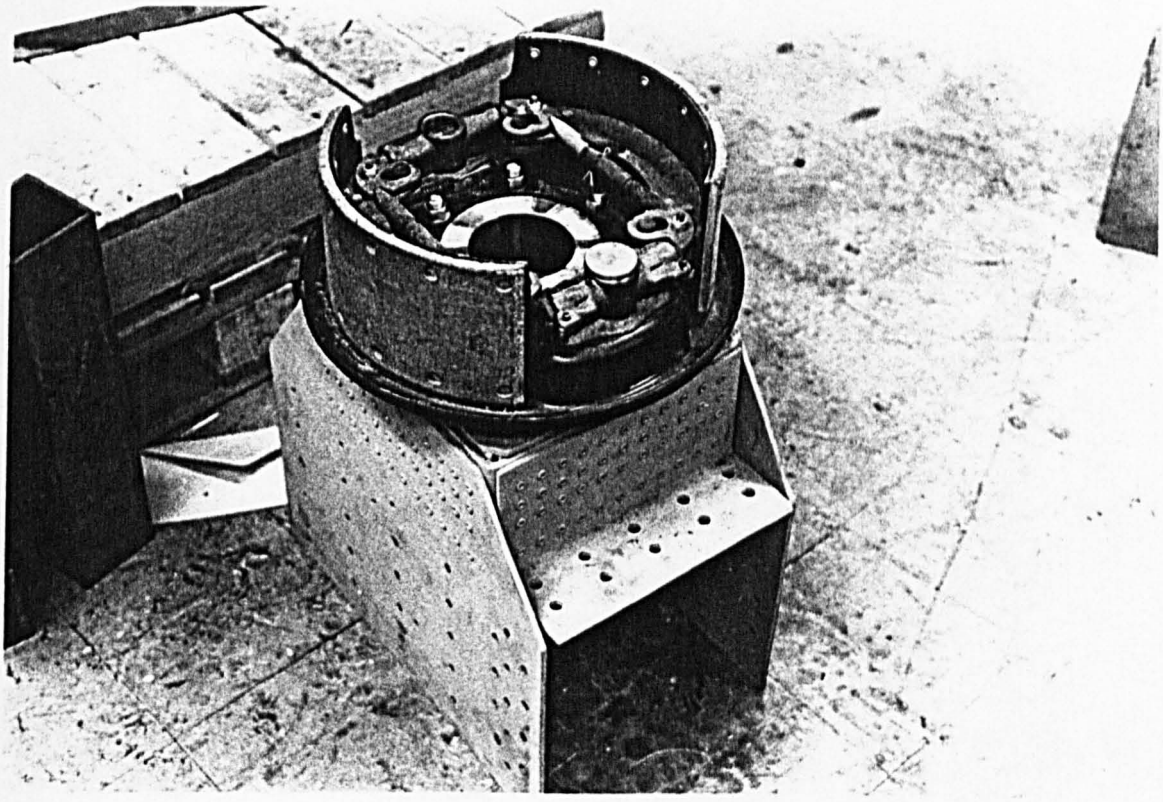

Figure 8.14: Lucas Girling 12(⅜)" x 5" 2LS type lorry brake used as the mechanical brake on the low speed shaft of the wind turbine

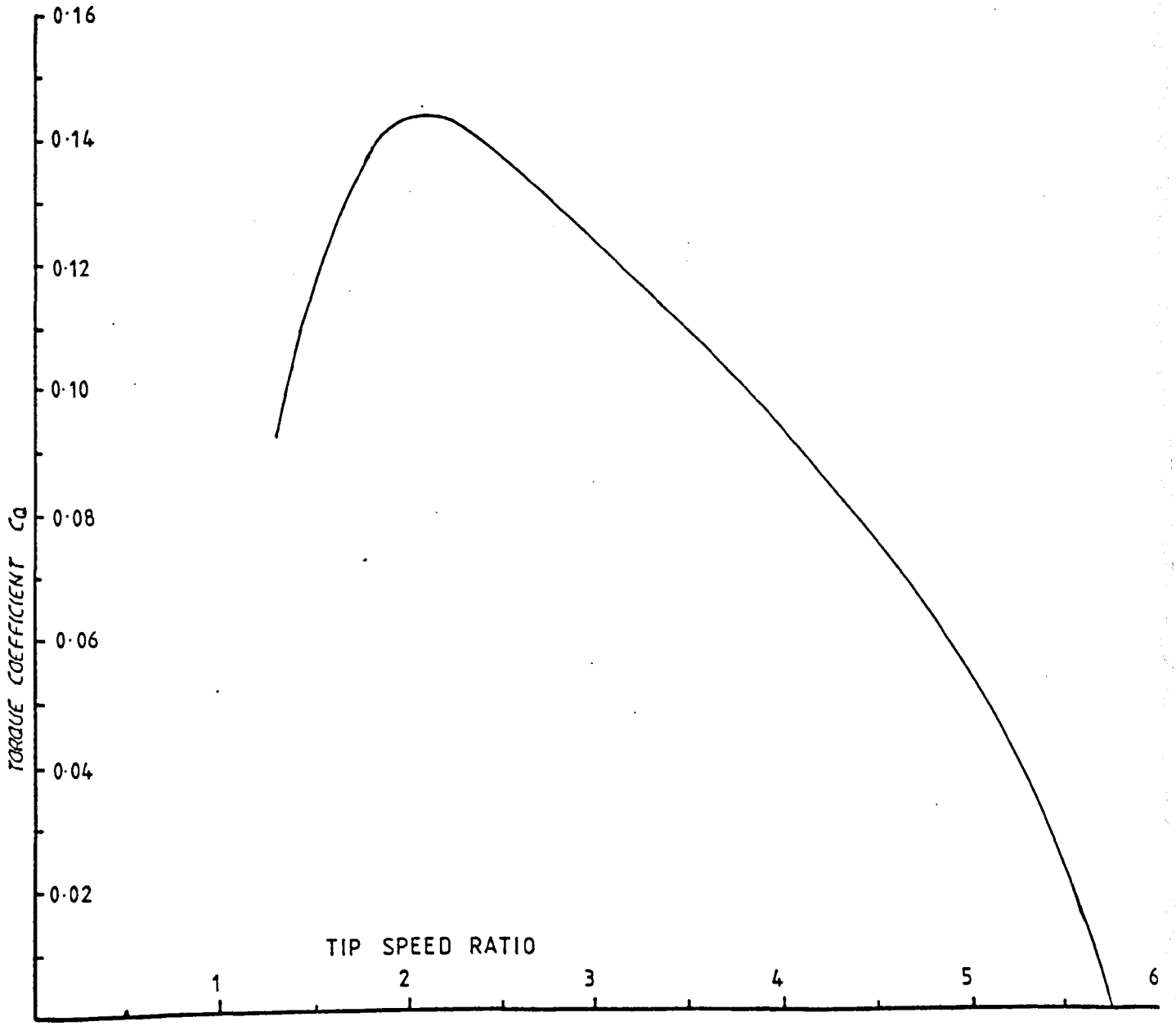

Figure 8.15: Predicted C /X Characteristics for 3 bladed sailfoil HAWT rotor with linearised blades

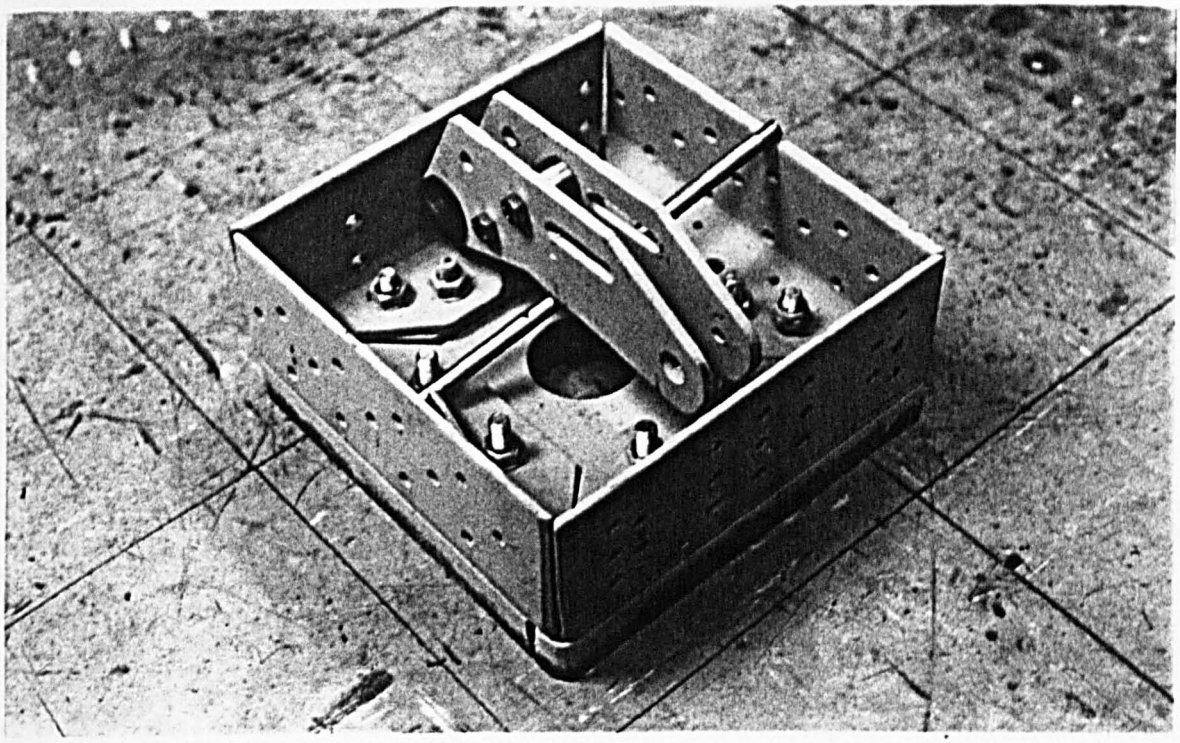

Figure 8.16a: Detail of the linkage mechanism used to convert the vertical pull from the (ground mounted) brake lever to a horizontal pull on the brake actuator

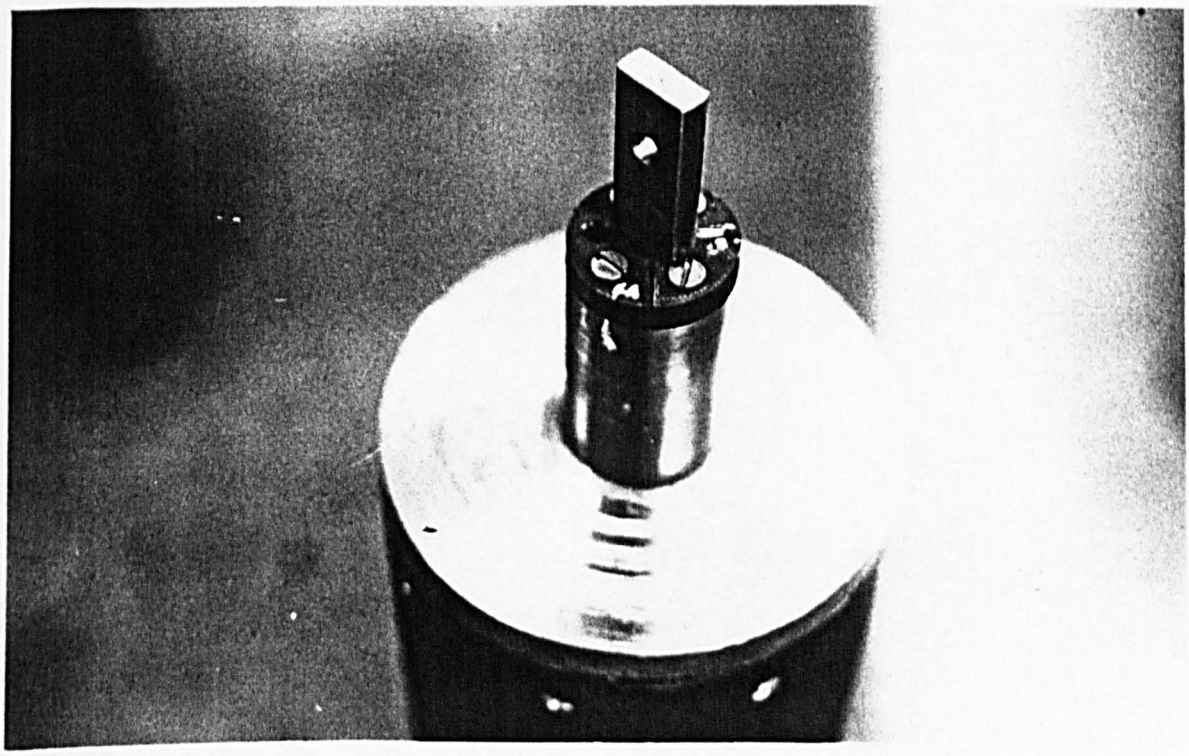

Figure 8.16b: Detail of the vertical actuator to be attached to the above linkage mechanism via a pin through the slots in the linkage. Also shown is vertical spindle and mast cap

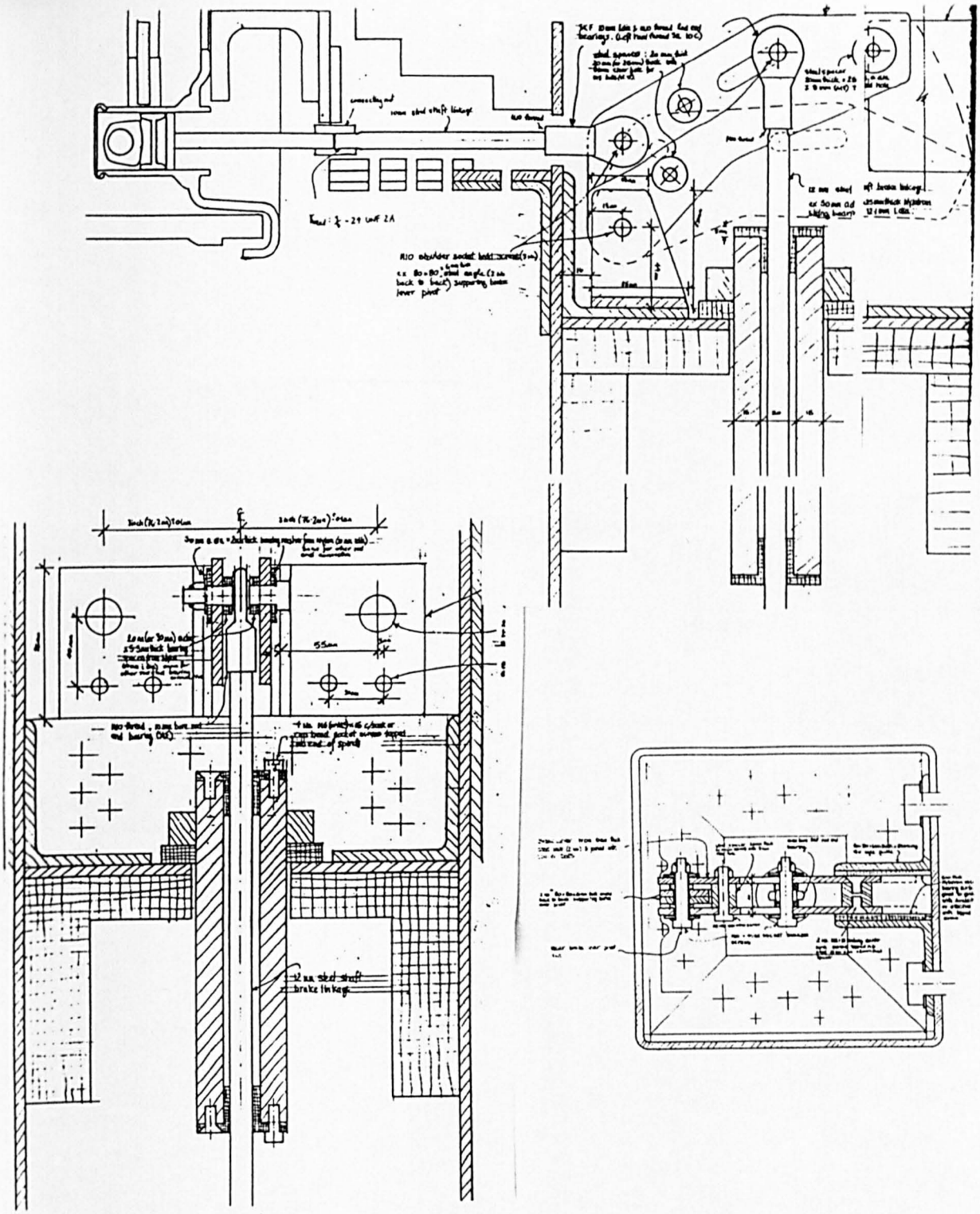

Fig. 8.17 Long and cross section and plan view of brake actuator mechanism.

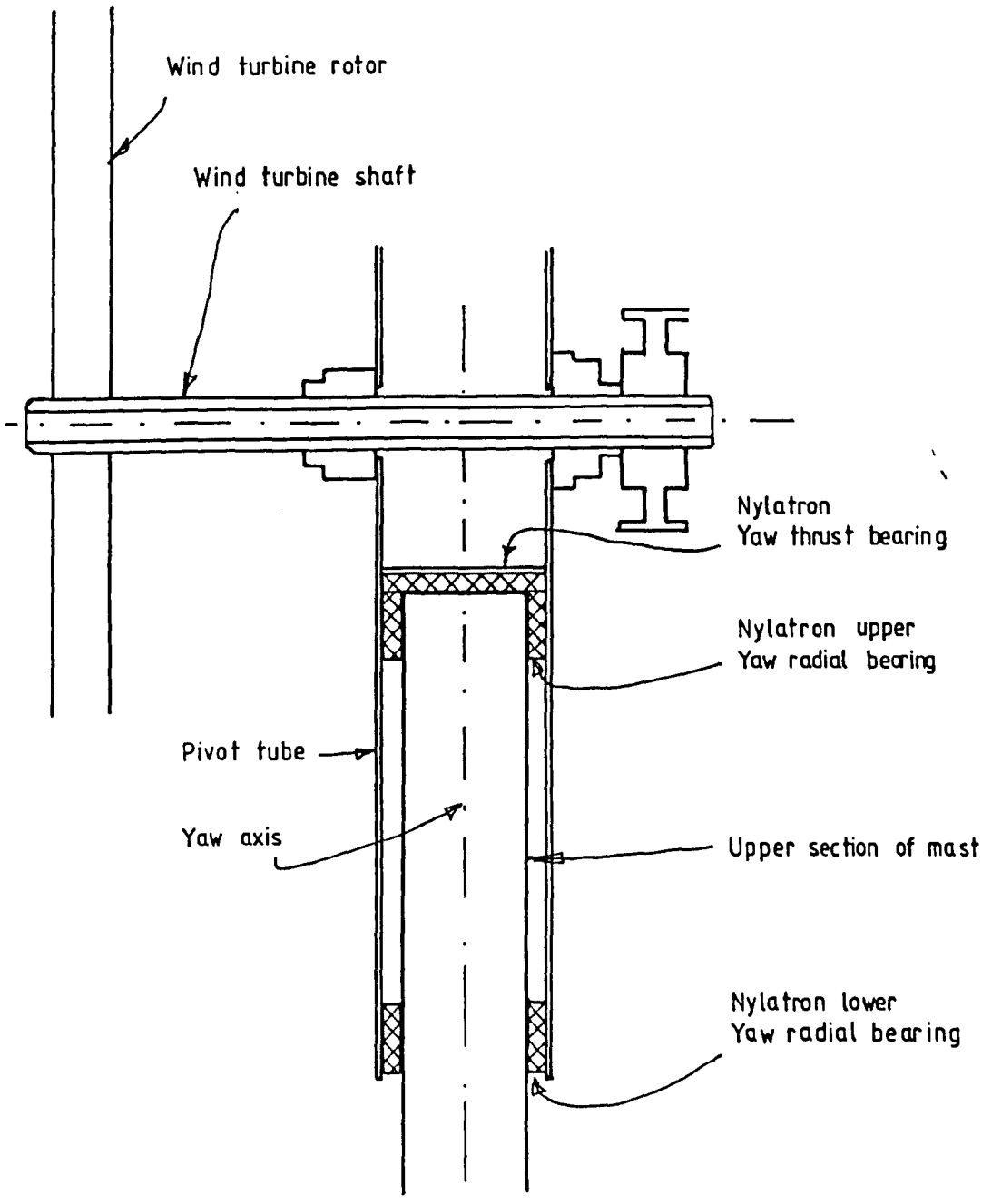

Fig. 8.18 Yaw bearing.

CHAPTER 9

WIND TURBINE TEST FACILITY

9.1 INTRODUCTION

In order to test the performance of the wind turbine under free air conditions a wind turbine field test facility was designed by the author and has been installed on the Open University campus.

The wind turbine field test facility (WTTF), Figure 9.1, consists of a wind turbine test rig, four wind instrumentation masts, and instrumentation/monitoring equipment located in a small cabin on the site.

9.2 WIND TURBINE TEST RIG

The test rig has been designed to allow for easy modification and adaption so that various types of wind turbines and rotors can be evaluated.

To allow for the testing of wind turbines of different tip speed ratios, a V belt transmission system (Fig 9.2) is used to permit changes in gear ratios.

To facilitate easy access to the wind turbine machinery and to the rotor itself, a tiltable guyed mast is used (Fig 9.3). This mast was produced to the author's specifications by Northumbrian Energy Workshop Ltd. It can be configured in several heights up to 10 metres and

modified to accept certain types of Vertical Axis Wind Turbines.

It is mounted on a pivoted base and can be tilted up or down in a few minutes by means of two Tirfor winches.

The power output from the test rig's alternator is fed to a resistive load consisting of 3 immersion water heaters located in a water tank.

9.3 INSTRUMENTATION AND MONITORING EQUIPMENT

The instrumentation and monitoring equipment used on the WTTF was designed and constructed to the author's specification and consists of the following.

Four 10 metre instrumentation masts are situated at equidistant intervals around the wind turbine test rig and about the prevailing wind axis (Fig 9.4 & Fig 9.5). These masts support four digital and two analogue anemometers to measure wind speed, and one wind direction vane.

On the test rig itself, and in the instrumentation cabin, are sensors for measuring wind turbine shaft rotation speed, torque, power, rotor azimuth position and alternator field current.

Signal cables carry the output from these sensors to the

instrumentation and monitoring cabin which has an unrestricted view of the test site. The cabin houses instantaneous read out instruments which display wind speed (Fig 9.6), rotor rpm, rotor azimuth position, logged rotor revolutions (Fig 9.7), power output (Fig 9.8) and alternator field current and voltage (Fig 9.9).

As well as being displayed instantaneously, these data values are also fed into a Microdata Prolog M1680 data logger (Fig 9.10) and recorded on to a magnetic tape cartridge for later computer analysis. A Northumbrian Energy Workshop Windlogger (Fig 9.11) is used for continuous monitoring of the wind speed.

A six channel Rostol/Pantos pen chart recorder (Fig 9.12) is also used for recording instantaneous analogue data.

The cabin also houses a Commodore 8032 microcomputer. This is used for fast data recording, via a CIL PC1000 Analogue to Digital converter, in order to carry out testing of wind turbine rotors using the 'acceleration' technique first developed by David Sharpe (Sharpe 1976). It is also used for analysing the data recorded in other tests by the data logger.

Figure 9.13 shows the circuit diagram of the WTTF instrumentation system and Tables 9.1 to 9.3 give a description of the instrumentation parameters.

Fig 9.14 shows the Sailfoil HAWT installed on the test rig.

REFERENCES FOR CHAPTER 9

Sharpe, DJ (1976): A Theoretical and Experimental Study of the Darrieus Vertical Axis Wind Turbine, research report, School of MAP Engineering, Kingston Polytechnic, October 1977

TABLE 9.1: INSTRUMENTATION AND MONITORING EQUIPMENT

Equipment	Manufacturer	Characteristics and Specification
Digital Anemometers (4 No)	Brookes & Gatehouse Model 193	2 pulses per second Calibration = =.42 m/s per revolution
Analogue Anemometers (2 No)	Vector Instruments	D.C. output voltage = 198 mV/m/sec
Digital Wind Direction Vane	Vector Instruments Model W200G	4 Bit Gray Code 22½° resolution
Wind Turbine Shaft Rpm Sensor	OU Electronics Common Facility	1 pulse per rpm. 60 magnet inset into side of V belt pulley No. 1 with sensor located close to.
Wind Turbine Rotor position sensor (Azimuth)	OU Electronics Common Facility	Series of magnets inset into internal circumference of V belt pulley No 1 with sensor located close to.
Yaw Sensors	OU Electronic Common Facility	Series of 36? magnets inset onto disc attached to yaw or pivot tube to measure yaw position, total yaw revs.
Wind Turbine Shaft Torque Sensor	OU Alternative Technology Group	Torque strain gauges attached to shaft and arranged in 4 gauge full Wheatstone Bridge. Data transmitted via single channel Astec Telemetry System.
1 Channel Telemetry System	Astech SA3A	

TABLE 9.2: INSTANTANEOUS DISPLAY INSTRUMENTS

Equipment	Manufacturer	Characteristics and Specifications
Electronic Watt meter		
Alternator Field current and Voltmeters	OU Electronics Common Facility	
Instantaneous Wind Speed Meter	" "	
Combined meters displaying:	" "	
Rotor rpm		
Rotor Azimuth Position		
Logged Rotor Revolutions		
Yaw Position		
Logged Yaw Revolutions		
Torque Meter	Astech	Microstrains displayed

TABLE 9.3: RECORDING, LOGGING AND CONTROL EQUIPMENT

Equipment	Manufacturer	Characteristics and Specifications
Prolog M1680 Data Logger	Microdata	20 channels available Analogue or Digital inputs. Sampling time - digital channels. 1m sec and 25m sec to 65m sec for analogue inputs. IEEE & RS232 Interfaces.
Multi-channel Pen chart recorder	Pantos/Rostol Unicorder Model U-626DS	6 analogue input channels 1 cm/min to 1 cm/hour chart speeds.
CBM 8032 Micro computer	Commodore	32K RAM Micro computer used for variety of tasks but principally for logging in acceleration tests.

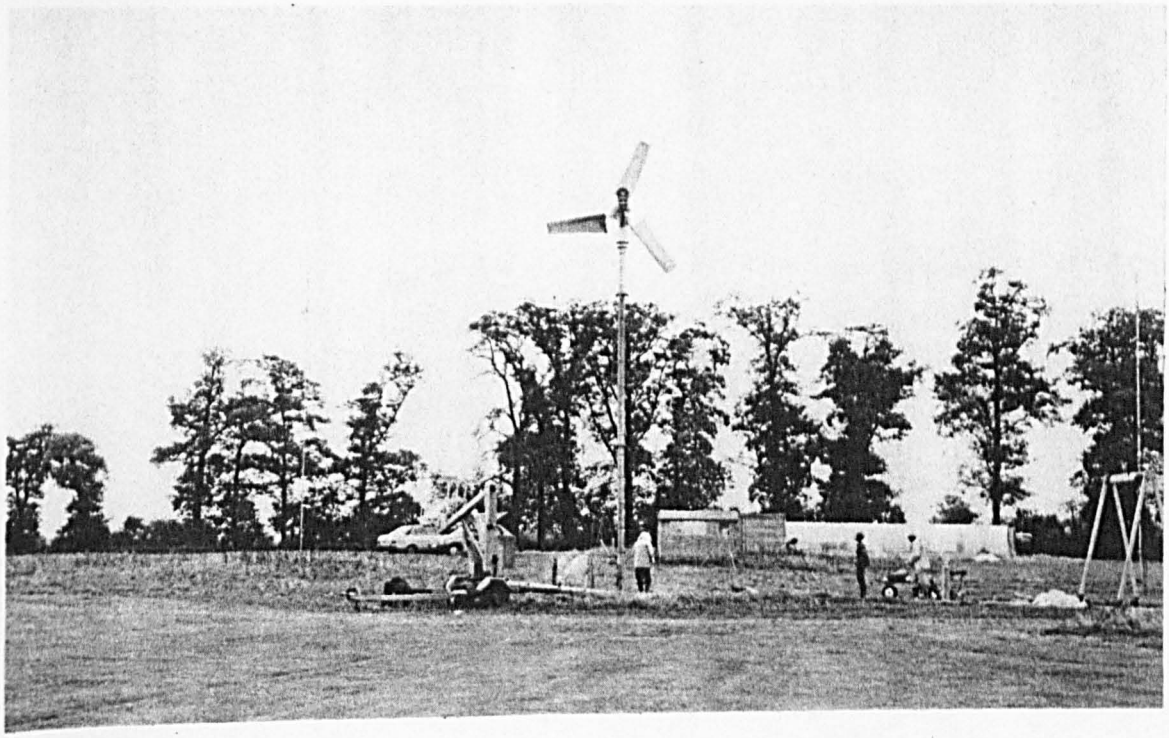

Fig 9.1:A.T.G. Wind Turbine Test Facility

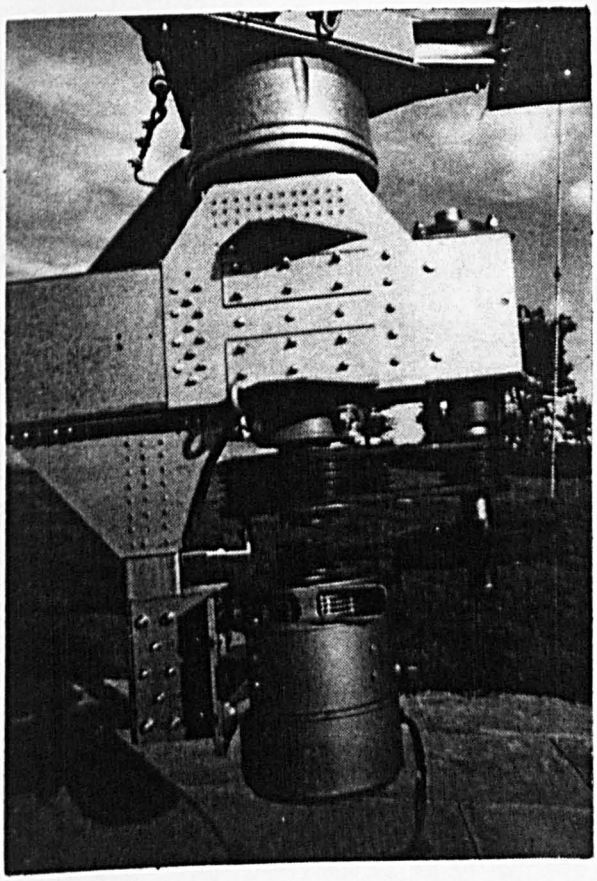

Fig 9.2: V Belt Transmission System

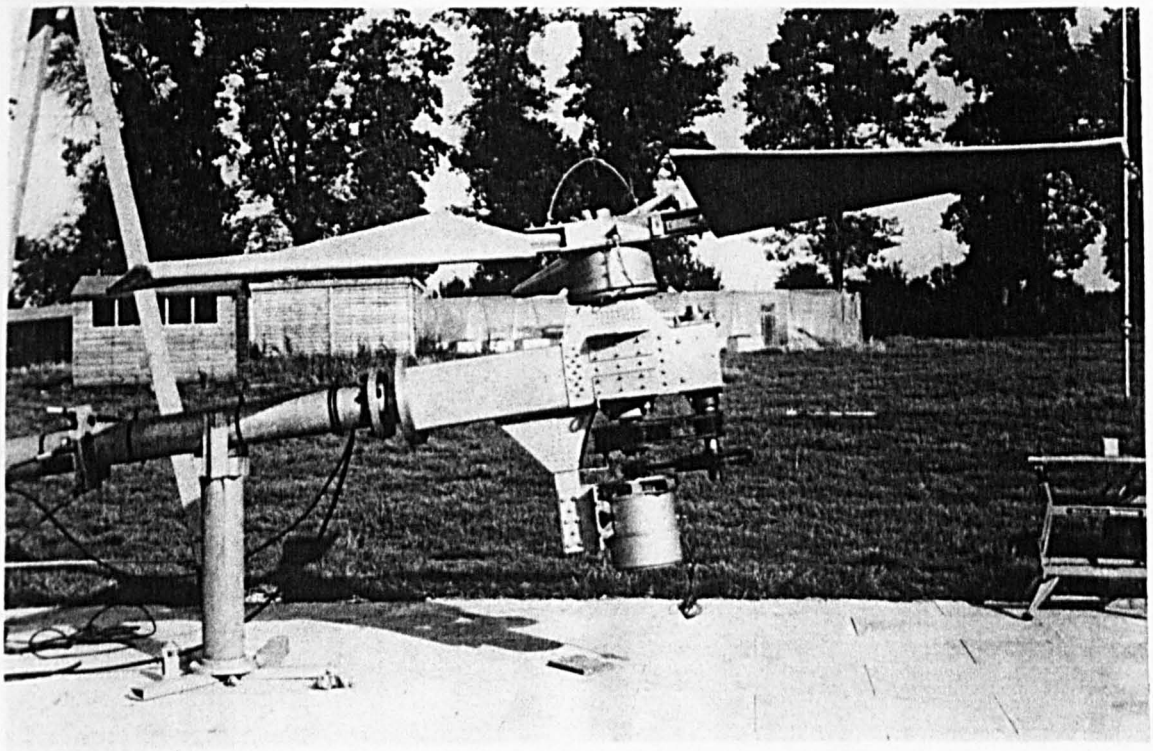

Fig 9.3: A WTTF Mast in LOWERED position providing easy access to machinery and rotor.

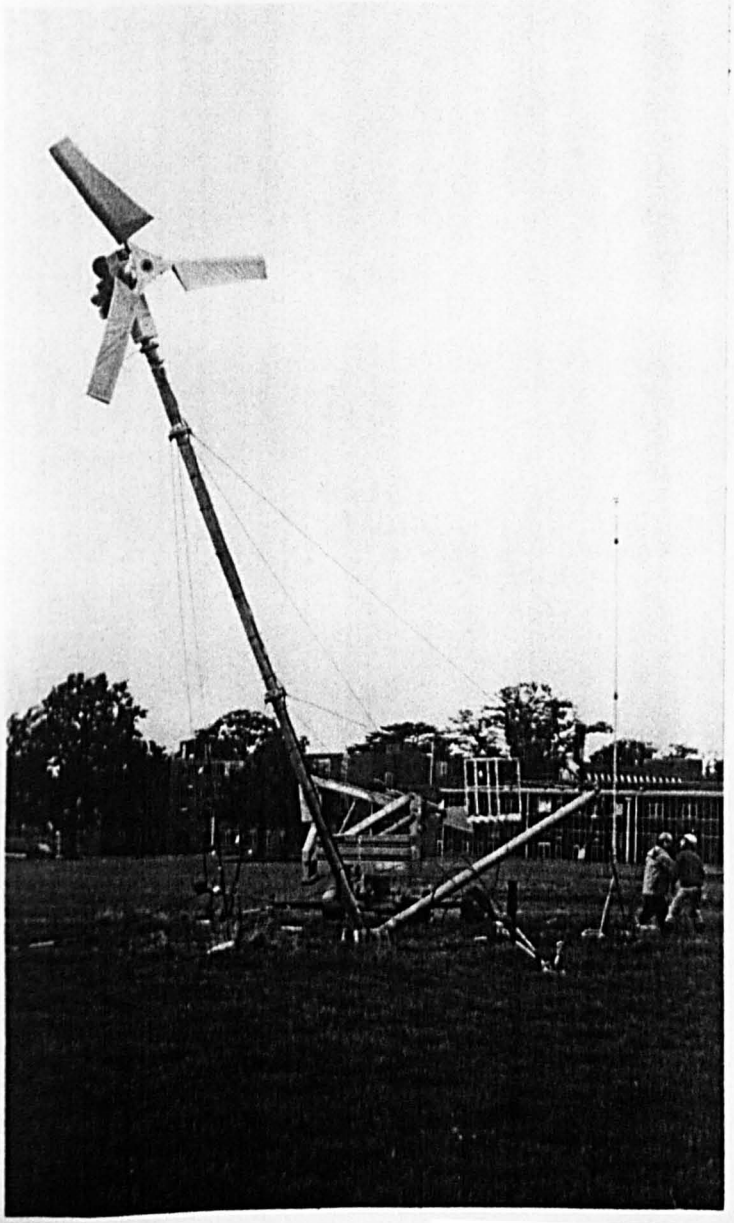

Fig 9.3b: Raising/Lowering of WTTF Mast.

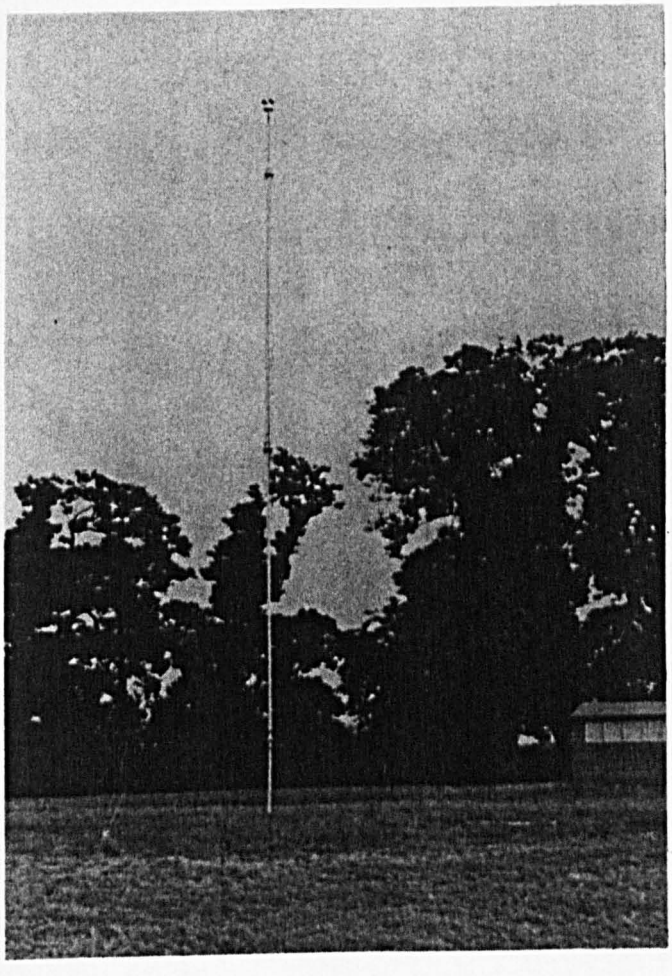

Fig 9.4: Instrumentation Mast.

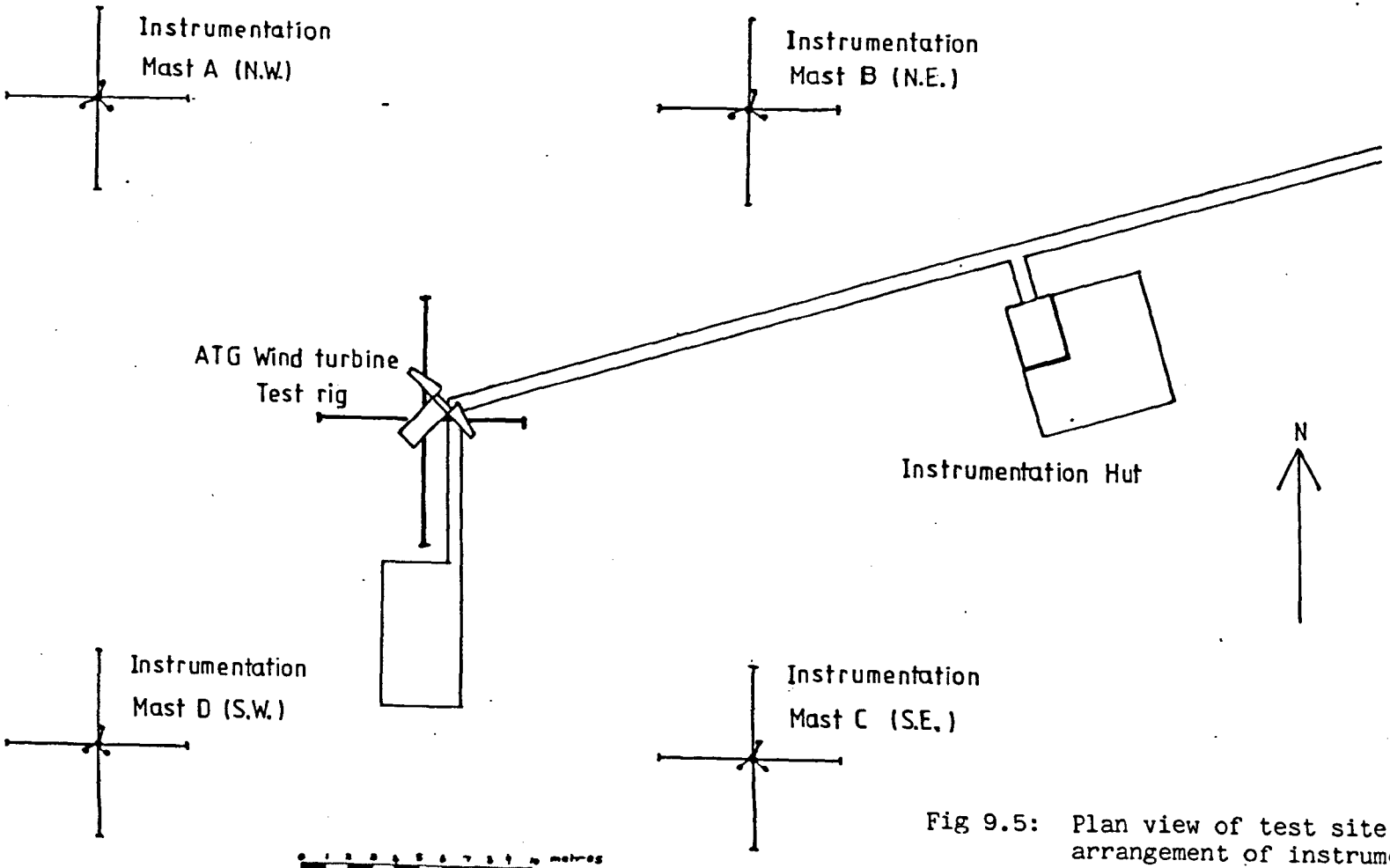

Fig 9.5: Plan view of test site showing arrangement of instrumentation masts about prevailing wind axis.

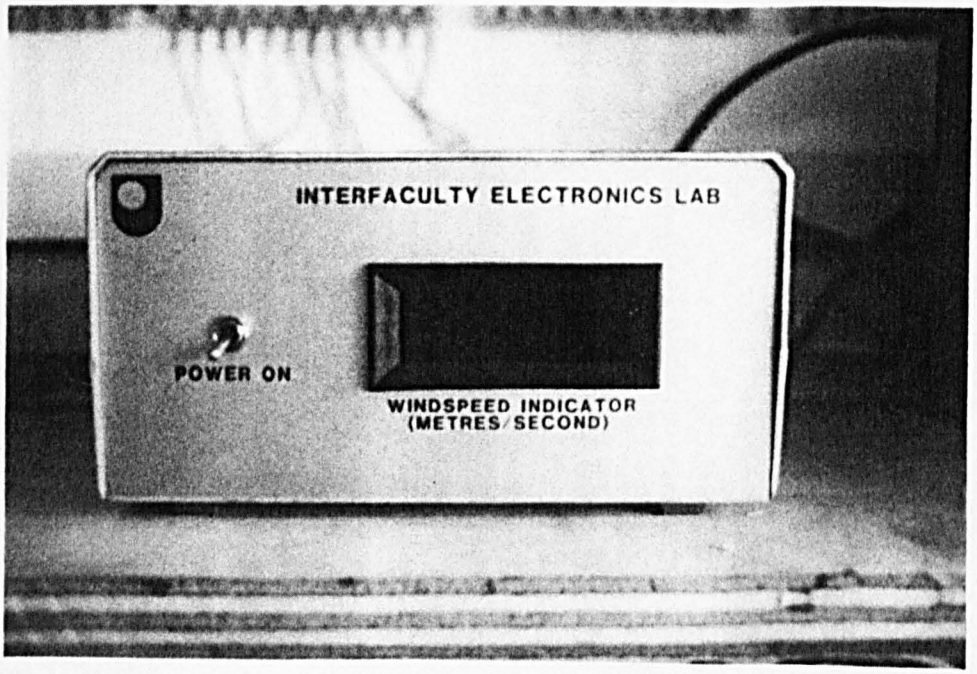

Fig 9.6: Instantaneous wind speed meter.

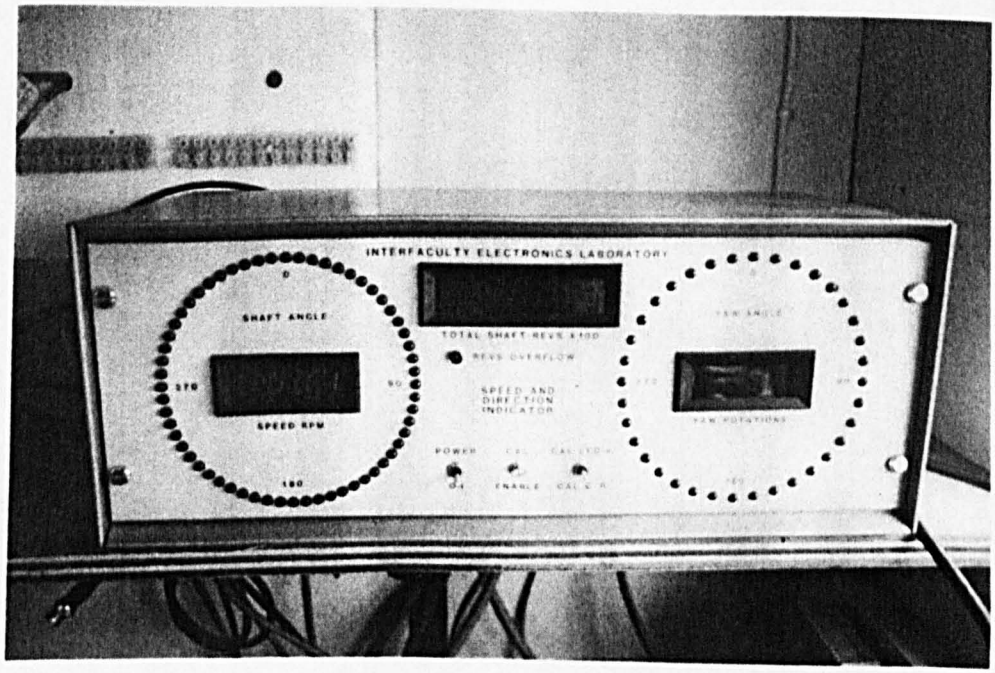

Fig9.7: Combined meters displaying: Rotor RPM; Rotor Azimuth position; Logged Rotor revolutions; Yaw Position; Logged Yaw revolutions.

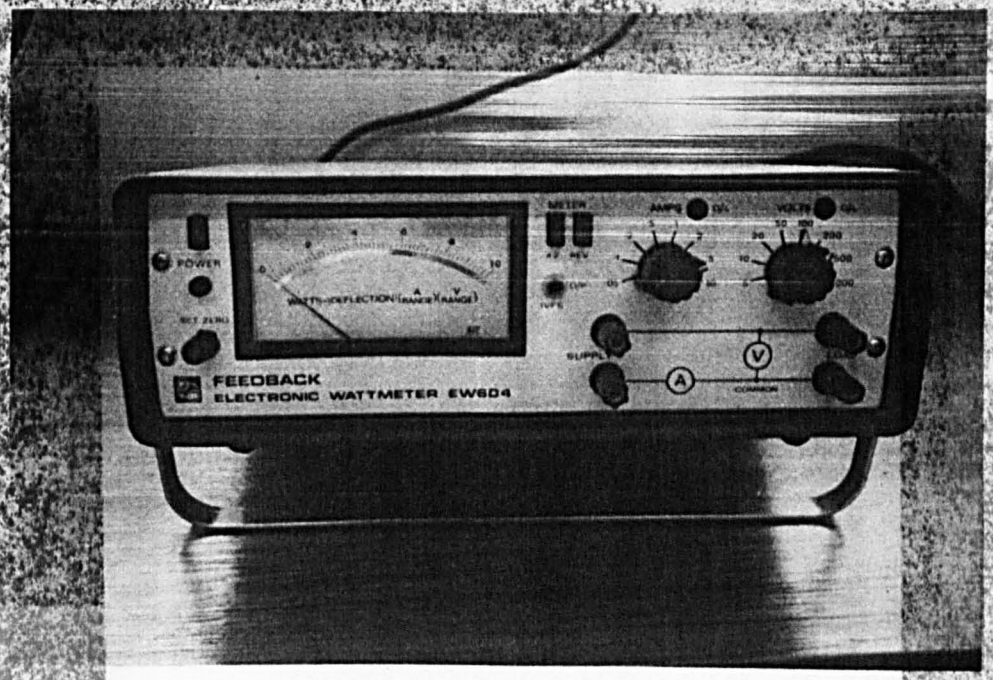

Fig 9.8: Electronic Wattmeter

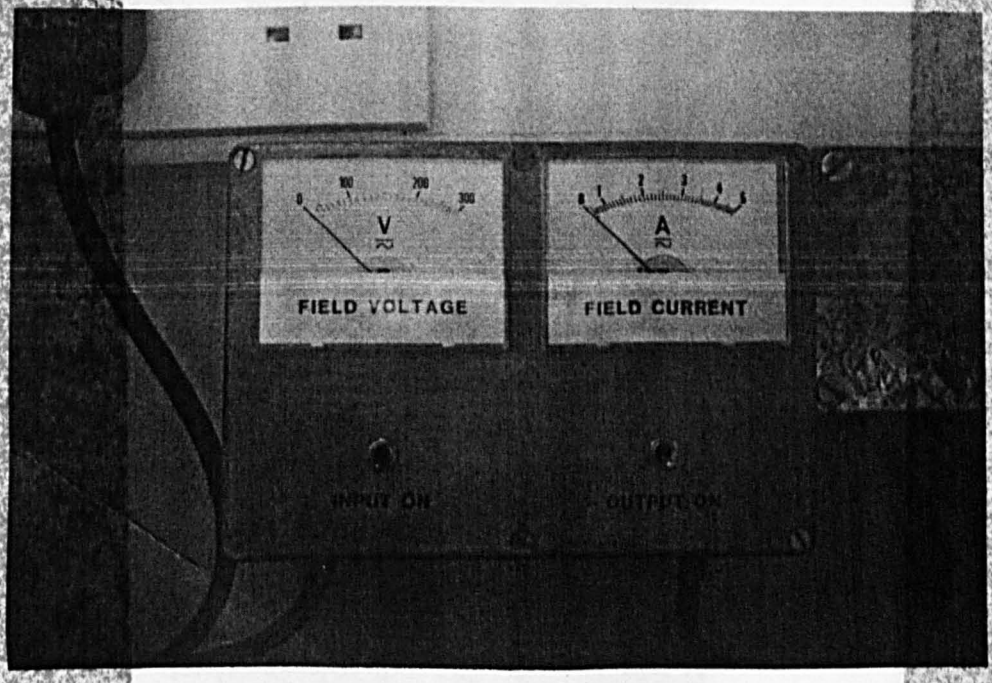

Fig 9.9: Alternator Field Current and Voltage meters

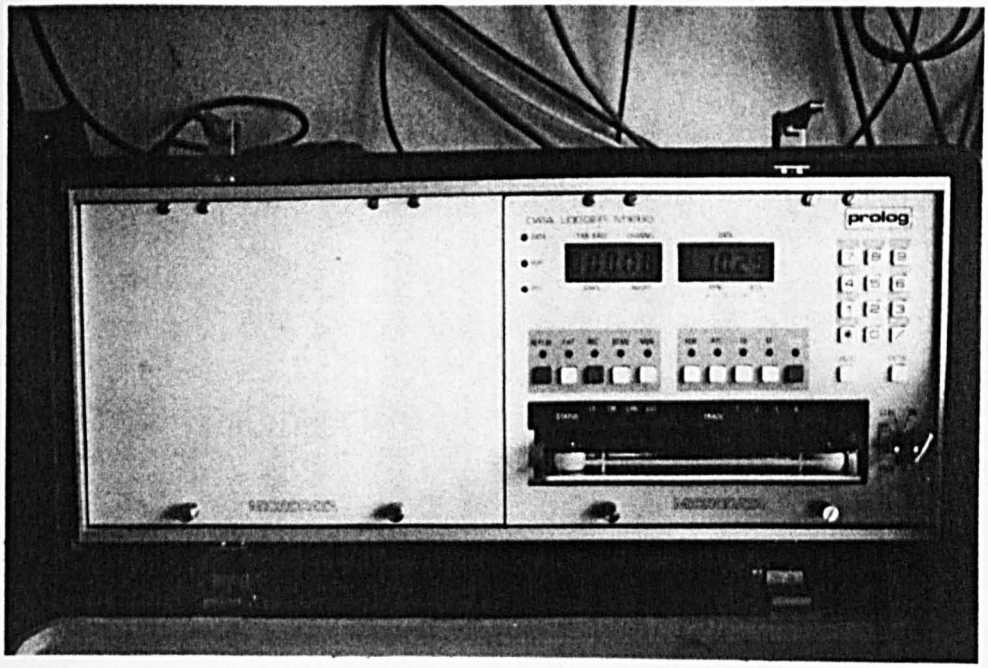

Fig 9.10: Microdata Prolog M1680
Data Logger

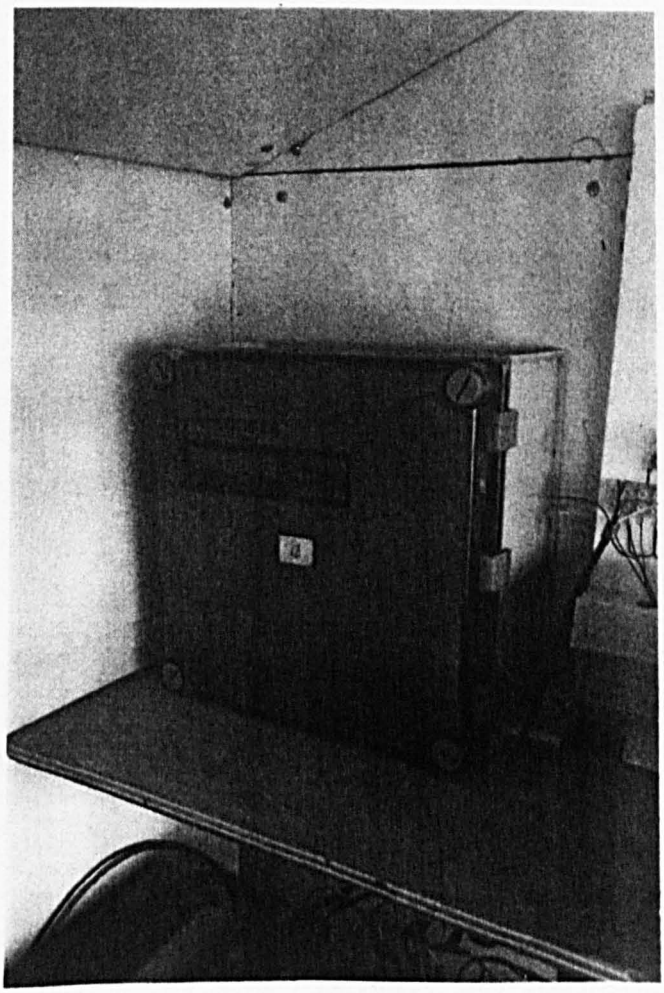

Fig 9.11: N.E.W. Windlogger

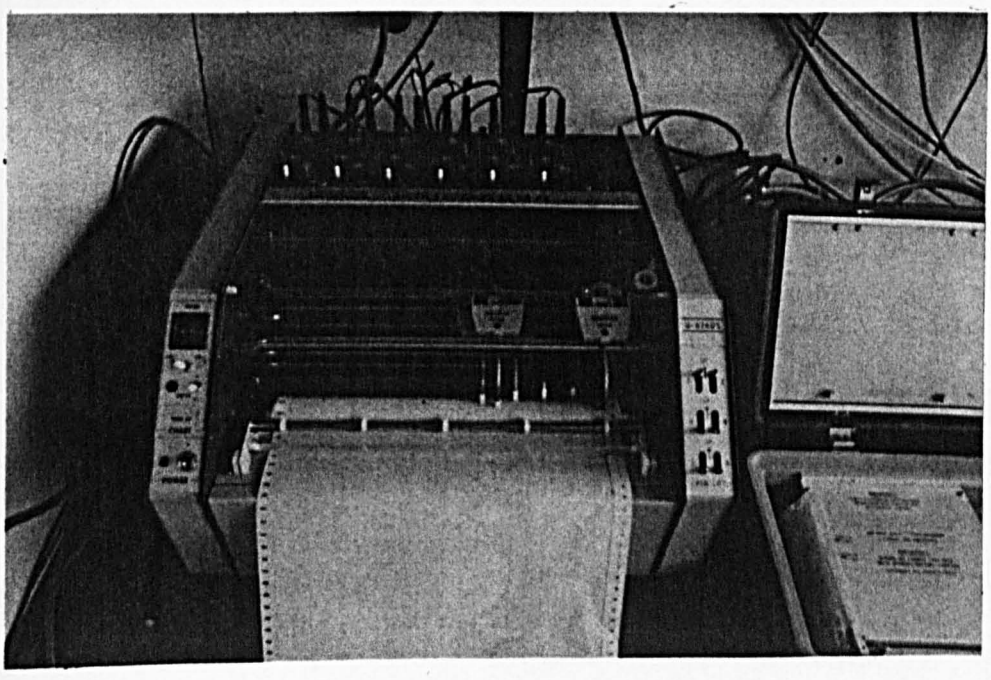

Fig. 9.12: Pantos/Rostil Unicorder
U-626DS 6 channel
Pen chart recorder.

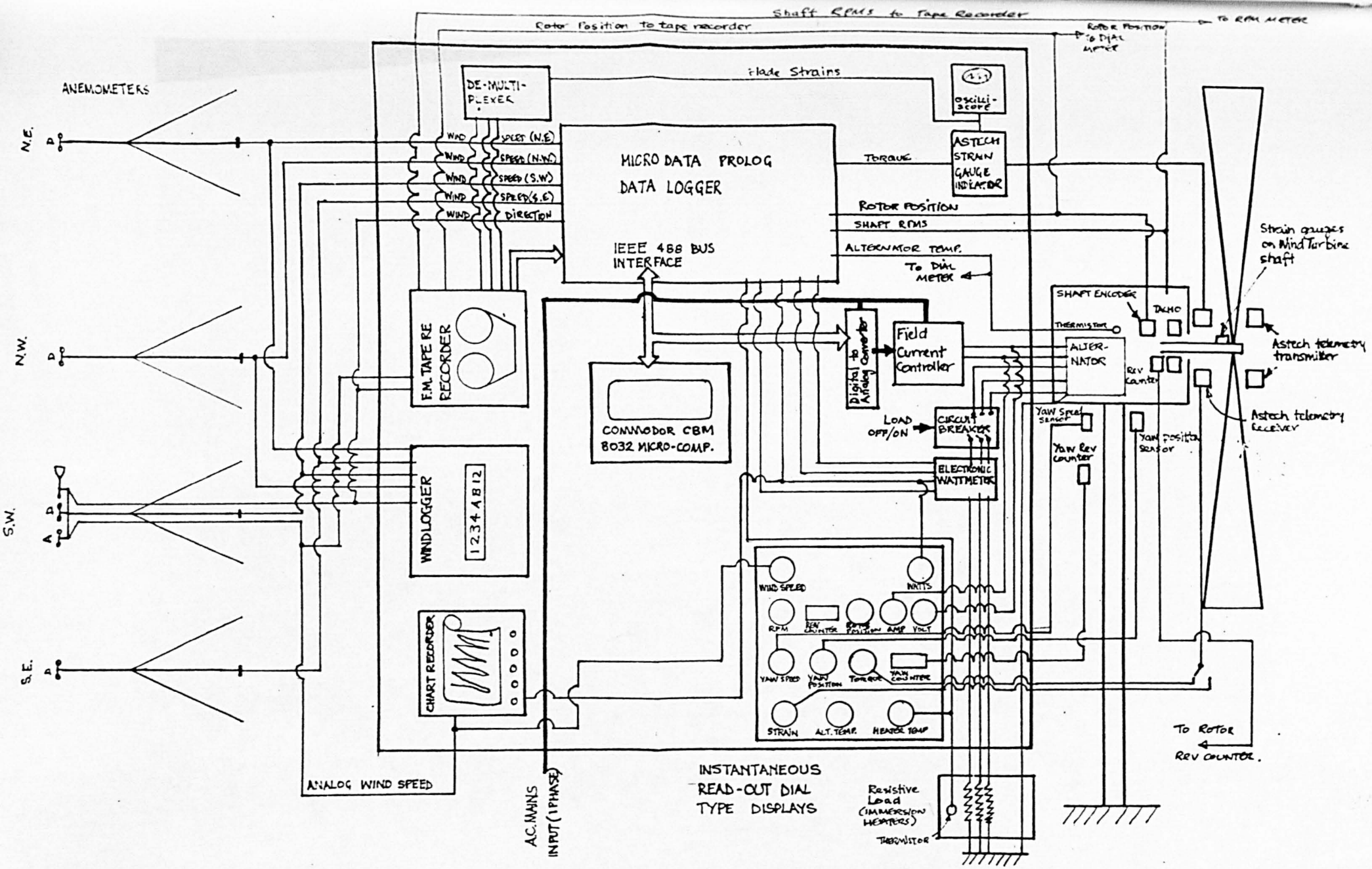

Fig 9.13: Instrumentation Circuit Diagram.

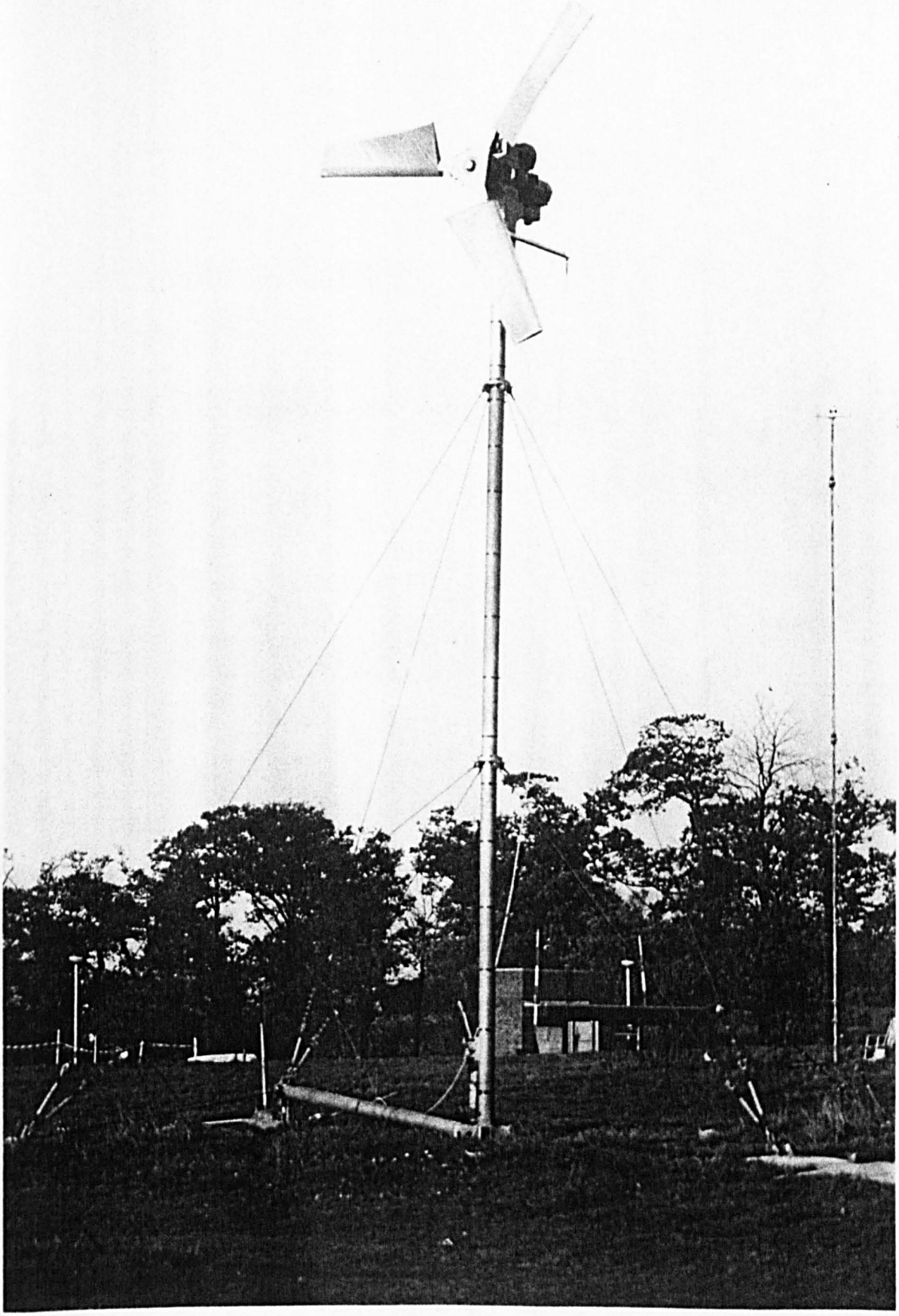

Fig 9.14: ATG 4m Dia Sailfoil HAWT
under test on ATG Wind
Turbine Test Facility

CHAPTER 10

PERFORMANCE TESTING OF SAILFOIL HAWT

LIST OF SYMBOLS FOR CHAPTER 10 (TESTS)

Ac = Acceleration of wind turbine rotor (rad/s^2)

bg = The number of blade passes until the weight Ml reaches the ground.

br = The further number of blade passes until the rotor stops.

bt = The total number of blade passes until the rotor stops.

CP = Rotor power coefficient eq (4-36)

CQ = Rotor torque coefficient eq (4-35)

g = Acceleration due to gravity g = 9.81 m/s^2

hw = Height from which weight falls to ground level.

Im = mass moment of inertia of wind turbine rotor.

Ml = Mass of laboratory weight.

ng = The number of revolutions of rotor for weight Ml to reach the ground.

nr = The further number of rotor revolutions of the rotor
until the rotor stops.

nt = The total number of revolutions till the rotor stops.

P = Wind turbine rotor power eq (10-2) and (10-3).

Q = Rotor torque Nm eq (10-1).

R = Tip radius of rotor.

rp = Radius of pulley No. 1.

t = Time taken for weight to reacn the ground.

V_e = Acceptable range of wind speed values between 2 readings (0%, 10% & 50%).

Vo = Undisturbed wind velocity.

X = Tip speed ratio.

Ω = Omega = Angular velocity of the wind turbine rotor rad/s

ρ = rho = Air density eq (4-35)

10.1 INTRODUCTION

In order to obtain the performance characteristics of a wind turbine it is necessary to carry out some test measurements.

These test measurements can be carried out either in a wind tunnel or in the open air real wind conditions. Whilst wind tunnel testing can be carried out quickly and the conditions can be controlled, it is mostly used for small scale models, because of the expense of using large wind tunnels. The use of small models of larger turbines in wind tunnels can produce results which are not directly comparable with the performance of a full-size machine in real wind conditions, due to blockage effects and the difference in Reynolds number. It was decided, therefore, to attempt to carry out performance testing under realistic open air conditions.

An open air Wind Turbine Field Test Facility was designed by the author (see chapter 9) and built on the Open University's Walton Hall Campus by the Alternative Technology Group.

The most appropriate type of test to carry out on a wind turbine operating in the open air is one which compares

the power output of the turbine against wind speed. This is also the most useful type of test for an operating wind turbine as it gives a characteristic curve which is then able to be used with wind speed data for a particular site to predict the amount of energy which the turbine would be expected to produce on that site.

In addition to determining the power versus wind speed characteristic curves for a wind turbine, it is also useful to have the power and torque coefficient versus tip speed ratio characteristics of the wind turbine. Obtaining these power and torque coefficient characteristics is more difficult with a variable speed wind turbine operating in the real wind than with one tested in a wind tunnel.

Two basic types of tests were undertaken to measure the performance of the Sailfoil rotor. These can be described as BINNING type tests and ACCELERATION TESTS. Both types of test were carried out on the test facility.

10.2 BINNING TYPE PERFORMANCE TESTING PROCEDURE

This type of performance testing procedure was used to measure the performance of the Sailfoil wind turbine with the generator wired up to its resistance load.

The testing procedure was derived from Akins guidelines for performance testing of wind turbines, (Akins, 1979). The technique is intended for producing power/wind speed curves for actual wind turbines operating in the real wind and under normal operating conditions.

The generator chosen for this wind turbine was a Markon rotating armature 5kW alternator. This was selected for its relatively low rotation speed (1500 rpm) and because, being a wound field machine, it could be operated in variable speed mode, ie, the field current could initially be set to zero, to minimise the starting resistance of the wind turbine, then gradually increased as the rotor accelerated. By actively varying the alternator field current in this way, the power absorbed by the alternator could be adjusted to match the power being generated by the wind turbine rotor, over a range of wind speeds.

The alternator of the Sailfoil wind turbine was connected to a simple 3 phase resistive load consisting of three 1.5kW immersion heaters in a tank of water.

Transducers measuring wind speed, shaft rpm, shaft torque, electrical power output and alternator field current were connected to the Microdata 1680 data logger. Data was recorded during a test at 1 second intervals and stored as data strings on the logger's 4 track magnetic tape cartridge. This data was later

transferred to the CBM 8032 microcomputer and stored in floppy disc format.

A computer program WINDPOWERTEST was written by the author to read and analyse this data. This program produces power/wind speed curves.

The program reads each data string (which corresponds to one instant in time), it also sorts the shaft power data (derived from torque and rpm measurements) and the electrical power data into wind speed 'bins' 0.5 m/s wide.

10.2.1 POWER/WIND SPEED TESTS

Each wind speed bin accumulates all the power values that occur within its specified wind speed range. A running average is also calculated each time a power value corresponding to a particular bin occurs, and that value is plotted on the computer screen. As more data points are accumulated, the averaging process gradually minimises the effect of any erroneous data points. In addition, successive test runs were carried out and the data values from successive tests compounded to produce an overall plot of the turbine's typical power/wind speed curve.

Figure 10.1 shows the shaft power versus wind speed curve, and Figure 10.2 shows the electrical power versus wind speed curve for the Sailfoil HAWT when tested

according to this procedure on the ATG Wind Turbine Field Test Facility.

Figure 10.3 shows the theoretically predicted shaft power/wind speed curve and Fig 10.4 shows the theoretically predicted electrical power/wind speed curve.

10.3 ACCELERATION TESTING TECHNIQUE

The acceleration test technique was developed by David Sharpe (1976), originally for testing wind tunnel models of wind turbines, in order to provide a means of measuring the torque produced by small models without using elaborate instrumentation.

The principles of the method are as follows:

The mass moment of intertia Im of the wind turbine rotor not coupled to a load is calculated, or measured under calm conditions. Once the mass moment of Inertia Im is known, the wind turbine rotor is placed in the windstream and allowed to accelerate without any load. By recording its angular velocity at regular intervals, the turbine's acceleration can be calculated. Since the wind speed is known, it is possible to obtain the rotor's torque characteristic by the following expression: (10-1)

$$Q = Im \; Ac \qquad (10\text{-}1)$$

Where Q = rotor torque (N.m)

Im = mass moment of Inertia of the unloaded Sailfoil Rotor ($kg.m^2$)

Ac = acceleration of rotor (rad/s^2)

The rotor's power characteristic is given by expression (10-2):

$$P = Q * \Omega \qquad (10\text{-}2)$$

Where Ω = Omega

= angular velocity of the rotor (rad/sec)

Combining these expressions yields:

$$P = Im \; Ac \; \Omega \qquad (10\text{-}3)$$

The expressions (4-35) and (4-36) for rotor Torque and Power Coefficients, CQ and CP, from Chapter 4, are as follows:

$$CQ = Q/(0.5 \; \rho \; R^3 \; Vo^2 \; \pi) \qquad (4\text{-}35)$$

$$CP = P/(0.5 \; \rho \; R^2 \; \pi \; Vo^3) \qquad (4\text{-}13)(4\text{-}36)$$

Substituting expression (10-1) into expression (4-35) we obtain the following relationships (10-4) between torque coefficient and acceleration:

$$CQ = \frac{Im \; Ac}{(0.5 \; \rho \; R^3 \; Vo^2 \; \pi)} \qquad (10\text{-}5)$$

A similar relationship between power coefficient and acceleration is shown by substituting expression (10-3)

into expression (4-36) as follows:

$$CP = \frac{Im\ Ac\ \Omega}{0.5\ \rho\ R^3\ Vo^2\ \pi} \qquad (10\text{-}6)$$

This technique therefore provides a relatively straight-forward method of obtaining the performance characteristics of a wind turbine rotor.

The way in which this method was applied will now be described.

10.3.1 ROTOR MASS MOMENT OF INERTIA

The mass moment of Inertia Im was measured by means of a standard physics experimental technique (F Tyler, 1966) with the rig's mast tilted down almost to ground level and in still wind conditions.

The wind turbine chassis was oriented so that its shaft was horizontal and rigidly braced (to prevent movement other than the rotation of the wind turbine shaft) at a height sufficient to allow the rotor to rotate freely.

The V belts coupling the wind turbine shaft to the secondary shaft were disconnected to allow the rotor to spin freely and unloaded.

A number of laboratory weights were attached to one end of a cord, the other end of which was coiled around

pulley no. 1 so that the weight was wound up to a height of around 1.5 metres. The weight was then allowed to fall to the ground, turning the rotor in the process. The number of rotor cycles or blade passes and time taken for the weight to reach the ground from a measured height were recorded, as were the number of rotor cycles or blade passes and time taken for the rotor to come to rest. Because of the use of small weights the velocity of the rotor was very small, so that the distorting effects of air resistance on the measurements was negligible. Figure 10.5 illustrates the experiment.

The mass moment of Inertia of the Sailfoil rotor is then derived from the following relationship (10-7) (Tyler, 1966):

$$Im = Ml\ rp^2 \left[\frac{(g\ t^2) - 1}{(2\ hw)} \right] \left\{ \frac{nr}{(nr - ng)} \right\} \quad (10\text{-}7)$$

Where Im = mass moment of Inertia in $kg.m^2$

Ml = mass of laboratory weight

rp = radius of pulley no. 1 (0.157m)

t = time taken for weight to reach the ground

ng = the number of revolutions of rotor for weight to reach ground = bg/3

bg = the number of blade passes until weight reaches the ground.

nr = the further number of rotor revolutions of the rotor until the rotor comes to rest
= br/3

br = the further number of blade passes till rotor comes to rest

nt = the total number of revolutions till rotor comes to rest = ng + nr

bt = the total number of blade passes till the rotor comes to rest.

g = acceleration due to gravity

hw = height that weight falls to ground level

These experiments were repeated 16 times with 3 different falling weights of mass 3kg, 4kg and 6kg.

The results of these experiments are shown in Table 10.1. The mass moment of Inertia, Im, was then calculated for each of the tests and the mean value for Im was then calculated to be 42.267 $kg.m^2$.

10.3.2 ACCELERATION TESTING OF SAILFOIL HAWT ROTOR

A computer program, originally written by David Sharpe, for testing wind tunnel models of wind turbines using the acceleration method, was modified for use on ATG's Wind Turbine Field Test Facility. The program runs on ATG's Commodore CBM8032 micro-computer and is entitled 'CP-L TESTS'.

The program uses analogue data from an Evershed Tachogenerator (having a 3 volts/1000 rpm output characteristic), driven by a friction roller in contact with the wind turbine shaft, and wind speed from a Vector Instruments analogue anemometer A100.

These analogue signals were fed to a 12 bit CIL analogue-to-digital converter and the converted signals were fed to the computer via the IEEE-488 parallel bus.

The program uses the computer's on-board clock to calculate the acceleration of the rotor from the input angular velocity and then determines the power coefficient for the input wind speed data. It does this with all the successive data readings it receives and sorts the calculated value of Power Coefficient into a Tip Speed Ratio bin of a width equal to 1/8th of a unit of Tip Speed Ratio.

It also keeps a running average value of each CP value in that bin, so that as more data points are accumulated the effect of any erroneous data points is minimised.

Up to 500 data points were collected during one acceleration test run and these were plotted on the screen. Successive test runs were then compounded to provide further smoothing, so eventually the overall CP-X curves for the wind turbine Sailfoil rotor are produced.

10.3.3 POWER COEFFICIENTS FROM ACCELERATION TESTS

Three methods of treating the acceleration test data were utilised to see which technique provided the most

satisfactory means of reducing the scatter.

10.3.3.1 Power Coefficients Derived from Raw Acceleration Test Data

With this method the data was simply sorted and binned as described above. In the CP-X curves based on raw data, there was considerable scatter. This is because the acceleration test technique was first designed for use in the wind tunnel where the wind speed can be kept constant. There, the acceleration of the wind turbine has a direct correlation with the torque imparted to it by the wind.

In the open air, however, the wind is very unlikely to be constant for more than a fraction of a second. Since the turbine rotor (due to its inertia) cannot instantaneously respond to the variations in wind speed, the relationship between wind velocity and the wind turbine's acceleration (and therefore its torque output) is subject to distortion.

10.3.3.2 First Order Refinement of Power Coefficients from Acceleration Test Data

In order to reduce the distortion effects caused by the varying wind speed, a refinement to the analysis of the data was introduced by means of a computer program CPCQ PLOTPRINT which was written by the author (see

Appendix).

This technique entailed filtering the data in such a way that all consecutive wind speed values that were not identical (ie, the wind speed was not constant between readings) were eliminated.

Figure 10-6 shows the acceleration test results that after refining in this way. There is a marked reduction in scatter, especially in the ascending part of the curve. However there is still some scatter at higher tip speed ratio end of the curve. This seems likely to be principally due to the fact that there are fewer data points to be averaged at the higher (and less frequent) tip speed ratios.

With the inclusion of this filtering refinement, the acceleration testing technique appears to provide a satisfactory means of testing the performance characteristics of variable speed wind turbines operating in the free wind.

REFERENCES FOR CHAPTER 10

Akins, RE (1979): Full-Scale Performance Evaluation of Wind Turbines, American Society of Civil Engineers Convention, Boston, April

Sharpe, D.J.(1976): A Theoretical and Experimental study of the Darrieus Vertical Axis Wind Turbine, Research report, School of M.A.P. Enegineering, Kingston Polytechnic, October 1977.

Tyler, F. (1966): A Laboratory Manual of Physics. Edward Arnold

TABLE 10.1: LOG OF SAILFOIL ROTOR MASS MOMENT OF INERTIA MEASUREMENTS

Mass of weight M1 (kg)	Height of weight at start hw (m)	Time taken for weight to reach ground t (sec)	No. of blades passes till weight on ground bg	No. of rotor revs for weight to reach ground ng	No. of blade passes till rotor at rest br	Further revs till rotor at rest nr	Mass moment of Inertia I ($kg.m^2$)
6	1.57	12.5	5	1.66	12.8	2.6	43.9
6	1.54	12.5	4.5		11		43.4
6	1.61	12.7	4.8	1.6	13.5	2.9	46.738
6	1.59	12.6	4.7	1.566	10	1.766	38.31
6	1.52	12.0	4.6	1.533	14	3.13	46.044
1	1.36	41.2	4.5	1.5	9	0.66	46.42
3	1.66	22.2	5.2	1.733	8	0.933	37.66
3	1.64	25.1	5	1.66	8	1	52.35
3	1.66	21.9	5	1.66	8.5	1.166	43.22
3	1.62	20	5	1.66	8.5	1.166	36.92
3	1.64	21.1	5	1.66	8.1	1.03	37.75
4	1.62	16.5	4.8	1.6	9.8	1.66	41.41
4	1.63	16.1	5	1.66	10.6	1.866	40.65
4	1.56	17.3	4.8	1.6	8.3	1.166	39.07
4	1.58	17.6	4.8	1.6	7.9	1.033	37.166
4	1.59	18.5	4.8	1.6	8.5	1.233	45.27
					Sum of moment of intertias =		676.278
					Mean moment of Inertia I =		42.267

r = pulley radius = 0.157m

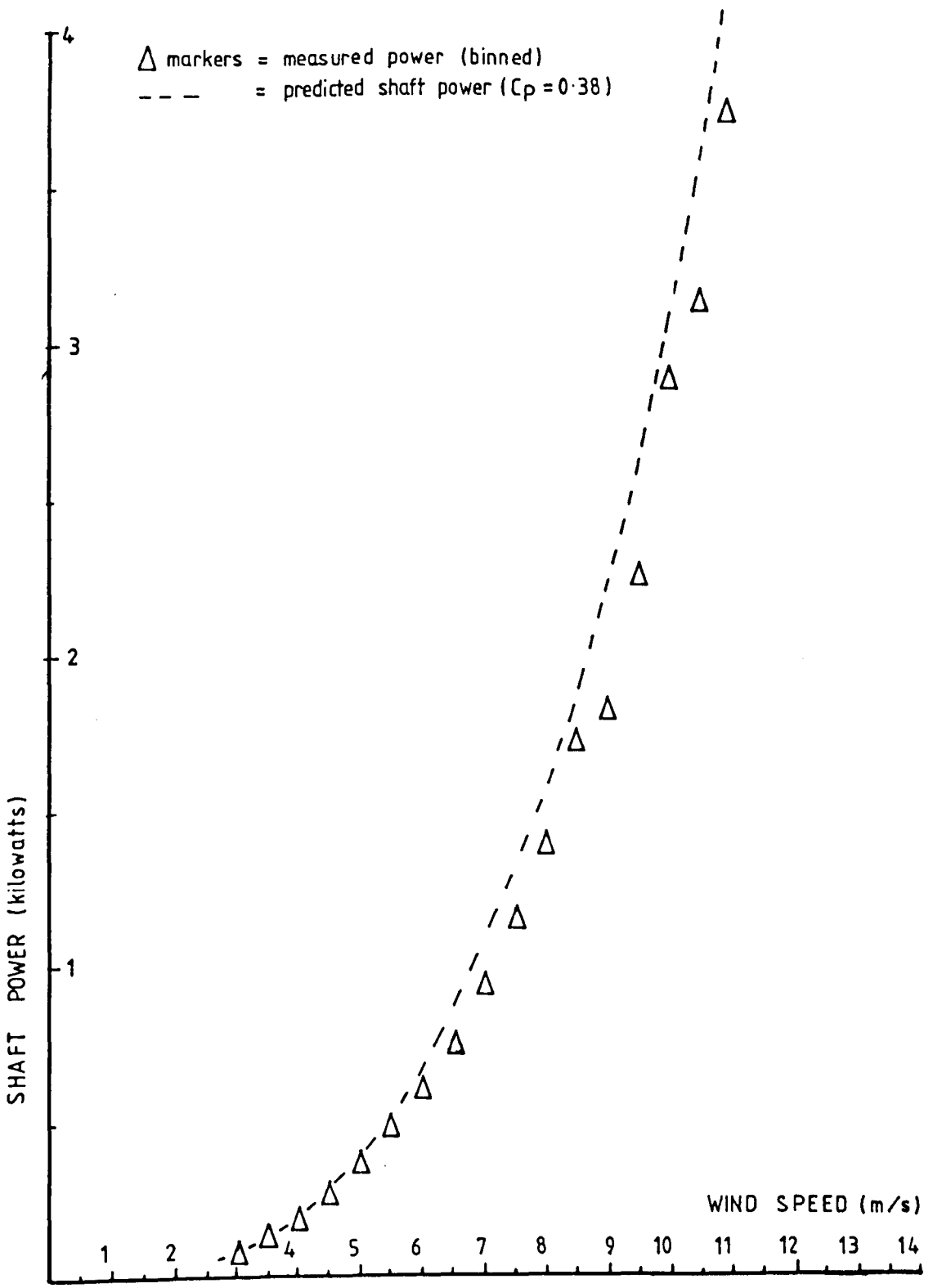

Fig. 10.1 Measured power/wind speed curve for the shaft power output of variable speed sailfoil wind turbine.

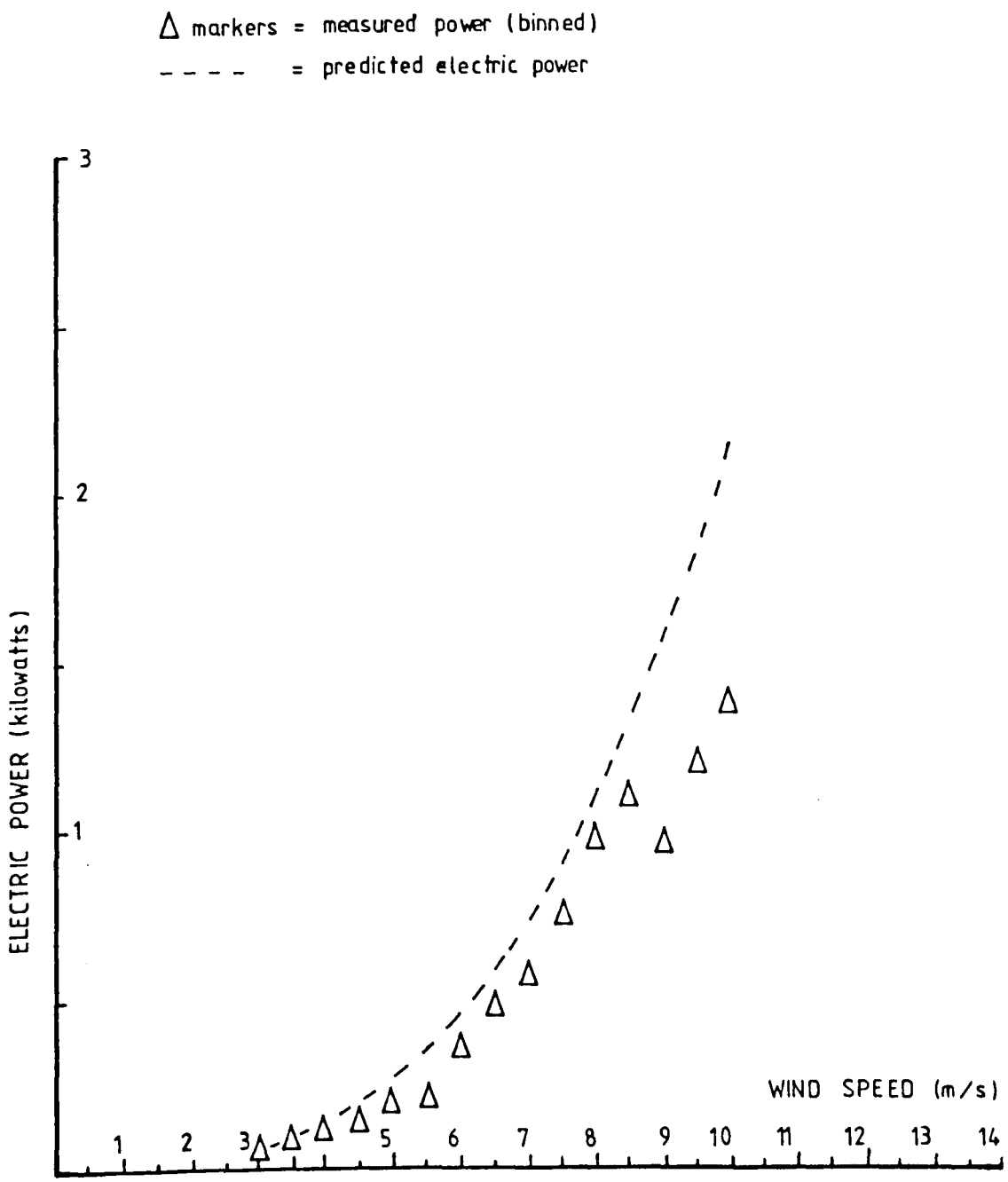

Fig. 10.2 Measured power/wind speed curve for the electrical power output of variable speed sailfoil wind turbine.

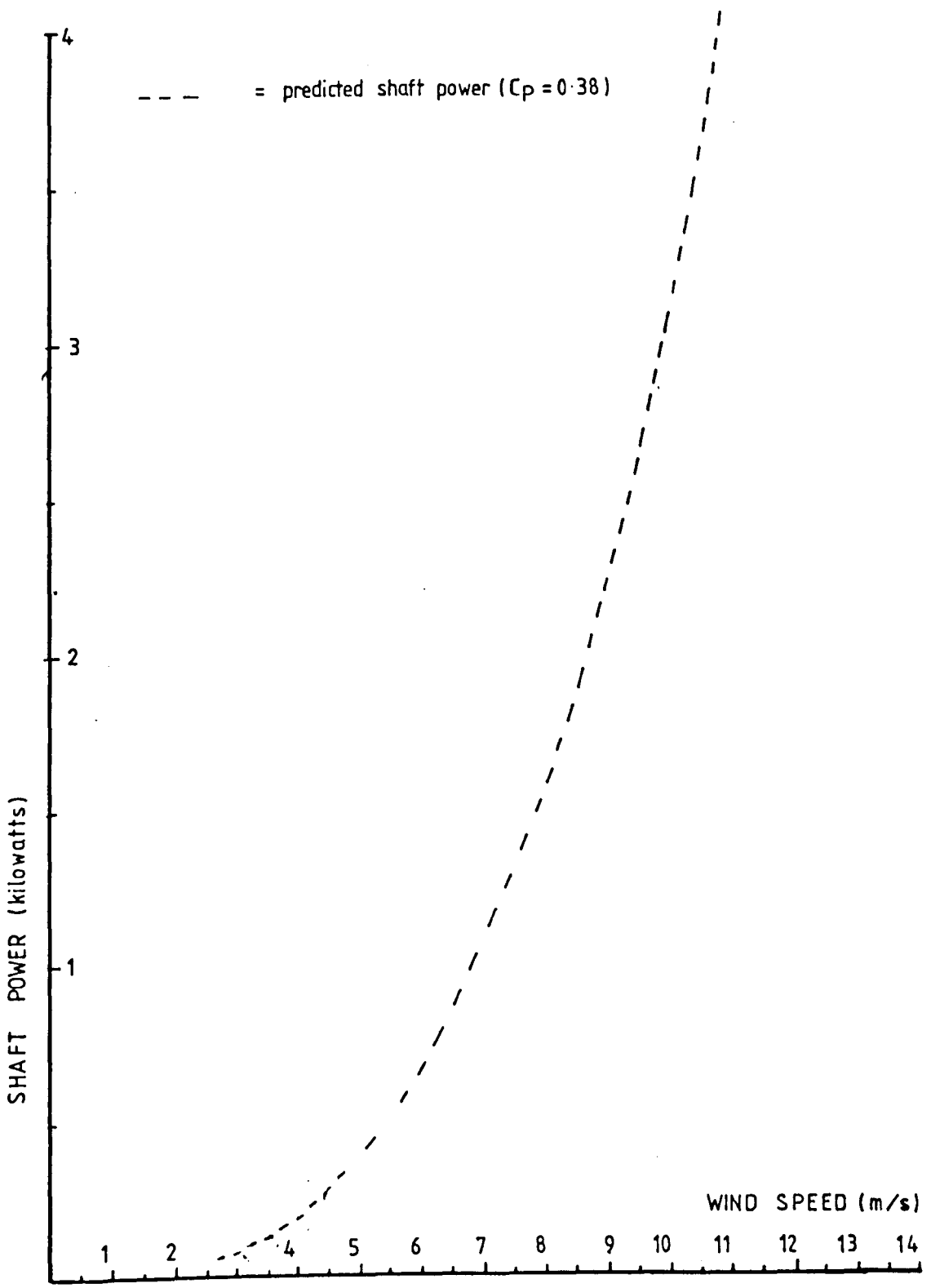

Fig. 10.3 Predicted power/wind speed curve for electrical power output of variable speed sailfoil wind turbine.

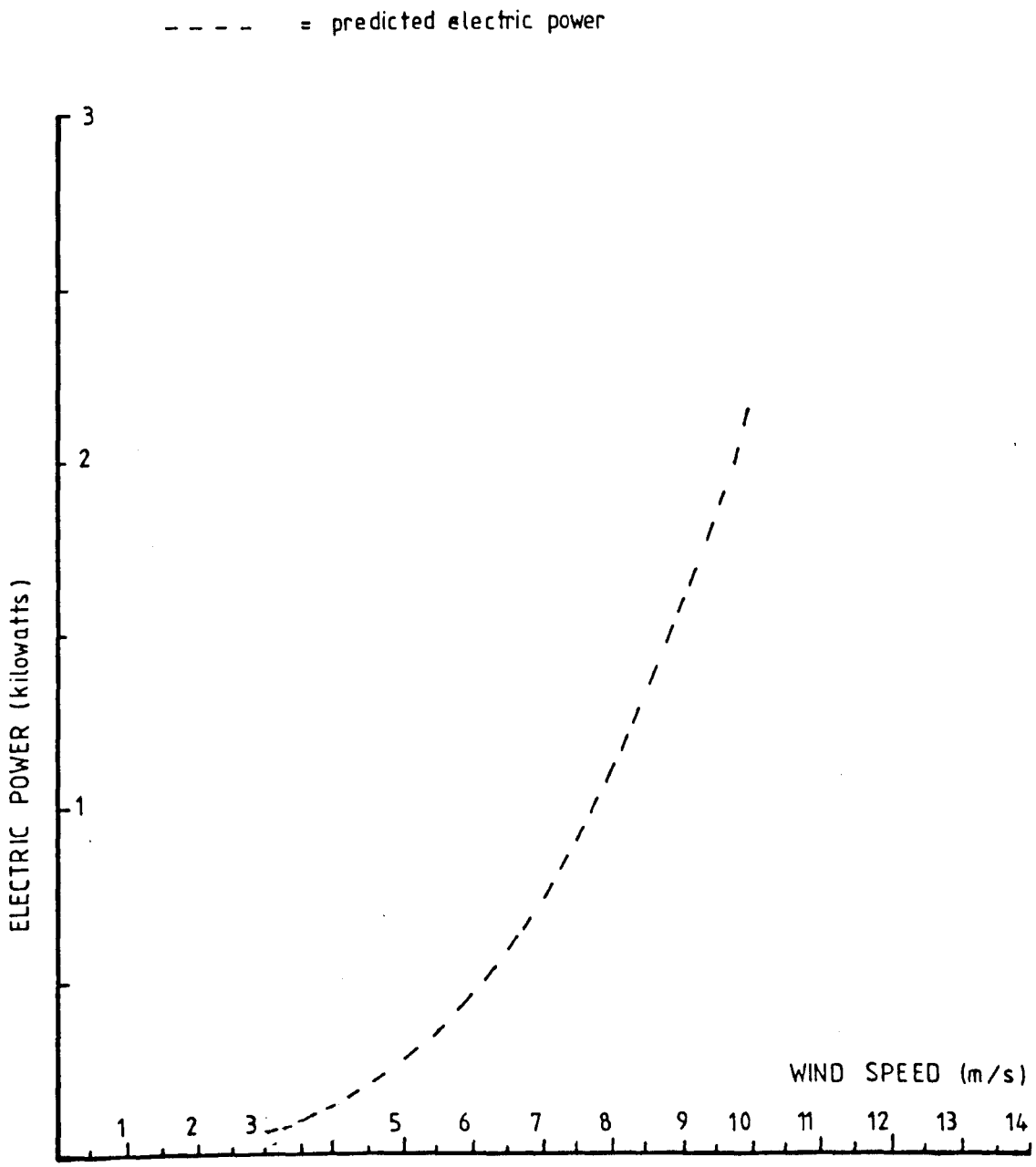

Fig. 10.4 Predicted power wind speed curve for electrical output of variable speed sailfoil wind turbine.

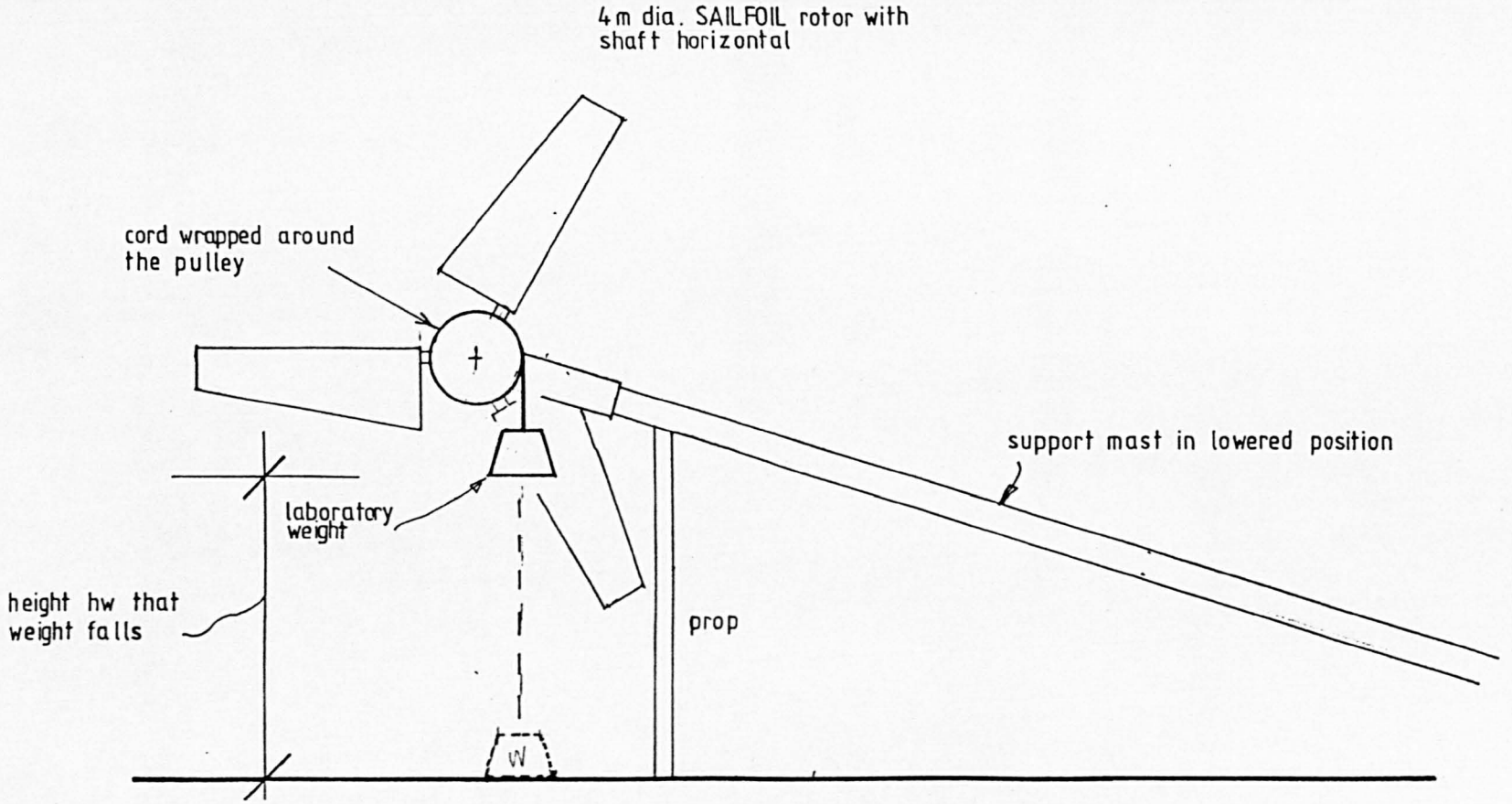

Figure 10.5: Experimental measurement of wind turbine's mass moment of intertia

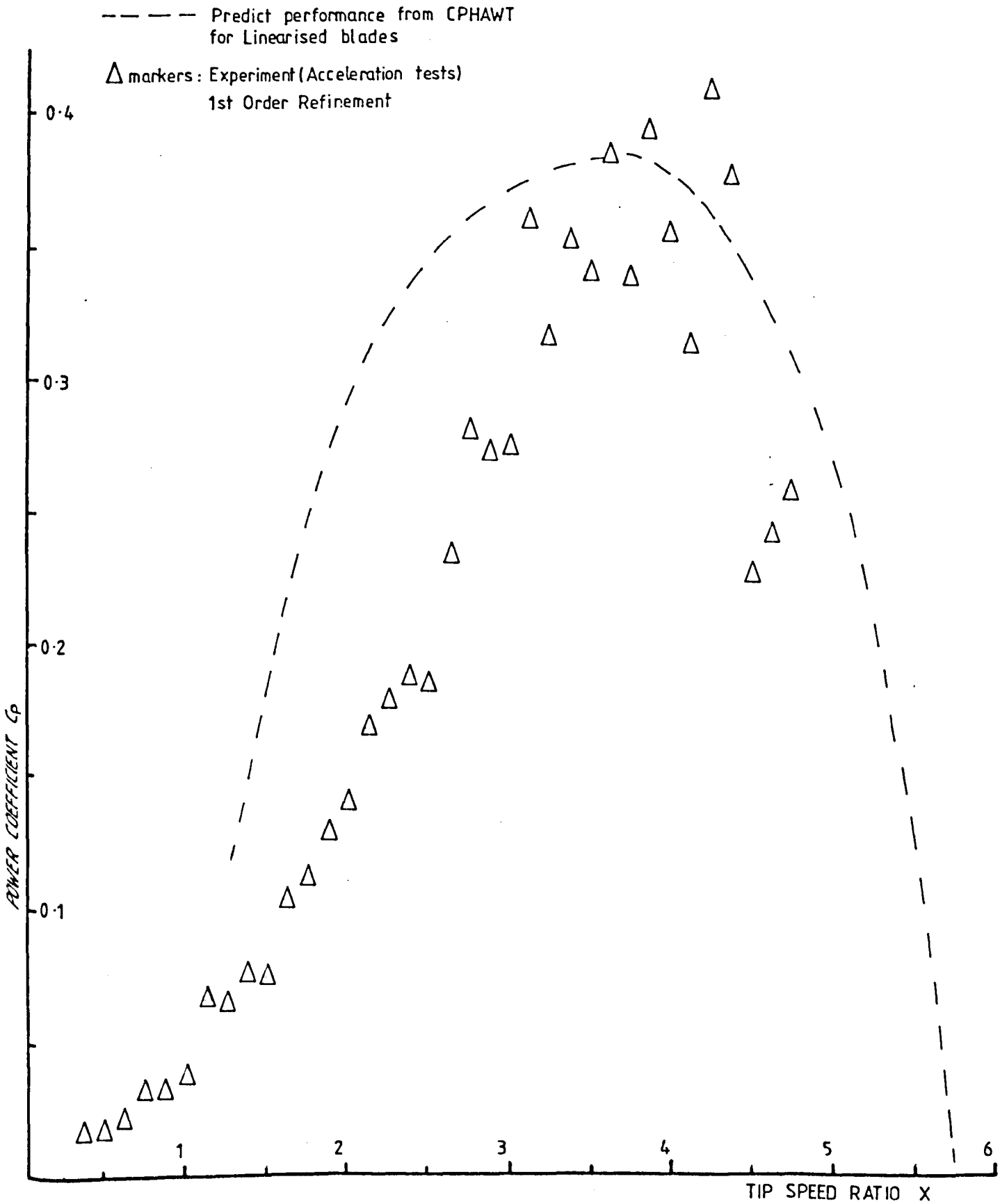

Figure 10.6: Measured CP-X curve for Sailfoil wind turbine - 1st Order Refinement

CHAPTER 11

CONCLUSION

11.1 SUMMARY AND DISCUSSION OF RESULTS

A wind turbine blade of novel design, the Sailfoil, has been developed and constructed. A UK patent on the concept has been granted to the Open University on behalf of the author (Appendix 7).

A 4 metre diameter, 3 bladed horizontal axis wind turbine which utilised these sailfoil blades for its rotor was designed by the author and fabricated in the workshops of the Alternative Technology Group at the Open University.

An open air wind turbine field test facility was designed by the author and installed on a field site on the Open University's Walton Hall Campus primarily for the purposes of testing this novel blade design.

11.2 RESULTS OF PERFORMANCE TESTS

A 4 metre diameter, 3 bladed horizontal axis wind turbine rotor with Sailfoil blades was tested on the ATG test facility in free air conditions. Power/wind speed characteristic curves were produced.

Figures 10.1 and 10.2 compares the predicted shaft power/wind speed and electrical power/wind speed curves

respectively.

The predicted values were based on a peak rotor power coefficient of 0.38 at a tip speed ratio of 4. The field current in the alternator was actively varied by a CBM 8032 microcomputer to maintain the tip speed at 4 times the wind speed.

As can be seen from Figure 10.1, that whilst the theoretical values slightly over predict, there is an excellent fit between predicted and measured shaft power/wind speed values, especially for the lower wind speeds (where more data points were accumulated in the bins, due to the higher frequency of lower wind speed).

The alternator efficiency characteristic, used in the predictions in Figure 10.2 was based on bench test measurements on the alternator carried out with facilities in the Department of Electrical Engineering at Imperial College, Boyle et al (1983).

As can be seen form Figure 10.2, that whist theoretical predictions generally over estimate slightly, there is a good fit for the lower wind speeds, though there is a sizeable theoretical over prediction at wind speeds in excess of 8.5 m/s. This discrepancy is believed to due the fact that the frequency of wind speeds in excess of 8.5 m/s during tests was very much lower than wind speeds below 8.5 m/s. This meant that there were very

few data points in each wind speed bin, in contrast to wind speeds below 8.5 m/s.

Tests were also carried out to determine the CP-X characteristics for the rotor. This is a difficult task in the case of a variable speed machine operating in free air conditions.

To determine the CP-X characteristics of the Sailfoil wind turbine, the 'acceleration' test technique was employed. Modifications to the technique were introduced to compensate for the variable wind speeds which occur in open air conditions.

The CP-X curves generated by this modified technique (Fig 10.7) did not fit precisely to the predicted values. The predicted values were generally higher than the measured values. This discrepancy is in part due to the fact that the Princeton sailwing aerofoil data used in the design of the Sailfoil HAWT rotor blades was based upon a thickness-to-chord ratio of 12%, whereas with the Sailfoil rotor this ratio was somewhat greater than 12% at the tips and less than 12% at the root. The reason for this was that a round, tubular spar with a constant diameter was used (this type of tube being more readily available), rather than a tapered spar which would have produced a constant thickness to chord ratio. If aerofoil data for a sailwing aerofoil with other than 12% thickness to chord ratio had been available then it

would have been possible to improve the prediction of performance by allowing for the changes in thickness to chord ratio along the blade.

Another difficulty in predicting the performance of a soft-sailed blade of this type is that the actual aerofoil that is 'seen' by the wind is not, strictly speaking, the same as that assumed theoretically. This departure from the aerofoil shape is because of the effect of the blade twist on the membrane of the fabric sock and is also due to the change in profile caused by the air flow across its surfaces. No doubt these phenomena could be modelled using an elaborate computer program but this was not considered justified within the time scale and resources of this project.

There was also a tendency for the membrane to exhibit ripples on its surface (which would tend to increase drag), even though every effort was employed to reduce these effects during construction. Other drag increasing factors may have included the effect of the stitched joints, though these were taped over smoothly. For simplicity of manufacture, the tip end of the blade took the form of a square cut edge which added to the drag of the rotor. This could be improved by gradually rounding off the tip edge.

The modified acceleration test technique does appear to be a useful and rapid method of testing a variable speed

wind turbine in the real wind.

Power versus wind speed curves were obtained for the Sailfoil HAWT. These give the most important performance characteristics required for an actual wind turbine installation

11.3 AEROFOIL DATA

There is a dearth of aerofoil data for 'D spar' type sailwing or sailfoil profiles suitable for wind turbine design. Therefore there is a need for more testing to be carried out on such aerofoils if soft-sailed wind turbines are to be developed and improved. Also, see comments on availability of data in section 11.2 above.

11.4 POSITIVE ATTRIBUTES OF THE SAILFOIL ROTOR

Although the turbine has not been in continuous operation, it has been exposed to the weather at all times and the Sailfoil sock fabric has stood up successfully to this exposure for over two years.

The blade fabrication technique has shown that a low technology blade can operate at reasonable efficiency on a wind turbine system in the open air.

11.5 POSSIBLE IMPROVEMENTS AND DEVELOPMENTS OF THE SAILFOIL ROTOR

There are a number of measures that could be carried out to improve the performance of a wind turbine utilising Sailfoil blades.

These include using a tapered spar in order to keep the thickness/chord ratio constant and at the optimum value.

Alternatively, the spar could be made out of laminated wood, using standard techniques employed for timber beams. This would be more straightforward than making a complete blade out of laminated timber, as the complex curved and twisted surface required is achieved automatically by the Sailfoil membrane.

Sailfoil profile could also be improved if the round trailing edge tube was replaced by a flat or wedge shaped bar to give a sharper trailing edge and improve airflow as it leaves the trailing edge.

A feature that lends itself to the Sailfoil is that of blade torsion. If the spar or root is designed in such a way that it can twist relatively easily, the blade could be designed so that it is constructed flat and untwisted and attached to the hub at a coarse pitch. As the rotor began to rotate the blade would then be twisted into a more efficient shape due to centrigual

force acting on mass weights attached to the blade spar. Using a similar concept, a small wind turbine has already been made in the USA (Bergey 1980) which uses a solid composite rotor blade. If successful, this method would also reduce the cost of a Sailfoil blade as it would not require a twisted 'D' spar to be constructed.

The same technique could also be employed as a means of speed and power regulation, either passively or actively operated, in much the same manner as a conventional variable pitch blade control mechanism but without the need to use bearings. A composite blade rotor developed by United Technologies (Cheney 1976) also uses this method.

A possible future development is as follows. Normally the 'D' spar sailwing or sailfoil type of blade is not suitable for use on vertical axis wind turbines due to the built in one way camber that they introduce. The author, however, has originated a novel concept, which has also been patented on the author's behalf by the Open University (Taylor 1981) known as the 'variable droop' sailwing/sailfoil, which should enable this type of blade to be employed on a vertical axis wind turbine (Fig 11.1).

The basic idea is that the 'D' spar is attached to a circular main spar via bearings so that it is able to swivel to positive or negative pitch as the turbine

rotates around the vertical axis and 'sees' the wind from first one surface and then the other. This could be a promising development since the blade does not have to be twisted or tapered for a vertical axis wind turbine, so the airfoil shape should be somewhat easier to predict and to construct. It should also have some improved performance (due to its reversal camber) over rigid fixed pitch blades, which have to be of symmetrical section.

CONCLUSION

This project has shown that wind turbines utilising Sailfoil blades, though simply made with off-the-shelf components, are durable and can achieve good efficiencies. Figure 11.2 compares the Sailfoil CP-X curve with other wind tubines (BWEA, 1982). If the Sailfoil is taken up by a sailmaking company or similar enterprise, it could provide an alternative to existing blade designs. In addition to its good performance and simple construction, the Sailfoil facilitates onsite repairs and also has potential as an uncomplicated design for homebuilt wind turbines.

In addition, sailfoil blades and sailfoil based turbines could be manufactured easily in Third World countries, especially where traditional sailmakers and light engineering shops or blacksmiths already exist.

Whether or not the Sailfoil type of blade could compete economically in high volume production with current standard mass produced GRP blades would depend on the choice of spar type, spar material and whether modern techniques of computerised automatic sail-making could be employed.

However, the author's experience in obtaining small numbers of GRP or timber blades for other small wind turbines indicates that the Sailfoil is likely to be competitive for small volume production of small scale wind turbine blades.

REFERENCES FOR CHAPTER 11

Boyle, GA, Taylor, DA & de Montmarin, G (1983): Experimental Bench Testing of a Wind Turbine Alternator, ISES Solar World Congress, Perth, Australia

Bergey, K (1980): Development of High Performance, High Reliability Windpower Generators, American Wind Energy Association's Summer Conference, Pittsburgh, Pennsylvania, USA

BWEA (1982): Wind Energy for the Eighties, Peter Peregrinus

Cheney, M (1976): Composite Bearingless Rotor, 1st International Symposium on Wind Energy Systems, BHRA, Cambridge

Taylor, DA (1981): Variable Droop Sailwing , Patent Office, London

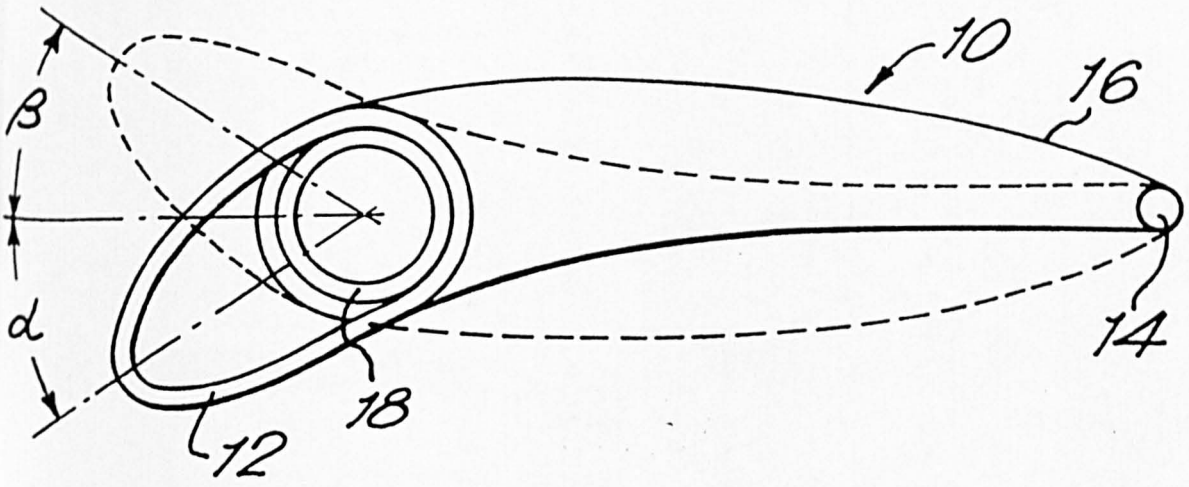

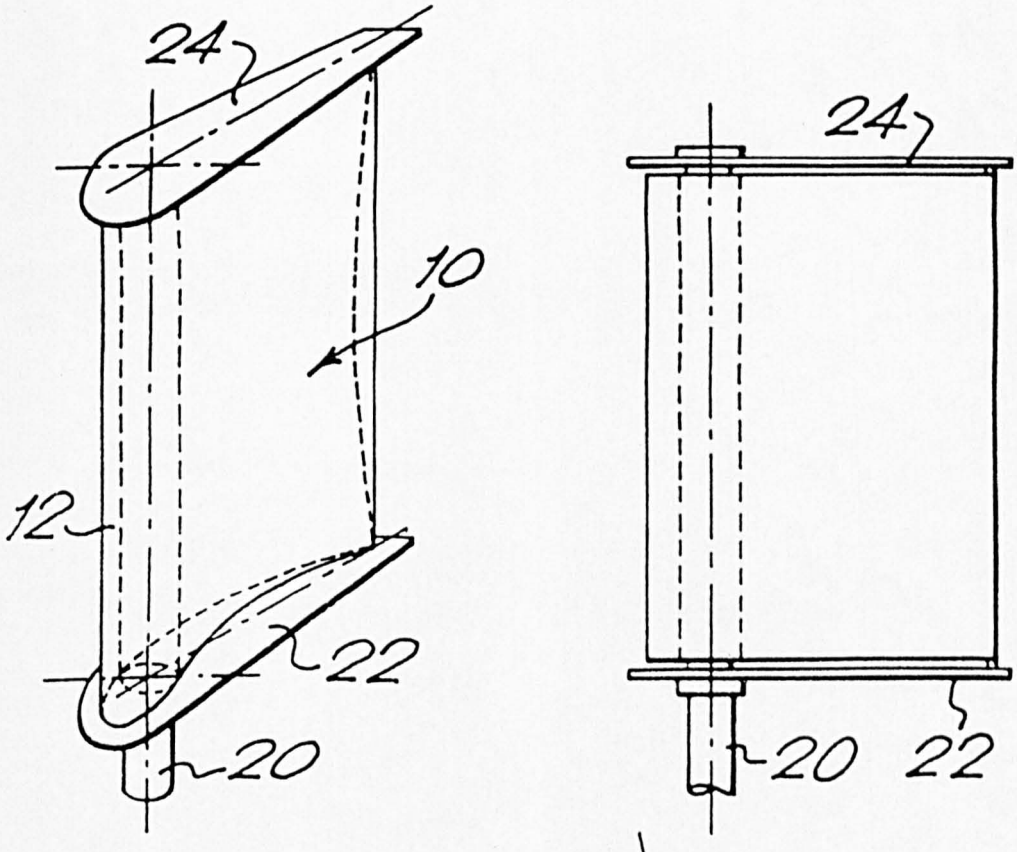

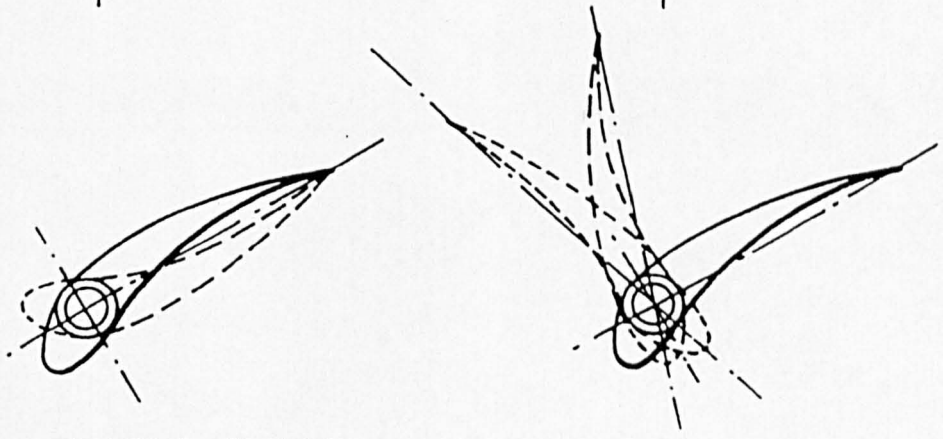

Fig. 11.1 Variable Droop Sailwing.

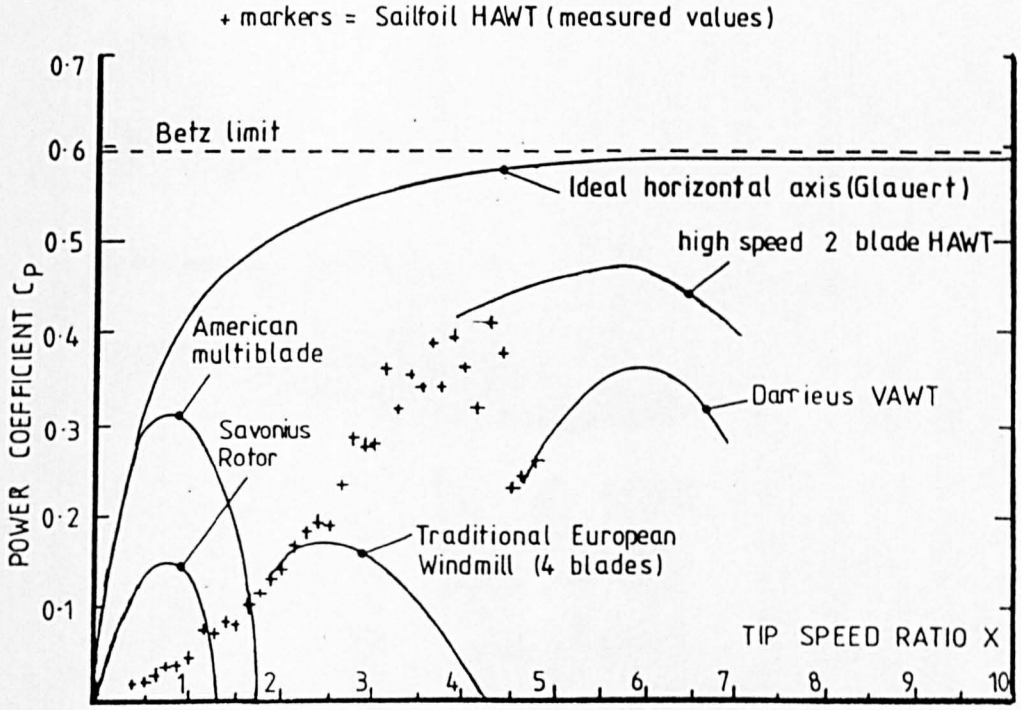

Figure 11.2: Comparison of Wind Turbine Power Coefficients With Experimental Power Coefficient - Tip speed ratio values for Sailfoil HAWT

NOTIFICATION OF REDACTION

THESIS TITLE:
The design and testing of a horizontal axis wind turbine with sail foil blades

AUTHOR:
Derek Taylor

YEAR:
1985

CLASSMARK:
621.312136 TAY

The following pages/sections have been redacted from this thesis:

Page No.	Item/section redacted
	APPENDICES 1 - 8